

**EVALUATION OF SELECTED RADAR CROSS SECTION  
MEASUREMENT RANGES**

**Vol. I: Range Parameters, Range Evaluation,  
Problem Areas and Recommendations.**

By

**Thomas M. Smith, Eugene F. Knott and Ralph E. Hiatt  
The University of Michigan Radiation Laboratory  
Department of Electrical Engineering  
Ann Arbor, Michigan**

December 1968

Contract AF30(602)-3872

Prepared for:

**Rome Air Development Center  
Griffiss Air Force Base, New York**

7462-1-F = RL-2157

## NOTICE

When Government drawings, specifications, or other data are used for any purpose other than in connection with a definitely related Government procurement operation, the United States Government thereby incurs no responsibility nor any obligation whatsoever; the fact that the Government may have formulated, furnished, or in any way supplied the said drawings, specifications, or other data, is not to be regarded by implication or otherwise as in any manner licensing the holder or any other person or corporation, or conveying any rights or permission to manufacture, use, or sell any patented invention that may in any way be related thereto.

Copies of this report should not be returned unless return is required by security considerations, contractual obligations, or notice on a specific document.

**Evaluation of Selected Radar Cross Section Measurement Ranges**

**Vol. I: Range Parameters, Range Evaluation, Problem Areas  
and Recommendations.**

Prepared by

**T.M.Smith, E.F.Knott and R.E.Hiatt  
The University of Michigan Radiation Laboratory  
Department of Electrical Engineering  
Ann Arbor, Michigan**

December 1968

**Contract AF 30(602)-3872**

**Rome Air Development Center  
Griffiss Air Force Base, New York**

## FOREWORD

This report (RADC-TR-68-238 , 7462-1-F) was prepared by The University of Michigan Radiation Laboratory, Department of Electrical Engineering, under the direction of Professor Ralph E. Hiatt under Air Force Contract AF 30(602)-3872 "Radar Scattering Investigation", Task 651207, Project 6512. The work was administered under the direction of the Rome Air Development Center, Griffiss Air Force Base, New York. The Task Engineer was Mr. D. M. Montana.

This report covers the period July 1965 through April 1968.

## ACKNOWLEDGEMENT

The authors are pleased to acknowledge the contributions of Dr. T. B. A. Senior on several phases of the program. Thanks are due to Mr. Tony Hsu for his considerable help in reading patterns and organizing the data.

This technical report has been reviewed and is approved.

MILTON L. WASSER  
Contracting Officer



## ABSTRACT

A program under which selected radar cross section measurement ranges were evaluated is described. Some details are given on the test models involved and on the test procedures used. Test results are summarized and the ranges are assigned ratings according to their performance in an evaluation that includes many points of comparison. Problem areas in radar cross section measurements are outlined and some recommended solutions are given. Some suggestions for the optimum utilization of radar cross section ranges are given for the benefit of the potential range user.

## TABLE OF CONTENTS

I	INTRODUCTION	1
II	SHORT HISTORY OF THE MEASUREMENTS PROGRAM	2
	2.1 Description of the Project	2
	2.2 Delays and Slippage in Schedules	9
	2.3 A Few Mistakes	15
III	RANGE COMPARISONS	18
	3.1 Facilities, Techniques and Procedures	18
	3.1.1 Frequency	18
	3.1.2 Near Field Effect	20
	3.1.3 Log	20
	3.1.4 Measurement Time	21
	3.1.5 Total Range Time	21
	3.1.6 Measurement Procedures	22
	3.1.7 Calibration Techniques	22
	3.1.8 Handling Facilities for Large Targets	23
	3.1.9 Sheltered Storage	23
	3.1.10 Confidence in Data	24
	3.1.11 Data Format	24
	3.1.12 Final Reports	25
	3.2 Accuracy of Cylinder VV and HH Data	25
	3.3 The Reliability of Cross Polarized Measurements on Cylinders	29
	3.4 The Accuracy of the Satellite RCS Data	30
	3.5 Ability of Make Specified Measurements	32
	3.6 Summary	33
IV	IDENTIFICATION OF PROBLEM AREAS AND RECOMMENDATIONS FOR IMPROVEMENT	35
	4.1 Measurement Errors	35
	4.1.1 Equipment and Facilities	36
	4.1.1.1 Near Field Measurements	38
	4.1.2 Measurement Procedures	40
	4.1.2.1 The Transmitter	40
	4.1.2.2 Receiving and Analog Recording System	41
	4.1.2.3 Turntable and Model Support	43
	4.1.2.4 Field Probe	44
	4.1.2.5 Background Evaluation	47
	4.1.2.6 Calibration Procedures	50
	4.1.2.7 Preliminary Analysis of Data	54
	4.1.3 The Range Crew	54

Table of Contents, Cont'd

4.2	Other Problem Areas	55
4.2.1	Cross Polarized Measurements	55
4.2.2	Phase Measurements	56
4.2.3	Digital Recording Systems	57
4.2.4	Data Display	58
4.2.5	Underestimating Range Time	60
4.2.6	Weather	63
4.3	Summary	63
V	GUIDE TO THE CHOICE AND UTILIZATION OF RADAR CROSS SECTION MEASUREMENT FACILITIES	67
5.1	Guidelines for Range Utilization	67
5.1.1	Adequacy of Facilities	67
5.1.2	Range Personnel	69
5.1.3	Costs	69
5.1.4	Schedules	69
5.2	Range Selection by a Potential User	70
VI	CONCLUSIONS	73
	REFERENCES	77
	DD FORM 1473	

## LIST OF ILLUSTRATIONS

2-1	Geometry for Typical Ground Plane Radar Cross Section Measuring Facility.	3
2-2	Test Program Began with Assembly of All Models to be Measured at Conductron Range.	10
2-3	Comparison of Planned and Actual Flow of Work.	12
4-1	Full Scale and 4/10 Scale Satellite Data for Fixed Aspect Angle and Polarization	37
4-2	RCS Pattern for Two Foot Cylinder, 2720 MHz VV Polarization from Conductron Corporation Range.	51

## LIST OF TABLES

II-1	Some Characteristics of the Sites.	5
II-2	Matrix of Frequency vs. Scale for Closed Right Cylinder.	6
II-3	Matrix of Frequency vs. Scale for Satellite Type Objects.	6
II-4	Description of the Models Used in the Measurements.	8
II-5	Shipping Costs of the Models.	16
III-1	Comparison of Facilities, Techniques and Procedures.	19
III-2	Distances Used for the Largest Model were Always Less than $2L^2/\lambda$ .	20
III-3	Summary of Range Tests for Five Points of Evaluation.	26
III-4	Rating on Cross Polarized Measurements on Cylinders	30
III-5	Rating on Satellite RCS Measurements.	31
III-6	Ability of Make Phase and Amplitude Measurements Specified in Tables II-2 and II-3.	33
III-7	Range Comparison Summary	34
IV-1	Comparison of Range Pattern Scales	59
IV-2	Summary of Range Quotations	61
IV-3	Revised Summary of Range Quotations	61
V-1	List of the Number of Errors 1 dB or Less When Measurements Compared with Theory for End-on and Broadside.	71
V-2	Range Selection for a Variety of Requirements.	72

# I

## INTRODUCTION

This report is Volume I of a three part report summarizing the results of work accomplished under Contract AF30(602)-3872. The objectives of this project were:

- 1) To evaluate existing radar cross section measurement facilities.
- 2) To provide a guide to optimum utilization of existing radar cross section measurement facilities.
- 3) To identify critical problem areas in radar cross section measurements.
- 4) To develop plans for attacking the critical problem areas identified.

Special emphasis was placed upon the measurement of large objects (30' and longer).

This volume is intended to contain information of general interest to potential users of radar cross section ranges. It discusses the relative merits of the radar range facilities involved in the study. A short history of the investigation appears in Chapter II and serves to acquaint the reader with some of the problems encountered during the contract. Chapter III is a comparison of the radar ranges in several categories. In Chapter IV, we discuss problem areas and possible solutions, and in Chapter V some brief comments on optimum utilization of ranges are given. The important conclusions to the investigation are summarized in Chapter VI.

The measurement techniques, the measurements themselves and the evaluation of the data are discussed in Volumes II-a and II-b of this Final Report. Volume II-a contains a detailed description of tests performed on five cylinders while Volume II-b presents the results on the satellite models.

## II

### SHORT HISTORY OF THE MEASUREMENTS PROGRAM

#### 2.1 Description of the Project

We present here a brief chronicle of the measurements program and itemize some of the reasons which caused the original scheduling to slip. We will single out the major errors committed early in the contract so that other potential radar range users, who may well encounter the same problems, may benefit from our experience.

The work requirements of this program called for a series of radar back scatter measurements to be made at the ranges operated by the contractors listed below:\*

Conductron Corporation, Ann Arbor, Michigan

Radiation Incorporated, Melbourne, Florida\*\*

General Dynamics, Fort Worth, Texas

RAT SCAT, Holloman Air Force Base, New Mexico

Micronetics Incorporated\*\*\*, San Diego, California

Air Force Avionics Laboratory, Wright-Patterson Air Force Base, Ohio.

With the exception of Micronetics, all the outdoor ranges make use of the ground plane geometry in their measurements. In the typical ground plane range, the antenna and target heights are adjusted so that the target is placed at a peak of the first lobe formed by the in-phase addition of the direct and ground reflected waves as shown in Fig. 2-1 (Bachman et al, 1963). At Micronetics the ground reflections are minimized by using a mound of asphalt in the shape of an inverted V which extends along the path between the transmitter and the target.

---

\* For the convenience of the reader we will refer to these organizations in the remainder of the report as: Conductron (CC), Radiation Services (RSC), General Dynamics (GD/FW), RAT SCAT (RSS), Micronetics (MC) and Avionics Laboratory (AL).

\*\* The reflectivity range operated by Radiation Incorporated is now an independent organization called Sigma Incorporated.

\*\*\* This organization was later changed to Micronetics Division, Teledyne Incorporated, Teledyne Systems Company.

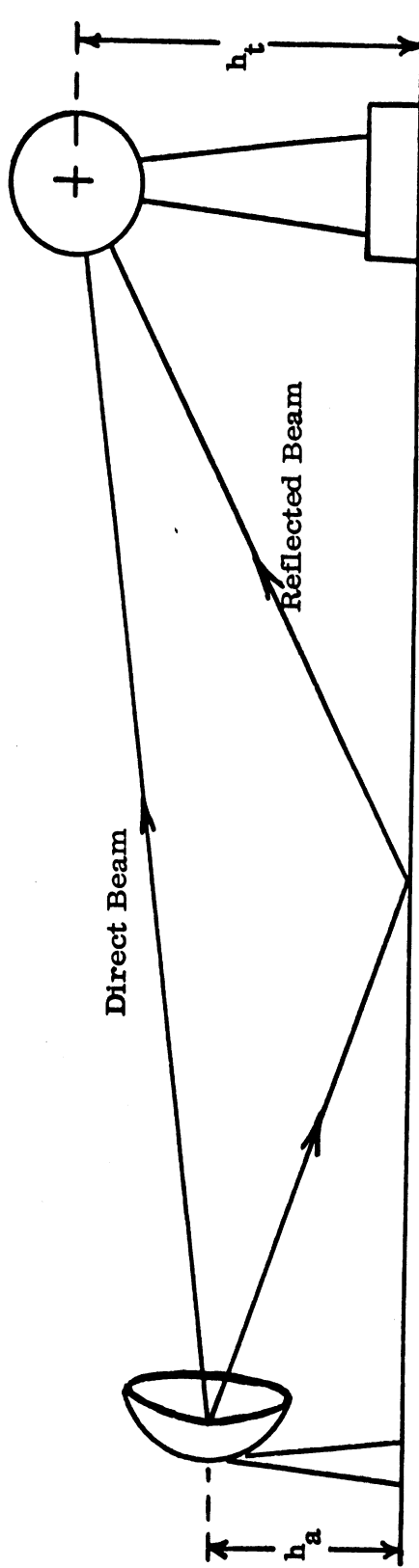


FIG. 2-1: GEOMETRY FOR TYPICAL GROUND PLANE RADAR CROSS SECTION MEASURING FACILITY.



With this arrangement the target and antenna heights are not as critically dependent on one another as with the conventional ground plane geometry.

Conductron Corporation uses a CW transmitter and employs a balanced RF bridge to separate the transmitted signal from the received. The other four ranges used pulsed radar systems with pulse widths between 1.0 and 0.1 microseconds and repetition rates on the order of a few KHz. When pulsed equipment is used the transmitted and received signals are separated in time and range, making it possible to gate out unwanted returns originating outside the target area. Blacksmith et al (1965) give more details on these types of systems and measurement techniques.

All the ranges have similar systems for recording amplitude data in analog form on rectangular pattern paper. The dynamic range of the recorders is 40 or 50 dB depending on the facility (Table II-1). Digital data are also recorded, and at two of the ranges, phase information is recorded. The type of equipment used at each range is also indicated in Table II-1.

For more detailed information on the ranges, the reader is referred to the following: (Conductron, Wren 1964), (Radiation Services, Landfried and Williamson 1964), (General Dynamics, 1968), (RAT SCAT, Marlow et al 1965), (Micronetics, Honer and Fortner, 1964), (Avionics Laboratory, Bahret, 1964), as well as more recent sources listed in the References.

Measurements were performed on five cylinders and three satellite objects at the frequencies shown in Tables II-2 and II-3. The frequency tolerance was to be  $\pm 0.1$  percent. Four polarization combinations, HH, VV, HV and VH were required at all frequencies and both phase and amplitude data was to be recorded for all facilities which have the needed polarization and phase capabilities. In the above abbreviations, H and V refer to horizontal and vertical respectively. The first letter indicates the transmitted and the second letter indicates the received polarization. Amplitude and phase information was to be provided as a function of target aspect angle through

TABLE II-1: SOME CHARACTERISTICS OF THE SITES

Site	Transmitter	Max Range Used (ft.) <sup>1</sup>	Geometry	Type Data Recorded	Dynamic Range	Digital Equipment
CC	CW	200	Ground Plane	Amplitude	40 db	Paper Tape
RSC	Pulse	1000	Ground Plane	Amplitude	40 db	Punch Cards
GD/FW	Pulse	1800	Ground Plane	Amplitude Phase	50 db 360°	Paper Tape
RSS	Pulse	1200 <sup>2</sup>	Ground Plane	Amplitude Phase (L-band)	50 db 360°	Paper Tape
MC	Pulse	600 <sup>3</sup>	Direct	Amplitude	40 db	Magnetic Tape

<sup>1</sup>Desired maximum range 2840' for the 32' cylinder at 1360 MHz.

<sup>2</sup>RAT SCAT has a 2400' range but did not use it to measure the full scale cylinder at 1360 MHz.

<sup>3</sup>Micronetics has a 1000' range but did not use it to measure the full scale cylinder at 1360 MHz.

**TABLE II-2: MATRIX OF FREQUENCY VS SCALE FOR CLOSED RIGHT CYLINDER.**

Scale \ Frequency MHz	Full	1/2	1/4	1/8	1/16
170	170	85			
340	340	170	85		
680	680	340	170	85	
1360	1360	680	340	170	85
2720	—	1360	680	340	170

Numbers shown represent equivalent full scale frequency

**TABLE II-3: MATRIX OF FREQUENCY VS SCALE FOR SATELLITE TYPE OBJECTS.**

Scale \ Frequency MHz	Full	4/10	1/8
170	170	—	—
425	—	170	—
1360	—	—	170
425	425	—	—
1062.5	—	425	—

Numbers shown represent equivalent full scale frequency

360° about a plane containing the longitudinal axis of the model. Phase data were to be provided only if the ranges were normally equipped to measure phase (see Table II-1). In all cases, measurements were to be made for a single, specified roll angle except that at one installation (RSS) the satellite models were to be measured at three roll angles for one frequency and for HH and VV polarizations. The 1/8 scale satellite type object was to be measured only at GD/FW. Measurements at AL were limited to the 1/8 and 1/16 scale cylinders at 1360 and 2720 MHz. Because of this limitation, the AL facility was not evaluated in the same sense as the other facilities. However, the data obtained there were useful as an additional yardstick for the study.

In order to make a comparative evaluation of the ranges it was planned to have each measure the radar backscatter from a standard electromagnetically simple physical object for which theoretical cross section computations could also be made (a cylinder in several scaled dimensions) and a more complex representative utilitarian target (full-scale satellite and two scaled models). The cylinders were furnished by the Radiation Laboratory. The largest is 32' long and 5' in diameter. The other four cylinders are 1/2, 1/4, 1/8 and 1/16 scale models of the larger cylinder. All satellite models were furnished by the United States Air Force. The full-scale satellite was obtained from Lockheed Missiles and Space Company and the two scaled models were obtained from General Dynamics/Fort Worth. The largest of the satellite models is 32' 6" long and 5' in diameter. The smaller models are 4/10 and 1/8 scale versions of the full scale satellite.

The target dimensions and weights are summarized in Table II-4. The 4/10 scale satellite was probably the least satisfactory with respect to details in structure and craftsmanship. Some of the cross section ranges noted this in their reports. More information on dimensions and tolerances for the cylinders are given in Vol. II-a, and by Hiatt and Smith (1966). Some detailed information is also given there, and in Vol. II-b the discrepancies between the 4/10 scale satellite and the full-scale model are listed.

**TABLE II-4: DESCRIPTION OF THE MODELS USED IN THE MEASUREMENTS.**

Model	Diameter (Inches)	Length (Feet)	Approximate Weight (Pounds)
Cylinder	60.0	32.0	1300
Cylinder	30.0	16.0	250
Cylinder	15.0	8.0	30
Cylinder	7.50	4.0	30
Cylinder	3.75	2.0	25
Full Scale Satellite	59.6 (max.)	32.6	900
4/10 Scale Satellite	24.0 (max.)	13.0	250

We knew before any measurements could be made on the satellite targets that they would have to be modified if we expected to be able to scale the data obtained from one model to another. The engine of the full scale model was somewhat exposed and because the fine engine details were not reproduced in the 4/10 scale model, it seemed best to remove some of the parts of the large model and shield others with conducting flat plates. After making these changes, it was still obvious that the 4/10 scale model was not an exact scale model of the larger satellite. It was our opinion, however, that the differences were not sufficient to warrant the considerable time and effort that would be required to perfect the scale. After consultation with the sponsor, it was agreed that the measurements should proceed without further changes. In the meantime, we arranged to have the five cylinders constructed. Eventually the models were ready for measurement, although not all at the same time, and we began shipping them to the cross section ranges. The radar data obtained from the tests are described, analyzed and compared in Volumes II-a and II-b of this Final Report; a summary of the results from these tests is presented in Chapter III of this volume. The Radiation Laboratory was responsible for monitoring the performance of the ranges but the measurements themselves were made by the operators of the individual ranges.

In addition to comparing the measurements of each object at each range, comparisons were made at the Radiation Laboratory between the measured

data and theoretically computed cross sections for the cylinder models. For this purpose, theoretical calculations based on a physical optics model provided by the Radiation Laboratory and digital computations provided by the Norair Division of Northrop Corporation under its contract with the Air Force Avionics Laboratory (AF33(615)-3166) were used.

## 2.2 Delays and Slippage in Schedules

The logistics involved in assembling the models and routing them from one range to another was far simpler than, say, a military operation, but it is nonetheless instructive to examine our plans as summarized in Fig. 2-2. Each line there represents a particular model or group of models and each box represents the location of a cross section range or the site of model origin. In the early months of the investigation we planned that all the models would converge at the Conductron range and would be measured before the winter of 1965 had set in. As we will see, the three largest cylinders were fabricated by Brooks and Perkins of Detroit, the two smallest in University of Michigan shops and the full scale and 4/10 scale satellites originated at Lockheed Missiles and Space Company (Sunnyvale) and General Dynamics/Fort Worth, respectively.

After measurements at Conductron, the models would be shipped south to Radiation Services, then westward to General Dynamics. The two smallest cylinders would then be shunted north to Wright-Patterson AFB while the remainder of the models would advance to RAT SCAT. In due time, the smaller cylinders would rendezvous with the main convoy of models at RAT SCAT after which the entire phalanx would press on to Micronetics in San Diego. After measurements there, the full scale satellite would embark on its last leg of the journey, heading back to Sunnyvale, while the rest of the models would be destined for RAT SCAT.

It will be quickly apparent to anyone keeping abreast of our progress that our schedule began slipping at the very beginning. Our first task was to solicit official quotations from several local fabricators for construction

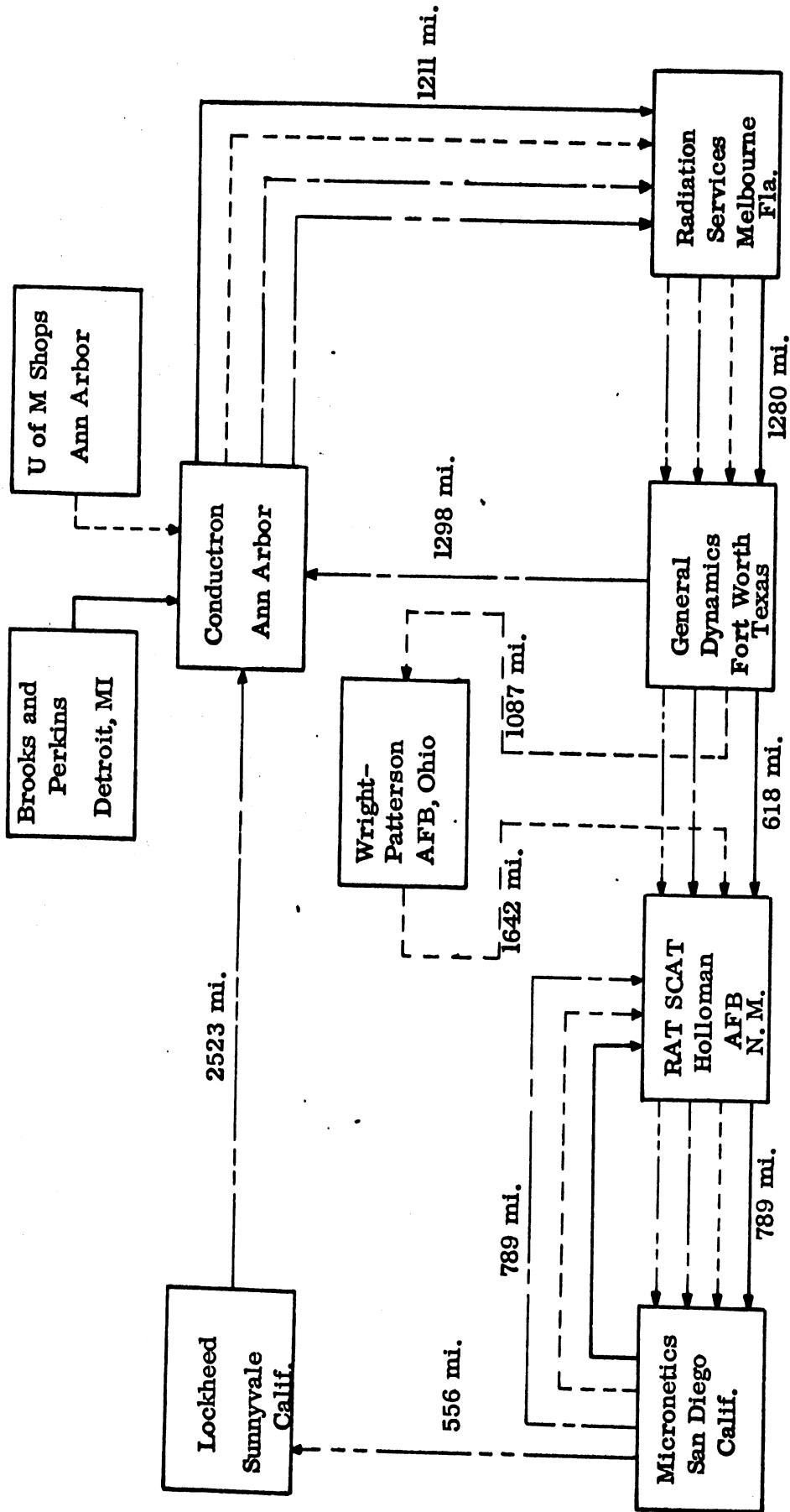


FIG. 2-2: TEST PROGRAM BEGAN WITH ASSEMBLY OF ALL MODELS TO BE MEASURED AT CONDUCTRON RANGE.  
 — 3 Large Cylinders, - - - 2 Small Cylinders, - - - 4/10 Scale Satellite, — Full Scale Satellite.

of the three largest cylinders required for the study. We requested these quotations be submitted to us by 30 July 1965, but none responded within the stated time. From this point on, our story is one of delays — the schedule slippage can be determined from Fig. 2-3 where we present our original plans (from the first Monthly Status Report, 7462-1-L, August 1965) together with the rate at which progress was actually made (shaded portion).

After the official quotations had been received, we felt Brooks and Perkins, Incorporated (B-P) of Detroit Michigan would do the best job of producing the three largest cylinders and an order was placed with them. In September 1965, we learned that B-P had encountered labor troubles and its non-salaried employees had struck the company. In an attempt to meet its obligation, B-P sub-contracted the construction job to National Light Metal and Plastic Tile Company of Caro, Michigan and fully expected the finished products would meet specifications. National Light Metal, however, found it difficult to meet our tolerance requirements and we subsequently relaxed them, but retained realistic specifications. When we inspected the 32' cylinder on 9 February 1966, we saw that it failed to meet even the relaxed specifications. To get the project under way, we accepted the model in spite of its shortcomings, with the proviso that the 16' and 8' models fully meet the specifications. \* Brooks and Perkins announced the completion of these two smaller models on 4 April 1966 and after inspection, they too, were accepted. The model construction phase of the program was thus completed about five months later than originally planned.

We did not anticipate the delay in model procurement, nor perhaps, did B-P. It was primarily due to labor strife and B-P was an innocent victim. We feel, on the other hand, that B-P could have sensed trouble afoot before it actually occurred and could have alerted us that a delay might be imminent.

The late model procurement had a lasting effect on the measurement program. Our plan was to provide Conductron with a complete set of models

---

\* As judged from radar cross section measurements of the 32' cylinder, the decision proved to be a sound one.



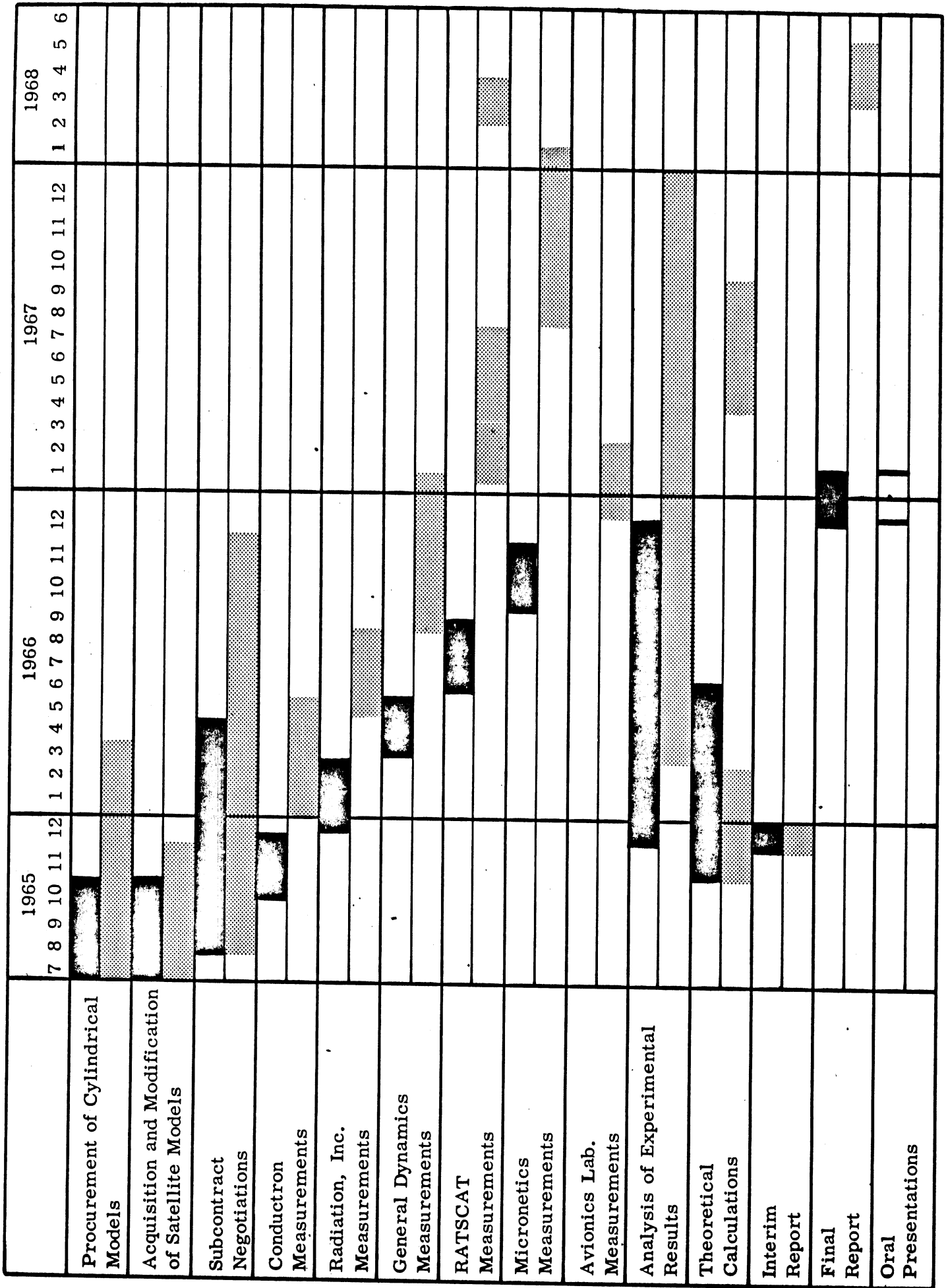


FIG. 2-3: COMPARISON OF PLANNED AND ACTUAL FLOW OF WORK.

before the capricious Michigan winter had set in and thus permit Conductron to finish its measurements well ahead of adverse weather conditions. But, due to lack of models (as well as modifications that had to be made upon the satellite targets), the Conductron work was started early in January 1966, and took place through practically all of that winter and most of the following spring. The measurements were finished on 26 May 1966, more than five months beyond schedule, the precise delay encountered in model procurement .

Radiation Services received the models shortly and discharged its measurement obligation in a scant two or three weeks beyond the estimated time allocated. / We note that it began measurements before Conductron had finished because some models had been shipped onward to expedite the program. Measurements were finished in Florida on 10 August 1966, barely five months beyond schedule, again the amount of model procurement delay. Thus far, our schedule had slipped only by the initial delay and neither Conductron or Radiation Services had contributed to further delays. We note in passing that the price for the data provided by Radiation Services, whether measured in dollars or in range time, was the best that any range provided.

After receiving the models from Radiation Services, General Dynamics of Fort Worth did nothing with them for almost two months. At about this point we began to realize that we had made a mistake in scheduling; it takes a finite amount of time to transport the models between ranges and, moreover, some ranges want to examine the models, decide how to set up the range, and otherwise prepare for actual measurements after accepting the models from the trucker. After GD/FW eventually started work, it finished in less than three months, and thus its actual range time (measurement time) was less than that of any other facility. The delay between receipt of models and commencement of measurements, however, amounted to two months and our scheduling had slipped to about 7 1/2 months by 11 January 1967. During the journey from GD/FT to RAT SCAT in mid January 1967, some of the models were damaged but the people at RAT SCAT were able to make all necessary repairs. In the interim, the two smaller cylinders were shunted

from GD/FW to Wright Field, were measured, and sent on to RAT SCAT by the first of March 1967.

We were unaware at the time, but very serious delays were in store for us after all the models showed up at RSS. Measurements were started there on 17 March 1967, 9 1/2 months beyond schedule, and because RSS declared it must discharge measurements with higher priority than ours, the slippage grew worse. In the summer of 1967, the models were still at RSS; after four months, and in exasperation, we arranged to ship them onward to Micronetics in San Diego, after which they could be returned to RSS for the possible completion of measurements there since this would eventually be their final destination anyway.

Micronetics began measurements early in August 1967, eleven months beyond the target date of our tattered schedule. As at other ranges, the work at MC was delayed by weather, higher priority measurements, and equipment failure. With the exception of one model and one frequency, the tests at MC were completed by 23 January 1968. The data on the 32' cylinder at 170 MHz were not obtained because the Micronetics crew lost the 32' cylinder from atop its column and the model was severely damaged. We will comment on this event later.

All the cylinders except the damaged 32' cylinder were then shipped to RSS to await completion of the test program. The 32' cylinder had already been completely measured there and detaining it for repairs at MC was no problem. In addition to these four cylinders, the 4/10 scale satellite was also shipped to RSS and the large satellite was returned to Lockheed in Sunnyvale, California. Thus, by the first of February 1968, RAT SCAT once again had all the models necessary to complete its test program.

---

The models remained untouched at RSS for a month. The sponsor then decided that the measurement phase of the program should be terminated by mid-March 1968 whether the work was completed or not. Upon being made aware of this decision, RSS rearranged its schedules and completed the measurements within the above time limit.

In summary, the delay in cylinder construction led a parade of subsequent delays, but was unavoidable and unforeseeable ; we ascribe the blame to no one. The delays that we experienced at the radar cross section ranges were due to (in the order of their importance), 1) adverse weather, 2) higher priority work, 3) the tendency of range operators to do very careful, and thus time-consuming work, since the results would be a badge of their competence, 4) finite shipping time between ranges and 5) preliminary range preparation. We were especially disappointed in RAT SCAT's inability to meet schedules but we could do no more than periodically prod them with anxious questions about measurement progress. It should be noted, however, that they were probably forced to pay closer attention to government priority ratings than the other ranges.

### 2.3 A Few Mistakes

We made most of our errors early in the contract and they were largely confined to model handling and transportation. It turned out that the two larger models (32' cylinder and full scale satellite) each occupied more than half a standard trailer and there was not enough room left in either trailer to accommodate the 16' cylinder. Consequently, portions of no fewer than three trailers were required for a complete shipment of the test models and two of them generally had an "exclusive use" rate for freight charges because more than half the trailer was required. The minimum "exclusive use" charge is based on a load of 12,000 or 14,000 pounds (it seems to depend on the particular freight route used) and since our models were much lighter than this, the shipping charges far exceeded our original estimates. Had we been able to fit all the models into a single trailer, the exclusive rate would have reduced our costs by 15 percent, but the final costs turned out to be about double our original estimates. The total weight of the shipment was less than 4000 pounds and the actual per mile costs per cwt listed in Table II-5 are based on this weight.

TABLE II-5: SHIPPING COSTS OF THE MODELS

Shipped From	Distance (Miles)	Cost (Dollars)	Cost/Mile (Dollars)	Cost/Mile/cwt. (Dollars)
Detroit to				
Melbourne to	1211	1244	1.025	.0256
Fort Worth to	1280	1795	1.401	.0350
Holloman AFB to	618	1410	2.280	.0570
San Diego	789	1903	2.380	.0604

A second error was our underestimation of the amount of abuse a shipment receives in the trucking process. On the first major leg of the trip, the loading was supervised by a Radiation Laboratory engineer and the models were received in good condition at Melbourne Florida; only the 4/10 scale satellite was damaged, and it was easily repaired. Between Melbourne and Fort Worth much more model damage was noted. An end plate of the large cylinder had received two or three dozen small pits due to contact with either another object loaded in the same trailer or the walls of the trailer itself; the forward retaining ring of the carriage supporting the full scale satellite had been damaged, and the nose cone of the 4/10 satellite needed repainting. Between Fort Worth and Holloman Air Force Base, the 16' cylinder had received a dent in its flank, the 4/10 scale satellite had been damaged again, and the shipping carriage for the full scale satellite needed repairs for the second time.

The full scale satellite was cradled in a large metal framework equipped with small jack-stands and dolly wheels. This fixture had a pair of heavy rings that encircled the model and clamped it tightly to the framework, and is apparently a universal support for handling the vehicle. It was a difficult piece of cargo to load or unload in trailers and difficult to handle with fork-lift equipment because the support fixture was shorter than the model it supported and was relatively open framework. Although the satellite was shipped in two pieces, with the smaller piece in an open crate, the loading process was often cumbersome.

The 32' cylinder was carried by a relatively weaker structure that did little more than support the model and keep it from rolling about the trailer. The shipping pallet was simply a pair of longitudinal timbers spanned transversely at three points by heavy plywood cradles in which the cylinder rested. The pallet was fitted with four lifting eyes that were apparently seldom used, and the model was strapped down by three belts at the points of support. The 16' cylinder was borne by a similar, but smaller, skid and the 4/10 scale satellite was shipped in a closed crate. The three smaller cylinders shared a foam-padded plywood box not unlike a coffin.

We were not concerned about the relative openness of the shipping skids for the two larger objects (the cylinder and full scale satellite) because both models were much stronger than any container would have been. It appears, however, that we were not careful enough in our efforts to protect the models. The large cylinder was originally covered by a pair of heavy tarpaulins and this should have been adequate but these were apparently not in place between Melbourne and Fort Worth. Even the 4/10 satellite model was damaged and since it was protected by its own crate, we wonder how stout a packing crate must be. It appears that no matter how much attention is given to designing a protective shipping container, models will be damaged unless loading and unloading is supervised, or if adequate loading equipment is not on hand. A simple device would be an unloading dock, or if this is too costly for a cross section range to possess, even a long unloading ramp would suffice. A few dollars worth of block and tackle would be a worthwhile investment. Several of the cross section ranges had, or could have quickly built, lifting equipment to hoist models from the trailers, but the trailers were all covered and the models had to be withdrawn horizontally from the rear.

### III

#### RANGE COMPARISONS

In this chapter we examine the capabilities and performance of the five ranges from several points of view and, based on our findings, we assign ratings as appropriate. Our examination is divided into five areas and the results are contained in five tables. Note that these groupings are not considered to be of equal importance.

#### 3.1 Facilities, Techniques and Procedures

Table III-1 is one list of ratings by which the five cross section ranges may be compared and the reader will note that each basis of comparison is a question. The ratings themselves do not specifically answer the question but are intended only to indicate how well the individual ranges performed in each instance. Twelve points of comparison are listed, but not in any particular order, and the potential range user will have to judge for himself which of the comparisons are important to his own needs. The ratings run from A through E and indicate our assessment as follows:

A = Very good; B = Good; C = Acceptable; D = Barely Acceptable; E = Intolerable

Note that only two entries in Table III-1 have the lowest possible rating of our scale of value. We will now briefly discuss each point of comparison.

##### 3.1.1 Frequency

A University of Michigan engineer measured the seven frequencies which were used at each radar cross section range with a superheterodyne frequency meter. The device uses a zero beat technique in which an unknown signal is compared with a harmonic of a known internally generated signal. Since four of the five ranges used pulsed systems, the measurement was really that of the center frequency of a power spectrum; not all the ranges produced the same pulse shape. Two of the ranges were able to hold frequency within 0.02 percent (RMS over the seven frequencies), two held it under 0.1 percent, and one slightly exceeded the  $\pm 0.1$  percent which was the limit specified in the subcontracts. It appears that frequency errors are the least troublesome aspects of radar cross section measurements. Radiation Services used 2712 MHz in place of

2720 MHz due to its inability to obtain the correct frequency source. This caused no noticeable errors in the data at this frequency for the cylinder models. An error of this size (approximately 0.3 %) in frequency for the satellite targets might have caused some fluctuation in the satellite data due to the location and nature of the scattering centers on these models.

TABLE III-1: COMPARISON OF FACILITIES, TECHNIQUES AND PROCEDURES

<u>Basis of Comparison</u>	<u>CC</u>	<u>RCS</u>	<u>GD/FW</u>	<u>RSS</u>	<u>MC</u>
1 How closely did they hold frequency to specifications?	A	B	A	A	A
2 Were they in the far field?	E	C	B	C	D
3 Did they maintain a good log?	B	B	A	A	C
4 How long did it take to record a pattern of the large model?	C	C	B	B	A
5 How long were the models held at the range?	B	A	D	E	D
6 Did they use good measurement procedures?	B	B	A	B	D
7 How did they handle cross polarized calibration?	B	B	B	B	B
8 Are there handling facilities adequate for large models?	B	C	A	A	A
9 Do they have enough sheltered storage?	B	B	A	A	B
10 Are they confident of their data?	B	B	A	C	C
11 How good was the data format?	C	B	A	A	B
12 How good was the final report?	A	A	B	D*	C
Average	B-	B	B+	B	B-

\* RAT SCAT was originally given a mark of E because its report was not available for evaluation at the end of the contract. The RAT SCAT final report was received on July 8, during the final revision of this volume but this was far too late to be of use in our analysis of the data. We note that the report it finally submitted was good (B) but a grade of D has been assigned because the report was not available for our use.



### 3.1.2 Near Field Effect

We have rated all five ranges on their far field distances, for the largest models only, since this is one of several gauges with which data are judged. For a 32' target at a frequency of 1.36 GHz, the required far field distance ( $2L^2/\lambda$ ) between the target and antennas is about 2840 feet; the actual distances used for this measurement are shown in Table III-2.

TABLE III-2: DISTANCES USED FOR THE LARGEST MODEL WERE ALWAYS LESS THAN  $2L^2/\lambda$ .

Range	R, Distance Used (Feet)	$\frac{R\lambda}{2L^2}$
Conductron Corporation	200	0.07
Radiation Services	1000	0.35
General Dynamics/Ft. W.	1800	0.63
RAT SCAT	1200	0.42
Micronetics	600	0.21

Accepted practice calls for  $R\lambda/2L^2$  to be equal to or greater than unity. Note that Conductron's measurements were performed well in the Fresnel zone and this seems to be characteristic of CW systems due to the relatively low power. (Low power requires that the target be close for sufficient sensitivity in the receiving system.) General Dynamics/Fort Worth used the greatest distance of all ranges, and RAT SCAT used only 50 percent of its range capability; we were not told why RAT SCAT did not use its full 2500' range capacity. Although Micronetics has a 1000' range, it chose to measure the 32' cylinder at 600' and this introduced a serious near field distortion in the broadside return at 1360 MHz.

### 3.1.3 Log

The intent of a log is to provide a history that may be consulted to find the answers to questions that often arise after an experiment has been completed and the apparatus dismantled. It can describe the conditions under which a measurement was made and is thus a simple method of bookkeeping that

will identify raw data. It can also be a repository for other raw data that the observers perhaps would not even consider data. Not all the ranges were diligent in maintaining good logs, but if they had been, we would later be able to find the answers to what appeared at the time to be unimportant questions.

#### Examples

- What percent of range "down time" is due to wind?
- How often do birds destroy patterns by flying through the range gate?
- How many times must the grass be mowed during the summer months?
- How many patterns are destroyed by man-made disturbances such as automobiles, airplanes or Channel 7 ?
- Why are less than maximum range distances used when they cause near field distortions?

The answers to many of these questions can be found in some of the logs, while others will tell only the frequency, polarization, and pattern number.

#### 3.1.4 Measurement Time

Many of the radar cross section ranges involved in this investigation use digital recording equipment which slows down the actual measurement time considerably, but one range, Micronetics, used a magnetic recorder that scarcely affected recording time at all. Since it is possible for signals to drift in both amplitude and phase in the duration of a measurement, the actual measurement time is, admittedly in a small way, a quality factor for data. It might also be a measure of the total time required by a range to complete a measurement program. We note, however, that the range that finished all its measurements in the shortest time required the longest time to record a single pattern.

#### 3.1.5 Total Range Time

By total range time we mean the length of time that a given range consumed between the receiving the first, and shipping the last, model to be measured. Radiation Services scored best on this critical question and RAT SCAT scored poorest of all the ranges.

### 3.1.6 Measurement Procedures

Most of the ranges used the commonly accepted measurement procedures. Model alignment and orientation were carefully checked at all ranges and support columns appropriately guyed at most of them. All ranges made preliminary probes of the structure of the incident field over the volume occupied by the targets, in both horizontal and vertical planes. Some ranges took it upon themselves to measure the effects of target roll, looking for asymmetries in the models that could cause errors. Some ranges were very careful about their model support columns and fashioned elaborate fixtures that supported the smaller models on slender foam fingers, much like a professional waiter carries his tray. Micronetics was surprisingly casual and plopped its models atop a fat column with perfect innocence; the operators of this range later discovered that more care is required than they had first supposed.

### 3.1.7 Calibration Techniques

All the ranges calibrated their co-polarized patterns with spheres and Micronetics supplemented the calibration with disks. (In a co-polarized measurement the polarization of the transmitting and receiving antenna are the same). All the ranges except Conductron pre-calibrated their patterns; this permitted them to label the pattern amplitude grid in convenient scales so that radar cross sections in dB relative to a square meter (dBsm) may be read directly from the patterns without the need for interpolating or counting dB's from a calibration level. While this admittedly makes the patterns easier to read, it also demands very careful observance of gain and attenuator settings and maintenance of a good log. Conductron installs the calibrating device after a measurement and the user of the data must execute mental gymnastics in order to determine the radar cross section in dBsm. The data, however, are more or less raw and are likely to contain fewer human errors than the pre-calibrated data of other ranges.

Calibration of the cross-polarized data varied from range to range. Conductron calibrated against the copolarized return from a sphere. With a

sphere as a target and with the antennas cross-polarized, fine polarization adjustments were made to minimize the return. The level of the cross-polarized return was obtained by referencing it to the copolarized return while maintaining the frequency and power level constant. To verify the fact that the system was properly cross-polarized when this procedure was followed, use was also made of a 45° inclined wire. Radiation Services calibrated a 45° inclined wire against a sphere; GD/FW and RSS used a corner reflector stationed outside the range gate. The cross-polarized return of this secondary standard was calibrated against the copolarized return of a sphere. In addition, GD/FW used a 45° inclined dipole as an alternate standard. Micronetics used a corner reflector as a secondary standard and carefully re-checked the calibration with an inclined wire. General Dynamics occasionally used an "electronic reference" composed of an appropriately attenuated sample of the transmitted signal piped directly to the receiver, but only for the very low frequencies. This reference was calibrated against a sphere.

### 3.1.8 Handling Facilities for Large Targets

RAT SCAT appeared to have more equipment than the other ranges for handling large targets and GD/FW was also well equipped, but with older and less sophisticated gear. Micronetics recently acquired its own crane (Fall, 1967) but Radiation Services had to rent a crane for its large models. Conductron used a large A-frame to hoist and carry large models and, though adequate, was often cumbersome to use.

### 3.1.9 Sheltered Storage

All of the ranges had provisions for sheltered storage of large models, and the ratings we assign are chiefly of degree. Both RAT SCAT and GD/FW had large sheds on wheels that served as shelter as well as model installation and retrieval equipment. The others had sufficient enclosed buildings to accommodate the models, but if several large models must be received at some of the ranges, conditions could become crowded. We should point out that the

climate in San Diego and New Mexico is relatively dry and models will not ordinarily suffer from outdoor exposure. We learned, however, that sudden and severe storms can erupt and pelt the desert with raindrops the size of grapes, and that the blowing alkali can abrade the skins of some targets. At Fort Worth, Melbourne and Ann Arbor, rainfall is more frequent and in these locations shelter is more desirable. All the facilities could adequately house classified models.

#### 3.1.10 Confidence in Data

The General Dynamics/Fort Worth people were probably the most competent and confident of all the range personnel with respect to their techniques and results. The strongest test was that of cross-polarized data collection and GD/FW executed the measurements with aplomb. The Micronetics personnel were wary of even their co-polarized patterns and Conductron and Radiation Services personnel were suspicious only of their cross-polarized data. The RAT SCAT people were noncommittal about their work and they kept their esteem for the patterns more or less to themselves.

#### 3.1.11 Data Format

Radar cross section ranges are virtually at the mercy of the equipment vendors in regard to the form of recorded analog data. All the ranges submitted radar cross section patterns on standard sized charts (~11" x 20" ) and these patterns must be either photographically reduced to manageable size for inclusion in reports, or be submitted in a separate folder of unmanageable size. All the patterns were approximately the same size, but often inter-range comparisons could not be made directly because the patterns were not exactly the same size. Thus, for purposes of inter-range comparison, we had to examine every pattern and read off certain data, such as broadside, end-on, and first sidelobe amplitudes, and the positions of various important nulls of the patterns. The lists of such data then had to be compared against each other for different ranges. The effort required in this comparison led us to conclude that the format in data presentation is a problem area and we will discuss it further in the next chapter. The grades for Item 11 in Table III-1 are based on how easy we found it to read and interpret the data.

### 3.1.12 Final Reports

Each of the ranges submitted a final engineering report at the end of the subcontract period and we have decided to compare them. Both Conductron and Radiation Services included some theoretical discussions, the former to account for near field effects and the latter to present some results for comparison with theory. General Dynamics and Micronetics presented no theoretical discussions, but merely explained and described the experimental results. Conductron failed to discuss cross polarized calibration procedures and Micronetics omitted any mention of its range crew dropping the 32' cylinder. We feel this latter omission to be ill advised since an organization should admit its mistakes. A discussion of the cause of the accident and means for avoiding such accidents in the future would have been in order.

### 3.2 Accuracy of Cylinder VV and HH Data

Without question, data accuracy is an important, probably the most important, criterion to be considered in evaluating range performance. This and the next two sections are devoted to an examination of measurement accuracy. Attention is given first to the data resulting from the co-polarized (VV and HH) measurements on the cylinders.

Cylinder data, in the form of patterns and tabulated results are presented in considerable detail in Volume IIa. The co-polarized data are analyzed and evaluated based on five points of comparison with the results presented in the form of tables and display graphs. Here we summarize the results in Table III-3 with a brief discussion of the points of comparison. (This is a duplicate of Table VI-4 in Volume IIa.) In this table we include entries from Avionics Laboratory (AL), who provided data only for the two and four foot cylinders, the smallest models used in the program.

The constant  $ka$  row in the table results from the comparison of end-on and broadside returns from one cylinder-frequency combination with another cylinder frequency combination having the same  $ka$  value where  $k = 2\pi/\lambda$  and  $a$  is the radius of the cylinder. Where equal  $ka$  values are involved with a

**TABLE III-3: SUMMARY OF RANGE TESTS FOR FIVE POINTS OF EVALUATION. Numbers indicate errors 1 dB or less for the range listed.**

<b>Range Test</b>	<b>CC</b>	<b>RSC</b>	<b>GD</b>	<b>RSS</b>	<b>MC</b>	<b>AL</b>
<b>Constant ka (52 possible)</b>	40	46	43	45	41	4 (of possible 4)
<b>End-on Polarization (18 possible)</b>	17	18	18	16	17	4 (of possible 4)
<b>End-on Theory (36 possible)</b>	17	30	24	27	33	4 (of possible 8)
<b>Broadside Theory (36 possible)</b>	21	30	34	33	15	8 (of possible 8)
<b>Special Low ka Test (74 possible)</b>	36	53	52	46	30	not evaluated
<b>Total Number of Errors (216 possible)</b>	131	177	171	167	136	20 (of possible 24)
<b>Percent</b>	60	82	79	77	63	83
<b>Grade</b>	D	B	C	C	D	B

2 to 1 size difference the cross section of the larger model will be 6 dB higher than that of the smaller model. Out of the eighteen model frequency combinations to be measured (Table II-2) there are thirteen equal ka pairs with a 2 to 1 size ratio. Each of these have two aspects, 0° and 90° and two polarizations to be compared. This provides for a total of 52 points for intra-range comparison for each facility. We show in Table III-3 the number of comparison points that deviate from 6 dB by less than 1 dB. We consider this to be a critical test; the ratings range from 39 to 46, neither poor nor excellent.

The next row, End-on Polarization, summarizes a comparison based on the theory that the HH and VV returns for end-on aspects should be equal. The theory is completely dependable and errors must be charged to calibration errors or other improper range procedures. There is a single comparison for each frequency-range combination making it possible for each range to have eighteen readings with less than 1 dB error. The ratings are good here with four of the major ranges having no more than one error greater than 1 dB. All four of the Avionics Laboratory's values had less than 1 dB error.

The third row, labeled End-on Theory, is based on data presented in Table VI-1 and earlier figures in Volume IIa. The entries in this row are the number of errors under 1 dB between the theory and the measured end-on returns for both polarizations. This is seen to be a more sensitive test than the end-on polarization comparison; note that only one of the major ranges (MC) rates an A grade. More information on the theory and experiment as well as a plot showing the distribution of errors is given in Volume IIa.

In the fourth row (Broadside Theory), we present the results obtained when the measured broadside returns are compared with the theoretical estimates. Since broadside returns depend upon polarization, the errors were determined separately for each polarization based on data presented in Figures 6-2 and 6-3 of Volume IIa. The entries we show in Table III-3 of this report represent the average for the two polarizations. Two of the major



ranges, GD/FW and RSS, as well as AL, rate an A on this test. Two other ranges, CC and MC, do poorly, partly as a result of errors caused by using insufficient range length. This and other sources of error are discussed in Section 6.2 of Volume IIa.

In the fifth row of Table III-3, the results of a special low ka test are presented. Special attention was given to certain measurements involving the ka value of 1.36 where unusually large discrepancies were found in the experimental data. The experimental data along with the theory are contained in Figures 6-7 to 6-10 of Volume IIa and a detailed discussion of the comparison is contained in Section 6-4 of that report. The experimental data are VV and HH measurements of the 16-foot cylinder at 170 MHz and the 4-foot cylinder at 680 MHz. The theory used is obtained from the Norair SDT program. Comparisons are made at 5° intervals from 0° to 90° with certain omissions to avoid extreme nulls in the pattern. The scores given in this test, as shown by the entries in row five range from medium to poor. Possible causes for the unusually poor performance on these tests are discussed in the next chapter of this report as well as in Section 6-4 of Volume IIa.

Some final comments on the comparison of the co-polarized cylinder data are in order. Table III-3 encompasses and summarizes the results from almost all of the analyses performed on these data. The data represent a major part of the results from the entire program and they have proven to be the most satisfactory when used as a basis for comparing range performance. The tests represented by the individual rows show that three of the outdoor ranges rather consistently earned the three highest ratings and this is also shown in the row which indicates the accumulated rating. From this we see that Radiation Services comes out as number one and General Dynamics and RAT SCAT are within five percent of the number one position. These three ranges rank well above Conductron and Micronetics on the basis of these accuracy tests.

### 3.3 The Reliability of Cross Polarized Measurements on Cylinders

With the increasing need for cross polarized RCS data, it is important to consider the ability of the various facilities to make such measurements with the necessary reliability. We are not satisfied with our method of judging ability to perform cross polarized measurements. It is shown in Chapter VII of Volume IIa that there should be no VH or HV return from true cylinder models for the aspects measured. As observed elsewhere in these reports, we now know that other models or other aspects for these models would have provided a much better basis for judgement.

Under the test conditions employed, the recorded VH or HV return should have been random in nature and at a level close to the background return. The actual return was not random; in fact it rather closely resembled the VV or HH return except that its level in dBsm was on the order of 25 to 30 dB lower. We concluded that the return presented was essentially the co-polarized return attenuated by an amount equal to the isolation level between the VV and HH polarizations of the antenna(s) and associated rf components.

Since we could not judge performance on the basis of the form of the patterns we have used the only other available criterion, the amount of isolation between the co-polarized and the cross polarized return. This value was obtained by subtracting the near broadside VH return from the HH return and similarly the HV return from the broadside HH return. This is discussed in further detail in Volume IIa and in Tables VII-3 and VII-4 of that report, where all isolation levels so determined are presented. In Table III-4 we present only the values obtained by averaging the dB values from the above tables. A maximum of 36 VH and HV tests were considered in the isolation evaluations. The RAT SCAT and Radiation Service facilities completed all 36 tests. Table III-6 in a later section, shows the number of measurements made by all ranges.

TABLE III-4: RATING ON CROSS POLARIZED MEASUREMENTS ON CYLINDERS.

Range	Average Isolation Between Co-Polarized and Cross Polarized Broadside Returns	Grade
CC	32.2	C
RSC	30.7	C
GD/FW	27.2	D
RSS	31.5	C
MC	25.7	D

The required isolation needed to perform satisfactory cross polarized measurements is subject to question. It depends of course on the target being measured and the required accuracy. Based on our experience, we feel that a 30 dB isolation level is the minimum acceptable, hence we somewhat arbitrarily equate this to a grade of C and assign other grades accordingly.

Our position on this aspect of the evaluation should be restated. We consider the ability to perform accurate cross polarized measurements very important. The specified cross polarized tests do not provide a good basis for judging the ranges' capabilities to make such measurements. This is discussed further in the cross polarization chapters in Volumes IIa and IIb.

#### 3.4 The Accuracy of the Satellite RCS Data

In earlier chapters we have described the satellite models to be measured in this evaluation and the frequency model combinations involved are shown in Table II-3. Four of the ranges were able to measure the full scale and the 0.4 scale satellite at two frequencies and four polarizations each. GD/FW was asked to make the same measurement and was to measure the 1/8 scale satellite at a third frequency and with four different polarizations. The frequency-model combinations were such that two pairs of equal ka values could be obtained.

A considerable amount of data on the satellite tests is presented in Chapter III of Volume IIb and in Chapter IV of that volume and the data are analyzed and evaluated. For that reason and in order to avoid having any classified information in this report our discussion of the satellite data here will be brief.

In both the constant ka tests and in the inter-range tests, comparisons are based on RCS values at nose-on, broadside and tail-on. Hence, in the constant ka tests for VV and HH polarizations, twelve intra-range comparison points were possible. For perfectly scaled models, an 8 dB difference in RCS values should have been measured. In Volume IIb we present the values obtained and show the distribution of errors, categorized in 2 dB steps. The grade we assigned as a result of our evaluation was based on the number of errors less than 2 dB. We used a more relaxed standard here than for the cylinder data since we are dealing with a target more complex and more difficult to measure. We wanted also to allow for the effect of possible modeling errors in the scaling. The results are given in Table III-5.

TABLE III-5: RATING ON SATELLITE RCS MEASUREMENTS

Range	Co-Polarized Tests		Cross Polarized Tests
	Constant ka	Inter-Range	
CC	D	D	? ?
RSC	C	C	? ?
GD/FW	D	B	? ?
RSS	D	B	? ?
MC	E	C	? ?

In the inter-range tests of the co-polarized measurements, we have available four patterns for each of two polarizations and with three aspect angles being examined we thus have 24 points to be compared with the average value. These data for all five ranges are contained in Tables IV-4 through IV-6 in Volume IIb. From these data we determine the deviations between

the measured and average values and show the distribution of errors arranged in steps of 1.5 dB. The assigned letter grade which appears in the second column in the above table is based on the number of errors less than 1.5 dB. Modeling errors are not a factor in the inter-range tests, thus a more restrictive standard than that used for the constant ka tests is appropriate.

In Volume IIb we present a substantial amount of cross polarized data. The data are analyzed and we use several approaches in an attempt to evaluate the HV and VH data. We finally decided that it is not feasible to rate the cross polarized data due to the small number of samples and the wide divergence that exists in patterns that should be identical. We acknowledge that the lack of agreement may be due in part to modelling inaccuracies, a factor that is particularly difficult to evaluate in cross polarized measurements. Modeling inaccuracies, however, should not effect the inter-range comparisons but here the position and the level of the major lobes showed too little agreement to give any credence to an average value. It is possible that a single pattern in the various comparison tests or even all of the RCS patterns of one range are the correct and accurate patterns but we doubt this very much. We doubt if any of the cross polarized satellite data should have an accuracy rating of better than 3 dB.

### 3.5 Ability to Make Specified Measurements

In this section we note and summarize the ability of the ranges to make the measurements specified in this program. In evaluating a range's performance on the basis of accuracy, we did not, in most cases, include as a factor the inability to perform some of the measurements. At the start of the program, the range operators were advised that they should respond to the request for proposal on an "as is" basis. They were not asked, for example, to add phase measuring equipment to their facilities to accommodate this program. Information on this and other capabilities are, however, needed by the potential user as he attempts to determine the range most suited for his needs. Table III-6 contains a summary of our information on the ability

of the five ranges to perform the measurements which were specified in this program. Much of this information is given elsewhere in this or the companion reports, e.g. Table II-1 of this report. With respect to the co-polarized amplitude measurements, entries there less than 100% in the case of Conductron are due to the lack of acceptable patterns where near field problems were particularly severe. For Micronetics, the same explanation holds, and in addition two measurements were not made as a result of severe damage to the 32 foot cylinder on that range.

TABLE III-6: ABILITY TO MAKE PHASE AND AMPLITUDE MEASUREMENTS SPECIFIED IN TABLES II-2 AND II-3

Range	Amplitude Measurements		Phase Measurements
	Co-Polarized	Cross Polarized	
CC	38/44	20/44	None
RSC	100 %	100 %	None
GD/FW	100 %	40/46	100 %
RSS	100 %	100 %	L Band Only
MC	42/44	40/44	None

Both Conductron and General Dynamics elected to omit some of the cross polarized measurements since the antenna systems were not well suited to provide the needed isolation. For Micronetics, the explanation given for the co-polarized measurements holds here also. As noted here and as was stated at the start of the program, three of the ranges do not make phase measurements and the RAT SCAT range provides phase data only at L Band (1000 to 2000 MHz in this case).

### 3.6 Summary

In this chapter we have compared the performance of the ranges based on information introduced here as well as data presented elsewhere in this report and in Volumes IIa and IIb. Our examination of the capabilities and performance of the ranges has been based on five points of comparison. In

four of these we have made an attempt to assign a letter grade indicating our estimate of the rating of each range. For the fifth area, having to do with the ranges' ability to perform the specified measurements, we provide a summary Table III-6. As indicated earlier, these points of comparison are not of equal importance. In Table III-7, we summarize the results of the range comparison and show the letter grade resulting from the first four ratings. Here we introduce a weighting factor to indicate our estimate of the relative importance of each of the four grades. In assigning the weighting factor, we were influenced also by our ability to judge range performance on the basis of the data available. This accounts to some extent for the smaller factor associated with cross polarized data and the satellite data. Judging from his specific requirements, the potential range user can, of course, substitute his own weighting factor and may thus see a lower rated range as best choice for his work.

**TABLE III-7: RANGE COMPARISON SUMMARY**

Range	Facilities Techniques and Procedures	Accuracy		
		Cylinder Data		Satellite Date
		Co-Polarized	Cross Polarized	
CC	B-	D	C	D
RSC	B	B	C	C
GD/FW	B+	C	D	C
RSS	B	C	C	C
MC	B-	D	D	D
<b>Suggested Weighting Factor</b>	<b>2</b>	<b>4</b>	<b>1</b>	<b>2</b>

## IV

### IDENTIFICATION OF PROBLEM AREAS AND RECOMMENDATIONS FOR IMPROVEMENT

We have had the good fortune of seeing range results coalesce at the Radiation Laboratory preceded by fairly comprehensive reports by Radiation Laboratory engineers who visited the ranges and observed actual measurements. The measurements, and the corroborating trip reports of these engineers, have delineated some distinct problem areas, and in this chapter we summarize our estimation of them and give our suggestions on possible improvements.

First, and foremost, is the problem of the accuracy of the data. Whether it is adequate or deficient depends, of course, upon the data user, but in several instances, it seems deficient. This is particularly true in the case of an object whose return is not easily predictable theoretically. We state that three requirements must be met to minimize measurement errors and much of this chapter is devoted to a discussion of these requirements.

We present additional comments on other problem areas most of which are not closely related to the measurement errors being analyzed here. We discuss cross-polarized measurements, phase measurements, digital recording systems, data display practices, range time estimates and weather problems.

#### 4.1 Measurement Errors

There may be some disagreement on the required degree of accuracy in radar cross section measurements. In considering the present program many users would be satisfied with the accuracy of the data obtained for the cylindrical models if the near field data were excluded. These data, however, may lack the accuracy desired in some applications even when the near field errors are disregarded. The seriousness of the accuracy problem becomes apparent when the satellite data is examined. A sample of this is



given in Fig. 4-1 for one angle of incidence. (The polarization and absolute dBsm scale is omitted for security reasons; see Volume II B for details.) Note that in this sample, the results obtained by different ranges for the same model and frequency differ by as much as 8 dB. Additional errors equal or greater in magnitude are shown in Volume II b. It is difficult to assign grades to the satellite data because no theoretical analysis is available for complex targets like these to substantiate what the cross sections should be.

Based on these results it is obvious that a careful examination of the cause of measurement errors is needed and, along with this, recommendations should be made how they can be minimized.

Three requirements must be met to insure accurate measurements. They are:

- 1) Adequate equipment and facilities.
- 2) The use of proven measurement procedures.
- 3) Careful, experienced and well-motivated operating personnel.

Let us consider these three requirements.

#### 4.1.1 Equipment and Facilities

It is our opinion that the performance of the equipment and facilities used in these tests proves that accurate measurements can be made and show also that no major deficiency exists in the equipment and facilities except for the cases where there is a near field problem. Evidence of this is seen in Fig. 6-3 of Volume II a. Note the results for  $ka = 1.36$  involving model lengths of 16, 8, 4 and 2 feet. Five ranges each contributing four measurements participated in this series of tests. All of these 20 datum points agree within  $\pm 1$  dB of the theory and are consistent among themselves.



4.1.1.1 Near Field Measurements. Since the near field problem is the major source of error associated with equipment and facilities we now consider it in some detail. None of the radar cross section ranges measured the largest cylinder at 1360 MHz at the generally accepted distance of  $2L^2/\lambda$ . We were not told why the required far field criterion was not satisfied, but in some cases it was a problem of receiver sensitivity; in others the fixed pit locations limited the range and in a few cases it appeared to be just a matter of indifference to recommended procedures.

As range is decreased from the standard  $2L^2/\lambda$  the first effect to be noticed is that the nulls begin to fill in, especially the first nulls off broadside. All the nulls of the pattern become shallow, but since pattern levels are low for intermediate aspect angles, the effect is often not noticeable. As range is decreased further, the sharp broadside lobe becomes wider and eventually splits into two or more perturbations superimposed over a broad variation of the pattern. The magnitude of the return decreases at the same time. By this time, the first and second, and possibly third, nulls off broadside have completely disappeared and even the returns at intermediate aspects are affected in some measure. Finally, if the range is decreased enough, the broadside echo drops below that of end-on for the cylinder patterns.

Near field measurements are more often encountered at CW radar cross section ranges than at pulsed ranges. This is due in part to the relatively low power levels that are available in CW sources. Even if the higher power were available, the poor isolation between transmitted and received signals could be a problem. Good isolation is possible in a pulsed system because there is no transmission during reception but CW systems depend on cancellation schemes to achieve isolation and these are highly dependent on frequency stability. Pulsed systems have another major advantage, when long ranges are involved, in their ability to gate out all unwanted foreground and background reflections except those near the target. For these reasons pulsed systems are much better than CW for making cross section measurements of large targets. This fact was pointed out in the first comprehensive study made of cross section measurement techniques (Fails and Fubini, 1949).

In discussing the limitations of CW ranges for measuring large targets at higher frequencies, one should note that the CW system has advantages in other situations. Many present day targets are small and have extremely low radar cross sections. For sensitivity reasons it is important to work at the minimum range consistent with far field requirements. Ranges as short as 10 to 20 feet may be suitable and these are easily achievable for CW systems. The minimum range for pulsed systems is limited by the receiver recovery time and in most cases it is well in excess of the above figures. As noted above, with a pulsed system it is possible to gate out unwanted reflections except those near the target. In a CW system when working at close ranges, reflections from the pedestal and those near the target will tend to be of most concern. An inherent characteristic of the CW system is its ability to cancel out such reflections. A phase coherent pulsed system is also able to cancel out these reflections but only a few such systems exist.

One recommended cure for the near field problem is quite straightforward: namely, design the equipment and range so that the target can always be in the far field. There is no simple rule that relates range length deficiencies to cross section error since this is a function of the target. The  $2L^2/\lambda$  distance is adequate or more than adequate in most cases. For a complete discussion of this question see, for example, Kouyoumjian and Peters (1965).

Another recommendation should be considered since, even though the above solution is straightforward, it is not always practical to operate at  $2L^2/\lambda$ . It is easy to see that the  $2L^2/\lambda$  rapidly becomes inconveniently large ( $\sim 38$  miles) when the cross section of a 100' airplane at X-band ( $\lambda = 0.1\text{ft}$ ) is needed. A range of almost 4 miles is needed even if a 1/10 scale model and a  $\lambda$  of 3 mm is used. To help find a solution to

this problem, an intensive study should be made to find an accurate method of transforming near field measurements to far field results. Some work has been done on this problem, (see, for example, Kay (1954) and Crispin and Siegel (1968)).

To summarize with respect to the first requirement, we believe it has been adequately demonstrated that the equipment and facility are sufficient to insure satisfactory accuracy if proper procedures are followed. Further comments will be made on the equipment in a later section but the points to be discussed are not closely related to measurement errors.

#### 4.1.2 Measurement Procedures

Any outline of procedures is subject to modification to better fit the characteristics of a particular range or measurement problem. Admitting this limitation, it is believed that the following outline will help reduce measurement errors.

4.1.2.1 The Transmitter. Whether CW or pulsed, the transmitted signal should be stable in amplitude and free from signals of spurious frequencies. The source must be stable in frequency and this requirement is particularly important for the CW system since to a large extent it determines the degree and the duration of the balance or isolation in the system. The required isolation is a function of the target cross section and range and typical numbers range from 90 to 115 dB; a frequency stability of one part in  $10^7$  or better is needed.

Sources with even higher frequency stability are needed in pulsed systems employing phase coherence. Phase coherence has been incorporated into pulsed systems (e.g. GD/FW and part of the RAT SCAT system) for the measurement of phase and to help cancel unwanted reflections emanating from within the range gate.

Use should be made of an oscilloscope or spectrum analyzer to be sure that the transmitted spectrum is up to specifications. This, together with a check of the frequency and amplitude stability and the absolute level of the transmitted power will in general be sufficient to insure the satisfactory performance of the transmitter. The frequency and power stability should be monitored prior to the beginning of a series of runs for a time period equal to twice that of a normal run. A good check is to retrace the second pattern over the first. If there is a close overlay, one thus obtains a check of the stability of the entire system. In recording any  $360^\circ$  pattern, the operator has an opportunity to check stability by noting whether or not the starting and stopping point (e.g.  $\pm 180^\circ$ ) coincide to within  $1/4$  dB or so. If not the pattern should not be accepted. It is a useful practice to have the scope or spectrum analyzer and a frequency meter or counter available to continuously monitor the power level, the signal spectrum and the frequency of a sample of the transmitted power.

Except for isolated instances where components failed, the transmitters caused little trouble in this series of measurements; the transmitters are not a likely source of significant measurement errors.

4.1.2.2 Receiving and Analog Recording System. The receiver must have the required sensitivity, stability and linearity. The receivers and recorders used on present day ranges are commonly comprised of a super-heterodyne receiver and a Scientific Atlanta rectangular recorder such as their model 1520. For the receiver itself, use is made of custom-made equipment or one of the Scientific Atlanta series 1600 receivers or modifications thereof. These receivers have a sensitivity ranging from -95 to -110 dBsm for the frequency range involved in these tests and this is comparable to the sensitivity of the receivers specially designed for the pulsed transmitters. The receiver-recorder systems have a dynamic range usually selectable at 40, 50 or 60 dB and they are rated to be linear in dB to  $\pm 1/4$  dB.

The following checks should be made at the start of each series of runs or when poor performance occurs.

- a) Check the stability of the receiver -- this will ordinarily be done along with the stability check of the transmitter unless separate checks are found necessary.
- b) Determine the sensitivity; a value below the rated level is an indication of a malfunction in the system.
- c) Check the response of the recorder servoloops that operate the pen and the chart azimuth motion. Amplitude errors are caused both by a sluggish as well as by a too tight control.
- d) Check the linearity of the receiver-recorder combination. This can be done with a signal generator or by the use of a precision rf attenuator when receiving a signal from a large cross section target. It is reasonable to demand linearity good to within  $\pm 1/4$  dB over the dynamic range being used. If there is a problem, separate checks of the receiver and recorder should be made.
- e) To the extent possible, check to see that the digital system is operating satisfactorily. This will be discussed further in a later section.
- f) For those ranges where phase is measured, the associated receiving and recording system should be checked for linearity. Use may be made of a calibrated phase shifter. For a more complete check, the phase of a rotating off-center sphere may be recorded and checked against theory.
- g) The synchronization between turntable position and recorded azimuth angle should be within  $\pm 0.10^{\circ}$ ; an occasional check should be made.

With a reasonable amount of care and attention, the receiver-recorder system should not be a source of error. We have seen no indication that it was a source of error in this series of measurements.

4.1.2.3 Turntable and Model Support. The turntable should be capable of supporting the weight and lateral stress imposed by the target and supporting structure with azimuth and elevation deflections no greater than  $\pm 0.1^\circ$  whether at rest or while rotating. In order to provide for guys when needed, the diameter of the rotating table should be an appreciable fraction of the target length. Along with the requirement for size and rigidity, there is a need for minimum RCS. This is accomplished by the use of an absorber covered turntable level with or below the surface of the ground. Even so, it is frequently necessary to cover exposed parts with radar absorbing material (RAM). This will be mentioned again as we discuss background. It is fortunate that with the typical ground plane system the turntable is not illuminated as strongly as the target. The axis of rotation of the turntable must be adjustable. In general, it must be tilted toward the antenna so that it will be perpendicular to the effective center of radiation.

When the target and frequency are known, the range distance,  $R$ , is selected according to the far field requirement and the proposed target height,  $h_t$ , is selected according to the equation

$$h_t = \frac{R\lambda}{4h_a}$$

where  $h_a$  is the antenna height,  $\lambda$  is the wavelength and the geometry is shown in Fig. 2-1. The quantity,  $h_t$ , is subject to further considerations depending upon the field probe to be described in the next section. Assuming the correct  $h_t$  is known, the model support must be chosen so that it is sturdy enough to provide secure support for the model but small enough and so shaped that its RCS will be 30 dB (hopefully) below the significant cross section values to be measured. Supports are generally made of styrofoam or Pelasan but in some cases where  $h_t$  and  $\lambda$  are large, fiberglass tubes are used.



It is desired also that the area of contact between the target and pedestal be a minimum to avoid undesired coupling. This can be accomplished by tapering the column to a smaller diameter at the top or by the use of "fingers" which make contact with the target. By coupling we refer to the interaction between the target and the support. It has been shown that the RCS of a long target can be significantly effected when there is opportunity for a strong surface wave to be propagated in the foam structure adjacent to the model (Senior and Knott, 1964). Ordinarily the supports are symmetrical about the axis of rotation but where low cross section shapes are being measured and where it is more important to have an accurate reading on the low part of the RCS pattern (e.g. the nose region of a re-entry vehicle) asymmetrical supports are used. This may be accomplished by tilting the column or by shaping its cross section to provide a lower than average return in the low RCS part of the pattern to be measured.

The final selection of the support is dependent on its performance when the background checks are made.

Based on the generally satisfactory background levels that were measured with the supports in position we conclude that the supports did not significantly contribute to measurement errors. The background measurements would not include possible coupling effects. With a large RCS target and relatively small support columns we believe this would also be insignificant.

4.1.2.4 Field Probe. The field probe is one of the most important checks associated with RCS measurements. RCS measurements are based on the assumption that the model is illuminated by a plane wave. Since this occurs only in free space and at infinity we must settle for an approximate plane wave condition. At a distance of  $2L^2/\lambda$ , the approximation is considered to be sufficiently good barring perturbations due to the intervening ground or other scatterers. Since the effect of the ground and other scatterers can not always be accurately predicted they must be measured. Experience has shown that for the ground plane geometry it is generally possible to

predict the azimuth field with some accuracy but the ground constants and their effect are not sufficiently well known to allow a reliable prediction of the elevation pattern except for its general shape.

Once the tentative target height is selected, the antenna(s) whose height has already been selected, is adjusted in azimuth and elevation for maximum signal at the point to be occupied by the center of the target. The field strength is then measured on a vertical line through the target center. If the target center does not coincide with the peak illumination, the support column height is changed or the antenna is adjusted and the vertical field is again probed. When the height is finally selected, a more thorough field mapping is needed to be sure that the field is uniform over the volume to be occupied by the model. This is accomplished by moving a small antenna vertically at selected (10 or so) stations along the horizontal axis of the model. This is the line that would coincide with the axis of the model if it were on the support with its horizontal axis in the broadside position. The horn is ordinarily moved by a pulley arrangement in a framework provided for this purpose and the signal received is recorded by hand or plotted automatically. In place of the receiving antenna probe, some ranges use a sphere and the two way signal strength is measured. Some ranges are accustomed to probing the horizontal field by rotating a sphere on the turntable at the proper height with the sphere several feet off center. This is adequate only if it covered the entire field of interest. Since the reflection coefficient of the ground varies with polarization it is important to probe the field with both vertical and horizontal polarization. The uniformity of the far field power level is advertised by some ranges to be

+ 0.5 dB. over the volume to be occupied by the model. With this degree of uniformity it is not likely that errors in RCS measurements of the model would exceed 1.0 dB. The error could be zero if the average illumination level over the illuminated portion of the model for all aspects was zero dB and if the calibration sphere had an average illumination of the same value. It should be noted, however, that field probes showed variations up to 1 dB for one range and up to 2 dB for another. Moreover in most cases the field was not probed as a function of range from the point occupied by the center of the model. The importance of this had not occurred to us until recently. Assume the 32 foot cylinder is being viewed end-on. It appears that we have no information on the average illumination over the 5 foot diameter circle occupied by the end of the cylinder and this illumination determines almost completely the end-on RCS. This cross section is calibrated against a sphere which would be located 16 feet down range from the end of the cylinder viewed end-on.

Traditionally we have not been much concerned about this; in a "free space" range the relative power (round trip) is proportional to  $1/R^4$  and when R is very large compared to the model length this factor is insignificant. It is not completely insignificant for a 32 foot model at a 200 ft range as was used by Conductron. The  $1/R^4$  effect over half the model length amounts to about 1.4 dB. We are more concerned, however, about the behavior of the field in the range direction where the ground plane geometry is involved. It is easy to suspect that the field variations at the position occupied by the cylinder end might be as large or perhaps much larger than those found elsewhere. End-on illumination is not likely to average out to equal the illumination on the calibration sphere partly because of the  $1/R^4$  effect.

We think this may account for the fact that there are greater discrepancies in end-on values than in the broadside values. We note also that Micronetics, which has the nearest approximation to a free space range, had the best results for their end-on values. From Table VI-1 of Volume IIa it is seen that 92 percent of their end-on returns were within 1 dB of theory. The corresponding average for the other 4 ranges is 68 percent. Conductron whose end-on illumination may have suffered both due to the ground plane geometry and the  $1/R^4$  effect had only 47 percent of its values within 1 dB of the theoretical prediction.

In summary, we recommend that the usual procedures for probing the field be carefully followed. It should include vertical and horizontal coverage for all polarizations to be involved and it should cover the volume to be occupied by the model -- not only for the broadside but also for the end-on position. A field uniform to within  $\pm 0.5$  dB is a desired objective but for large targets this may not be achievable. It is important that significant deviations in excess of  $1/2$  dB be noted in the pattern log, especially if an area large enough to illuminate an important scattering center is involved.

4.1.2.5 Background Evaluation. After the field probing is complete, with the selected model in place and the transmitter, receiver and recording systems properly operating, the turntable should be rotated to determine the contribution due to the background. For this test the CW system will be tuned to minimize the background contributions. In the pulsed system, all reflections outside the range gate will be largely excluded. The background return will be plotted on the recorder and calibrated in terms of dBsm. The acceptable background level is dependent on the accuracy required. It introduces errors by adding in or out of phase with the desired signal. The upper and lower limits of the error are plotted in several references, see for example Fig. 3 of Blacksmith et al (1965). A background of -20 dB may

cause errors of about  $\pm 0.9$  dB while the maximum error for a -30 dB background is less than 1/2 dB. If the background is not sufficiently low a search should be made to determine the cause. Any extraneous scatterers should be removed. For a CW system this includes any scatterers illuminated by the antenna; for a pulsed system scatterers in the range gate should be removed or covered with RAM. If this does not reduce the background sufficiently, the target support might be temporarily removed, if this is feasible. This move will indicate whether or not the support column is satisfactory. For low cross section measurements, the return from a styrofoam column can be considerably decreased for a spot frequency by adjusting, or tuning its diameter (Senior et al, 1964). If further adjustments are needed, a careful examination of the turntable is in order. Additional RAM or improved RAM should be added to cover exposed areas. If a RAM covered barrier is being used, a minor adjustment in its position may be needed.

Once the background is properly cleaned up, further changes should not be necessary until a frequency change or some change in the physical set up is made, but background checks should be made several times each day. For a CW system, checks are made after each pattern.

In the present series of measurements, the background was not high enough to cause errors of more than 1/2 dB in the broadside and end-on returns. This is based on a background -25 dB below the end-on return. More typical values are -35 dB. One exception to this should be noted. At GD/FW, the interference due to an outside electronic source was particularly troublesome at 170 MHz. It was erratic in time and amplitude but was frequently high enough to add spikes to the patterns submitted. A number of reruns were made in hopes of obtaining a clean pattern. This interference was troublesome but easily recognizable; it did not add to the tabulated measurement errors.

At this point it is important to note another possible source of error. It is related to background but would not be measured in the background tests just described. We refer to secondary reflections which strike nearby scatterers before or after being reflected by the target. If scattered towards the receiving antenna, these will cause errors in measured RCS values. Rays being scattered as intended by the "mid-area" in the ground plane geometry are, of course, not to be considered here.

Scatterers most likely to cause trouble might be the edges of the turntable pit or nearby rough areas on the ground. These will be more strongly illuminated where frequencies and targets combine to form low  $ka$  or  $kl$  conditions thus resulting in wide beam scattering from the target. In the present series this might be expected to cause more trouble when the 16 foot cylinder is measured at 170 MHz and perhaps with the 8 foot and 4 foot models at 340 and 680 MHz since for these cases  $ka$  is small and the antenna beamwidth tends to broaden. It is not feasible to predict the effect of this secondary scattering and since it will not be detected in the standard background checks, another test is needed. A rotating off-center sphere will give some clue to the presence of secondary reflections but this will not be quantitative since the sphere scattering pattern will differ from that of the model. The nose rock test commonly used in anechoic room RCS measurements and used by Conductron on its outdoor range would indicate more specifically whether or not secondary reflections were effecting the RCS of the model being measured. This consists of moving the target toward or away from the antenna with the target on the support and rotated to the aspect of interest. A movement of a wavelength or so is needed to allow for the in-phase and out-of-phase addition of the contribution of the unwanted scatterer. Zero change in the RCS value shows that there is no problem. An alternate method is to run the pattern at ranges  $R$ ,  $R + \lambda/4$  and  $R + \lambda/2$ . If secondary reflections are indicated they should

be eliminated or their presence and the extent of their contribution should be noted. Changes which may remove secondary reflections include small change of height, variations and the adjustment or addition of RAM and (of course) the removal of any suspect scatterers.

Judging from the data it is not possible to prove or disprove that RCS errors were caused by secondary reflections. Since the measurement errors are more pronounced for low  $ka$  and low frequency tests there is good reason to suspect that secondary reflections were a contributor. Our only data which includes results at range  $R$  and  $R + \lambda/4$  is from Conductron for the 2 foot cylinder at 2720 MHz for VV and HH. See Fig. 4-2 for the VV patterns. The differences in RCS for the two ranges are less than 0.2 dB for broadside and end-on values. The variation amounts to 1 dB in the first end-on side lobe for VV. In this test  $ka = 2.72$ , so we are not dealing with our smallest  $ka$  value; this and the high frequency would lead us to expect only minor errors from secondary reflections. It indicates, we think, the likelihood of more pronounced effects under less favorable conditions suggested above.

For those ranges that can not move their turn table in range, an alternative is to move the model longitudinally on its support. This can give the desired  $R + \lambda/4$  change for near nose-on and tail-on aspects but it will have little effect on the broadside aspects. It will, however, help also to indicate the presence or absence of coupling with the support which we mentioned in 4.1.2.3.

4.1.2.6. Calibration Procedures. The commonly accepted method of determining the absolute level of a scattering pattern is to compare its return with that of a standard scatterer. The preferred standard scatterer is the precision sphere since it presents no orientation problems and its RCS has been accurately calculated. In most ranges where pulsed systems are used the calibration is accomplished before the pattern is run. A

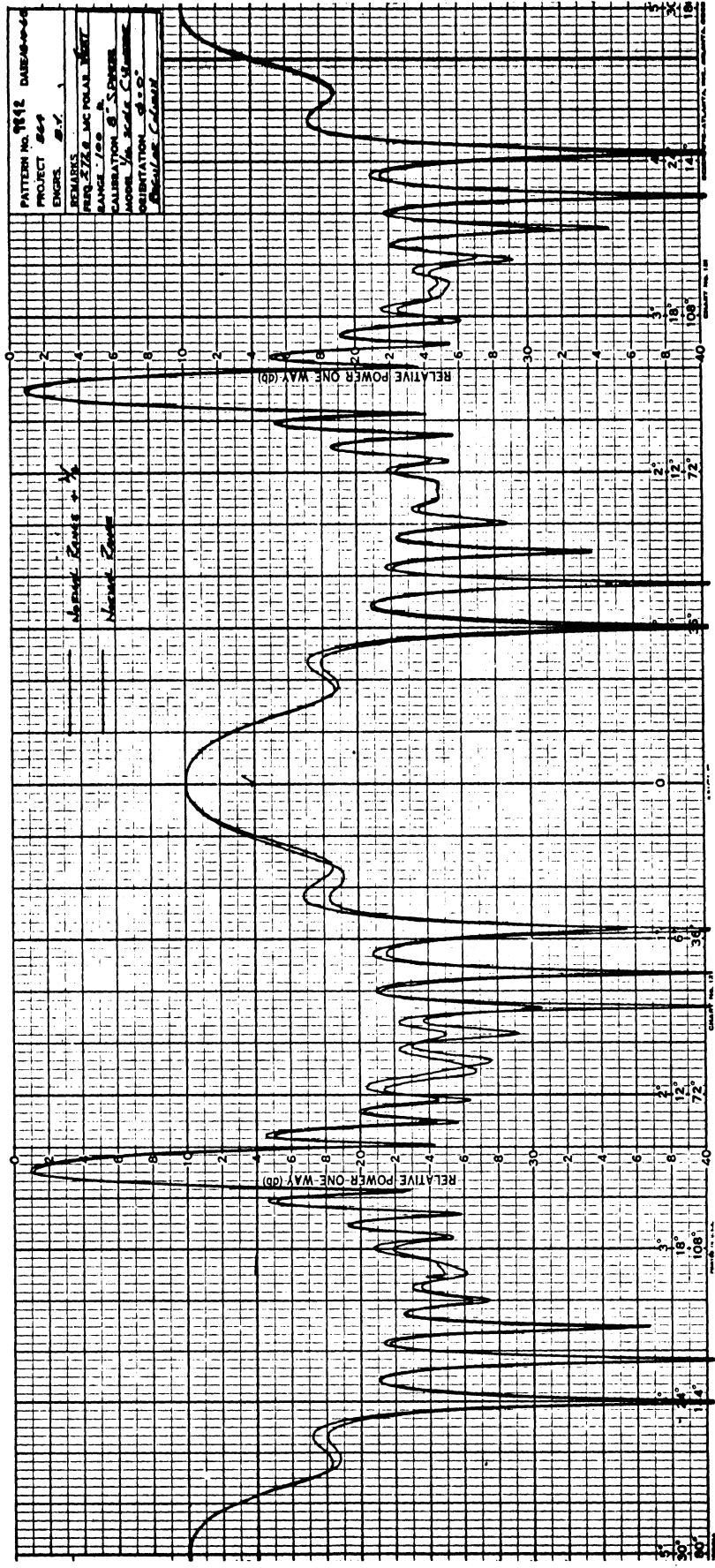


FIG. 4-2: RCS PATTERN FOR TWO FOOT CYLINDER, 2720 MHZ, VV POLARIZATION, FROM CONDUCTRON CORPORATION RANGE. Shows effect of secondary reflections.



suitable sphere, preferably one with an RCS within 10 dB or so of the target's average cross section is placed on the support column and the receiver gain is usually adjusted so that 0 or some multiple of 10 dBsm coincides with a 10 dB line on the pattern paper. At the start of a series of runs, it is advisable to use two or three standard spheres selected so that their returns are well distributed in the dB range of the pattern to be recorded. This not only provides a second check on the linearity of the system but it also checks range performance for different scattering patterns. On CW ranges the procedure is essentially the same except that the calibration is more commonly done after the pattern is run.

Some pulse ranges, use a secondary or transfer standard located outside the range gate that contains the target. By calibrating the transfer standard in dBsm, the system can be checked before and after each pattern simply by moving the range gate. A recheck should be made with the sphere after several hours or several patterns. If the sphere and secondary standard do not recheck, the patterns taken since the previous sphere calibrations should be invalidated.

Cross polarized patterns must be calibrated by other means since a sphere theoretically has no cross polarized return. This will be discussed in more detail in Section 4.2.1; briefly however, the cross polarized pattern may be calibrated against the co-polarized (HH or VV) return of a sphere or against the return of a  $45^{\circ}$  inclined wire. For a  $45^{\circ}$  inclined wire the return for VV, HH, HV and VH are equal.

If 1 dB accuracy is required, we believe a more elaborate type of standard is needed in many cases. As has been stated above, the measurement errors on the satellite models were large, much higher than for the cylinders. We have concluded that most range operators will stay with a model until they measure an accurate scattering pattern providing they have reliable information on the true pattern. The accurate pattern is obtained

by removing effects about the range or the equipment that contribute to error until the desired accuracy is obtained. This is not possible when working with a satellite or similar complex model since its scattering characteristics can not be predicted accurately. Even if all the above guide lines are carefully followed, one would have no way of knowing that his results were correct. To help improve this situation it is proposed that a series of standard scatterers be developed that tend to approximate typical targets being measured. Closed circular cylinders would be appropriate for satellite models for example. Two should be used, so chosen that they would bracket the target return with an upper and lower bound.

The procedure might be as follows: Carefully perform all of the range checks then measure the pattern of one of the cylinders whose end-on and broadside values are known. If the test cylinder doesn't perform according to theoretical predictions, start over again and repeat until a good pattern is obtained from the first cylinder. As a further check on the facility and procedures, measure the second cylinder. If this does not check according to theoretical predictions find the reason and repeat until the correct patterns can be obtained from the two cylinders one after the other.

The complex (satellite) model should now be measured using all the care exercised on the cylinders. Additional patterns should be taken until it is demonstrated that a satisfactory repeat pattern can be taken after the model has been removed and replaced on the support column. If this proves to be difficult due to sensitivity to frequency, roll or pitch alignment, a study should be made to determine the degree of sensitivity to these factors. Proper control of the factors causing the sensitivity should then make it possible to produce the desired repeat pattern. Following this, one of the two standard cylinders should be run again. With this procedure one should be able to state that the satellite pattern was as nearly correct as the final repeat pattern on the cylinder. If the cylinder pattern did not repeat sufficiently well, all or part of the process should be repeated until a satisfactory check pattern is obtained.

It is obvious that this procedure will be time consuming and costly but it should produce patterns of unknown scatterers to which a reliable confidence rating can be assigned. It is recognized that the intended use of scattering data does not, in many cases, require the accuracy that would result from this costly procedure. Based on a "cost effectiveness" philosophy the user of the scattering data must decide how many dollars he is able to spend to achieve a given degree of accuracy.

4.1.2.7 Preliminary Analysis of Data. Before they are released, all data should be reviewed by a qualified analyst experienced in RCS analysis and familiar with experimental procedures as well. The average range operator can be expected to determine if a pattern is acceptable from the standpoint of background noise, pattern symmetry, apparent calibration accuracy and repeatability, but in many cases he will not be able to make a very accurate prediction of the expected scattering pattern. We believe that the cylinder data obtained in this program benefited from this type of preliminary analysis and such an analysis should probably be done by a man who, to some extent, acts as an inspector. He should be a little apart from the operating crew and willing to take a purely objective point of view in deciding if data is acceptable.

#### 4.1.3 The Range Crew

We stated earlier that to insure accurate RCS measurements, the requirements included adequate equipment and facilities, proven measurement procedures and a careful, experienced, well-motivated range crew. We feel that this third requirement is an important as the other two but once this is recognized and acknowledged, little more needs to be said. Some range operators say that there is still some "black magic" in the art of producing good patterns. This may be true to some extent - an operator will learn the fine points about the equipment and procedures only by experience with the system.

The need for careful and dedicated workers is obvious. We believe that they require a good understanding of the users' requirements, and where feasible, a knowledge of the ultimate use of the data. This may help to solve another problem; too often a user will ask for measurements or accuracy that he doesn't need. A detailed discussion between a technical man representing the user and the range operator and the analyst will help to eliminate confusion and delineate the more important aspects of the requirements. Such procedures will help to maintain the needed motivation of the range operators.

#### 4.2 Other Problem Areas

In this section we review other problems which became apparent during the program. Some deserve early attention, some are in the nuisance category and some, such as the weather problem, we can't do much about.

##### 4.2.1 Cross Polarized Measurements.

Some of the ranges were well prepared for cross polarized measurements while others had to do some homework. It can be shown that the cross polarized return from a perfectly conducting right circular cylinder is zero if measured in a principal plane, but none of the data produced by the ranges approached this. One can argue that the support column, ground reflections, and imperfect models have some depolarizing effect and hence contribute to a cross polarized return, but we feel it is the impurity of the illuminating wave that causes most of the trouble. We are told by antenna experts that even good pyramidal horns emit a cross polarized component that is down only 30 dB or so from the dominant polarization. Even if a perfect feed (ellipticity of zero) horn is used with a parabolic dish, the reflecting surface, as well as the feed support struts, will cause some depolarization. It is not surprising, then, that most of the cross polarized patterns are near facsimiles of HH or VV patterns, or possibly combinations of both. The cross polarized data are analyzed in Volume II-a and we concluded there that the purity, or ellipticity of the transmitted wave, was no better than 20 to 30 dB for most radar cross section ranges.

A study should be made to determine how much isolation is needed between the direct and cross polarized radiation to obtain satisfactory results for most practical cases. For cylinders and principal plane patterns, 30 dB is not enough to produce the expected random pattern. It might, however, be enough for targets having a large amount of cross polarized return. The fact that General Dynamics/Fort Worth have been able to use its cross-polarized data and scattering matrix techniques to calculate scattering data for new polarizations (later verified experimentally) is evidence that their cross polarized data is accurate enough.

Once we learn the amount of needed isolation, the factors contributing to the inferior isolation should be determined and appropriate remedies could then be made. One possible remedy would be to add polarization gratings to the antenna aperture to screen out the unwanted polarization. When the antenna problem is solved, attention should then be given to the range. It is quite likely that the ground plane range and possibly the pedestal add considerably to the cross polarized return. Perhaps the following test has been made, but if not, it would be informative to do the following. With a good linearly polarized pick up antenna in free space and in the far field, measure the polarization ellipticity from the transmitting antenna. Then make the same measurement with the pick up antenna at the target location on the ground plane range. If the results differ, a study should be made to eliminate this effect of the ground plane if possible.

#### 4.2.2 Phase Measurements

Up to now, little has been said about phase measurements. As was stated in the original University of Michigan proposal, we planned to make little or no use of the phase data in our evaluation of the ranges. As a matter of fact, we have made no use of the phase data. This is partly because only two ranges were able to provide phase data and then for only part of the frequencies. / It is difficult or impossible to make good use of phase data unless it is properly calibrated against a reference point that can be identified. From what we have been able to determine and from informal conversations with General

Dynamics/Fort Worth personnel, the phase data they provided were not adequately calibrated. RAT SCAT submitted phase data for the 32' and 16' cylinder at 1360 MHz only.

Despite this we consider it very important that the major ranges have the ability to provide phase data over a wide frequency range. The need for phase data is well known. The primary requirement for phase data is in the measurement of the scattering matrix. Scattering matrix data have been obtained on a point-by-point basis for several years but only recently have we begun to realize some of its potential as the measurement equipment becomes more fully automatic. The most important use for scattering matrix data is in the identification of radar targets. Considerable efforts are being made to solve the inverse scattering problem and part of this effort is concerned with scattering matrix measurements. Scattering matrix data can also be used to calculate cross section data when information for many polarizations is required.

Phase data are also of use in the vector subtraction method that has been used to cancel out target support contributions. Another potential use for phase data may be in the solution of the far-field requirement problem. Phase data provide an additional parameter which may prove important in the derivation of far field measurements when only near field data is available.

#### 4.2.3 Digital Recording Systems

Three kinds of digital recording systems were used at the various ranges to provide stored digital data for use in data analysis or for reproducing the analog patterns. Three ranges used punched paper tape, one used punched cards, and one used magnetic tape (see Table II-1). The punched cards were the slowest (since a pattern can be run no faster than the data can be punched on the cards) and they occasionally contained punching errors that had to be manually corrected later. The cards can be processed by computer directly. Punched paper tape was not much faster than the cards, but suffered serious problems due to

frequent breaking. The paper tape often broke during recording as well as during the later read-out of the stored information. Magnetic tape was the fastest since the rate of information storage is very high, and patterns could be obtained rapidly as the range crews felt was physically safe for the targets installed on the pedestal. In earlier installations, paper tape systems may well have been the best means of obtaining digital data but with the proven superiority of magnetic tape a change to it is in order. In addition, the Air Force should determine the preferred data format and advise all ranges accordingly.

Another problem with digital data became obvious during the program. There are few opportunities for the range operator to adequately check the performance of the digital equipment. From time to time his data may be checked out by others at the computing center but this will generally occur too late for the range operator to correct any errors that may exist. Equipment should be readily available at the range to allow frequent checks of the accuracy and adequacy of the digital data. The analog output of the D to A converter should be on a scale identical to that of the original analog pattern to allow for quick checks by the use of overlays.

#### 4.2.4 Data Display.

Data users can be classified into two groups: those who roll up their sleeves and work with cross section patterns, reading off amplitudes to the nearest tenth of a decibel and positions to the nearest 1/2 degree; and those who make only a cursory inspection of a pattern, noticing amplitudes to the decibel or two and positions within five degrees. Data users of the first kind are particularly keen on detail and would prefer to use original patterns to work with while those of the second kind look for gross effects and leave the details to users of the first kind. There are many more of the latter than the former.

A typical raw analog pattern is of the order of 11" x 20" in size and may have 40, 50, or 60 dB full scale amplitude range. To include such a pattern in a report means that it must either be photographically reduced in size by about 50 percent, or that the final report be in two separate volumes (one part being the text printed on standard 8 1/2 x 11 paper; the other being the 11 x 20 patterns), or that the patterns be included in the standard size report as foldouts. None of these solutions is ideal.

Our solution is to have the recording equipment modified to produce not only its regular size patterns but also patterns whose overall size is about 5 x 9 inches. Such a pattern could be read with nearly the same precision as the present sizes are and it would be far easier to reproduce. When there is a particular concern for detail, the larger patterns could still be used.

Another small, but annoying, problem is the lack of standard sizes of chart paper grids. This is not ordinarily a problem, but in our investigation many inter-range comparisons had to be made which could not be simply done because of the variety of amplitude scales used by the five radar cross section ranges. This variation is illustrated in Table IV-1, in which we have compared the amplitudes of the various range patterns' scales. The full scale amplitude range of the chart paper in all cases covered 9 7/8 inches; this makes more sense when one realizes it is precisely 25 centimeters. Here we recommend that a standard be established so that all 40 dB paper has the same grid size; similarly for 50 dB and 60 dB paper. In an evaluation such as ours, it would make sense to insist that all ranges supply their data on identical chart paper.

TABLE IV-1: COMPARISON OF RANGE PATTERN SCALES.

Range	Full Scale Pattern Deflection (dB)	Smallest Division (dB)
Conductron	40	1.0
Radiation Services	40	0.5
General Dynamics/FW	50	0.5
Micronetics	40	1.0
RAT SCAT	50	0.5



Finally, with regard to data display, there is a small problem that CW ranges experience in post-calibration. It is tradition at CW ranges that the calibration standard is installed or measured after the pattern of the desired target has been measured and this calibration level generally does not coincide with any convenient amplitude scale on the chart. The ranges using pulsed systems, on the other hand, pre-calibrate their patterns and thus assign convenient amplitudes to the scale printed on the chart. This makes it easy to read values off the pattern in dBsm, or any other desired unit, with scarcely any effort. The post-calibration technique, on the other hand, requires that the cross section of the calibration target be first ascertained and this rarely turns out to be a convenient number, either in dBsm or  $\text{dB } \lambda^2$ , and then the difference between its level and an amplitude on the pattern must be counted relative to the calibration level.

The solution is obvious. CW ranges could, if they desired, pre-calibrate their data like the pulsed ranges do. The two measurements (of the target and of the calibrator) take place next to each other, in time, and it matters little which is done first. In fact, patterns could be both pre- and post-calibrated at CW ranges. The net result is that radar cross section patterns produced at CW ranges would be much more readable.

#### 4.2.5 Underestimating Range Time.

In the summer of 1965 we solicited the five cross section ranges for quotations and the particulars of their responses are shown in Table IV-2. The measurement times seemed reasonable, although GD/FW and MC required a full four to eight weeks more than the other ranges. It should be noted that the measurements to be provided for the quotations were not the same for each range. Most of the ranges declined to bid on phase measurements while others could not provide cross polarized data at certain frequencies. Table IV-2 is intended only to show the original estimates of range time according to the preliminary quotes submitted to us.

Note that we have included the lead time each range required in order to prepare for the measurements; this varies from 2 weeks for Conductron to as long as three months for Micronetics. We more or less assumed that the

lead time was a negligible factor in the measurements program because we had encountered model procurement delays early in the investigation and had kept the various ranges informed of expected delivery dates for the models. Apparently however, our assumptions were wrong because the measurements at most of the ranges required approximately the sum of estimated measurement time plus estimated lead time.

TABLE IV-2: SUMMARY OF RANGE QUOTATIONS

Range	Lead Time	Measurement Time	Quotation Good For	Cost
Conductron	2 wks	8 wks	--	39,872
Radiation Serv.	2 mo.	7 wks	45 days	16,674
General Dyn.	2 mo.	3 mo.	75 days	46,880
Micronetics	3 mo.	4 mo.	90 days	62,200*
RAT SCAT	--	6 wks	-	GFE

\* The \$62,000 quotation was later revised to \$38,700.

By the beginning of 1967, we had advised the ranges of delays due to model procurement problems and many of them had revised their estimated range time; Conductron held to its 8-week estimate, GD/FW stood by its 13-week estimate, Radiation Services now asked for 13 weeks, Micronetics asked for 16 weeks and RAT SCAT 6 weeks. If we add the lead time originally requested by each range to its revised range time estimate, we obtain the numbers listed in the first column of Table IV-3. The ranges required from 19 to 28 weeks to receive the models, measure them and ship them out again.

TABLE IV-3: REVISED SUMMARY OF RANGE QUOTATIONS

Range	Lead Time + Estimated Range Time (Weeks)	Actual Range Time (Weeks)
Conductron	10	21
Radiation Services	22	21
General Dynamics/FW	22	19
Micronetics	29	26
RAT SCAT	39	28

We hasten to caution the reader against judging the ranges too harshly on the basis of Tables IV-2 and IV-3. It might appear the Conductron and Radiation Services badly underestimated their range times but we believe the 21-weeks they each used does not reflect their true performance. The models dribbled into each range over a 12-week period and it is therefore not entirely their fault that they had the models longer than estimated.

Both General Dynamics/Fort Worth and RAT SCAT, on the other hand, had been informed of measurement progress at preceding ranges and could have been better prepared for measurements when the models finally appeared. Both these organizations waited a full eight weeks after receiving the models before commencing their measurements. General Dynamics discharged its obligations a scant eleven weeks after starting measurements, however, RAT SCAT felt it advisable to release the models to Micronetics long before its measurements were done. Micronetics made a few token measurements after receiving the models but its work was performed in short spurts interrupted by long delays due to weather, equipment trouble and "higher priority" commitments.

Twenty-odd weeks seem to be a long time to obtain 92 radar cross section patterns, but this is typically the time we encountered. Had the measurements been of entirely unknown targets (by "unknown" we mean targets whose returns could not have easily been predicted theoretically) the range times might have been much less. Since each cross section range knew it was part of an evaluation program, each probably took much more time than it might have ordinarily.

It is difficult to make a significant recommendation that will help to solve this problem. One might offer a cash incentive for every week a range finishes ahead of a schedule and impose penalties for every week it consumes beyond the promised schedule. To avoid delays due to higher priority measurements, one should make use of ranges with as small a work load as possible, other things being equal. If the need is great enough, the price paid per measurement can be raised to increase the level of competition and the number of ranges .

#### 4.2.6 Weather

We grossly underestimated the effects of weather and apparently so did some of the range operators. Regardless of location or season, the weather was hostile. The wind was the worst offender, since it always threatened to blow the models off their support columns and, in one case, this actually occurred with disastrous results. Conductron's CW system required the quietest of conditions and its work was done almost exclusively at night. General Dynamics/Fort Worth had the boldest operators who even made a few measurements in 15 to 20 knot winds. Yet range managers tend to ignore weather when they bid a job and the evidence lies in the fact that no range completed its work in the time specified in its quotation. Thus, we learned that quoted range time estimates are usually unreliable; models will be detained at a range from a minimum of two weeks to as much as several months longer than specified in an official quotation.

With respect to weather advantages, and range location, we feel that the weather tends to be more adverse at the Conductron range location. To a large extent, however, this was compensated for by the "try harder" attitude of the range personnel as evidenced by the extensive amount of their night work. Poor weather was given as a frequent cause of delay by Radiation Services, RAT SCAT and Micronetics. For this series of measurements, we would rate these locations as nearly equal with respect to time lost due to weather and General Dynamics would receive a slightly higher rating.

Our recommendation in connection with the weather problem is to allow for delays due to weather; a minimum of 25 percent lost time would seem to be a reasonable estimate.

#### 4.3 Summary

In this chapter we have pointed out problem areas, discussed the source of the problems when known and to the extent possible we have made recommendations for solutions. The major problem area is the lack of

measurement accuracy. We suggest that accurate measurements can be obtained (1) if one has adequate equipment and facilities, (2), if proven operation procedures are used, and (3) if the range is operated by careful experienced and well motivated personnel. We conclude that the equipment and facilities are adequate except for the near field limitation. We list the major steps to be followed in our suggested measurement procedure, call attention to specific problem areas, and we briefly discuss the importance of a qualified range crew. Other problem areas not so closely related to measurement accuracies are also discussed.

It would be helpful at this point to be able to pinpoint the several problem areas and cite the specific deficiencies at each range that caused their results to be less than perfect. Except for a few instances this can not be done. One of the easiest problems to identify has been mentioned, perhaps too many times. We refer to the near field problem. This problem exists at the Conductron range and it was well recognized by them and it was treated very thoroughly in their report. This limitation, which in their case is difficult to overcome, did not prevent them from producing quite satisfactory data in many of their measurements. Perhaps more to be criticized are those organizations who had long ranges available but still worked at near field distances and turned in some faulty data as a result. Micro-netics and to a lesser extent RAT SCAT and Radiation Service measured targets at distances less than  $L^2/\lambda$  when longer distances were available.

Another less critical deficiency that is easy to identify is the pattern errors due to rf interference experienced by GD/FW in its 170 MHz measurements. This, too, is a well recognized problem and errors due to it are easily corrected.

It is not possible, however, to tie down the causes of the bulk of the measurement errors and link the problems to one or more specific range. We believe that the situation is too complex to do this. In our opinion there are two or three probable causes of errors in addition to those just mentioned.

Judging from the random nature of the errors it is quite possible that all the ranges were deficient in one or more ways and these deficiencies could well have varied with model size or frequency.

It is our opinion that most of the errors not already mentioned are due to (1) lack of uniform field, (2) secondary reflections, (3) insufficient attention to test procedural details. The first point was discussed in detail in 4.1.2.4. We show that a field variation of n dB could result in an error of about this magnitude if it happens to occur over much of the position to be occupied by a principal scatterer. To our knowledge few of the range operators examine their field in the target-antenna direction and it is in this direction that errors in this field pattern could be linked directly to changes in the RCS values. This problem could exist on any range but it is more likely to exist on the ground plane ranges than on the Micronetics range.

Secondary reflections, discussed in 4.1.2.5 are a known major source of errors in anechoic room RCS measurements and are almost certain to exist, although to a lesser extent, on outdoor ranges. Evidence of this was cited; its presence is shown by measuring the RCS pattern at two slightly different ranges. Its presence will sometimes (but not always) be indicated by rotating a sphere off center. The common background check where the support column only is rotated will not reveal the effect of secondary scattering. Until proven otherwise, one should assume that all five of the ranges experienced some inaccuracies due to secondary reflections.

We have mentioned also that measurement errors are caused by insufficient attention to test procedural details. Examples of this are seen in Fig. 5-3 of Volume IIa where VV and HH RCS values for end-on aspects are presented. All those involved are aware that the HH and VV values should be equal and yet there are two instances where the values differ by 1.75 dB and another with a difference of 2 dB. Had the operators been aware and concerned about this discrepancy they would have been able to ascertain the cause and correct

the errors. In the same figure GD/FW submits data which are quite suspect. Its data for the two foot cylinder at 1360 MHz is well below the theoretical value and about 8.5 (rather than 6)dB below its 680 MHz data for this value of ka. Precision cylinders are involved here so the fault cannot be with the models. We believe that these and other inconsistencies which could be pointed out are due to insufficient attention to details that would have become obvious had the operators been more alert.

One further point should be mentioned. The satellite data were considerably poorer than the cylinder data. There is a tendency to claim that this is largely due to imperfect models. It is agreed that the models did not scale as well as desired.

There were, however, two opportunities to compare the full scale and 4/10 scale models at the "same" ka value, namely in the 170/425 MHz and the 425/1062.5 MHz measurements where the first frequency in each case is that used for the full scale model. The differences and similarities which occurred in the first two patterns should have been repeated in the second two patterns. We found a number of inconsistencies in making these comparisons. These data and further discussion is found in Volume IIb of this Final Report.

In Section 4.1.2.6 we discussed calibration procedures at considerable length and suggested that other standard shapes such as cylinders should be used. We think of these auxiliary standards more as a method of checking performance over the entire pattern. We do not question the present calibration procedure for determining the RCS of a target if the system and the range are operating ideally.

## GUIDE TO THE CHOICE AND UTILIZATION OF RADAR CROSS SECTION MEASUREMENT FACILITIES

As was stated in the introduction, one of the objectives of this study was to provide a guide to optimum utilization of existing radar cross section measurement facilities. We have interpreted this to mean that a guide should be provided for the user or customer who requires the service of a range facility. While we believe that this entire report serves as such a guide, we provide in this chapter a list of guidelines which we think are most pertinent. In most cases we consider these points to be rather obvious and would expect most users to produce a somewhat similar list after a little consideration.

### 5.1 Guidelines for Range Utilization

#### 5.1.1 Adequacy of Facilities

The user should satisfy himself that the physical facilities are adequate for his needs - check the following points by inspecting the facilities and the results of previous measurements.

- a) Be sure that the operating frequencies available at the range include those required in the planned measurements.
- b) Polarization capability; some ranges are unable to measure cross polarized return or even co-polarized returns, except for vertical and horizontal planes.
- c) Antenna-to-target distance; to date there is no completely satisfactory method for eliminating deficiency in range length. If accuracy is important and good data is required for all aspects, the  $2L^2/\lambda$  formula should be applied. The near field effects begin to be intolerable for ranges less than  $L^2/\lambda$ .
- d) Signal-to-noise; this is most important for low cross section targets. Transmitter power and receiver sensitivity should be sufficient to prove a 20 dB S/N for critical data points. Expected cross sections and the range distance are, of course, important factors in any S/N computation.



- e) **Extraneous reflections:** The range should be as free as possible of unwanted reflections and means must be available to cancel out or gate out those which do exist. When accurate results are required, tests should be performed to map the field over the volume to be occupied by the target. A "quick and dirty" method for assessing background effects is to note the return of a sphere rotating on the target support in an off-center position. Choose a sphere whose return is less than or comparable to the critical values in the pattern to be measured. See also 4.1.2.4 and 4.1.2.5.
- f) **Target support:** The target support must be designed so as to eliminate the possibility of dropping the model under all reasonable circumstances. Equally important it must not significantly affect the return from the target. This is not a critical problem for the models measured in this series but it is a major problem for low cross section targets and it has been discussed widely in the literature. See, for example, Blacksmith et al, 1965, as well as 4.1.2.3.
- g) **Calibration standards:** The standard procedures for calibrating radar cross section returns are well known, and should be satisfactory for nominal accuracy for co-polarized returns. For measurements where accuracy is of critical importance refer to the discussion in 4.1.2.6. For calibrating cross polarized returns, secondary standards such as a  $45^\circ$  inclined wire should be used which in turn may be calibrated against the co-polarized return of a sphere.
- h) **Determine if the analog plots are adequate in dynamic range and angular extent.**
- i) **Digital data:** If required, magnetic tape or punch cards are preferable, depending on the user's own read-out equipment. Check to see that amplitude and angle increments are compatible with requirements.

- j) Phase measuring capability, if required: Be sure that phase data can be calibrated in a meaningful and usable manner.

#### 5.1.2 Range Personnel

The user should satisfy himself that the range supervisor and operating crew are experienced, competent and concerned about doing a good job. It is advisable for the customer to have an experienced representative on hand at the start of the measurements. A mutual understanding of the objectives and good rapport between the customer and range operators will help ensure a well-motivated crew and more accurate data. It is most desirable that the staff at the range facility include a qualified analyst who is available to answer questions concerning the data. He should examine the data periodically and point out obvious, or even subtle, errors in the measured results.

#### 5.1.3 Costs

Price quotations should be solicited from two or more ranges. Quotations for the measurements involved in this program differed by a factor of 3.7.

This factor was later reduced; the highest bidder reduced their quotation by more than 35 percent after a second solicitation. There is by no means a one-to-one relationship between cost and results.

#### 5.1.4 Schedules

If the user has a tight time schedule, he should make a special effort to negotiate an agreement to ensure that the schedule will be met. This procedure will, in most cases, eliminate delays resulting from work on other programs. As a partial protection against delays due to weather, the user can arrange to have his measurements made in that part of the country which traditionally has good weather for the time interval in question.

## 5.2 Range Selection by a Potential User

Shopping for precisely the "right" radar cross section range to use is much like shopping for a major household appliance. The typical consumer expects the appliance to be durable, perhaps with a life expectancy of 15 years, and he therefore seeks to make as wise a selection as possible. The potential range user has much the same outlook, since he will probably have his target measured only once.

Ideally we would like to present the potential range customer with a survey that tells him precisely which range to use but, because of the limited scope of the contract, we can do so only in general terms. This is because not all the ranges in the United States capable of measuring our targets were included in the investigation and only two basic shapes were used in the study. The reader must bear in mind that our conclusions are valid only for cylindrical or roughly cylindrical targets.

Since the potential user is likely to be interested in range performance for large targets and low frequencies, Table V-1 below has been generated from data evaluated in Volume IIa of the final report. In this table we present the same information in two different matrices. The numbers listed refer to the number of errors one dB or less, as judged by a comparison of theory and experiment, committed by the ranges in their end-on and broadside radar cross section measurements. Note that GD heads the list for the large cylinders, but falls last for small cylinders. Note also that RSC takes first place for the lowest frequency and ties for first place for the highest frequency. The table suggests that GD should be given the task of measuring large cylinders, that any of the other four can handle the smallest cylinders, and that RSC is the choice for both high and low frequencies (but not for all intermediate ones).

---

**TABLE V-1: LIST OF THE NUMBER OF ERRORS 1 dB OR LESS WHEN MEASUREMENTS COMPARED WITH THEORY FOR END-ON AND BROADSIDE. The same data are presented in both halves of the table but are categorized differently in each case.**

<b>Cylinder Size (feet) or Frequency (MHz)</b>	<b>CC</b>	<b>RSC</b>	<b>GD</b>	<b>RSS</b>	<b>MC</b>	<b>Total Possible</b>
32	4	9	13	11	8	16
16	8	16	17	15	10	20
8	7	15	13	15	13	16
4	11	12	10	11	10	12
2	8	8	5	8	7	8
170	2	7	4	4	2	8
340	4	10	10	9	6	12
680	12	11	16	14	12	16
1360	11	17	15	18	14	20
2720	9	15	13	15	12	16

Optimum range selection depends a great deal on the kind of information required (for example, amplitude or phase or both), the accuracy demanded, the price the customer is willing to pay, and the delay he will tolerate before he gets his data. Assume, for example, that a satellite target is to be measured at the frequencies spanned in our investigation and that the quality of the ranges has not changed since our targets were measured. By stipulating certain conditions, listed in column 1 of Table V-2 below, we postulate the range selections in column 2, based on our evaluation of range performance.

**TABLE V-2: RANGE SELECTION FOR A VARIETY OF REQUIREMENTS.**  
 None of the ranges can satisfy all the requirements.

Requirement	Range Selection
RCS amplitude with emphasis on accuracy	RSC, GD, RSS
Amplitude and phase at L-band	GD, RSS
Amplitude and phase at all frequencies	GD
Amplitude at lowest cost	RSC
Amplitude recorded on mag tape	MC
Very large targets	GD
Small targets	CC, RSC, RSS, MC, AL
Low frequencies	RSC

Finally we urge the reader to examine ranges other than those considered in this report. Depending upon the size of his targets and the frequencies of interest, there may be a dozen other ranges capable of performing the measurements. Some range descriptions and points of comparison can be found in Fritsch (1963), Buie and Mills (1963) and in the Radar Reflectivity Measurements Symposium (1964). From these descriptions, one feels that the Boeing (Wichita) and Lockheed ranges could have measured all but the largest cylinder, but these ranges were not specified in our contract.

VI  
CONCLUSIONS

In the Introduction, four objectives were listed, the first of which was to evaluate selected radar cross section measurement facilities. We did this in Chapter III based on data and opinions contained therein, and on the more complete data in Volumes IIa and IIb of this Final Report. To obtain an overall performance figure we rated the ranges from A to E for several points of evaluation, but in Chapter III these ratings were grouped into four major areas.

Some of the areas are much more significant than others and it is doubtful if a group of experts would agree on their relative importance. The cost of measurements (Table IV-2) is also significant. A summary of our evaluation is given in Table III-7, which we repeat here. Our own

**TABLE III-7: RANGE COMPARISON SUMMARY**

Range	Facilities Techniques and Procedures	Accuracy		
		Cylinder Data		Satellite Data
		Co-Polarized	Cross Polarized	
CC	B-	D	C	D
RSC	B	B	C	C
GD/FW	B+	C	D	C
RSS	B	C	C	C
MC	B-	D	D	D
Suggested Weighting Factor	2	4	1	2

estimate of the relative importance of the areas of comparison and our ability to judge based on the data available is indicated by a weighting factor which we introduced into the table. Any potential user should, of course, assign a weighting factor in accordance with the requirements of his particular needs. With certain exceptions such as inability to measure phase or insufficient range, all five of the facilities are able to make the measurements required. If the facilities are adequate, the most important requirements are to exercise extreme care in checking out range characteristics (field probe, background and secondary reflection effects) and the experience, competence and motivation of the personnel involved.

We note that range personnel and management change with time and it may be of interest to point out some of the major changes that have taken place during the three years of this evaluation. Radiation Services Company was sold to Sigma Incorporated by Radiation Incorporated and Micronetics was bought by the Teledyne Company. High level and intermediate management changes have occurred at Conductron Corporation, on the range and in the front office. Thus to a certain extent the findings of this investigation are dated, which points out the importance for range users to maintain an up-to-date person-to-person contact with the cross section facilities.

Other objectives were to identify critical problem areas and present plans for their solution. Several problems were cited in Chapter IV and to the extent possible, recommendations were given for their solutions. In examining the data, we are impressed with the evident accuracy of some of the measurements. On the whole, inter-range and intra-range comparisons are good and the theory is supported by the measurements. On the other hand, we find range-to-range deviations greater than 3 dB for some of the cylinder results but, more distressing, are the satellite data in which differences as large as 10 dB exist between the returns from the same model measured at two different ranges. We conclude that a range user cannot expect accurate results for a target whose return cannot be accurately predicted theoretically. The problem of measurement errors was discussed at length in Chapter IV

and, briefly, we feel that the customer must insist, with appropriate motivation, on much more care than currently is practiced in following through good measurement procedures. The major steps to be followed in RCS measurements were discussed in 4.1.2 not the least of which is the repetition of measurements to insure higher accuracy, a costly proposition. The customer should ask for all the data, both good and bad, to acquaint himself with the measurement problems and results.

Another critical problem occurs in measurements of large targets with insufficient target distance. This is a well-known problem with a well-known answer but it remained an obvious cause of error in this series of measurements. Aside from the obvious recommendation that all measurements should be made at a distance equal to or reasonably close to  $2L^2/\lambda$ , two other recommendations are made. A considerable effort should be made to develop much longer ranges at existing or new facilities so that large models can be measured at high microwave frequencies. Second, an effort should be made to exploit, if possible, near field data to produce far field results.

Most ranges are incapable of making phase measurements. As was pointed out in Chapter IV, phase data are needed to calculate scattering matrices, to study discrimination problems, to help eliminate errors in cross section measurements due to the pedestal support, and possibly to help calculate far field data from near field measurements. We recommend that ranges equip themselves for phase measurements as this becomes economically feasible.

Other problems considered in Chapter IV included cross polarization measurements, data display, digital recording techniques, weather problems, and inaccuracies in estimates on measurement schedules.

A problem area which was not discussed since it was not pertinent to this series of measurements, is the inadequate frequency coverage of outdoor ranges measuring large targets. There is a growing interest in radar cross section data just above and in the HF band and although some capabilities exist, they are usually makeshift setups. The difficulties in working at these frequencies are severe and demand careful equipment design.



We saw very little evidence of measurement capabilities at K-band or millimeter wavelengths and there is a need for more and better facilities to accomodate these frequencies. As shown in Chapter IV, millimeter frequencies will be needed for X-band and higher frequency measurements of large models. We believe that the RAT SCAT range at least should be equipped to make measurements at long ranges at these frequencies.

Another objective was to provide a guide to the selection and optimum utilization of radar cross section measurement facilities. It is felt that this information is contained in all parts of this report . To set them out more clearly, however, they are listed in Chapter V separately.

With the responsibility for evaluating these five radar cross section ranges, we play the part of the umpire and have been, perhaps, supercritical. In order to make comparisons we have used a more precise yardstick than is generally required. Most of the data would be considered satisfactory for a majority of applications and we emphasize that the ranges were asked to participate in these tests with as is facilities. They were not to make additions or modifications in order to increase their ability with respect to frequency coverage, cross polarized measurements, phase measurements or digital records. Ranges which had some problems with these measurements may well be able to provide more accurate data in other measurements.

## VII

### REFERENCES

- Bachman, C.G., H.E. King and R.C. Hansen (1963), "Techniques for Measurement of Reduced Radar Cross Sections," Microwave J., 6, Pt. 1, pp. 61-67. (February), Pt. 2, pp. 95-101 (March), Pt. 3, pp. 80-86 (April).
- Bahret, W.F. (1964), "Avionics Laboratory Radar Cross Section Measurements Facility," Radar Refl. Measurements Symp-II, RADC-TDR-64-25, AD 601365, pp. 201-282.
- Blacksmith, P., R.E. Hiatt and R.B. Mack (1965), "Introduction to Radar Cross Section Measurements," Proc. IEEE, 53, pp. 901-920.
- Buie, H.B. and E.E. Mills (1963), "Radar Cross Section Measurement Facilities Study," U.S. Army Missile Command, Redstone Arsenal, Report No. RE-TR-63-4, Vol. I.
- Crispin, J.W. and K.M. Siegel (1968), Methods of Radar Cross Section Analysis, Academic Press, New York, Chapter 12.
- Fails, W.A. and E.G. Fubini (1949), "Methods of Measuring Radar Cross Sections," Airborne Instruments Laboratory, Inc., Report 380-1 (January).
- Fritsch, Peter C. (1963), "Survey of Radar Reflectivity Ranges," MIT Lincoln Laboratory, Report PA-16 Rev. 1 (BMRS) No. 159.
- General Dynamics (1968), "Radar Cross Section Measurement Capabilities," General Dynamics/Fort Worth Report FZE-675 (June).
- Hiatt, R.E. and T.M. Smith (1966), "Radar Scattering Investigation," The University of Michigan Radiation Laboratory Report 7462-1-T, RADC-TR-66-35, AD 483471.
- Honer, R.E. and W.D. Fortner (1964), "Outdoor Pulsed Radar Reflectivity Range," Radar Refl. Measurements Symp. -II, RADC-TDR-64-25, AD 601365, pp. 274-285.  
See also: Micronetics (1968), "Equipment and Services in Microwave Instrumentation and High Resolution Backscatter Measurements," Micronetics, A Teledyne Company, 7155 Mission Gorge Rd., San Diego, California 92120.
- Kay, A.F. (1954), "Far Field Data at Close Distances," Technical Research Group, Contract No. AF 19 (604)-1126, October.
- Kouyoumjian, R.G. and L. Peters, Jr. (1965), "Range Requirements in Radar Cross Section Measurements," Proc. IEEE, 53, pp. 920-928.

- Landfried, J. E. and W. L. Williamson (1964), "Static Radar Reflectivity Measurement Facilities at Radiation Incorporated," Radar Refl. Measurements Symp. -II, RADC-TDR-64-25, AD 601365, pp. 299-302.  
See also: Sigma Incorporated (1968), "Reflectivity Range Capabilities," Sigma, Incorporated, Box 760, 3000 NASA Blvd., Melbourne, Fla, 32901.
- Marlow, H. C., D. C. Watson, C. H. VanHoover and C. C. Freeny (1965), "The RAT SCAT Cross Section Facility," Proc. IEEE, 53, pp. 946-953.
- Radar Reflectivity Measurements Symposium -II (1964) RADC-TDR-64-25, AD 601365 (April).
- Senior, T. B. A. and E. F. Knott (1964), "The Near Field of a Styrofoam Cylinder," Radar Reflectivity Measurement Symposium, RADC-TDR-64-25, Vol. 1, AD 601364.
- Senior, T. B. A., M. A. Plonus, and E. F. Knott (1964), "Designing Foamed-Plastic Supports," Microwaves, 3, pp. 38-51.
- Wren, A. W. (1964), "Conductron Corporation's Cross Section Range," Radar Reflectivity Measurements Symposium-II, RADC-TDR-64-25, AD 601365, pp. 359-362.  
See also: Conductron Corporation (1968), "Electromagnetic Range," Conductron Corporation, Box 614, Ann Arbor, Michigan 48107.

UNCLASSIFIED

Security Classification

DOCUMENT CONTROL DATA - R & D

(Security classification of title, body of abstract and indexing annotation must be entered when the overall report is classified)

1. ORIGINATING ACTIVITY (Corporate author) The University of Michigan Radiation Laboratory, Dept. of Electrical Engineering, 201 Catherine Street, Ann Arbor, Michigan 48108	2a. REPORT SECURITY CLASSIFICATION <b>UNCLASSIFIED</b>
	2b. GROUP N/A

3. REPORT TITLE  
Evaluation of Slected Radar Cross Section Measurement Ranges  
Vol. I: Range Parameters, Range Evaluation, Problem Areas and Recommendations.

4. DESCRIPTIVE NOTES (Type of report and inclusive dates)  
Final Report - Vol. I July 1965 through April 1968

5. AUTHOR(S) (First name, middle initial, last name)  
Thomas M. Smith, Eugene F. Knott, and Ralph E. Hiatt

6. REPORT DATE December 1968	7a. TOTAL NO. OF PAGES 78	7b. NO. OF REFS 18
---------------------------------	------------------------------	-----------------------

8a. CONTRACT OR GRANT NO. AF 30(602)-3872 b. PROJECT NO. 6512 c. Task 651207 d.	9a. ORIGINATOR'S REPORT NUMBER(S) 7462-1-F (Vol. I)
	9b. OTHER REPORT NO(S) (Any other numbers that may be assigned this report) RADC-TR-68-238

10. DISTRIBUTION STATEMENT

11. SUPPLEMENTARY NOTES	12. SPONSORING MILITARY ACTIVITY Rome Air Development Center Griffiss Air Force Base New York 13442
-------------------------	--

13. ABSTRACT

A program under which selected radar cross section measurement ranges were evaluated is described. Some details are given on the test models involved and on the test procedures used. Test results are summarized and the ranges are assigned ratings according to their performance in an evaluation that includes sixteen points of comparison. Problem areas in radar cross section measurements are outlined and some recommended solutions are given. Some suggestions for the optimum utilization of radar cross section ranges are given for the benefit of the potential range user.

14. KEY WORDS	LINK A		LINK B		LINK C	
	ROLE	WT	ROLE	WT	ROLE	WT
Radar Cross Section Study Radar Cross Section Measurements Radar Cross Section Ranges Evaluation of Radar Cross Section Ranges Radar Cross Section Standard Models						

EVALUATION OF SELECTED RADAR CROSS SECTION  
MEASUREMENT RANGES

Volume IIa: Cylinder Tests and Range Evaluation Procedures

By

Thomas M. Smith, Eugene F. Knott and Ralph E. Hiatt  
The University of Michigan Radiation Laboratory  
Department of Electrical Engineering  
Ann Arbor, Michigan

December 1968

Contract AF 30(602)-3872

Prepared for:

Rome Air Development Center  
Griffiss Air Force Base, New York

RADC-TR-68-238

7462-1-F

Evaluation of Selected Radar Cross Section Measurement Ranges  
Volume IIa: Cylinder Tests and Range Evaluation Procedures

Prepared by

T. M. Smith, E. F. Knott and R. E. Hiatt  
The University of Michigan Radiation Laboratory  
Department of Electrical Engineering  
Ann Arbor, Michigan

December 1968

Contract AF 30(602)-3872  
Rome Air Development Center  
Griffiss Air Force Base, New York

## NOTICE

When Government drawings, specifications, or other data are used for any purpose other than in connection with a definitely related Government procurement operation, the United States Government thereby incurs no responsibility nor any obligation whatsoever; the fact that the Government may have formulated, furnished, or in any way supplied the said drawings, specifications, or other data, is not to be regarded by implication or otherwise as in any manner licensing the holder or any other person or corporation, or conveying any rights or permission to manufacture, use, or sell any patented invention that may in any way be related thereto.

Copies of this report should not be returned unless return is required by security considerations, contractual obligations, or notice on a specific document.



## FOREWORD

This report (RADC-TR-68-328, 7462-1-F) was prepared by The University of Michigan Radiation Laboratory, Department of Electrical Engineering, under the direction of Professor Ralph E. Hiatt under Air Force Contract AF 30(602)-3872 "Radar Scattering Investigation", Task 651207 Project 6512. The work was administered under the direction of the Rome Air Development Center, Griffiss Air Force Base, New York.

This report covers the period July 1965 through April 1968.

The authors are pleased to acknowledge the contributions of Dr. T. B. A. Senior on several phases of the program. Thanks are due to Mr. Tony Hsu for his considerable help in reading patterns and organizing the data.

This technical report has been reviewed and is approved.

MILTON L. WASSER  
Contracting Officer

## ABSTRACT

This is the second part of a three part final report on the evaluation of radar cross section measuring facilities. In Volume IIa, the results from measurements on five right circular cylinders, which are scale models of one another, are discussed in detail. Evaluation procedures are set forth in order to determine how well each of the ranges performed their tasks. These procedures involve the comparison of measurements on cylinders which should give the same results, or results which should differ by known scale factors, and secondly the comparison of theoretical and experimental results for end-on and broadside aspect angles. Five outdoor radar ranges took part in this evaluation program. Limited tests were made on two of the smaller cylinder models at a sixth facility, an indoor range.

## TABLE OF CONTENTS

<b>I</b>	<b>INTRODUCTION</b>	<b>1</b>
	1.1 Objectives	1
	1.2 Work Requirements	2
	1.3 Some Difficulties in Evaluating Radar Ranges	4
	1.4 Evaluation Procedures	6
	1.5 Outline of Volume IIa Contents	8
<b>II</b>	<b>CYLINDER MODELS AND RANGE ENVIRONMENT</b>	<b>10</b>
	2.1 Cylinder Models	10
	2.2 Range Environment	16
<b>III</b>	<b>THEORETICAL BACKSCATTERING MODELS</b>	<b>20</b>
	3.1 Backscattering from Cylinders	21
	3.2 Cylinder Scattering Patterns	22
	3.3 End-on and Broadside Cross Sections	30
<b>IV</b>	<b>CO-POLARIZED EXPERIMENTAL DATA</b>	<b>38</b>
	4.1 Patterns for all ka Cases	38
	4.2 Patterns from Each Outdoor Range	45
	4.3 Near Field Distortion	56
	4.4 Comparison Between Theory and Experiment	60
<b>V</b>	<b>INTRA-RANGE EVALUATION TESTS</b>	<b>66</b>
	5.1 Constant ka Tests	70
	5.2 End-on Polarization Comparison	79
<b>VI</b>	<b>INTER-RANGE EVALUATION TESTS</b>	<b>84</b>
	6.1 End-on Data	84
	6.2 Broadside Data	87
	6.3 Sidelobe Symmetry	90
	6.4 Special Evaluation for ka=1.36	94
	6.5 Summary of Co-Polarized Measurements	101
<b>VII</b>	<b>CROSS POLARIZATION THEORY AND EXPERIMENT</b>	<b>106</b>
	7.1 Cross Polarized Theory	106
	7.2 Cross Polarized Measurements	109
	7.3 Evaluation of Cross Polarized Data	113
<b>VIII</b>	<b>CONCLUSION</b>	<b>119</b>
	8.1 Remarks on the Theoretical Models	120
	8.2 Remarks on the Co-Polarized Data	121
	8.3 Remarks on the Cross Polarized Data	123
	8.4 Final Remarks	124
	<b>REFERENCES</b>	<b>126</b>
	<b>APPENDIX A: PHYSICAL OPTICS MODEL FOR SCATTERING BY A FINITE CYLINDER</b>	<b>128</b>

DD FORM 1473

## LIST OF ILLUSTRATIONS

Figure No.	Caption	Page No.
2-1	Brooks and Perkins Preliminary Drawings for 32-foot Cylinder.	13
2-2	Brooks and Perkins Preliminary Drawings for 16-foot Cylinder.	14
2-3	Brooks and Perkins Preliminary Drawings for 8-foot Cylinder.	15
2-4	Geometry for Typical Radar Cross Section Measuring Facility.	17
3-1	Theoretical Patterns for $ka=1.36$ and $kl=17.4$ .	24
3-2	Theoretical Patterns for $ka=2.72$ and $kl=34.8$ .	25
3-3	Theoretical Pattern for $ka=5.44$ and $kl=69.6$ .	26
3-4	Theoretical Pattern for $ka=10.9$ and $kl=139.2$ .	27
3-5	Theoretical Pattern for $ka=21.7$ and $kl=278.4$ .	28
3-6	Theoretical Cross Section and Phase Patterns for $ka=5.43$ .	29
3-7	Theoretical Radar Cross Section Values at End-on and Broadside for 32'x5' Cylinder.	31
3-8	Theoretical Radar Cross Sections of Cylinders at End-on for VV and HH Polarizations, Inter-Range Display.	35
3-9	Theoretical Radar Cross Sections of Cylinders at Broadside for VV Polarization, Inter-Range Display.	36
3-10	Theoretical Radar Cross Sections of Cylinders at Broadside for HH Polarization, Inter-Range Display.	37
4-1	Experimental Patterns for $ka=1.36$ , 170 MHz, Range 400', 16-foot Cylinder.	39
4-2	Experimental Patterns for $ka=2.72$ , 340 MHz, Range 400' 400', 16-foot Cylinder.	40
4-3	Experimental Patterns for $ka=5.44$ , 680 MHz, Range 1000', 16-foot Cylinder.	41
4-4	Experimental Patterns for $ka=10.9$ , 1360 MHz, Range 1000', 16-foot Cylinder.	42
4-5	Experimental Patterns for $ka=21.7$ , 2720 MHz, Range 1000', 16-foot Cylinder.	43
4-6	Conductron Pattern for 32-foot Cylinder, VV Polarization, 340 MHz.	46

4-7	Radiation Service Pattern for 32-foot Cylinder, VV Polarization, 340 MHz.	47
4-8	General Dynamics Pattern for 32-foot Cylinder, VV Polarization, 340 MHz.	48
4-9	RAT SCAT Pattern for 32-foot Cylinder, VV Polarization, 340 MHz.	49
4-10	Micronetics Pattern for 32-foot Cylinder, VV Polarization, 340 MHz.	50
4-11	Conductron Pattern for 32-foot Cylinder, HH Polarization, 340 MHz.	51
4-12	Radiation Service Pattern for 32-foot Cylinder, HH Polarization, 340 MHz.	52
4-13	General Dynamics Pattern for 32-foot Cylinder, HH Polarization, 340 MHz.	53
4-14	RAT SCAT Pattern for 32-foot Cylinder, HH Polarization, 340 MHz.	54
4-15	Micronetics Pattern for 32-foot Cylinder, HH Polarization, 340 MHz.	55
4-16	Near Field Distortion for HH Polarization at $ka=10.9$	58
4-17	Comparison of Norair SDT Theory with Range Data for HH Polarization.	62
4-18	Comparison of Norair SDT Theory with Range Data for VV Polarization.	63
4-19	Differences between Theory and Experiment are Summarized for End-on and Broadside Aspect Angles.	64
5-1	Scattering Pattern showing the Points Recorded in Table V-1	67
5-2	Error Distributions for Constant $ka$ Tests.	78
5-3	Comparison Between Theory and Experiment at End-on for Cylinders, VV and HH Polarizations (I).	80
5-4	Distribution of Errors Between HH and VV Measurements of End-on Returns.	82
6-1	Distribution of Errors Between Theory and Experiment for End-on Incidence; Both Polarizations.	85

6-2	Comparison between Theory and Experiment at Broadside for Cylinders, VV Polarization.	88
6-3	Comparison between Theory and Experiment at Broadside for Cylinders, HH Polarization.	89
6-4	Distribution of Errors between Theory and Experiment for Broadside Incidence; Both Polarizations.	91
6-5	Comparison between Theory and Experiment at First Side-lobes Next to Broadside for Cylinder, VV Polarization.	92
6-6	Comparison between Theory and Experiment at First Side-lobes Next to Broadside for Cylinder, HH Polarization.	93
6-7	Comparison between Theory and Experiment for 16-foot Cylinder, VV Polarization, 170 MHz.	95
6-8	Comparison between Theory and Experiment for 16-foot Cylinder, HH Polarization, 170 MHz.	96
6-9	Comparison between Theory and Experiment for 4-foot Cylinder, VV Polarization, 680 MHz.	97
6-10	Comparison between Theory and Experiment for 4-foot Cylinder, HH Polarization, 680 MHz.	98
6-11	Error Distribution for special $ka=1.36$ Test.	100
6-12	Total Error Distribution of the Co-Polarized Cylinder Measurements.	102
7-1	Image Plane Geometry for the Cylinder Model.	107
7-2	Comparison between HH and VH Polarizations.	110
7-3	Cross Polarized Measurements are Best Performed in Cuts Angled $45^\circ$ to the Principal Planes.	118
A-1	Finite Cylinder Geometry.	129

## LIST OF TABLES

Table No.	Caption	Page
I-1	Frequency-Scale Matrix for Cylinder Tests showing Resulting $k_a$ Values.	3
II-1	Cylinder Dimensions .	12
II-2	Some Characteristics of the Sites .	19
III-1	Intra-range Data Display for Theoretical Cross Sections, End-on and Broadside.	33
IV-1	Required Range Distance (feet) as Determined by $2L^2/\lambda$ .	59
IV-2	List of Conditions in which Theory is Compared with Experiment.	60
V-1	Example of how Data was Reduced for each Pattern from each Range.	68
V-2	Conductron Constant $k_a$ Test.	71
V-3	Radiation Service Constant $k_a$ Test.	72
V-4	GD/FW Constant $k_a$ Test.	73
V-5	RAT SCAT Constant $k_a$ Test.	74
V-6	Micronetics Constant $k_a$ Test.	75
V-7	Avionics Laboratory Constant $k_a$ Test.	76
V-8	Constant $k_a$ Test Results.	77
V-9	End-on Polarization Test Results.	81
VI-1	Errors between Theory and Experiment for End-on Incidence.	86
VI-2	Errors between Theory and Experiment at Broadside for Both Polarizations.	90
VI-3	Range Ratings for Special Pattern Test ( $k_a=1.36$ ).	99
VI-4	Summary of Range Tests for Five Points of Evaluation.	103
VII-1	Summary of VH Cross Polarized Data for Peak Returns Near Broadside .	111
VII-2	Summary of HV Cross Polarized Data for Peak Returns Near Broadside.	112

VII-3	Isolation Comparisons for $\sigma_{HH}(90^\circ) - \sigma_{VH}(\approx 90^\circ)$ .	114
VII-4	Isolation Comparisons for $\sigma_{VV}(90^\circ) - \sigma_{HV}(\approx 90^\circ)$ .	115
VII-5	Isolation Averages.	116
VIII-1	Summary of Grades for All Evaluation Tests and Average Grades.	122



## INTRODUCTION

This is Volume IIa of the final report on the evaluation of radar cross section measurement facilities. A history and summary of the program are found in Volume I. Volume IIa contains a detailed analysis and evaluation of backscattering tests performed on five closed cylinder models which constituted the main portion of the evaluation program. Volume IIb is classified and is a summary of test results on two satellite models which represent a more typical target.

In a brief statement, the purpose of this volume is to describe the cylinder models, the range environment in which they were tested, the theoretical scattering characteristics of these targets, and most important, the analysis of the cylinder backscattering patterns submitted by the ranges taking part in this test program.

To begin our story we start with a restatement of the program and the required tests set forth by the contract, parts of which have already been stated in Volume I, then we briefly describe the procedure we used to reduce and evaluate the data. At the end of this introduction, we give a short outline for the remaining chapters in this volume.

The evaluation procedure is specified in detail in Exhibit A of the Contract. Summaries and excerpts are given below for those parts which apply to the cylinder models and tests.

### 1.1 Objectives

- a) To evaluate existing radar cross section measurement facilities.
- b) To provide a guide to optimize utilization of existing radar cross section measurement facilities.
- c) To identify critical problem areas in radar cross section measurements.

d) To develop plans for attacking the critical problem areas identified. Special emphasis is to be placed on the measurement of large objects (30 feet or longer).

## 1.2 Work Requirements

### 1.2.1 Experiments to be Performed

A series of radar backscatter measurements shall be performed at the following ranges.

- a) Conductron Corporation, Ann Arbor, Michigan
- b) Radiation Incorporated, Melbourne, Florida
- c) General Dynamics, Fort Worth, Texas
- d) RAT SCAT, Holloman AFB, New Mexico
- e) Micronetics, San Diego, California
- f) Air Force Avionics Laboratory, Wright-Patterson AFB, Ohio.

Measurements shall be performed on five cylinders at the frequencies shown in Table I-1. The frequency tolerance is  $\pm 0.1$  percent. Four polarization combinations, HH, VV, HV, and VH shall be required at all frequencies and both phase and amplitude data shall be recorded for all facilities which have the needed polarization and phase capabilities. Amplitude and phase information is to be provided as a function of target aspect angle through  $360^{\circ}$  about a plane containing the longitudinal axis of the model. In addition to the analog data, digital data is to be recorded in the finest increments of aspect and amplitude normally available from each of the several ranges. In all cases, measurements are to be made for a single, specified roll angle for the cylinders. Measurements at the Air Force Avionics Laboratory shall be limited to the 1/8 and 1/16 scale cylinders at 1360 and 2720 MHz.

### 1.2.2 Models

The Contractor (The University of Michigan) shall provide five cylinders, the largest of which is to be 32 feet long and 5 feet in diameter. The other four cylinders are to be 1/2, 1/4, 1/8 and 1/16 scale models of the largest cylinder.

1.2.3 Theoretical Computations

The Contractor shall compute expected radar cross section for each of the cylinders under the experimental frequencies and polarization conditions specified. To avoid duplication, the results of a parallel contract, AF 33(615)-3166, with the Norair Division of Northrop Corporation shall be used to the maximum extent possible.

1.2.4 Data Analysis

The Contractor shall perform an analysis of all data using the technique most appropriate for the attainment of the stated objective. Comparisons shall be made between measured data and theoretical calculations, between similar measurements at different ranges, and between full size and scaled measurements.

Comparisons shall be made of the total performance of the several ranges and any special measurement capabilities that are demonstrated should be noted.

TABLE I-1  
 FREQUENCY-SCALE MATRIX FOR CYLINDER TESTS  
 SHOWING RESULTING  $ka$  VALUES

Scale Frequency (MHz)	(32' Full	(1/2)	(1/4)	(1/8)	(1/16)
170	2.72	1.36	—	—	—
340	5.44	2.72	1.36	—	—
680	10.9	5.44	2.72	1.36	—
1360	21.7	10.9	5.44	2.72	1.36
2720	—	21.7	10.9	5.44	2.72

Explanations are needed for the meaning of the polarization terminology and the significance of Table I-1. The polarization terms HH and VV are the co-polarized and VH and HV are the cross polarized symbols. Here V and H refer to the orientation of the electric field vector relative to the ground; V indicates that the E field is vertical and H that it is horizontal. The first letter represents the polarization of the transmitting antenna and the second letter that of the receiving antenna.

Table I-1 is a summary of the frequency and size relationships and the  $ka$  values for each frequency - scale combination for which tests are performed;  $k$  is the wave number  $2\pi/\lambda$ ,  $a$  is the cylinder radius and  $\lambda$  is the incident wavelength. The five cylinders vary in length from 2 feet (1/16 scale) to 32 feet (1/1 scale) and the five frequencies vary from 170 MHz to 2720 MHz. These model sizes and frequencies are combined to produce five electric circumferences ( $ka$ ): 1.36, 2.72, 5.44, 10.9 and 21.7. This range in  $ka$  extends from the resonant region (1.36 and 2.72) into the physical optics region (10.9 and 21.7) with  $ka=5.44$  being in the transition region between the two. Patterns with the same  $ka$  and polarization should have identical forms but be shifted in absolute power levels by some multiple of 6 dB, depending on the ratio of the frequencies being compared. For example if the frequency ratio is 2 to 1 there is a 6 dB difference in power levels, if the ratio is 4 to 1 the difference is 12 dB, and so on.

### 1.3 Some Difficulties in Evaluating Radar Ranges

There are no formal standards set forth by recognized authorities by which radar cross section ranges can be evaluated because of the large variety of shapes that range customers need measured as well as the number of conditions under which the measurements can be made. An obvious standard might be the comparison of theory and experiment for a body whose scattering behavior is known exactly enough to be considered a standard, but, aside from the sphere, such a body is hard to come by. In subsequent portions of this report, we assume that the cylinder is understood well enough to be a standard in this context, but the reader will soon see deficiencies even in this simple model. Furthermore, even if the "standard" target is agreed upon, there arises the question what constitutes standard performance. Obviously, it is not logical to demand that a given range measure a given target with an accuracy of  $\pm 1$  dB without specifying if this figure applies to a 20 dBsm scatterer or a -10 dBsm scatterer, or if it applies to a flat plate or to a cone-sphere, or if it is to hold at 3000 MHz or at 300 MHz, or if it refers to the peak values of the static pattern or those on the slope of the fourth sidelobe. Range standards clearly involve many more parameters than we were able to investigate in this project.

Evaluation of the range data was colored by our concept of a typical range user. Being users of our own experimental facility, we had pre-conceived ideas how to judge the patterns the facility produces. Firstly, one looks for a calibration level and decides if the scatterer that produced it is an acceptable one, Secondly, one examines how well the pattern itself was centered on the grid of the paper. Then, because the target usually has features of symmetry, one folds the chart paper in half and holds it up to the light to verify symmetry in the recording itself. Further evaluation proceeds to finer and finer examination; sidelobe levels are checked against theoretical predictions if the body is simple enough, null depths are examined, and null locations compared about the points of symmetry. Near field effects are potential sources of degradation and missing sidelobes signal this possibility. As "typical" range users, we thought these were some of the possible ways data could be evaluated if time and resources permitted.

But the evaluation of data in truth depends upon the use to which it will be put. If one is designing a radar to be used to detect a class of objects, it is the level of expected cross sections one seeks to know and the measurement of specular echoes with an accuracy of 3 dB could well be sufficient. One might wish to develop a discrimination scheme that depends upon the number of nulls in a pattern, so that amplitudes are even less important. On the other hand, if range data are to be used for scattering matrix investigations, better accuracy is desired and the data should be recorded in digital form. Since we cannot foresee all the uses of the data from a typical radar cross section range, we will develop a generalized, as opposed to a specific, approach.

Throughout the report we present details of performance in such a way that the reader can assign his own rating if he disagrees with our ratings. We give tables listing, for example, the number of errors less than one dB that a given range produced for a given target at a given frequency; we assign a rating to that performance, but the reader is free to assign his own rating, depending upon his concept of the accuracy of the data he would need.

#### 1.4 Evaluation Procedures

An enormous amount of data were collected during the course of the range evaluation program. Seventy-two cross and co-polarized measurements were made on the five cylinder targets at each range to produce a total of 360 separate backscattering patterns for evaluation. One of the larger and more important tasks in this program was to determine efficient, informative, and accurate methods for reducing and presenting the raw scattering data. Unfortunately it is difficult for more than a few people at a given time and place to agree on universal and identical definitions for the three underlined adjectives in the previous sentence. As in many practical problems the underlined adjectives contradict one another in their extremes and a trade-off is necessary to achieve an optimum satisfaction of all three at the same time. What is optimum for one situation is not necessarily so for another and herein lies the problem of obtaining a universal evaluation process. Even if the reader disagrees with the methods used here we hope some of the techniques will be helpful to him in achieving a more acceptable form of evaluation.

Shortly after samples of the test patterns started to arrive in Ann Arbor, overlay comparisons were made on a light table between similar test data and between theory and measurements. Although the observer obtains much information by making the comparisons, he finds it difficult to represent the results of such a comparison unless facts and figures are recorded. In addition, we knew that patterns to be submitted by two of the ranges would have different scaling factors, thus restricting the effectiveness of direct comparisons on a light table. It appeared that whatever reduction method was used, some form of point by point recording technique would have to be developed to take the place of direct overlay comparisons. After considerable deliberation we decided to record the amplitude of pattern peaks and the angular location of pattern nulls. Heavy emphasis was placed on the lobe structure in the neighborhood of end-on and broadside angles of incidence where the only specular returns are located. Limited peak and null information was recorded in the aspect region near and about  $45^{\circ}$  also.

After 60 percent of the data were reduced and recorded in tables, some cursory examinations of these tabulations were made. We observed that there was sufficient disagreement in the end-on and broadside data alone to point out the difficulties each range had performing their tasks. Furthermore with 40 percent of the data expected to be available to us only in the closing days of the contract, we had to reduce the amount of data to be evaluated to a level which we could handle in the time allotted. After considering the surrounding circumstances we concluded that a detailed analysis of the two specular points ( $\theta = 0^\circ$  and  $90^\circ$ ) would allow us enough time to evaluate the data and at the same time sufficiently indicate the achievement of the ranges' measuring abilities for most radar applications. In our final critique of the measured data we pass judgement based largely on the amplitude of the end-on and broadside returns.

Comparison and evaluation tests are divided into two groups a) Intra-range tests and b) Inter-range tests. Intra-range tests are a comparison of scaled data from within a given range. No theoretical values are used in these comparisons. Data which should be scaled in 6 dB steps are examined and all deviations are noted. Also in the intra-range tests comparisons are made between the VV and HH returns at end-on incidence. These two values should be the same and any differences are considered errors.

In the inter-range tests measurements from all the ranges are compared with one another and theory on bar graphs. This is done for the amplitude at end-on (VV and HH together), VV broadside, HH broadside and the sidelobes immediately adjacent to broadside (VV and HH separately). Grades are assigned only to the performance at the end-on and broadside aspect positions.

For the cross polarized patterns (VH and HV) isolation comparisons are made. For pattern cuts taken in a plane of symmetry, such as in the case of these cylinder tests, theoretically there should be no cross polarized return. Thus the cylinder patterns recorded during this program should have no VH or HV return and any return that does exist is due to unwanted coupling, background or related effects. In the isolation test the maximum cross (VH or HV) returns (in dB)

are subtracted from the maximum direct (HH or VV) returns. As a rule, the maximum cross and direct returns are located near or at broadside. The larger the difference between the cross and direct returns the better the isolation. Final results showed that the isolation levels for the ranges are between 20 and 30 dB.

The measurements show that the patterns obtained by all the ranges for tests of the same model are similar in form. There are cases where differences larger than 2 dB were found between measurements of different ranges and between measurements and theory. The largest single cause of errors was near-field distortion, which occurs when the distance between the radar and the target is not sufficiently large. Near-field problems are easy to recognize and predict. For some applications, the size and rate of occurrence of the errors found in this evaluation may not be tolerable and for other applications they may be acceptable; the reader must be the final judge of this.

#### 1.5 Outline of Volume IIa Contents

The next chapter is a description of the cylinder models and the range environment in which they were tested. Chapters III through VI cover all the material related to the directly polarized VV and HH tests. Chapter VII covers all the cross polarized VH and HV tests and is similar in form to the previous four chapters. The final chapter (VIII) is the conclusion, but many additional remarks and suggestions are found in Volume I regarding the results presented here.

A further breakdown on the four chapters dealing with the directly polarized topics is as follows. Chapter III contains all the theoretical material for the VV and HH backscattering. Particular emphasis is placed on the physical optics model for calculating continuous theoretical patterns. More accurate calculations than the physical optics results are given for both polarizations at end-on and broadside aspect angles.



Experimental measurements for all the different pattern shapes encountered in the tests are shown in Chapter IV. Also shown here are samples of patterns from each of the outdoor ranges. Some of the difficulties that arose in the measurements are pointed out and analyzed.

In Chapters V and VI the procedures used to reduce and evaluate the data are discussed. Grades are assigned to each of the ranges for their performances in the various tests. These two chapters contain the main critique for the measurements.

## II

### CYLINDER MODELS AND RANGE ENVIRONMENT

The five scaled cylinders and the range environment in which they were measured are discussed in this chapter. Since part of the test program is based on a comparison of scaled frequency-model tests outlined in Table I-1, it was important that these models be carefully designed and constructed to insure that the accuracy of their dimensions would not be questioned. A short description of the ranges is given along with references to information which contain more details on each of the measuring facilities.

#### 2.1 Cylinder Models

Five right circular, aluminum cylinders were the primary models used in the evaluation program. The full scale cylinder is 32 feet long and 5 feet in diameter and the others are 1/2, 1/4, 1/8, and 1/16 scale models of the largest cylinder. A cylinder is well suited to this program since its scattering pattern can be described rather accurately for most aspect angles by readily available theoretical formulations. On the other hand, its scattering patterns are complicated enough, providing many peaks and nulls, to furnish healthy exercises for testing the ranges.

The scaled models are measured at five frequencies in such a manner as to produce a series of test results which are related to one another by multiples of 6 dB. When these measurements are compared, it is possible to check range accuracies independently of any theoretical calculations. Such tests are called intra-range tests in this report and are comparisons of scaled patterns having the same  $ka$  and polarization.

To avoid errors in the scaled measurements and in the theoretical experimental checks, high tolerances were set on the cylinder dimensions. The models were made with sufficient skin thickness and internal bracing to withstand normal handling without deformation or damage. The cylinder dimensions and specified

tolerances are given in Table II-1a. These are essentially as specified in the special instructions associated with the present contract.

The two smaller cylinders were made in The University of Michigan machine shops. The 2 foot cylinder was turned on a lathe from a solid bar of aluminum and the 4 foot cylinder was turned from a piece of standard, thick-walled aluminum tubing. No difficulties were experienced in the fabrication or in meeting the specified tolerances.

Due to the close tolerances and large size of the three larger cylinders, we found it difficult to find interested fabricators who had the capability to make the cylinders. After a careful survey a contract was awarded to Brooks and Perkins of Detroit, Michigan to design and build these three cylinders. Shortly thereafter this company experienced a work stoppage due to a strike. An effort was made to save time by the use of a subcontractor but this proved costly both in time and workmanship. After five months of delay and after a modest change in the required tolerances the cylinders were accepted and delivered. Test results indicate that the relaxed tolerances in Table II-1 b caused no problems.

The largest cylinders (32 foot, 16 foot, 8 foot) were formed by attaching pre-rolled skins to an inner framework of circular channels. The inner framework for the 32 foot cylinder included nine  $2\frac{1}{2}$ " x  $1\frac{1}{2}$ " x  $\frac{1}{8}$ " channels rolled into circles of the required diameter. The circular forms were supported by longitudinal channels and additional diagonal braces and the skin was held to the framework by a flat head rivets. The method of fabrication used for the 16 foot and 8 foot cylinders is similar except for a more simple inner framework design. For these cylinders, the rivets were countersunk into the skin in order to meet the surface roughness tolerances. The approximate weights of the 32 foot, 16 foot and 8 foot cylinders are 1300, 250 and 30 pounds respectively. Further information on the design of the cylinders is given in Figs. 2-1, 2-2, and 2-3 which are preliminary drawings of Brooks and Perkins.

TABLE II-1

CYLINDER DIMENSIONS

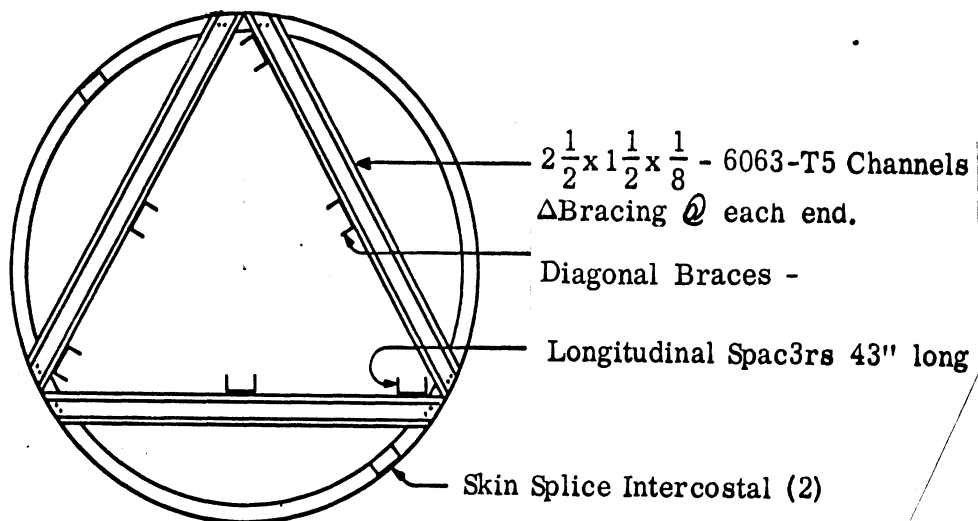
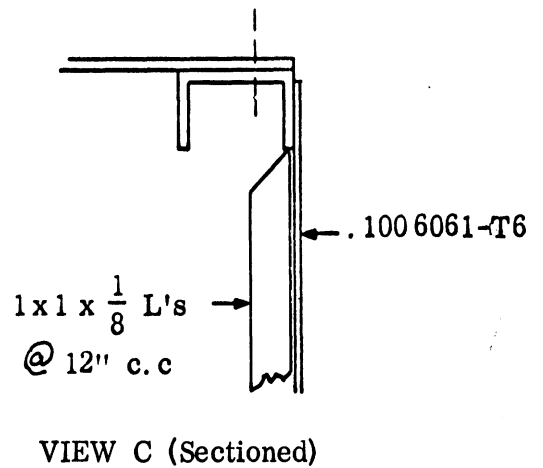
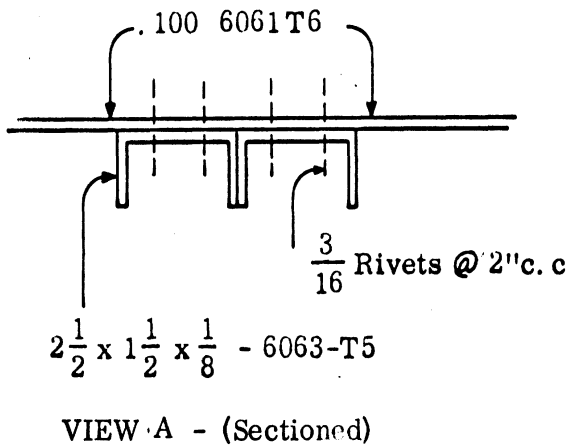
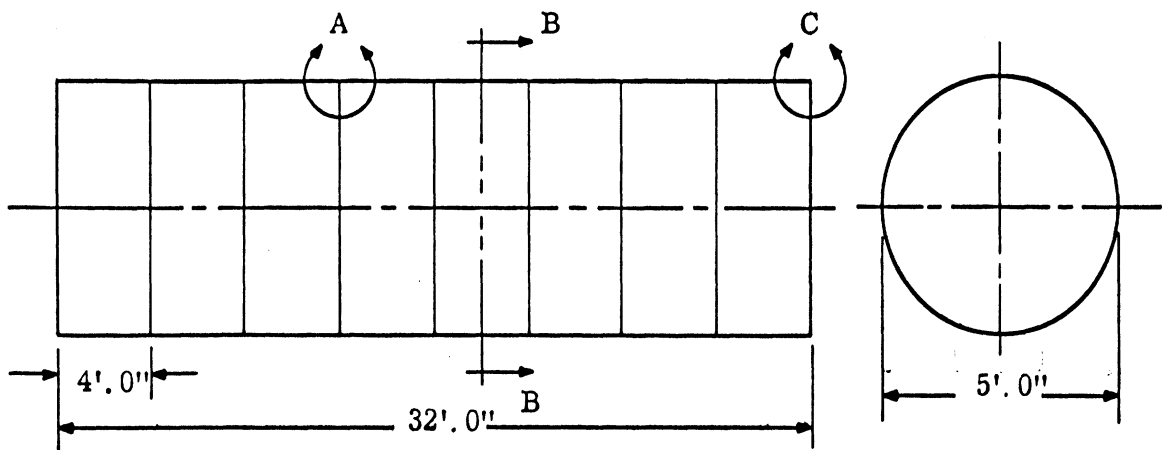
Length	Diameter <sup>+</sup> (inches)	(a) Original Tolerances		
		Surface Roughness (welds, rivet heads, etc) (inches)	Surface Irregularity <sup>++</sup> (straightness)	Skin Thickness (inches)
32' ± 1/2"	60 ± 1/4	± 0.087	± .033"/ft	0.100
16' ± 1/4"	30 ± 1/8	± 0.043	± .033"/ft	0.050
8' ± 1/8"	15 ± 1/16	± 0.032	± .033"/ft	0.050
4' ± 1/64"	7.5 ± .005	± 0.005	± .005"/ft	0.250
2' ± 1/64"	3.75 ± .005	± 0.005	± .005"/ft	0.125

<sup>+</sup> Cylinders are to be circular to within 0.1 percent of diameter.

<sup>++</sup> The axis of the cylinder is not to deviate from a straight line by more than .250, .125, .063" for the 32, 16 and 8' cylinders respectively. The ends are to be perpendicular to the cylinder axis to within 1/4°.

(b) Revised Tolerances (January 24, 1966)

	Surface Irregularities	Circularity
32' Cylinder	± 0.06"/ft	± 0.080"
16' Cylinder	± 0.043"/ft	± 0.043"
8' Cylinder	Same as above	± 0.030"

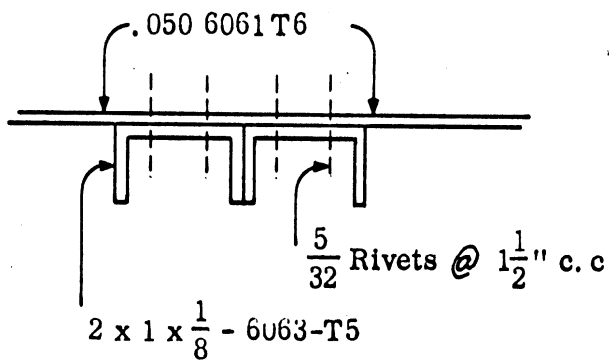
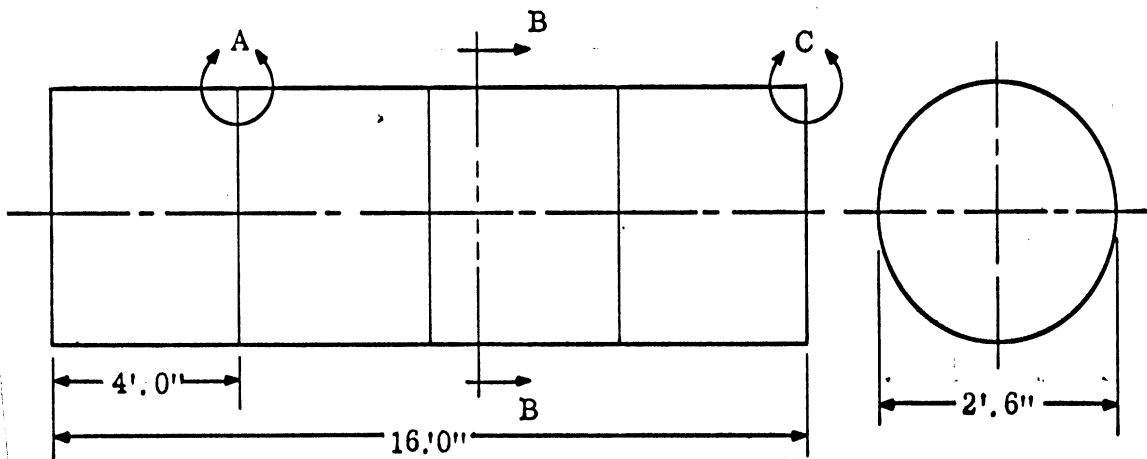


SECTION B-B

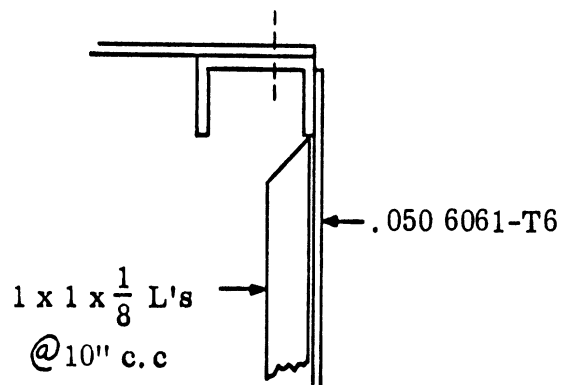
$16 - \frac{1}{4}$ " Vent Holes Required

Est. Wt. = 1280  
 Scale = None

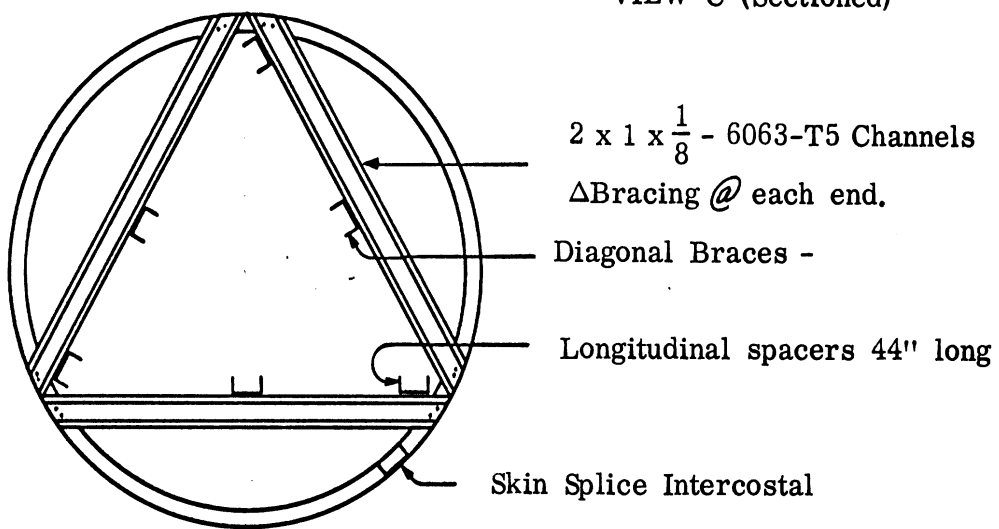
FIG. 2-1: BROOKS AND PERKINS PRELIMINARY DRAWINGS FOR 32 FOOT CYLINDER.



VIEW A - (Sectioned)



VIEW C (Sectioned)



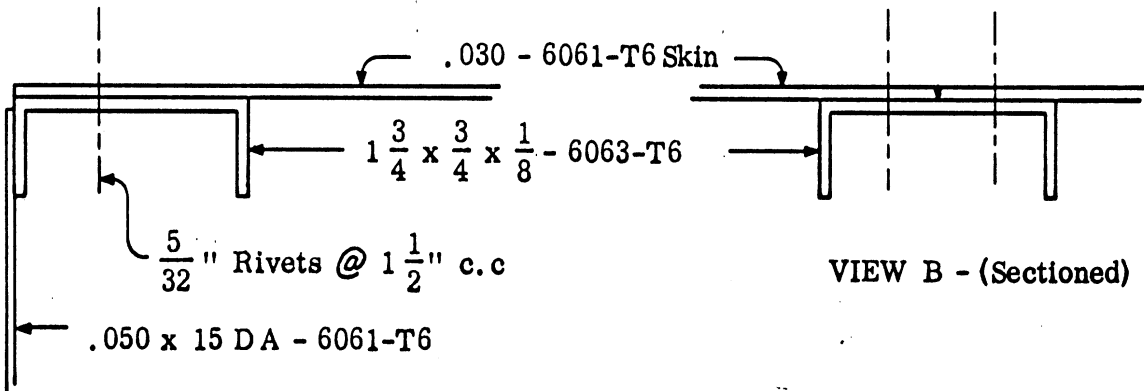
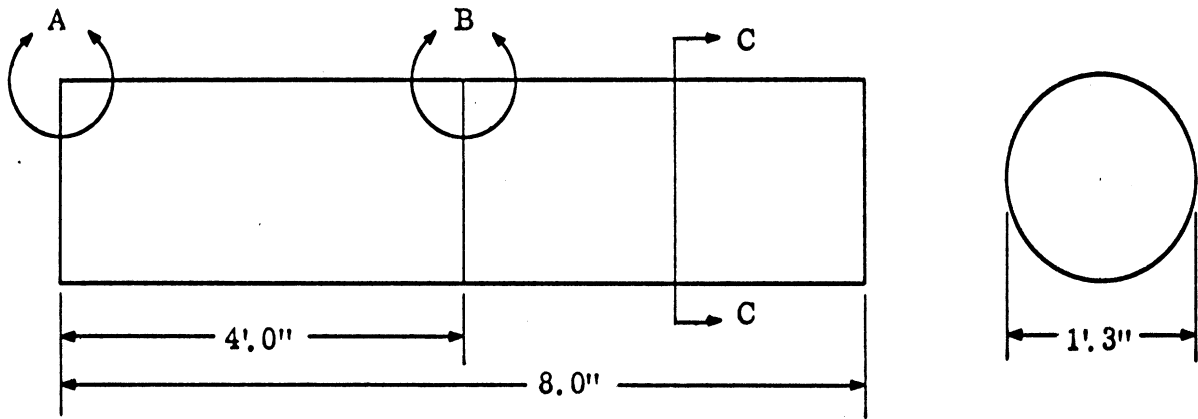
Est. Wt. = 240

Scale = None

SECTION B-B

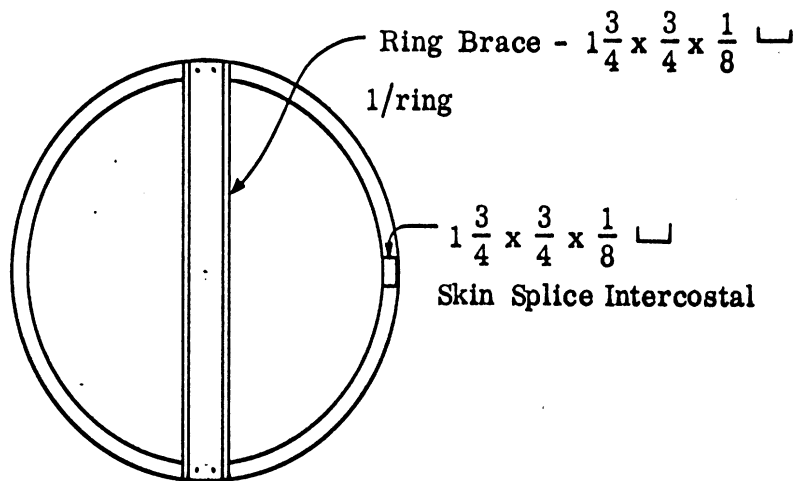
8 -  $\frac{1}{4}$ " Vent Holes Required

FIG 2-2; BROOKS AND PERKINS PRELIMINARY DRAWINGS FOR 16 FOOT CYLINDER.



VIEW A - (Sectioned)

VIEW B - (Sectioned)



Weight = 27

Scale = None

4  $\frac{1}{4}$ " Vent Holes Required

FIG. 2-3: BROOKS AND PERKINS PRELIMINARY DRAWINGS FOR 8 FOOT CYLINDER.

## 2.2 Range Environment

The typical model range geometry in which the targets were measured is shown in Fig. 2-4. In all the tests the cylinder was mounted on a pedestal with its axis in the horizontal plane. Rotation took place about the vertical axis with the aspect angle  $\theta$  being measured relative to the end-on position. For monostatic tests the transmitter and receiver are located together a distance  $R$  from the target.

With the exception of Micronetics, all the outdoor ranges made use of the ground plane geometry in their measurements. In the typical ground plane range, the antenna and target heights are adjusted so that the target is placed at the peak of the first lobe formed by the in-phase addition of the direct and ground reflected waves as shown in Bachman et al (1963). At Micronetics (Honer and Fortner, 1964) the ground reflections are minimized by a mound of asphalt in the shape of an inverted  $V$  which extends along the path between the transmitter and the target. With this arrangement the target and antenna heights are not as critically dependent on one another as in the ground plane geometry.

Conductron Corporation (Wren, 1964) uses a CW transmitter and employs a balanced RF bridge to separate the transmitted from the received signal. The other four outdoor ranges use pulse-type radar systems with pulse widths between 1.0 and 0.1 microseconds and repetition rates on the order of a few KHz. When pulsed equipment is used the transmitted and received signals are separated in time and range, making it possible to gate out unwanted returns originating outside the target area. Blacksmith et al (1965) give more details on these types of systems and measurement techniques.

Limited tests were made at the Air Force Avionics Laboratory which has an indoor facility with a maximum range of 50 foot (Bahret, 1965). Only VV and HH polarized tests were made on the 2 foot and 4 foot cylinders at 1360 and 2720 MHz.



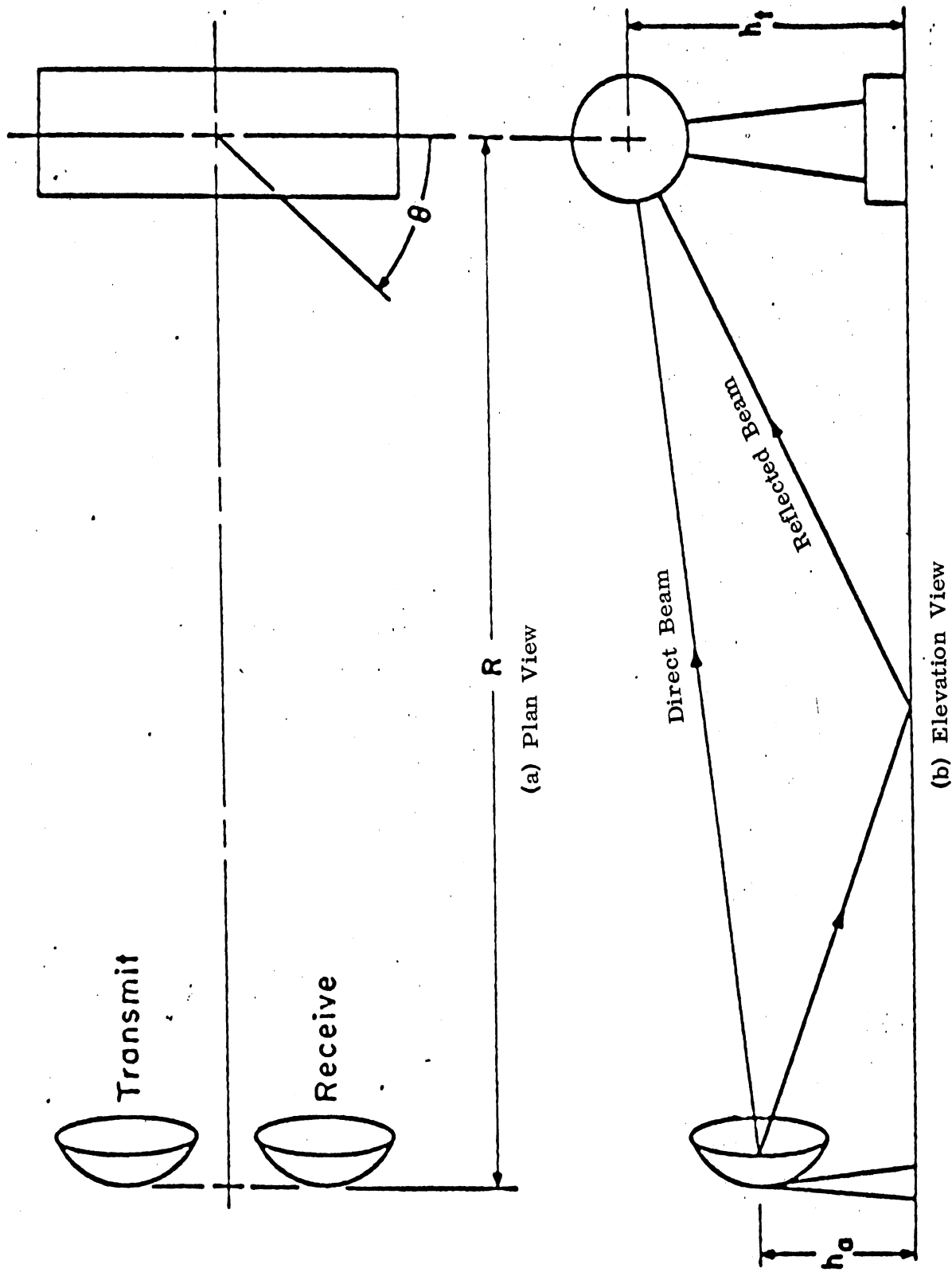


FIG. 2-4: GEOMETRY FOR TYPICAL RADAR CROSS SECTION MEASURING FACILITY.

Results from these tests are tabulated in the appropriate places, but due to the limited amount of data no final grades are assigned to this range. The overall evaluation is limited to the performance of the five outdoor facilities.

All the ranges have similar systems for recording amplitude data in analog form on rectangular pattern paper. The dynamic range of the recorders varies between 40 - 50 dB depending on the facility (see Table II-2). Digital data is also recorded and at two of the ranges phase information is recorded. The type of equipment used at each range is indicated in the same table.

In order for the target to be in the far field (Fraunhofer zone) the distance  $R$  between the transmitter and target should be  $R \geq 2L^2/\lambda$  where  $L$  is the maximum dimension of the target and  $\lambda$  the incident wavelength. The maximum  $R$  needed for the schedule of tests given in Table II-2 is about 2900 foot for the case where the 32 foot cylinder is measured at 1360 MHz. The actual ranges used and/or available at each facility are given in the table under "Maximum Range Used". Later, an example is presented showing the effects of insufficient range on measured data.

Since complete descriptions of the ranges to be evaluated are not given in this report, it is appropriate to cite additional references which provide descriptions of all ranges. The facilities and capabilities of the Radiation Incorporated range are described by Landfried and Williamson (1964). This range is the oldest of those being evaluated and during the tests it was operated by Radiation Service Company, a subsidiary of Radiation Incorporated. This facility is now operated by Sigma Incorporated and is described in their 1968 Company Brochure. A description of the General Dynamics/Fort Worth range is given in its brochure (GD/FW 1968). The RAT SCAT range is the newest facility being evaluated and is described in some detail by Marlow et al (1965). Additional information on measurements already made and on operating procedures is given in an Air Force brochure (AFMDC 1968). For more recent information on the Conductron and the Micronetics ranges the reader is referred to 1968 Company Brochures.

TABLE II-2  
SOME CHARACTERISTICS OF THE SITES

Site	Transmitter	Maximum Range Used*	Geometry	Data Recorded		Digital Equipment
				Type	Dynamic Range	
Conductron	CW	200'	Ground Plane	Amplitude	40 dB	Paper Tape
Radiation Service	Pulse	1000'	Ground Plane	Amplitude	40 dB	Punch Cards
General Dynamics	Pulse	1800'	Ground Plane	Amplitude Phase	50 dB 360°	Paper Tape
RAT SCAT	Pulse	1200'	Ground Plane	Amplitude Phase (L-band)	50 dB 360°	Paper Tape
Micronetics	Pulse	600'	Direct " $\Delta$ "	Amplitude	40 dB	Magnetic Tape
Avionics Laboratory	CW and Pulse	50'	Indoor Free Space	Amplitude	40 dB	None

\* Desired Maximum range 2900'

### III

## THEORETICAL BACKSCATTERING MODELS

In this chapter we discuss the theoretical models that were used to study and calculate the backscattering behavior of finite circular cylinders for VV and HH polarizations. Lest anyone be led astray and believe that there is an exact mathematical formulation available for determining the expected cross section of finite cylinders, let us state most emphatically that there is no such solution for this problem. All the techniques discussed here are approximate. Since there is no exact solution, precise limits of accuracy cannot be assigned to the approximate methods. Estimates of accuracy are made for those theoretical techniques which are used to evaluate the experimental data and these estimates are based on experience in dealing with both experimental and theoretical material for finite cylinders.

Continuous patterns for aspect angles between 0 and 90° are calculated for all five values of  $ka$  for the cylinders. For the two lower values (1.36 and 2.72) separate patterns for VV and HH polarization are given since for these cases the polarization differences are more noticeable. As  $ka$  grows larger, polarization differences in VV and HH patterns become smaller. For the larger values of  $ka$  (5.43, 10.86 and 21.72) the polarization differences are sufficiently small to represent the VV and HH patterns with the same theoretical pattern for most applications. Thus the physical optics model, which is developed in the Appendix, is used to determine the theoretical patterns for the three larger  $ka$  cases. This model becomes meaningful for large values of  $ka$  where the VV and HH patterns tend to look alike.

Particular emphasis is given to the calculation of the cross sections at end-on and broadside aspect positions, because these results are compared directly with experimental tests in later chapters. We estimate, based on experience, that these results should be accurate to within  $\pm 1.0$  dB. A more detailed discussion of the relationship between theory and experiment is given in the last section of Chapter IV.

### 3.1 Backscattering from Cylinders

The theoretical techniques used to analyze the radar cross section behavior of the cylinders are:

- a) Numerical solution to the integral formulation for the scattered field (Oshiro, 1967).
- b) Keller's geometrical theory of diffraction (Bechtel and Ross, 1966).
- c) Traveling wave approximation (Fisher, 1967).
- d) Phasor addition of physical optics contributions from a cylinder and disc.
- e) Separation of variables in two dimensions for a cylinder (Mentzer, 1955).
- f) Andrejewski's solution for backscattering by a conducting circular disc (Schmitt, 1959).

We employed all the models except (b) at one time or another to produce continuous patterns and/or to calculate precise cross sections at specific aspect angles. In particular, we used methods (a), (c) and (d) to generate continuous scattering patterns for aspect angles between 0 and 90° and used methods (e) and (f) to calculate cross sections only at broadside and end-on aspect positions.

The integral equation approach (a) is used to calculate cross sections in the resonant region ( $ka=1.36, 2.72$ ) where the differences in VV and HH polarized patterns are noticeable. This is a numerical technique for evaluating an integral equation representation for electromagnetic scattering. For  $ka$  values equal to or greater than 5.43 the computer time and memory requirements tend to become prohibitive in the numerical solution for this formulation, and other approaches to the problem such as methods (b) and (d) become more practical. Norair Division of Northrop Corporation developed the numerical technique called the Source Distribution Technique (SDT) and results from SDT were obtained for this evaluation program through the Air Force Avionics Laboratory. A description of the mathematical development and computer program can be found in a series of reports by Oshiro (1965, 1967).

Complete data from the SDT program was supplied only for VV and HH polarization for  $ka=1.36$ . Partial results were furnished for  $ka=2.72$  and  $5.43$  but these datum points were not sufficiently close together to construct continuous patterns. Fortunately, Fred Fisher (1967) of Radiation Service Company developed a traveling wave model (c) for VV and HH patterns for  $ka=2.72$ . Fisher's technique incorporates portions of methods (d) and (e) along with a traveling wave contribution for HH polarization. Although method (c) is not as accurate as the numerical approach of (a), it does show the salient features of the VV and HH patterns.

Method (d), the phasor addition of the physical optics contributions for a cylinder and disc, is discussed in detail in the Appendix. This formulation becomes more accurate for increasing values of  $ka$  (see Ch. IV). Continuous patterns for  $ka=5.43, 10.86$  and  $21.72$  are obtained for this model.

The last two techniques, (e) and (f), are used to calculate cross sections for all  $ka$  values and both polarizations at broadside and end-on aspect positions. In the last section of this chapter plots of cross section versus  $ka$  curves are given for the 32-foot cylinder based on these models. The cross sections of the other four scale models are found by subtracting the appropriate number of 6dB increments from the full scale values. Broadside and end-on cross sections are displayed in tables for all the cylinder models.

### 3.2 Cylinder Scattering Patterns

Ordinarily ten theoretical patterns would be necessary to describe all the experimental scattering configurations for VV and HH polarizations which arise during the cylinder measurements if they are normalized to the square of the wavelength ( $\lambda^2$ ). Mathematically, this corresponds to casting the scattering expression into a form like that in Eq.(A-14) in the Appendix. The ten patterns consist of VV and HH data for the five  $ka$  cases. Both polarized patterns are presented for  $ka=1.36$  and  $2.72$ . In the cases of the three larger  $ka$  values, the physical optics formulation was used to calculate the cross section data; thus the VV and HH theoretical patterns are the same. Because of this, seven

patterns instead of ten are needed to describe the scattering behavior of the cylinder tests. One phase pattern for  $ka = 5.43$  is shown and it was obtained from Eq. (A.16).

The parameters for the five cylinder and frequency combinations are:

Case	1	2	3	4	5
$ka$	1.36	2.72	5.43	10.86	21.72
$k\ell$	17.4	34.8	69.6	139.2	278.4

In all cases the cylinder dimensions are such that  $k\ell = 12.8 ka$ . Figures 3-1 through 3-5 present the scattering functions for  $\sigma/\lambda^2$  in dB as a function of aspect angle  $\theta$ . It is sufficient to display  $90^\circ$  of the pattern because of the target symmetry;  $\theta = 0^\circ$  is the end-on and  $\theta = 90^\circ$  is the broadside aspect position.

For Case 1 the VV and HH patterns are given in Fig. 3-1. Some noticeable differences in the two polarizations are the deeper nulls in the HH pattern and 3 dB higher broadside ( $\theta = 90^\circ$ ) return in that pattern. These patterns were obtained from the SDT (Oshiro, 1967) program through the Air Force Avionics Laboratory. Later experimental data from all the ranges will be superposed on these theoretical patterns.

There are still noticeable polarization differences in Case 2 (Fig. 3-2), namely the HH pattern has a significant traveling wave lobe near  $\theta = 20^\circ$  and a 2 dB higher broadside ( $\theta = 90^\circ$ ) return compared to the VV pattern. These patterns are based on Fisher's work (1967), method (c). These results do not agree as well with experiment as those in Fig. 3-1.

Cases 3, 4 and 5 are given in Figs. 3-3, 3-4 and 3-5. These patterns were obtained directly from the expression (A.14) which is method (d). For these larger  $ka$  patterns, polarization differences grow smaller with increasing size. Also the pattern oscillation increases, producing more lobes to such an extent that for Case 5 in Fig. 3-5, only the lobe peaks are shown beyond  $50^\circ$ .

An example of a phase pattern is given in Fig. 3-6 for Case 3. The cross section pattern in Fig. 3-3 has been reduced to the same angular scale as the phase pattern for the sake of comparison. This example of phase data is determined by method (d), physical optics, and is shown here to demonstrate the rapid fluctuations of a typical phase pattern.

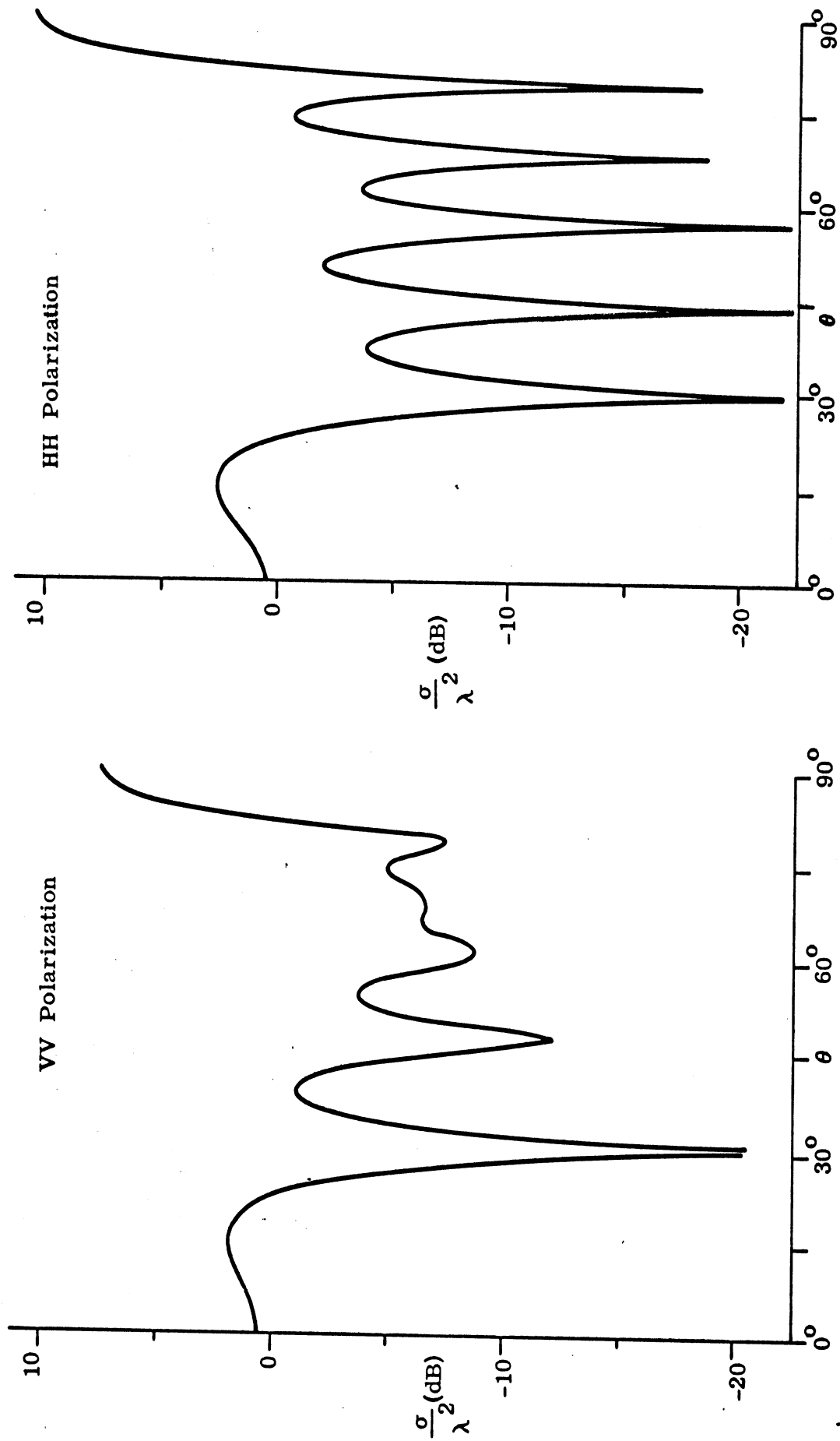


FIG. 3-1: THEORETICAL PATTERNS FOR  $k_a = 1.36$  AND  $k_l = 17.4$ .  
 Calculated by Method (a) NORAIR's SDT Method.



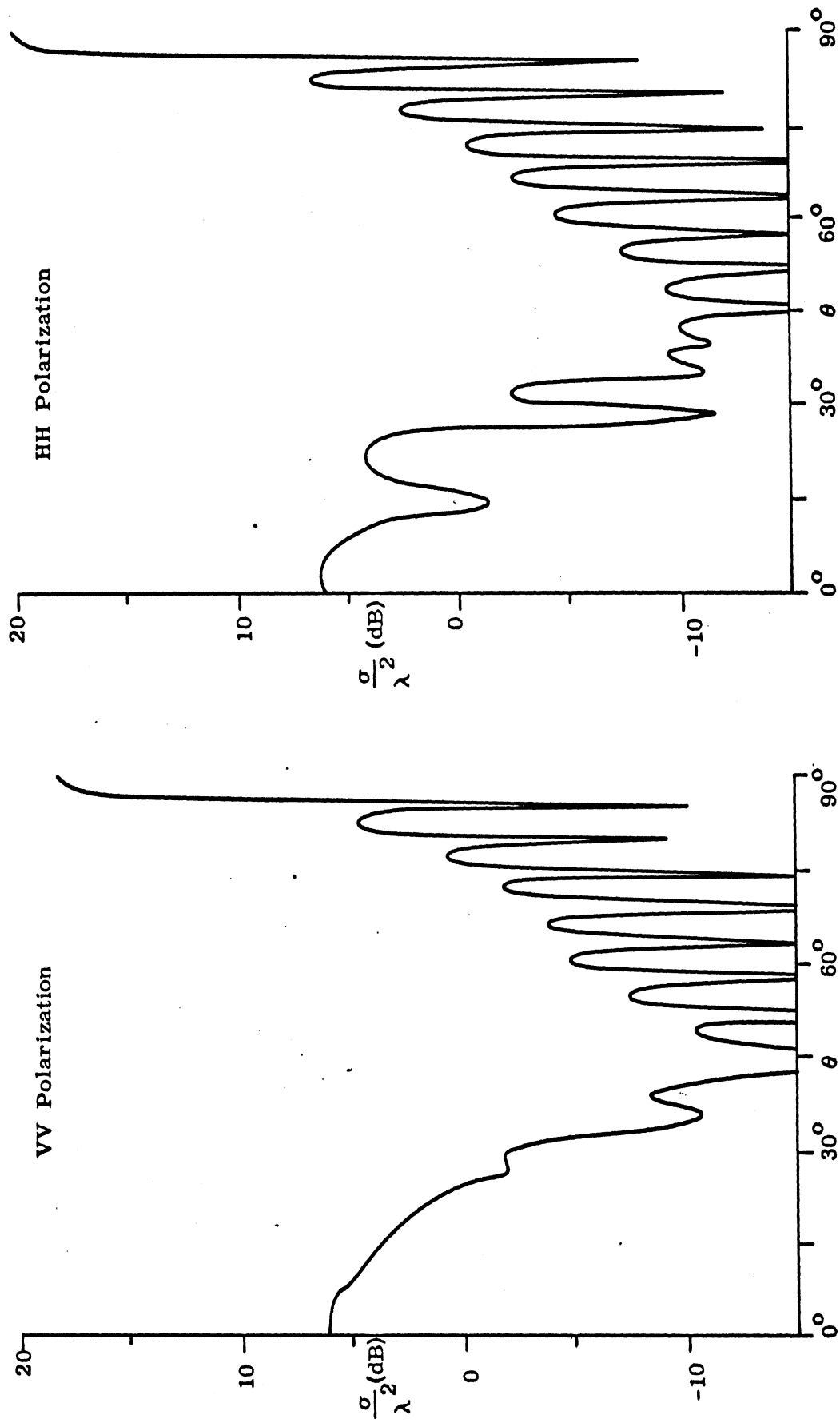


FIG. 3-2: THEORETICAL PATTERNS FOR  $k_a = 2.72$  AND  $k_l = 34.8$ .  
 Calculated by Method (c), supplied by Radiation Services.

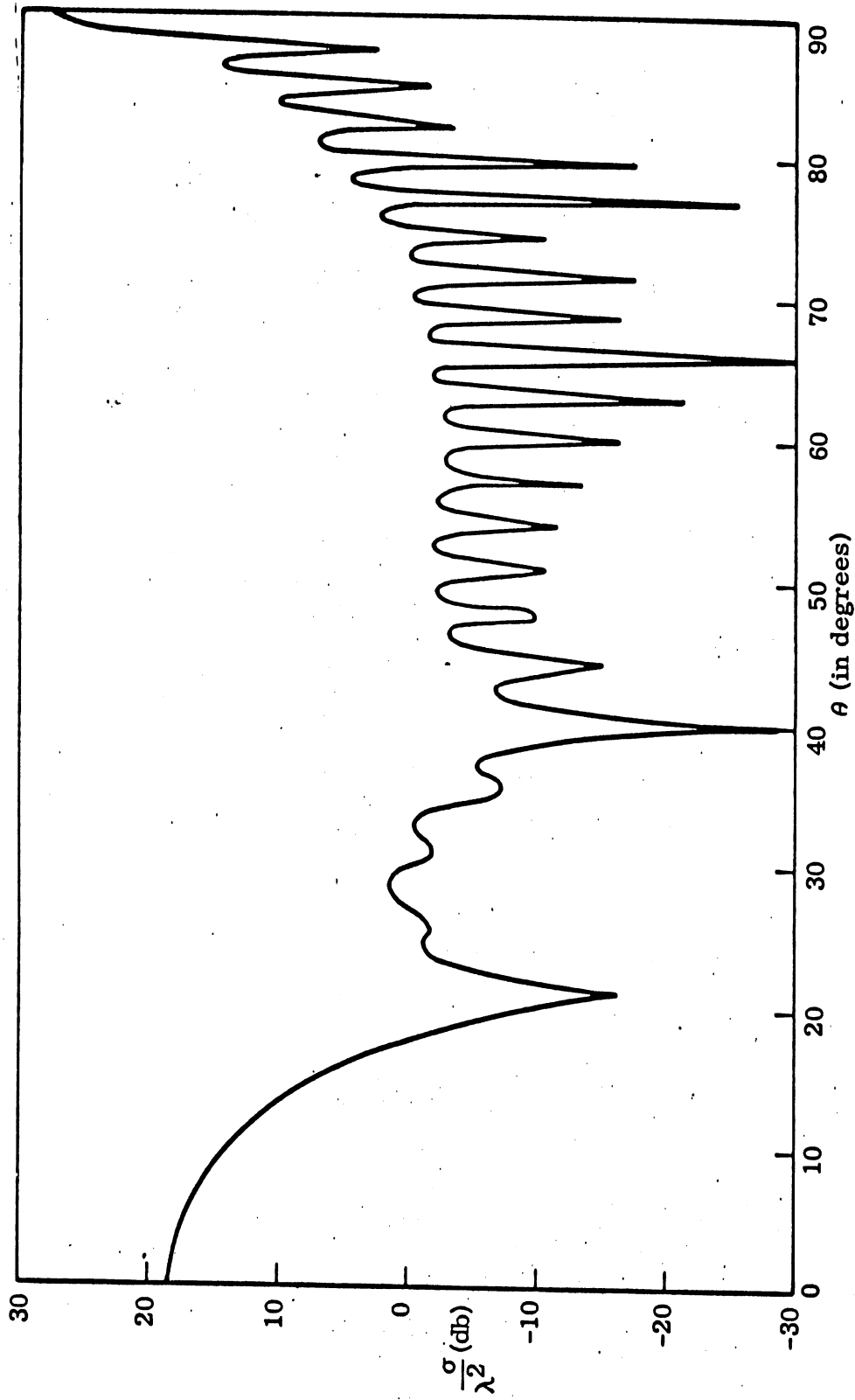


FIG. 3-3: THEORETICAL PATTERN FOR  $ka = 5.44$  AND  $kl = 69.6$ .  
 Calculated from Eq. (A. 14), Method (d) .

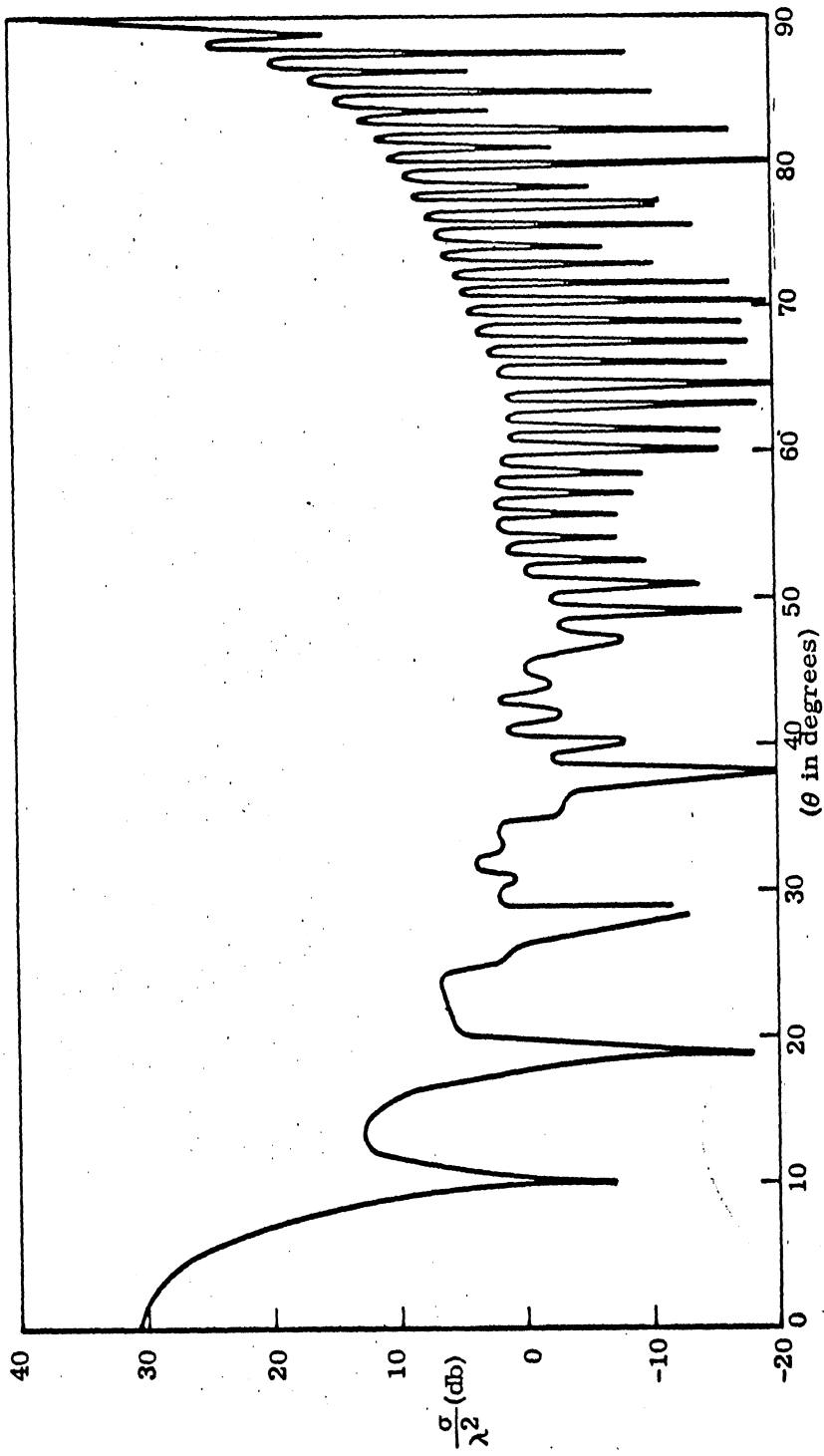


FIG. 3-4: THEORETICAL PATTERN FOR  $ka = 10.9$  and  $kl = 139.2$ .  
 Calculated From Eq. (A. 14), Method (d)

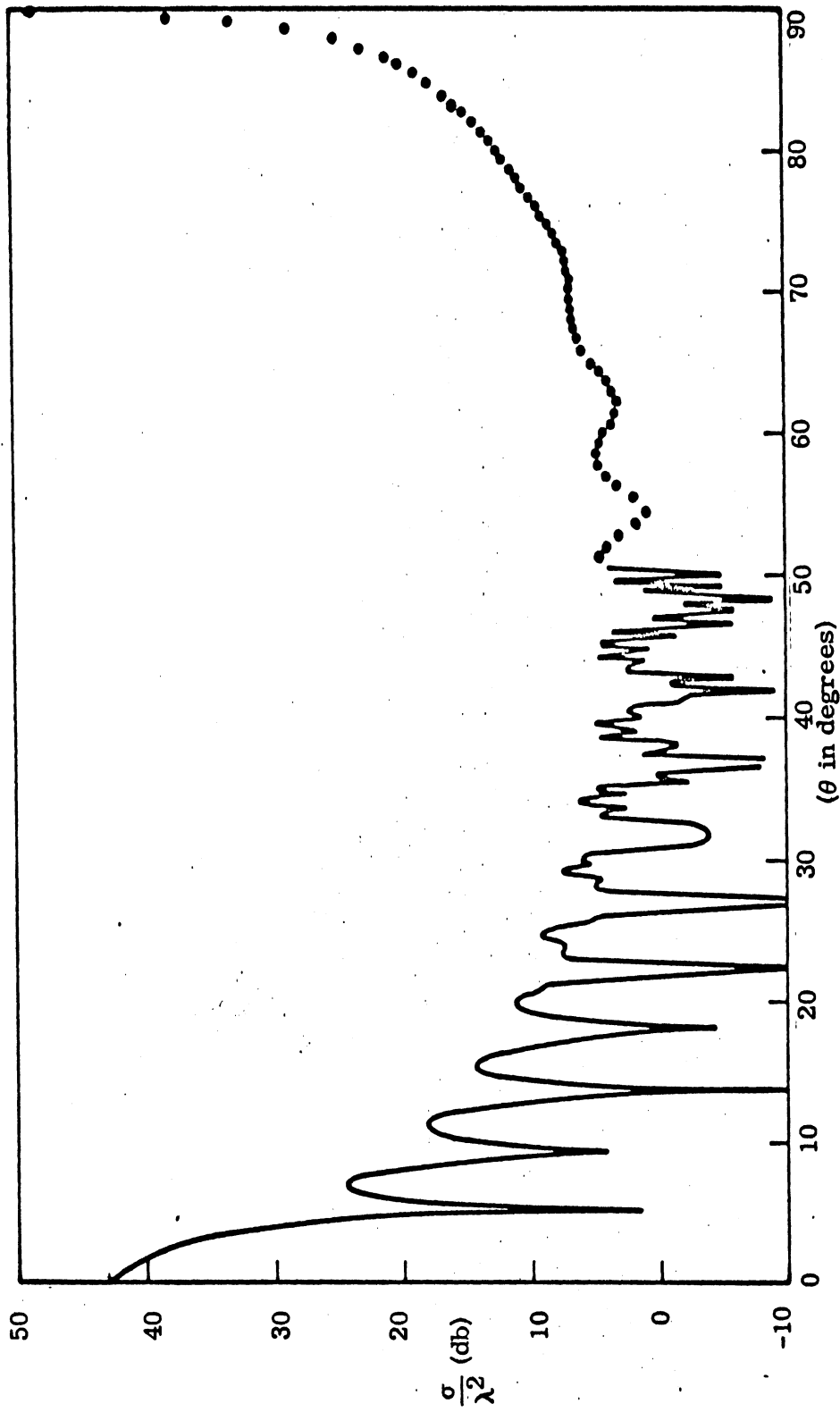


FIG. 3-5: THEORETICAL PATTERN FOR  $k_a = 21.7$  AND  $k_l = 278.4$ .  
 • Indicates peak positions for oscillations with  $0.65^\circ$  period.  
 Calculated from Eq. (A.14), Method (d).

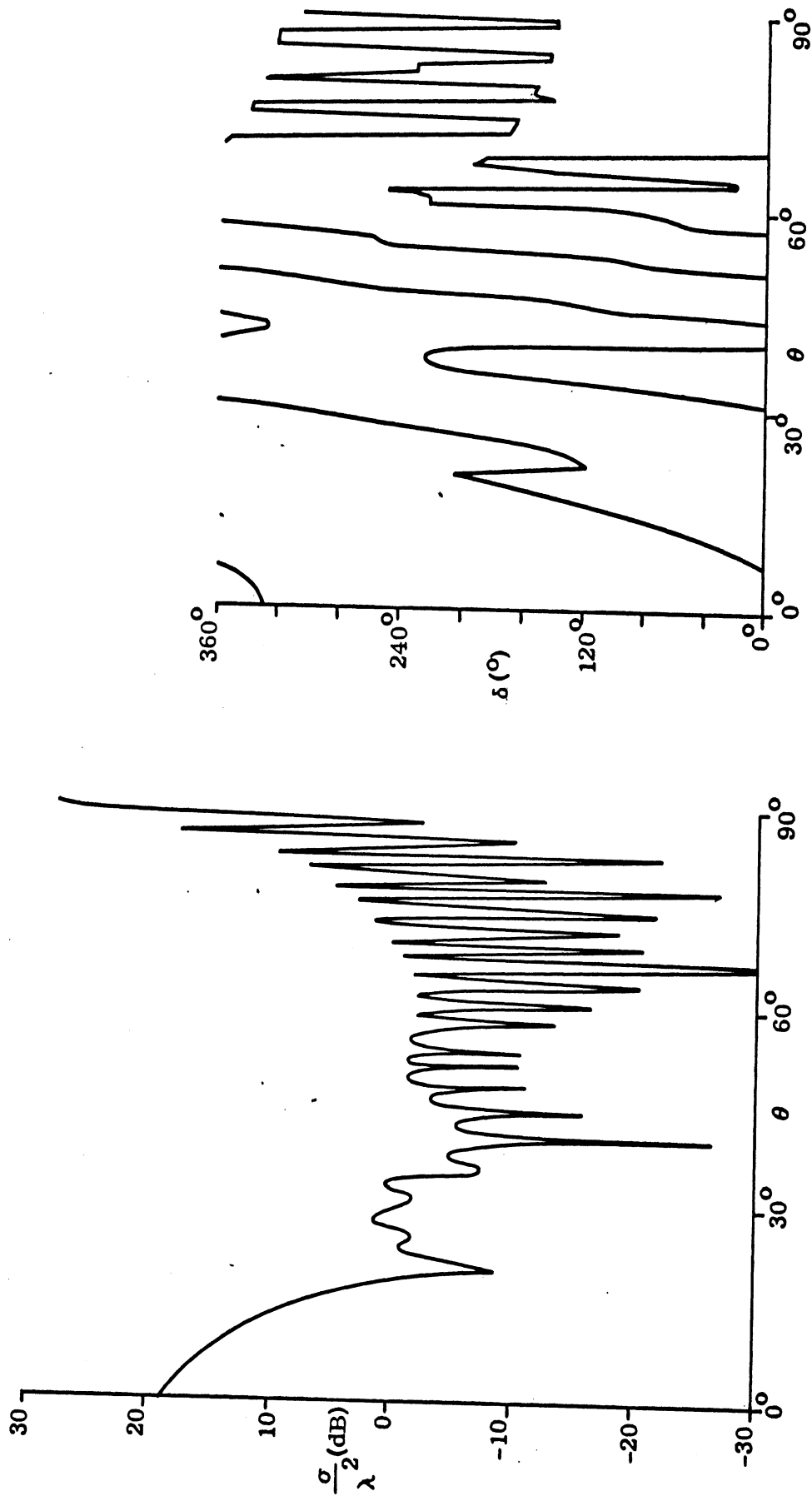


FIG. 3-6: THEORETICAL CROSS SECTION AND PHASE PATTERNS FOR  $ka = 5.43$ .  
 Calculated from Eqs. (A.14) and (A.16), Method (d)

### 3.3 End-on and Broadside Cross Sections

Detailed calculations are presented here for the cross sections at broadside and end-on and are based on methods (e) and (f). Using method (e), Mentzer (1955) obtains cross section expressions for VV and HH polarizations for a finite cylinder, which for broadside incidence, reduce to

$$\sigma_{\perp} = \sigma_{VV} = \frac{4\ell^2}{\pi} \left| \sum_{-\infty}^{\infty} (-1)^n \frac{J'_n(ka)}{H_n^{(2)'}(ka)} \right|^2 \quad (3.1)$$

and

$$\sigma_{\parallel} = \sigma_{HH} = \frac{4\ell^2}{\pi} \left| \sum_{-\infty}^{\infty} (-1)^n \frac{J_n(ka)}{H_n^{(2)}(ka)} \right|^2 \quad (3.2)$$

where  $a$  and  $\ell$  are the radius and length of the cylinder. The cylindrical functions  $J_n$  and  $H_n^{(2)}$  are the Bessel functions and outgoing Hankel functions of order  $n$ . Primes in (3.2) indicate differentiation with respect to the total argument  $ka$ . As  $ka$  increases beyond 5 or 6,  $\sigma_{\perp}$  and  $\sigma_{\parallel}$  approach the physical optics form

$$\sigma(90^\circ) = ka \ell^2 \quad (3.3)$$

which is (A.13) with  $\theta=90^\circ$ .

Plots of the expressions in (3.1) - (3.3) are shown in the upper curve of Fig. 3-7.  $\sigma_{\parallel}(90^\circ)$  and  $\sigma_{\perp}(90^\circ)$  differ in the region for  $ka < 10$ . When  $ka > 10$  they are the same as shown by the circle portion of the curve. The curves in Fig. 3-7 are cross sections in dB relative to a square meter (dBsm) as a function of  $ka$  for the 32'x5' cylinder. All other cross sections for the smaller cylinders can be derived from these curves and this will be done shortly.

The lower curve of Fig. 3-7 is the cross section of a circular flat plate or disc obtained from method (f) by Schmitt (1959). It is noted that the end-on view ( $\theta=0^\circ$ ) of the finite cylinder is a disc connected to the cylinder, whereas the theoretical curve in Fig. 3-7 is for a disc alone. For the smaller  $ka$  values it is to be expected that the disc model is less accurate than the broadside cylinder model, but it is the best theoretical method available for the end-on view.

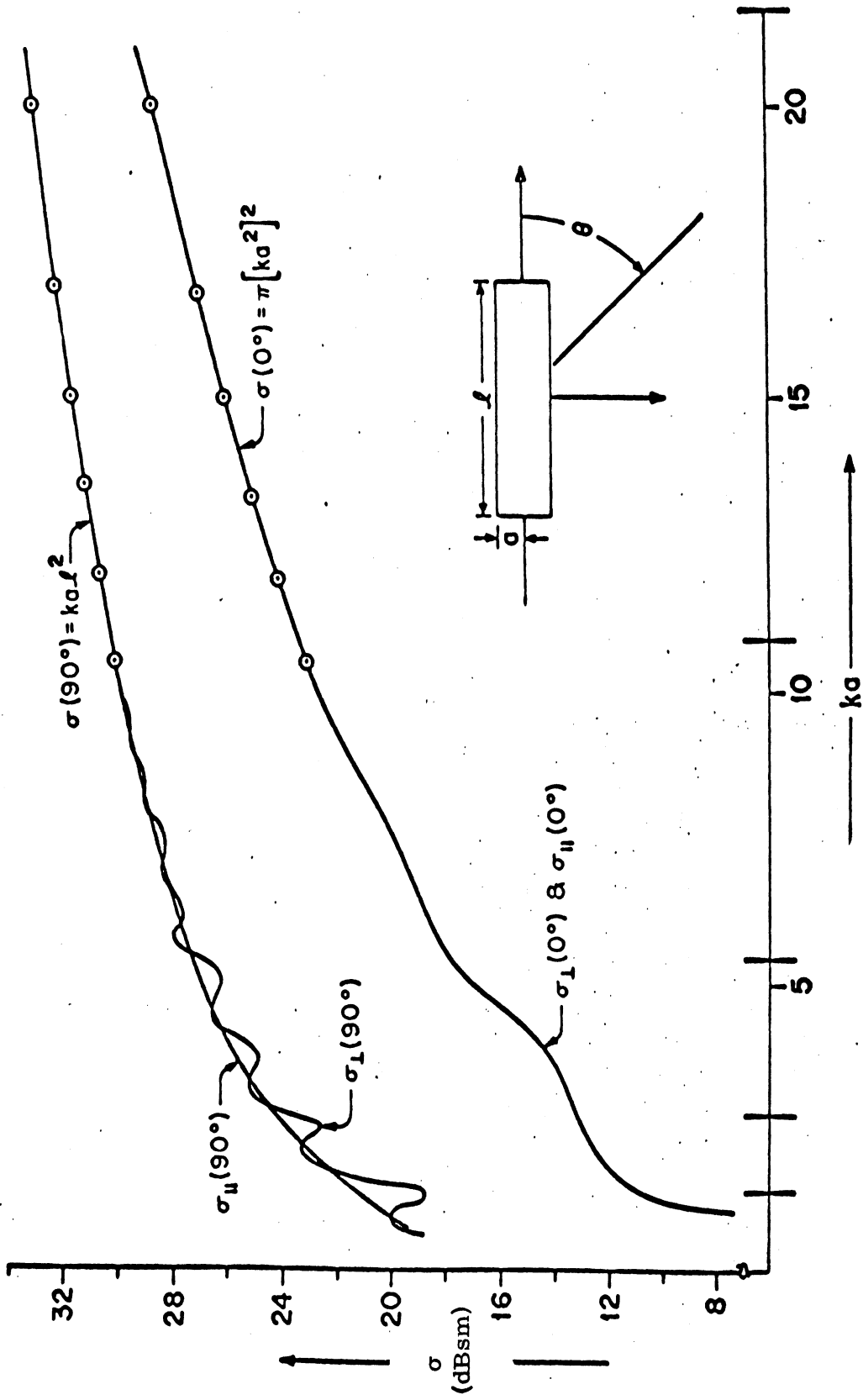


FIG. 3-7: THEORETICAL RADAR CROSS SECTION VALUES AT END-ON AND BROADSIDE FOR 32' x 5' CYLINDER. Method (e) was used to obtain the upper curve and Method (f) the lower curve.

Schmitt's technique is an extension of Andrejewski's thesis done at Technische Hochschule in Aachen, Germany in 1952. The form of the solution is uncommon and complicated; only the curve in Fig. 3-7 is presented here. The interested reader is referred to the article by Schmitt (1959). For the entire range of  $ka$ , the end-on cross section is independent of polarization:  $\sigma_{VV} = \sigma_{HH}$ . When  $ka$  is large enough ( $ka > 10$ ) the physical optics ( $\theta = 0^\circ$  in Eq. A. 13) expression is valid

$$\sigma(0^\circ) = \pi a^2 (ka)^2 \quad . \quad (3.4)$$

This portion of the curve is indicated by the circles.

A display of all the theoretical cross sections for the cylinder models at end-on and broadside for VV and HH polarizations is given in Table III-1. The display is arranged as a function of frequency and model size with constant  $ka$  along the diagonal lines connecting the boxes. The full scale values are the same as those in Fig. 3-7 which were obtained from methods (e) and (f). Although the 32-foot model (1/1 scale) was not tested for  $ka = 1.36$ , these values were also noted. The cross sections for the 16-foot model (1/2 scale) are found by subtracting 6 dB from the full scale cross sections with the same  $ka$ . This procedure holds for going from the 1/2 to the 1/4 scale and so on. Thus, as one moves down a constant  $ka$  line there are successive 6 dB reductions in the cross sections for each smaller model.

It would be reasonable to ask why both polarizations for end-on were listed in the table if they are always equal. This was done here because later the same type format will be used to display the experimental data in the intra-range test. By introducing the form of Table III-1 at this time, we allow the reader to become familiar with it. It will be seen that in the experimental results, the end-on cross sections for VV and HH differ by varying amounts which, of course, is an indication of error.



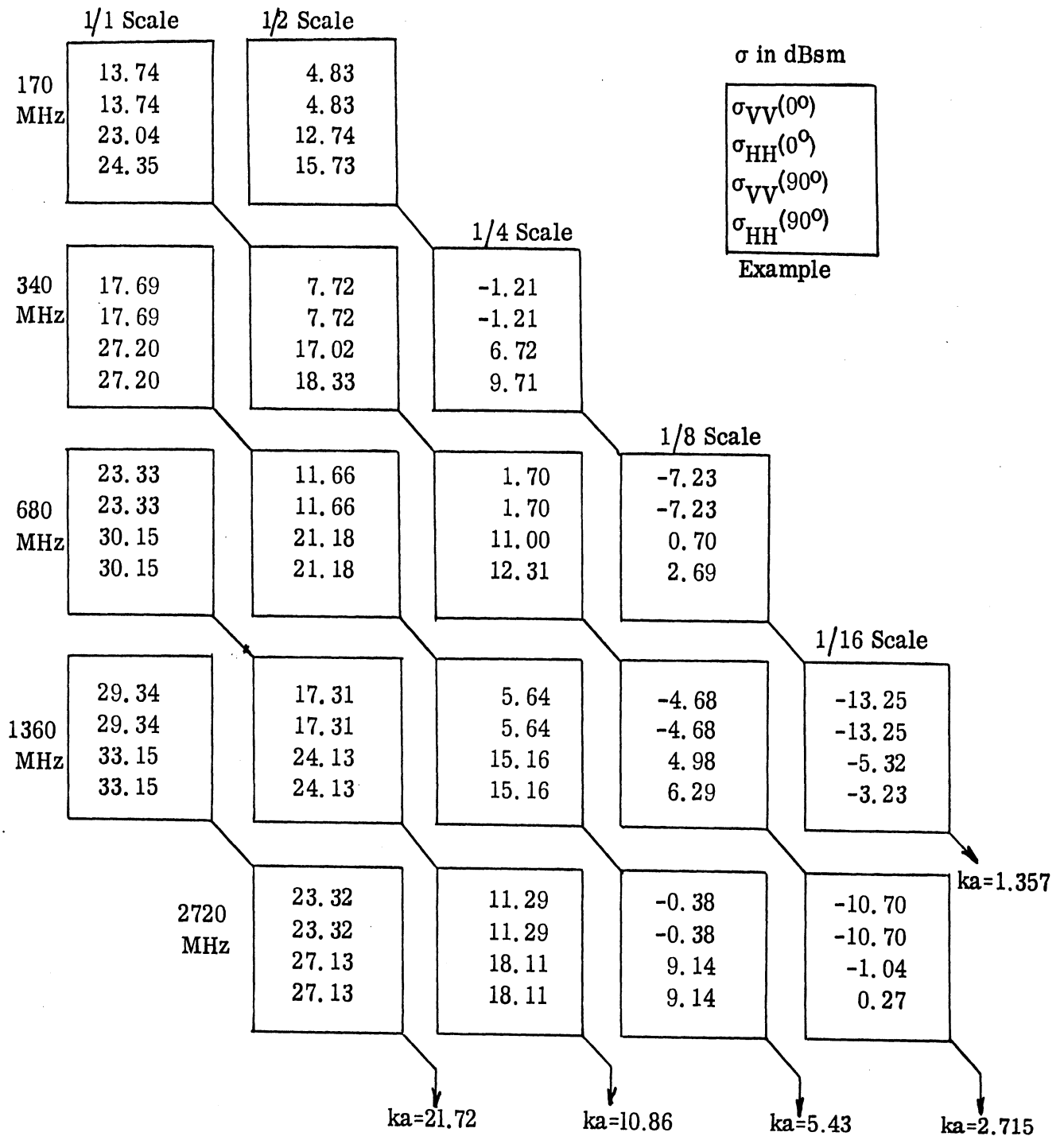


TABLE III-1: INTRA-RANGE DATA DISPLAY FOR THEORETICAL CROSS SECTIONS AT END-ON AND BROADSIDE.

The data in Table III-1 is presented in still another form to give the reader a preview of the inter-range data display. Figures 3-8 through 3-10 are plots of cross section (dBsm) versus frequency of the end-on, broadside VV, and broadside HH theoretical values. Note that the frequency scale is compressed in these figures. The cylinder size and constant  $ka$  lines are labeled in the figures. This form of display will be used for the comparison of experimental data from all the ranges and for comparison of experimental data with theory.

In this chapter all the necessary theoretical models were described to give the proper physical picture of the scattering behavior of cylinder targets and to obtain accurate cross section values for evaluating the experimental data in later chapters.

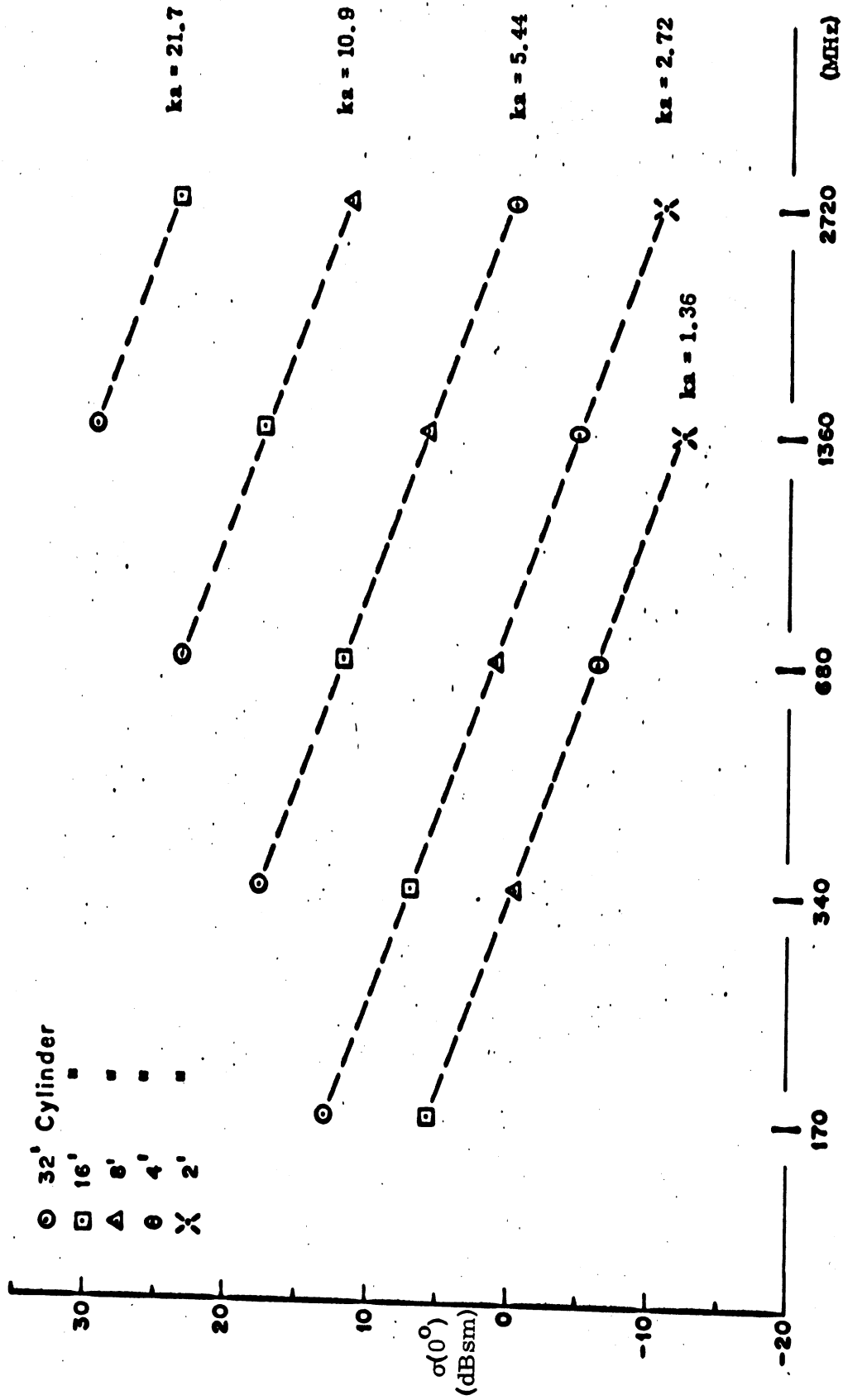


FIG. 3-8: THEORETICAL RCS OF CYLINDERS AT END-ON FOR VV AND HH POLARIZATIONS, INTER-RANGE DISPLAY.

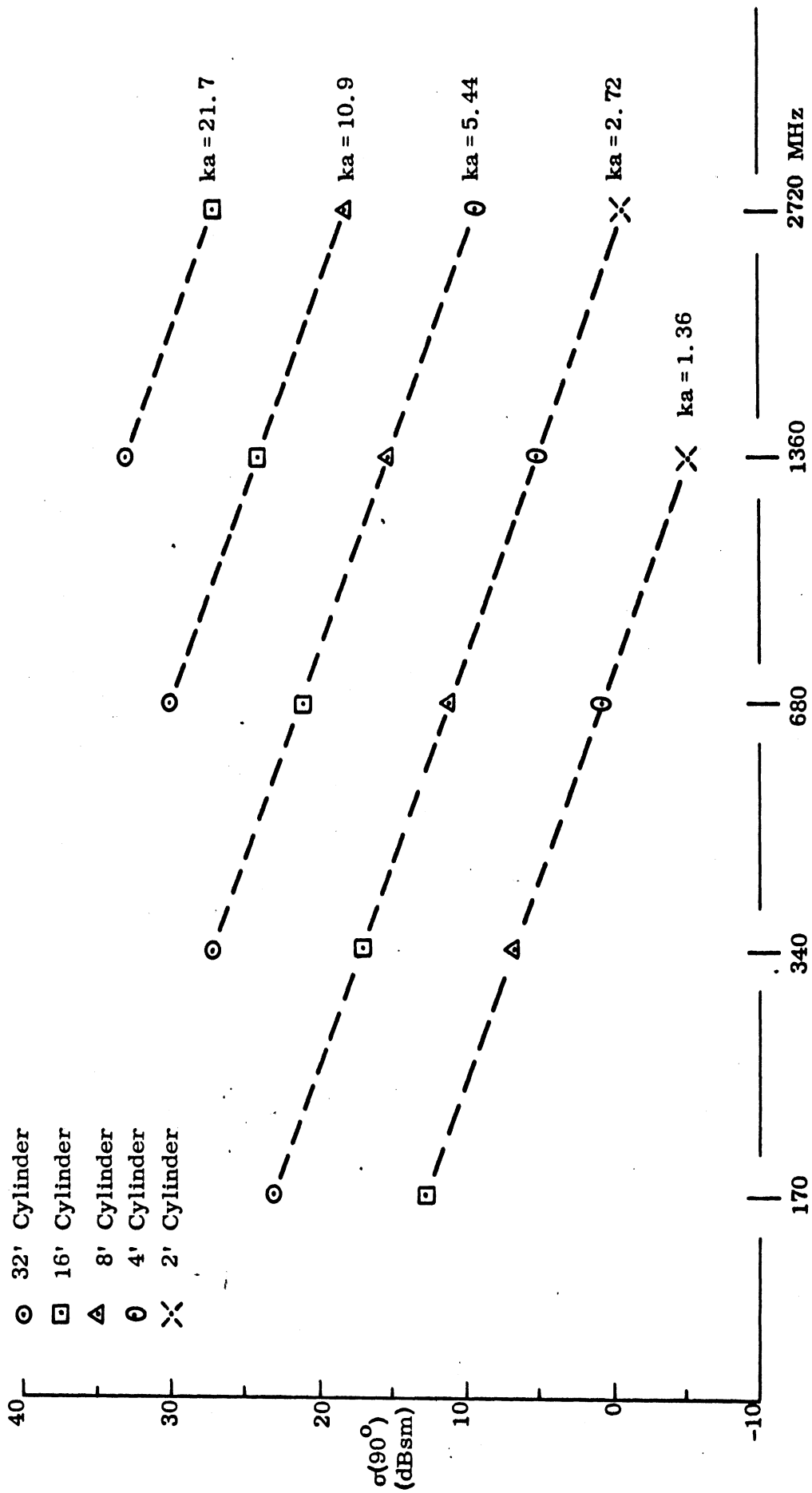


FIG. 3-9: THEORETICAL RCS OF CYLINDERS AT BROADSIDE FOR VV POLARIZATION; INTER-RANGE DISPLAY.

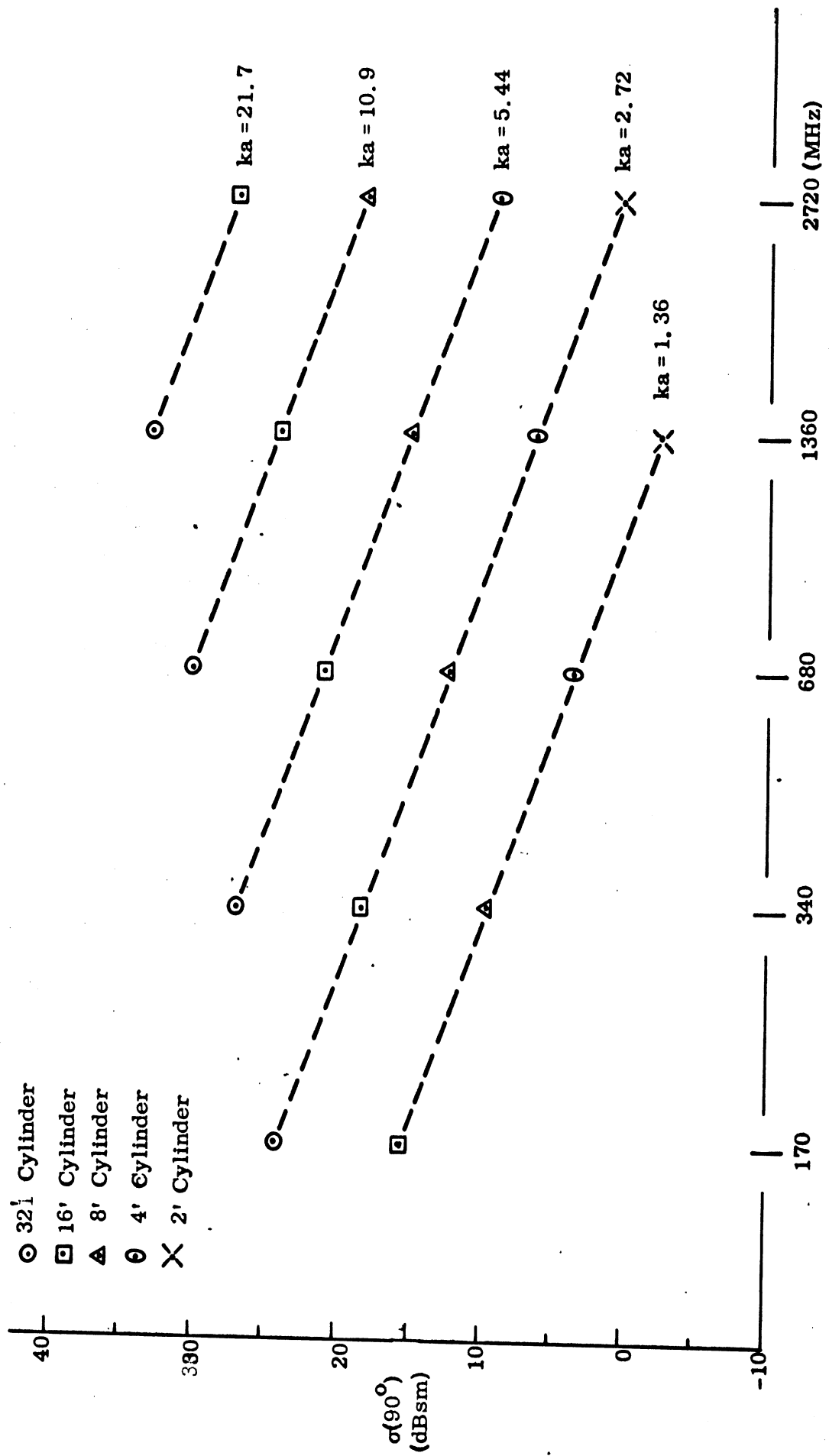


FIG. 3-10: THEORETICAL RCS OF CYLINDERS AT BROADSIDE FOR HH POLARIZATION; INTER-RANGE DISPLAY.

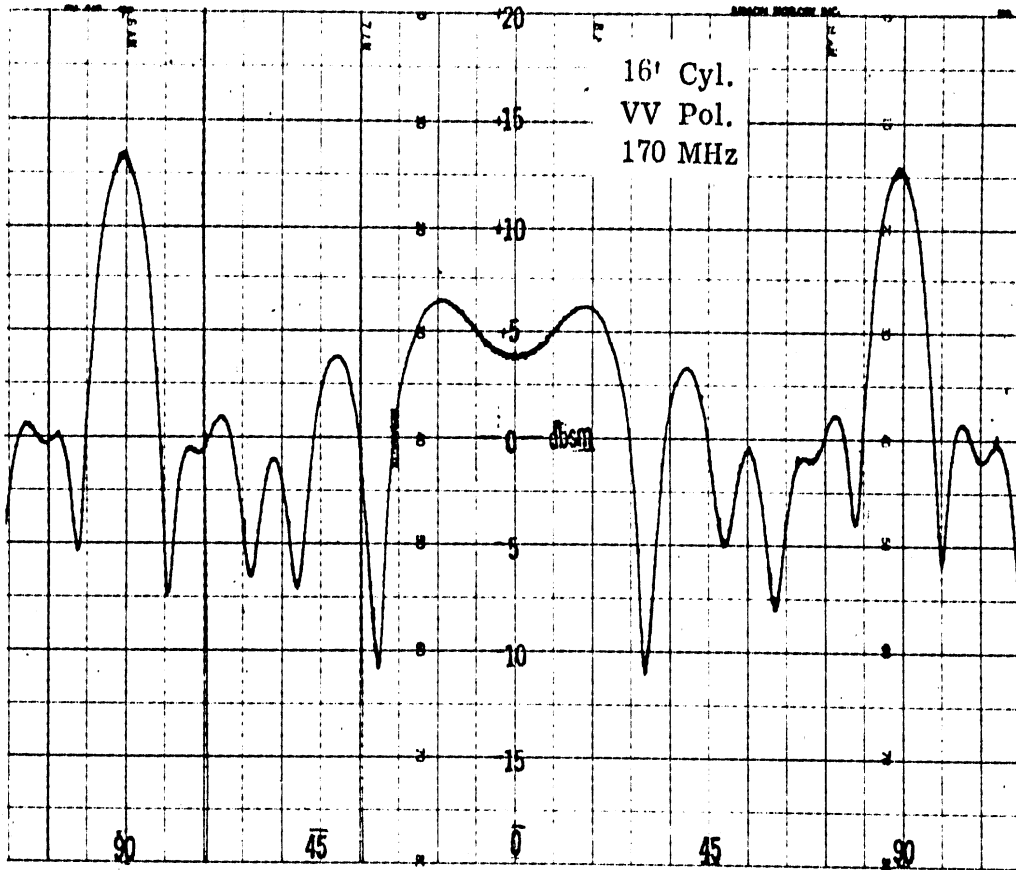
## IV

### CO-POLARIZED EXPERIMENTAL DATA

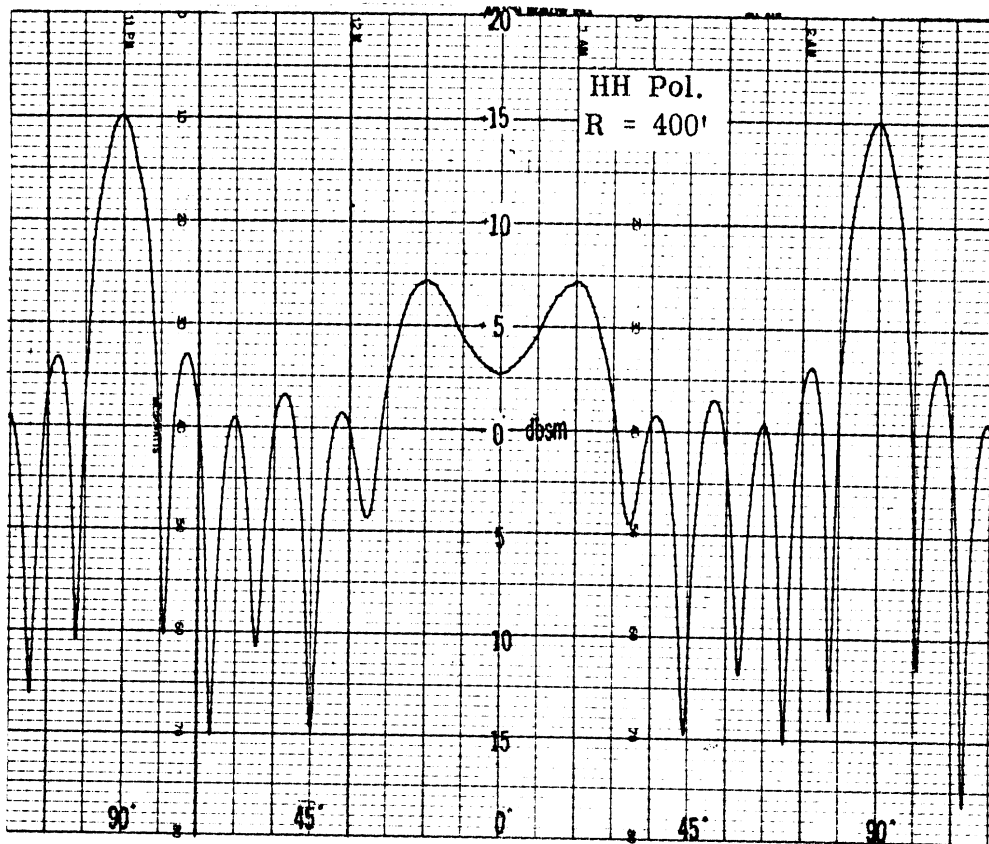
In the last chapter we saw how the data should appear by examining theoretical models; in this chapter we see how the measurements actually appear by examining experimental patterns. First, a group of ten patterns are examined including all  $ka$  co-polarized cases (VV and HH). Then a second group of ten patterns are presented to show samples from each of the five outdoor ranges for tests on the same target. The third topic is a discussion of near field distortions caused by insufficient distance between the target and radar locations. The fourth and last section describes a comparison between theory and experiment for  $ka = 1.36$ .

#### 4.1 Patterns for all $ka$ Cases

Figures 4-1 through Fig. 4-5 are examples of all the test pattern shapes which occur for the VV and HH cylinder measurements and correspond to the theoretical patterns in Figs. 3-2 through 3-6. These ten experimental patterns, which were recorded at Radiation Service in Melbourne, Florida, show radar cross sections for the aspect region between  $\pm 120^\circ$  in dBsm. Results are calibrated relative to a square meter rather than to a square wavelength as in the last chapter. All of the patterns are for the 16 foot (1/2 scale) cylinder starting with  $ka = 1.36$  (170 MHz) in Fig. 4-1 and ending with  $ka = 21.7$  (2720 MHz) in Fig. 4-5. Polarization, size, frequency, and range  $R$  are indicated in each figure. Data for the 16 foot model was chosen because it is the only one measured at every frequency and  $ka$ ; thus it is the only model for which there is a complete set of experimental results. Radiation Service data was chosen for this display because a uniform set of patterns (all from the same range) was desirable for comparison purposes and this data was available early in the program.



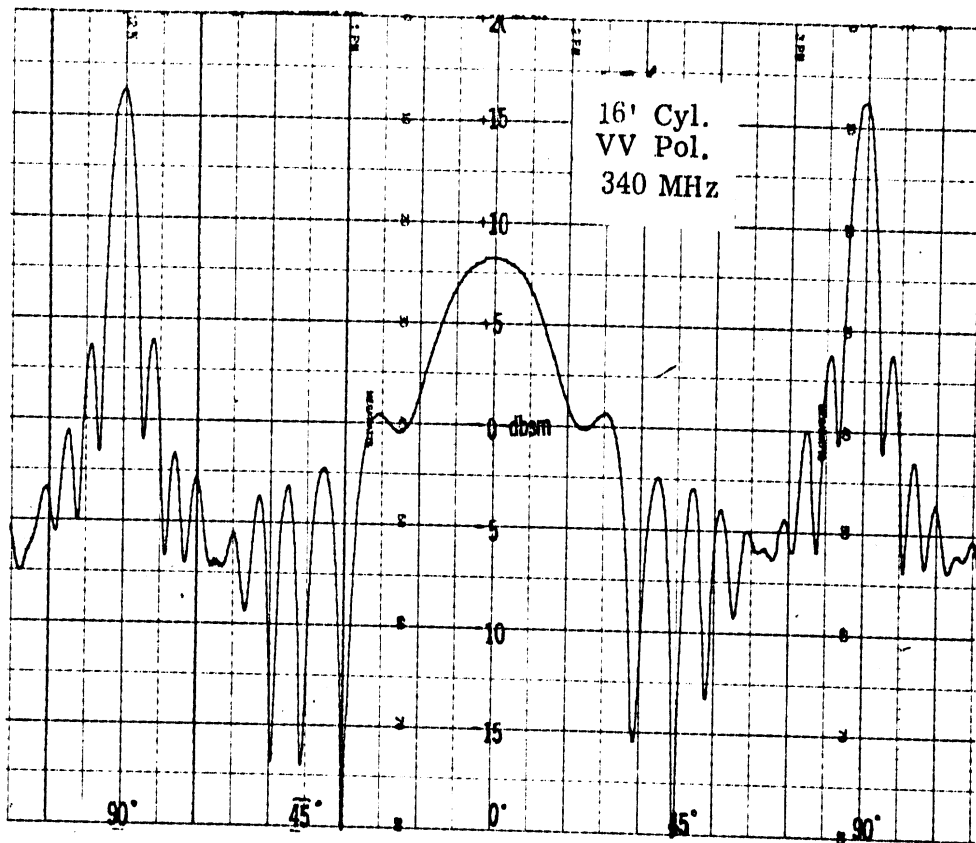
(a) VV Polarization



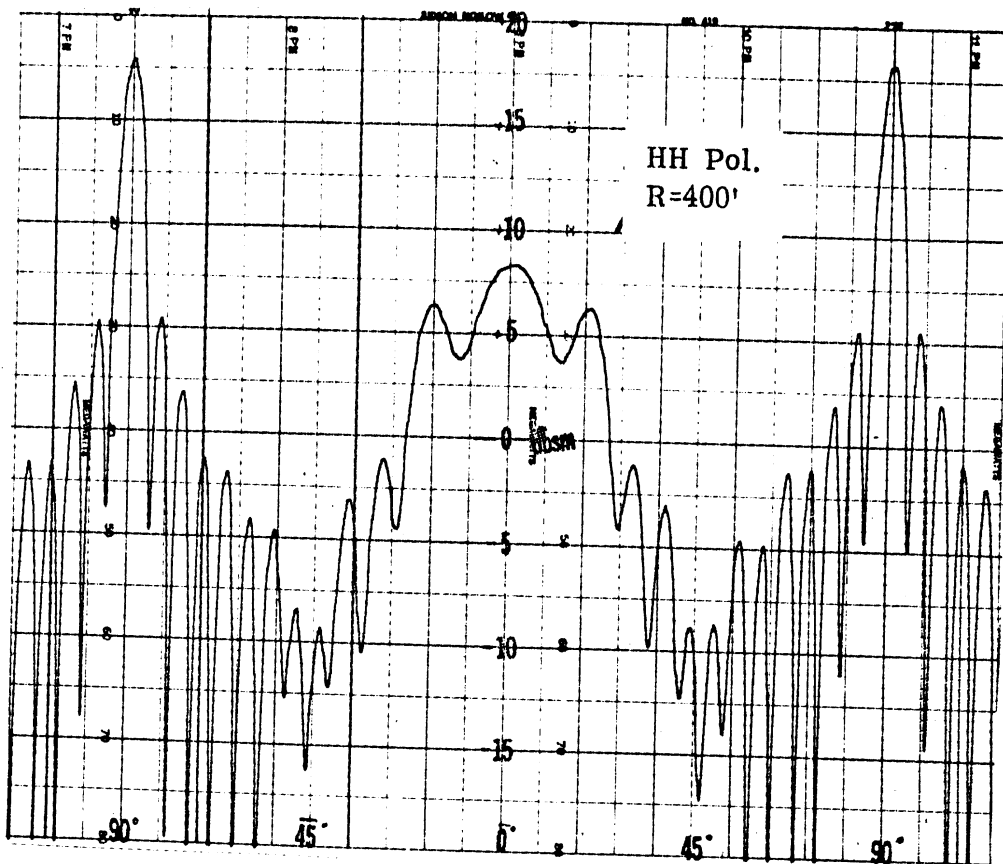
(b) HH Polarization

FIG. 4-1: EXPERIMENTAL PATTERNS FOR  $ka = 1.36$ , 170 MHz, RANGE 400 FEET, 16 FOOT CYLINDER.





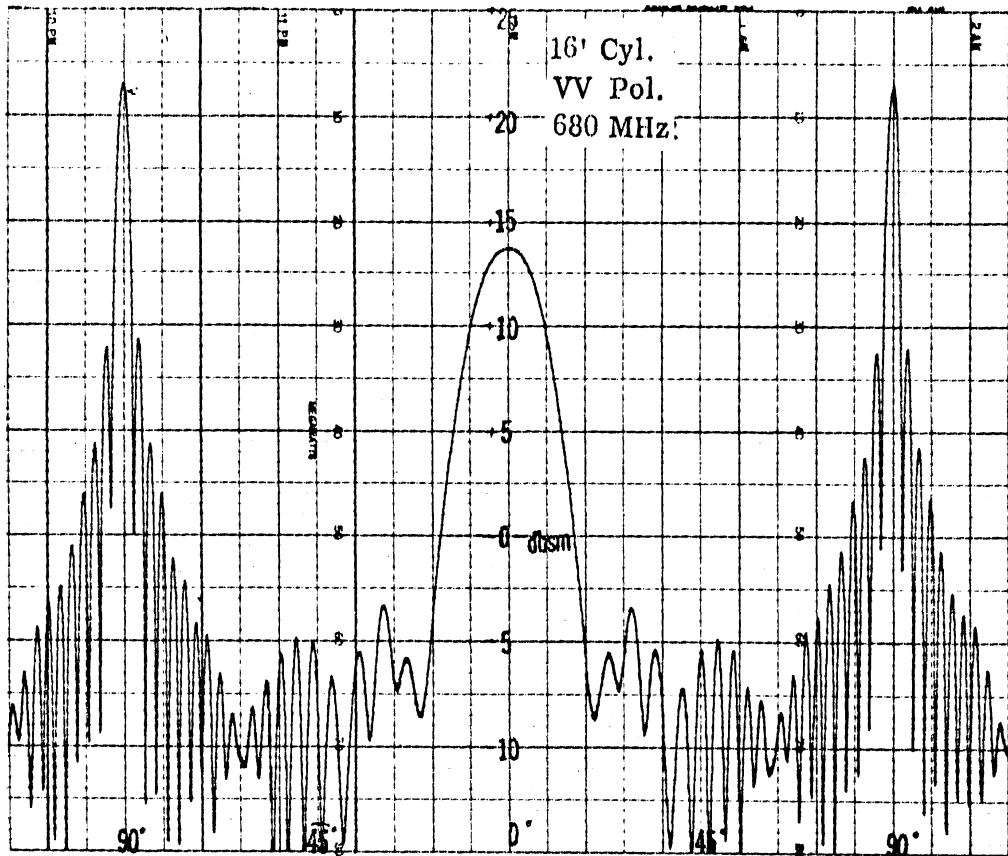
(a) VV Polarization



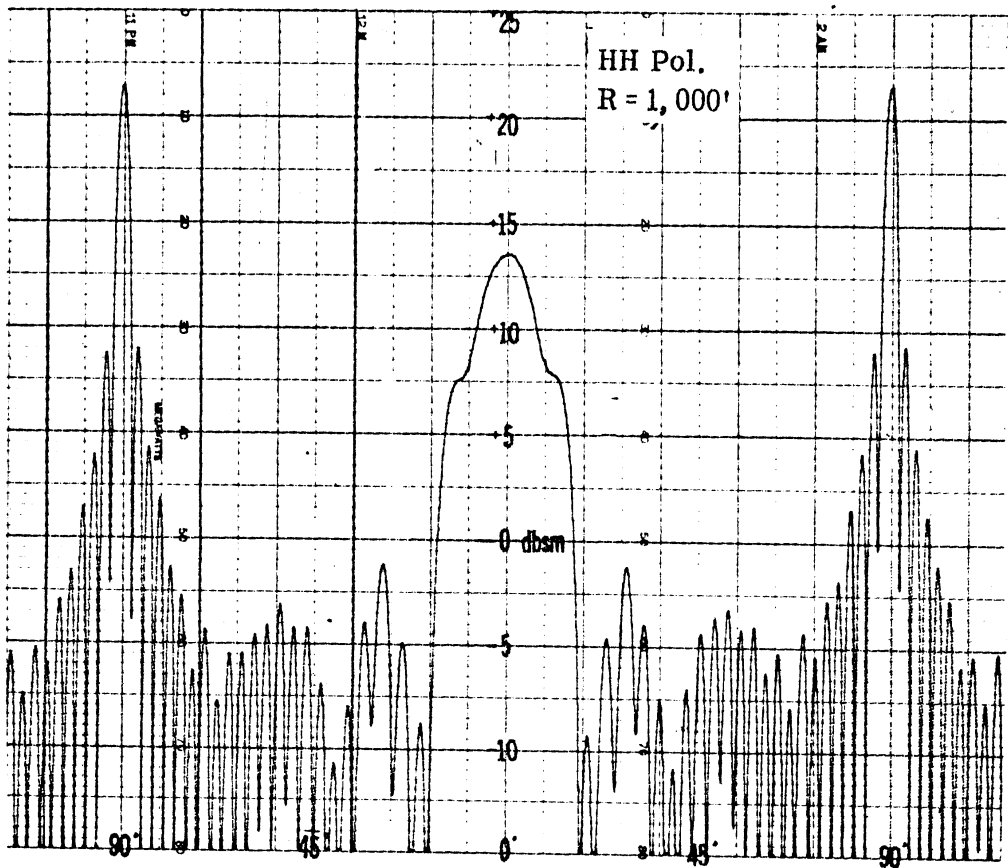
(b) HH Polarization

FIG. 4-2: EXPERIMENTAL PATTERNS FOR  $k_a = 2.72$ , 340 MHz, RANGE 400 FEET, 16 FOOT CYLINDER.





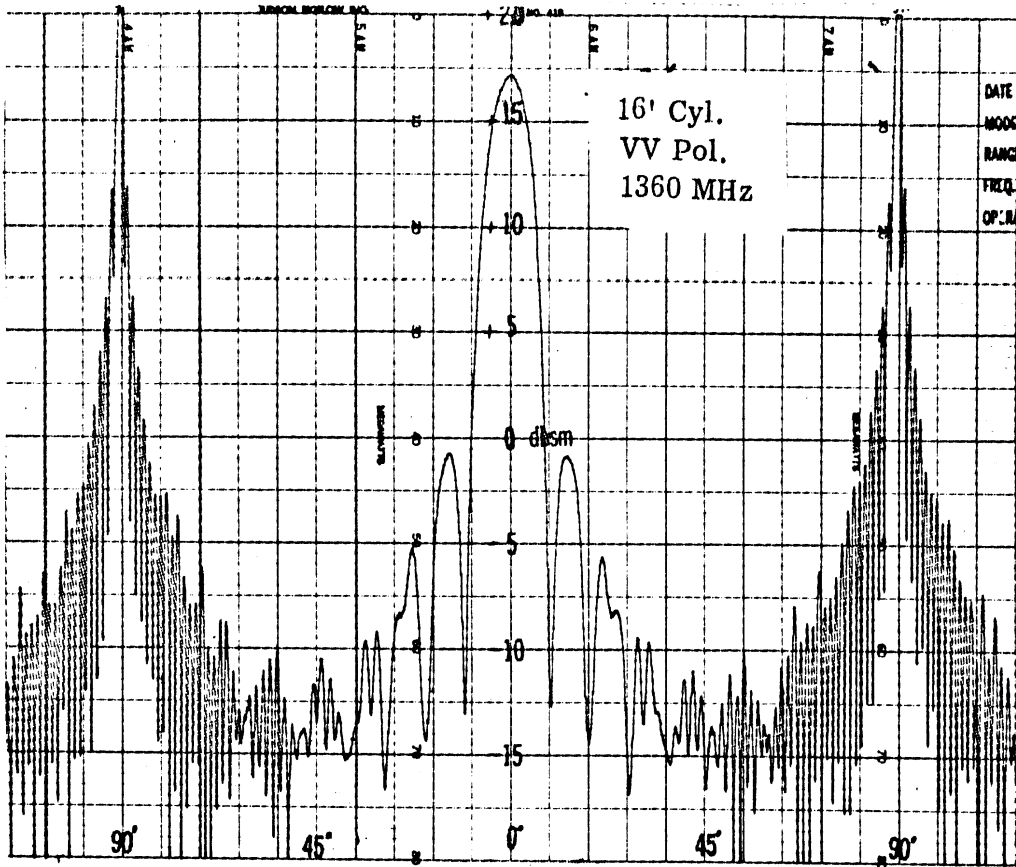
(a) VV Polarization



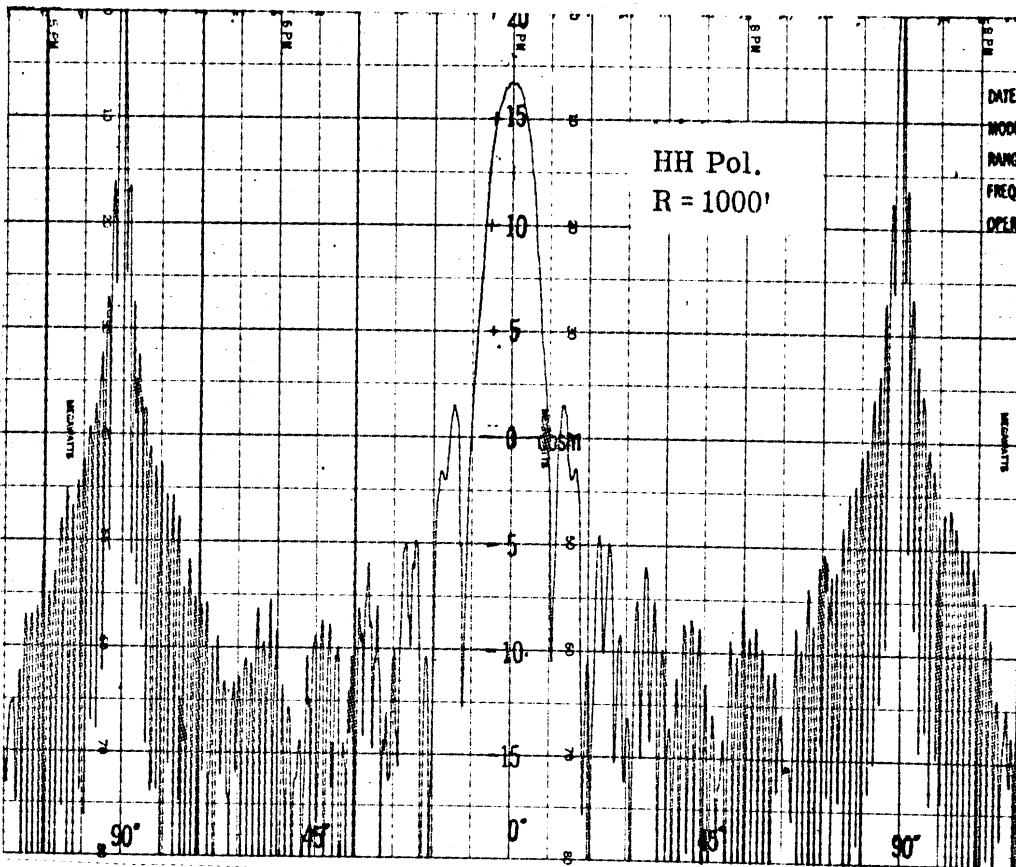
(b) HH Polarization

FIG. 4-3: EXPERIMENTAL PATTERNS FOR  $ka = 5.44$ , 680 MHz, RANGE 1000 FEET, 16 FOOT CYLINDER.



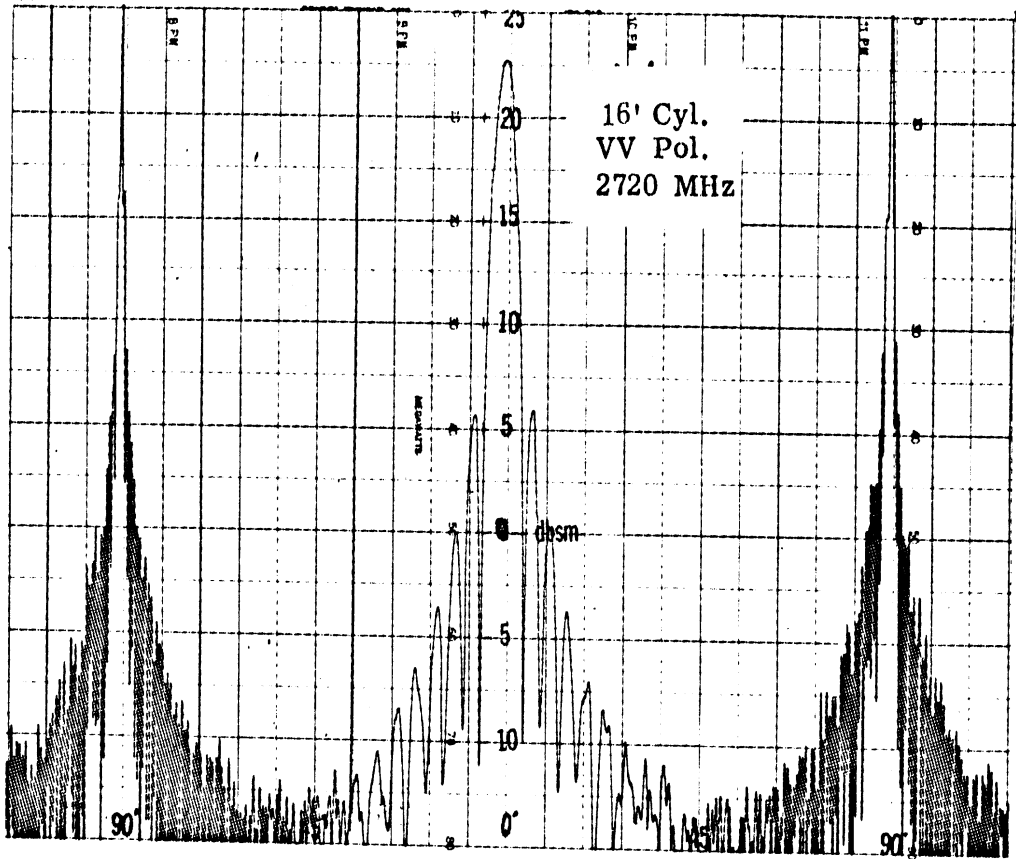


(a) VV Polarization

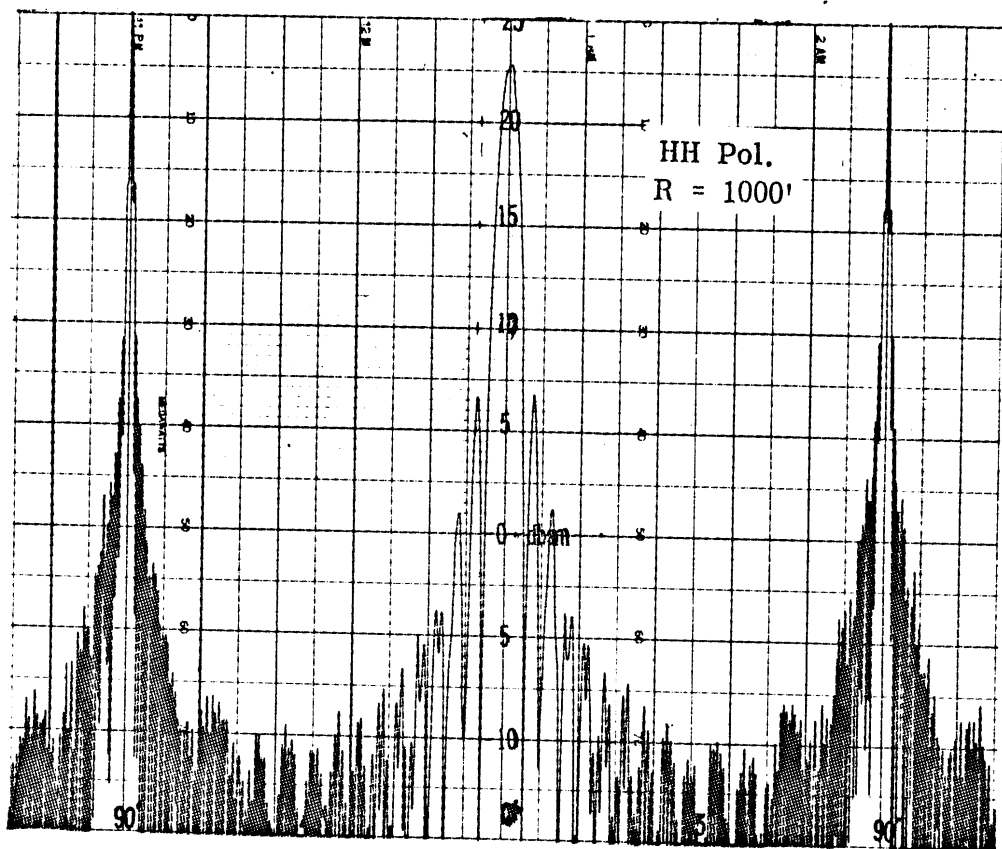


(b) HH Polarization

FIG. 4-4: EXPERIMENTAL PATTERNS FOR  $ka = 10.9$ , 1360 MHz, RANGE 1000 FEET, 16 FOOT CYLINDER.



(a) VV Polarization



(b) HH Polarization

FIG. 4-5: EXPERIMENTAL PATTERNS FOR  $k_a = 21.7$ , 2720 MHz, RANGE 1000 FEET, 16 FOOT CYLINDER.

If one compares these measured patterns with the corresponding theory in the last chapter it is seen that Figs. 4-1 and 4-5 ( $ka = 1.36$  and  $21.7$ ) agree in more detail with theory than the other three  $ka$  values, but that, in general, there is a reasonable amount of agreement between all theoretical and experimental cases. For the most part differences in pattern shape between theory and experiment are attributed to theoretical rather than experimental deficiencies. As will become evident in later discussions, the precise dBsm level for the experimental patterns may not be as accurate as the pattern shape due to experimental errors.

One criterion for judging range performance is pattern symmetry. That is, how close are lobe amplitude and shape features about points of symmetry such as end-on ( $\theta = 0^\circ$ ) and broadside ( $\theta = \pm 90^\circ$ ) for these cylinder models? In general all the ranges performed well in this respect. When poor symmetry was noticed it was usually accompanied by other errors. Some symmetry difficulties are noted in the VV polarizations near  $\pm 72^\circ$  for the first two cases, Figs. 4-1 and 4-2, although these are not serious. Other than for these instances, the symmetry for these ten patterns should be rated as excellent.

In Fig. 4-4 and 4-5 the broadside peaks run off the top of the recording paper. This occurs often and is done deliberately to show more of the details in the lower portion of the pattern. In most cases, as in the present one, additional patterns are recorded showing the complete broadside peaks moved down on the record. The second patterns are not included here but we note that the level of the broadside peaks for both the VV and HH patterns are tabulated in Table V-2.

In the highest  $ka$  pattern, Fig. 4-5, the pattern oscillations are so rapid that it is not possible to resolve the lobe width beyond  $\pm 45^\circ$  aspect angle. This difficulty was indicated in the theoretical pattern, Fig. 3-6,

where only the peak locations were given for  $\theta$  greater than  $50^\circ$ . All the ranges have the capability to avoid this problem by expanding the aspect scale on their records, but since the contract with each of these ranges did not call for expanded patterns, it was not done. This example points out the importance of adequate recording scales if the pattern lobe structure is to be examined in any detail.

#### 4.2 Patterns from Each Outdoor Range

Examples of measurements made at each of the outdoor ranges on the 32 foot cylinder at 340 MHz ( $k_a = 5.44$ ) are shown in Figs. 4-6 through 4-10 for VV and Figs 4-11 through 4-15 for HH polarizations. Like all the experimental patterns these cross sections are given in dBsm but here the complete aspect region,  $\pm 180^\circ$  is shown rather than just  $\pm 120^\circ$  as in the previous ten patterns. Though all the patterns were recorded on 10 inch by 20 inch chart paper, GD/FW and RAT SCAT have a 50 dB range over 10 inches while the other three facilities have 40 dB over 10 inches. Also it should be noted that during the photographic reduction, the angular scales were reduced by slightly different amounts. These discrepancies make it difficult to perform accurate, direct comparisons between the patterns from different ranges. Nevertheless it is informative to make cursory comparisons for this set of data.

On first inspection of these patterns one is probably aware of the noticeable distortion and asymmetry in the broadside region in the Conductron patterns, Fig. 4-6 and 4-11. This is caused by near field distortion, the largest single cause of errors in the patterns. Further discussion on this topic follows in the next section.

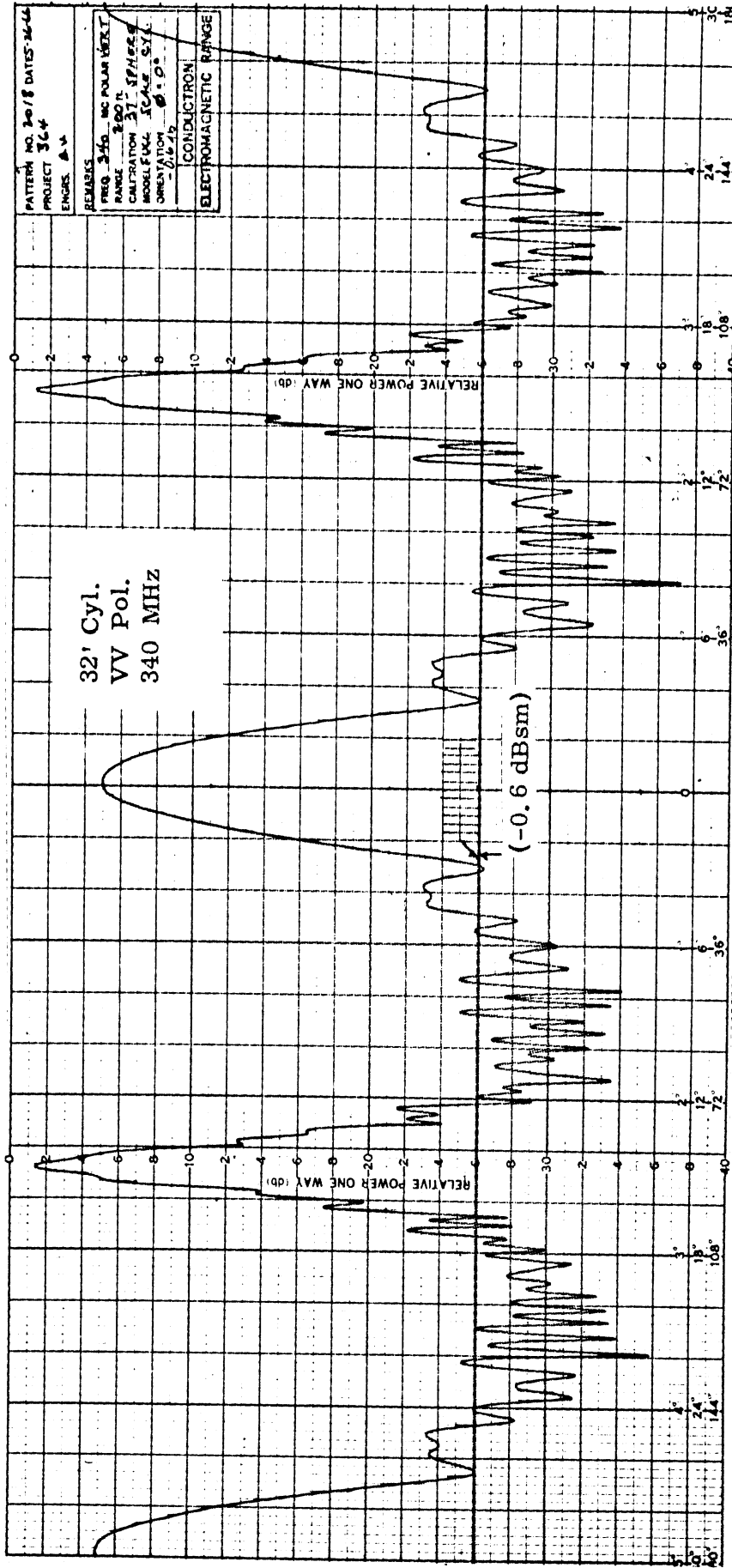


FIG. 4-6: CONDUCTRON PATTERN FOR 32 FOOT CYLINDER, VV POLARIZATION, 340 MHZ.

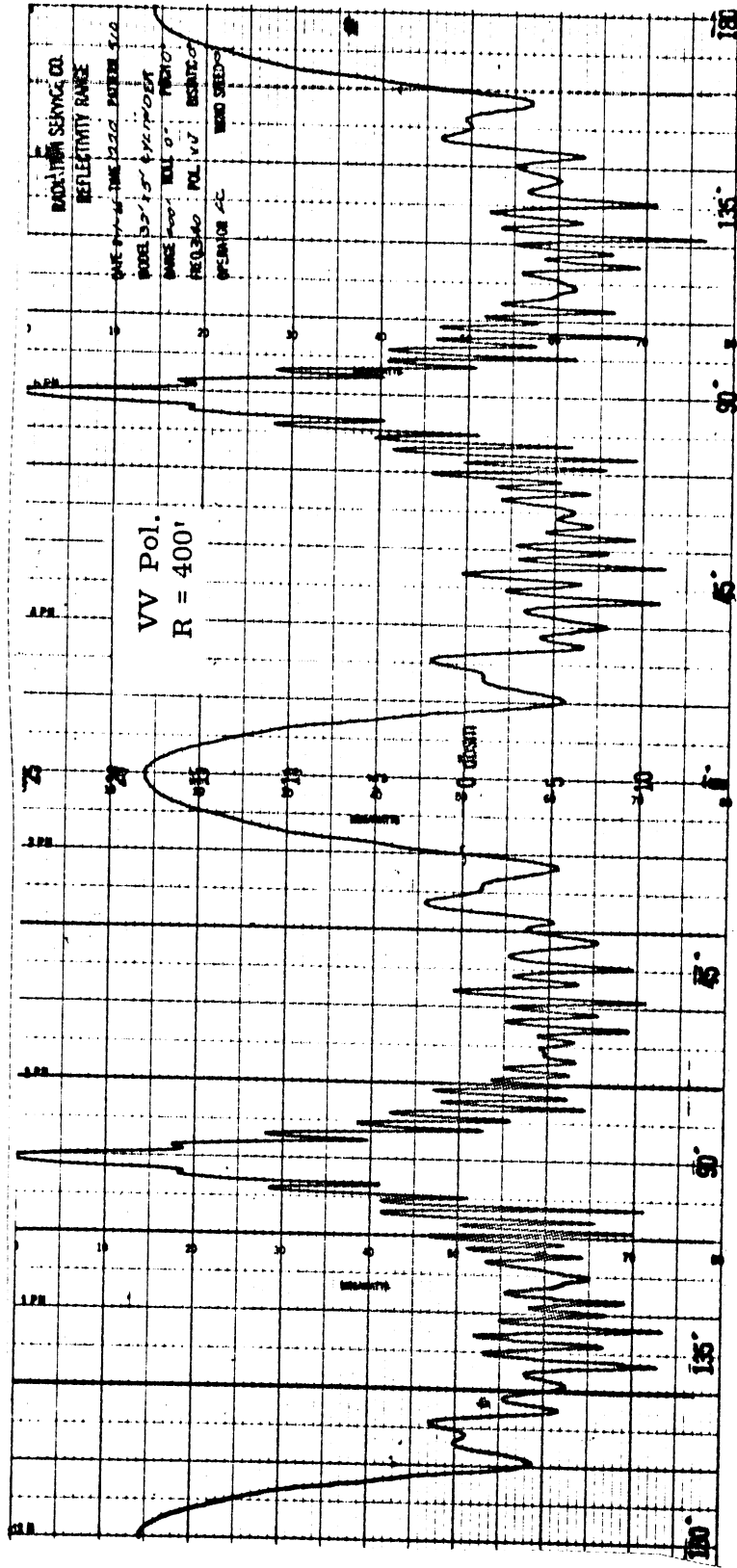


FIG. 4-7: RADIATION SERVICE PATTERN FOR 32 FOOT CYLINDER VV POLARIZATION, 340 MHZ.

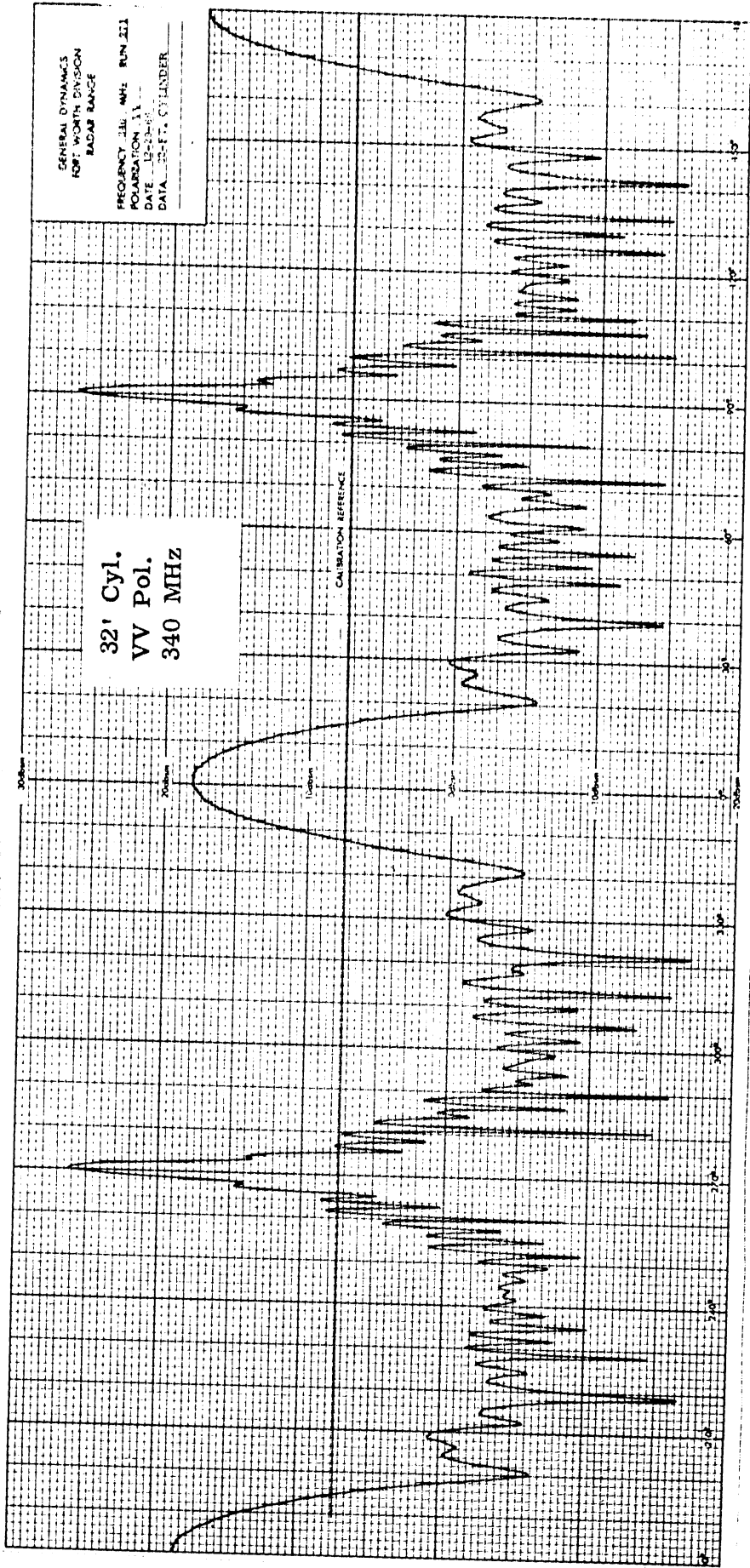


FIG. 4-8: GENERAL DYNAMICS PATTERN FOR 32 FOOT CYLINDER, VV POLARIZATION, 340 MHz.



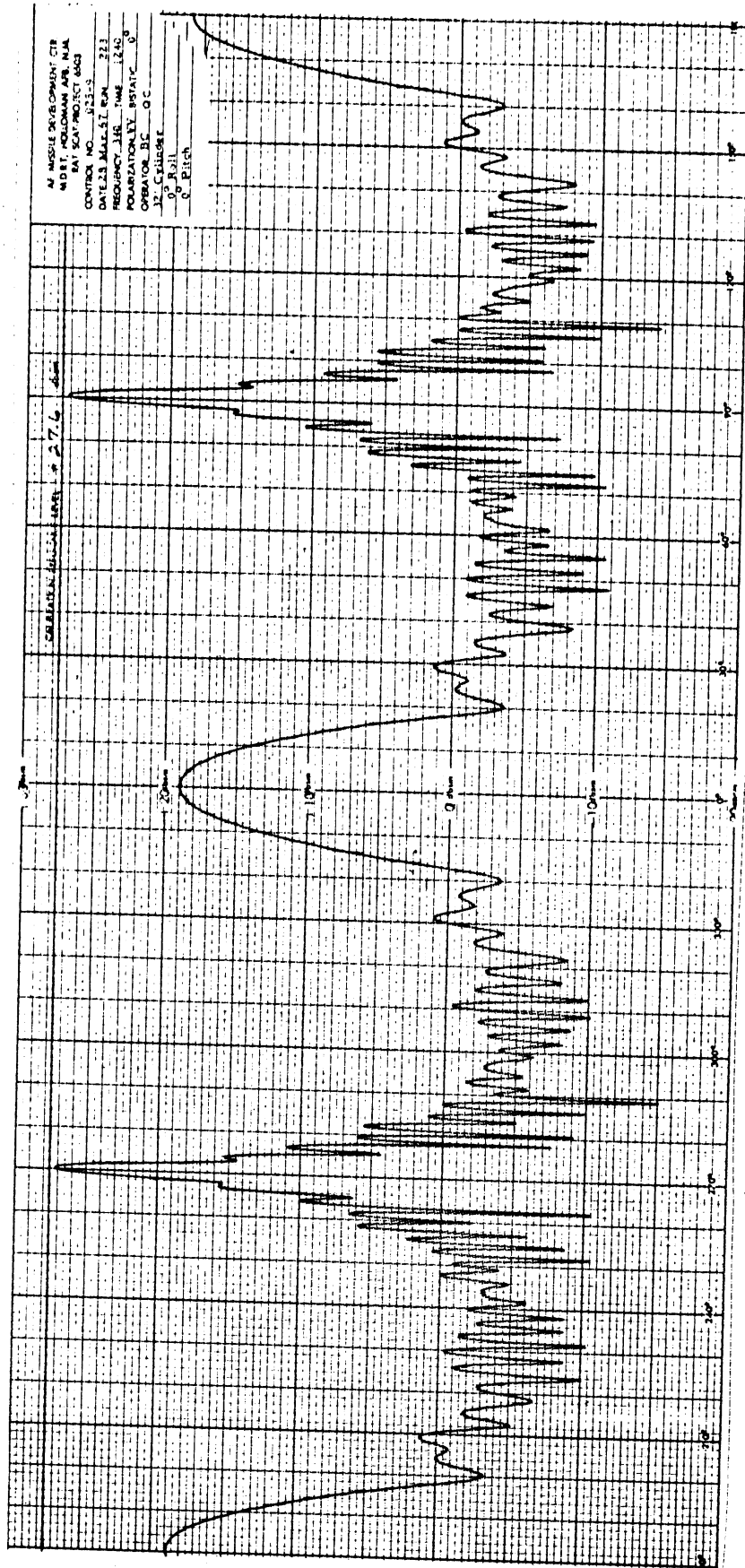


FIG. 4-9: RAT SCAT PATTERN FOR 32 FOOT CYLINDER, VV POLARIZATION, 340 MHZ.

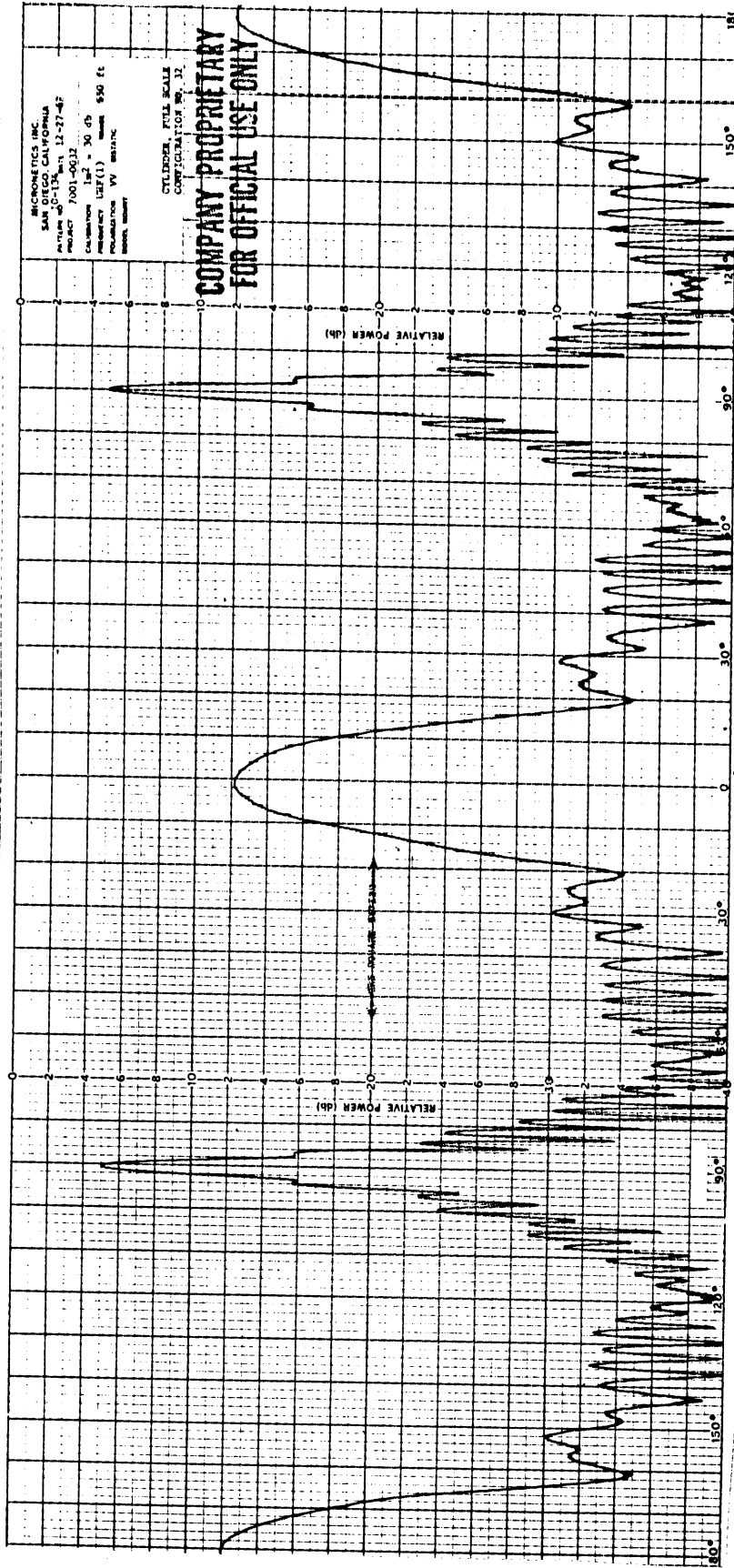


FIG. 4-10: MICRONETICS PATTERN FOR 32 FOOT CYLINDER, VV POLARIZATION, 340 MHZ.  
 (The horizontal arrows indicate the + 10 dBsm level).

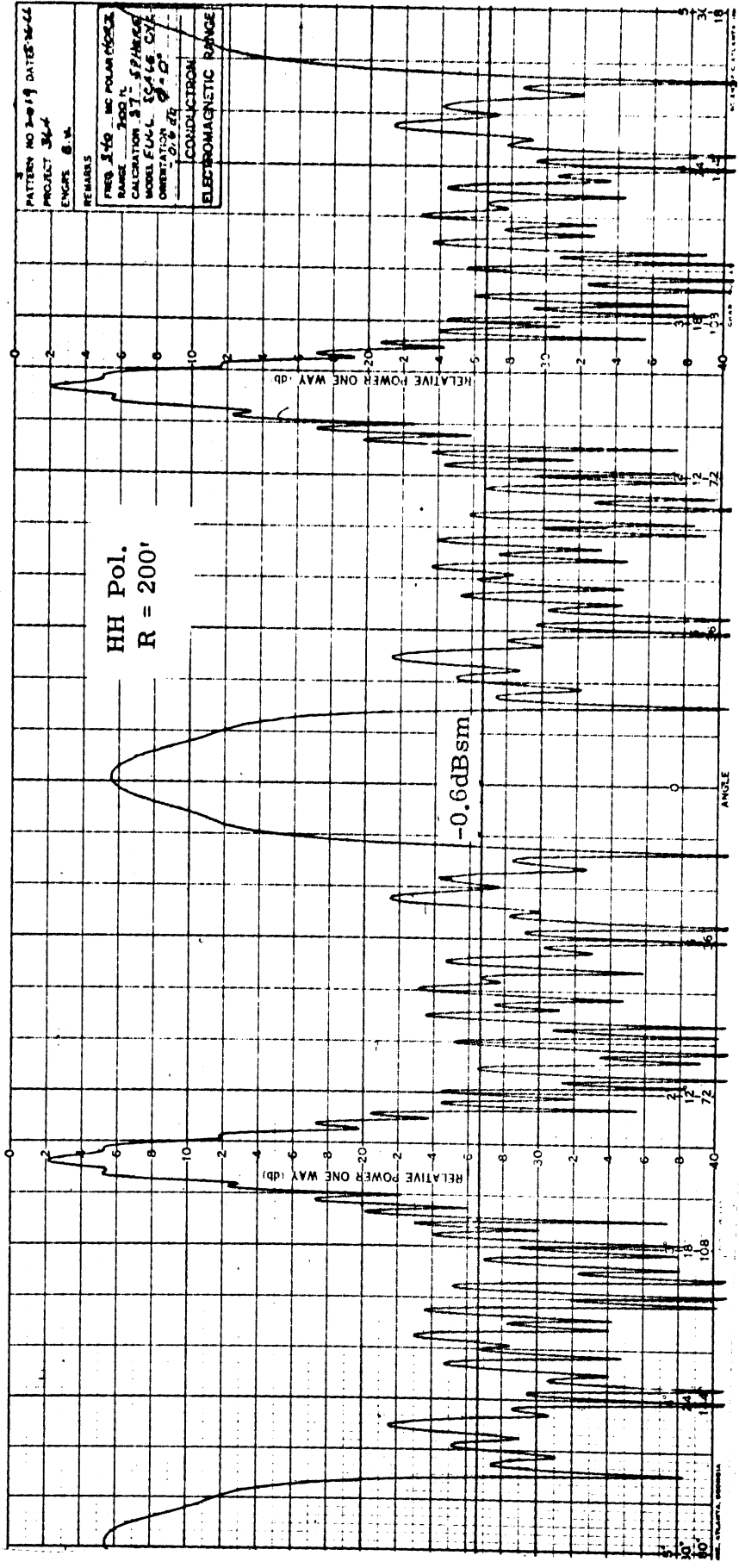


FIG. 4-11: CONDUCTRON PATTERN FOR 32 FOOT CYLINDER, HH POLARIZATION, 340 MHZ.

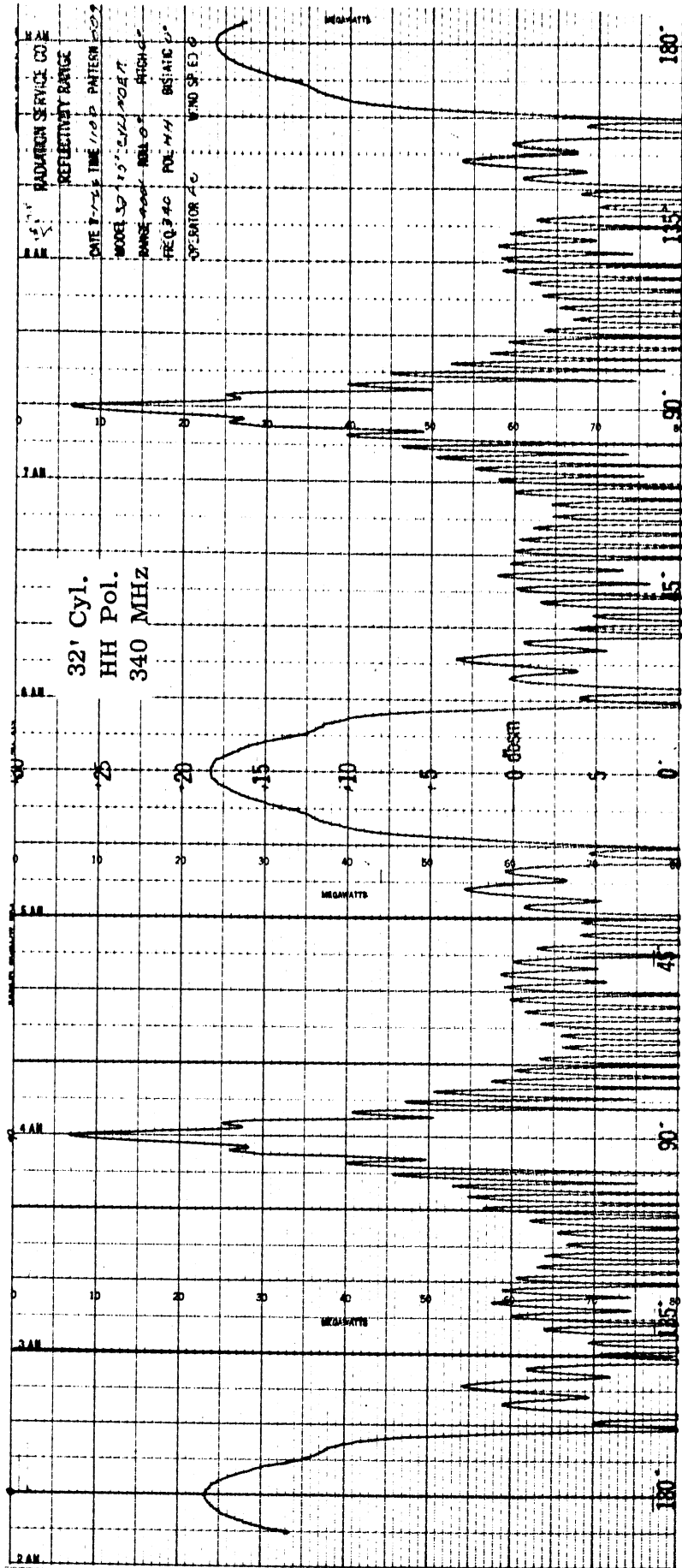


FIG. 4-12: RADIATION SERVICE PATTERN FOR 32 FOOT CYLINDER, HH POLARIZATION, 340 MHZ.

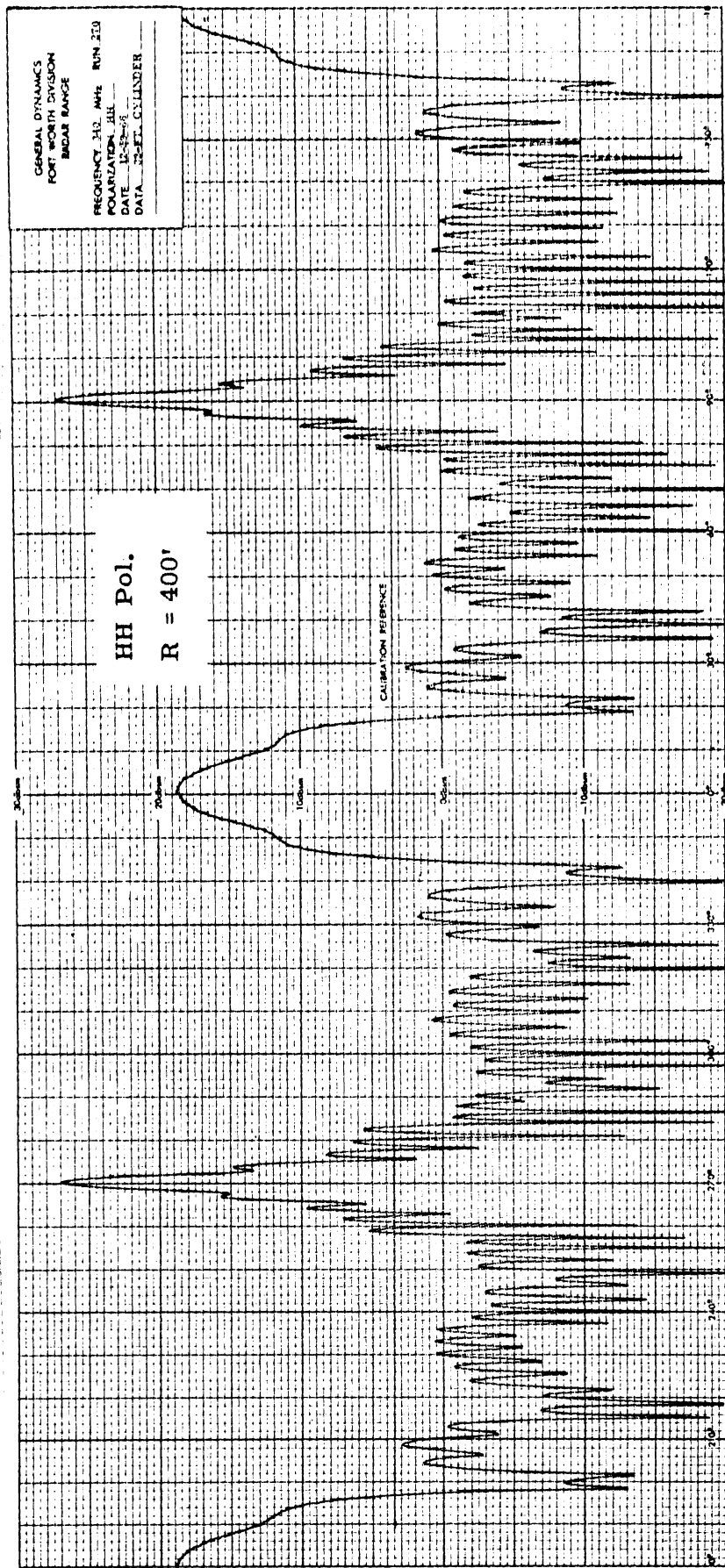


FIG. 4-13: GENERAL DYNAMICS PATTERN FOR 32 FOOT CYLINDER, HH POLARIZATION, 340 MHZ.

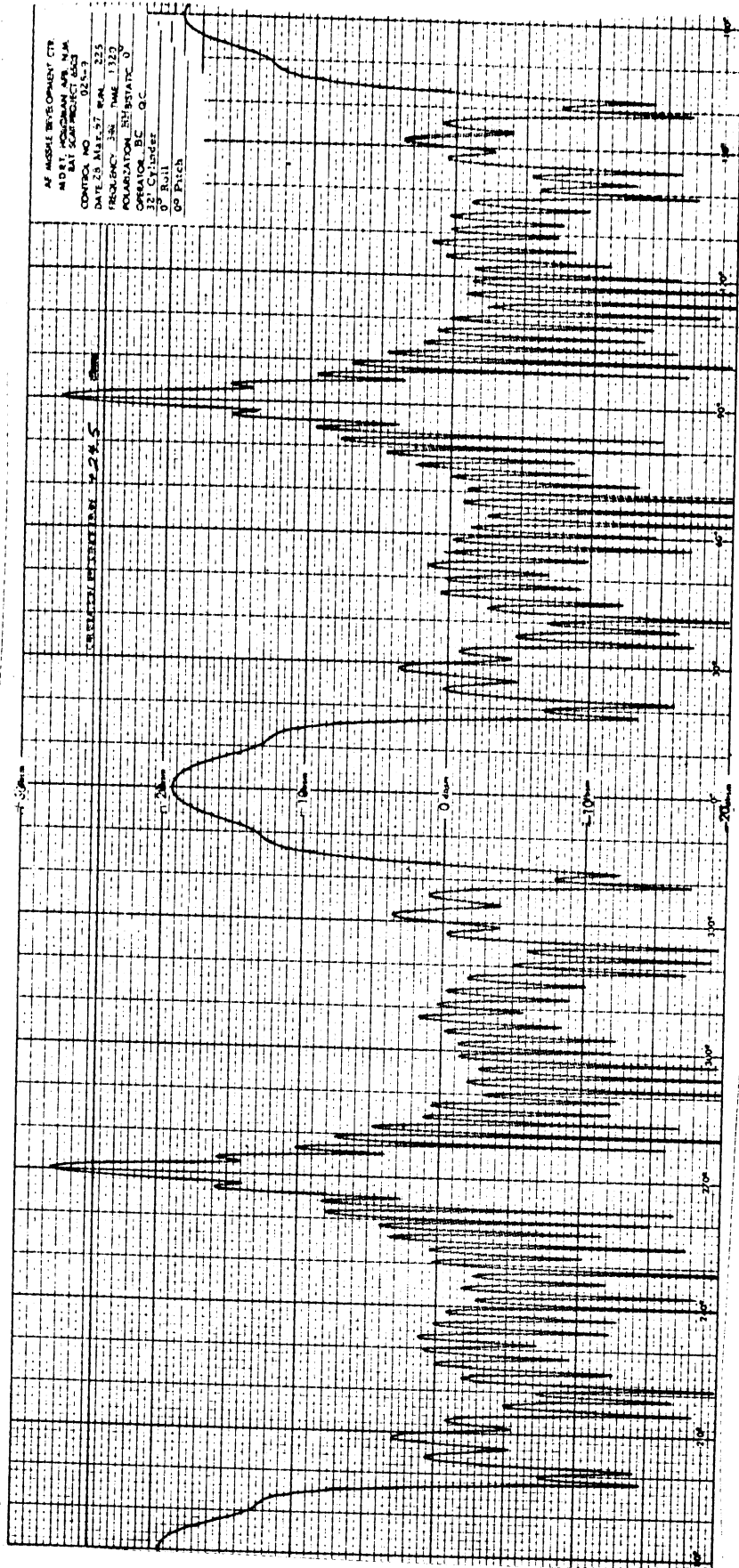


FIG. 4-14: RAT SCAT PATTERN FOR 32 FOOT CYLINDER, HH POLARIZATION, 340 MHz.

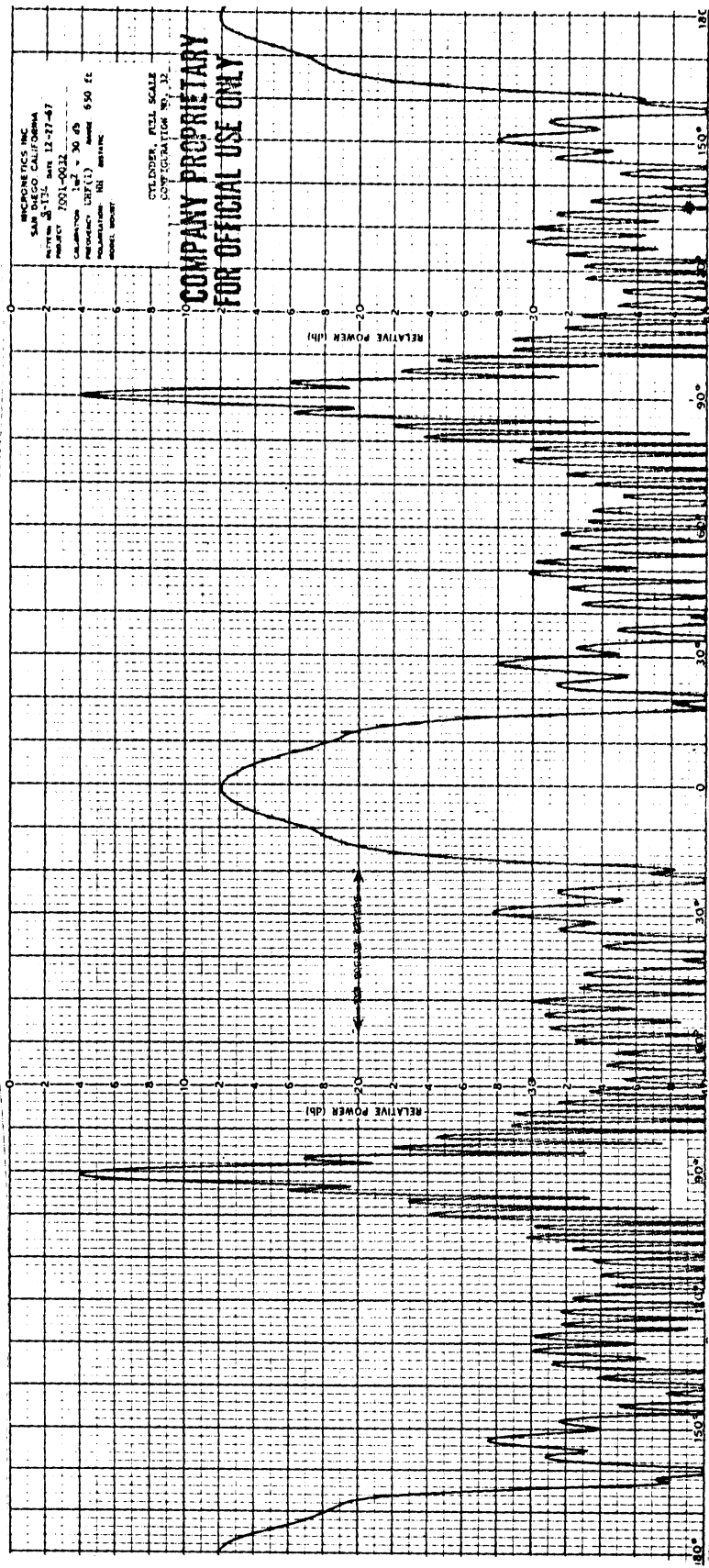


FIG. 4-15: MICRONETICS PATTERN FOR 32 FOOT CYLINDER, HH POLARIZATION, 340 MHZ.  
 (The horizontal arrows indicate the + 10 dBsm level).

An annoying feature of the Conductron pattern is that there is no convenient relation between the dBsm values and the dB level on the chart grid. This is a result of making pattern calibrations after the target pattern is measured, instead of before, and the format is clearly not as easy to read as is the pre-calibrated patterns of the other ranges. CW ranges can pre-calibrate their work like pulse ranges do with very little extra effort and we recommend that this be done.\* The pattern traces on the Avionics Laboratory data (not shown here) are placed on the recording paper in a manner similar to Conductron's but in addition their angular locations appear to be randomly placed on the recording paper, disregarding the angular markings, hence making their patterns even more difficult to read.

Additional comparisons can be made on the 32 foot cylinder data by referring to the 1/2 scale data for  $ka = 5.44$  in Fig. 4-3; this should have the same shape but be 6 dB less than the full scale data. A quick examination shows actual differences closer to 5 dB between the broadside peak for the full scale and the half scale patterns. The approximate 1 dB error is in the full scale data and is due to near field effects also.

#### 4.3 Near Field Distortion

Noticeable near field distortions have been pointed out in Figs. 4-6 and 4-11, but a further examination indicates that all of the patterns in Figs. 4-6 through 4-15 are beginning to show near field effects compared to the patterns in Fig. 4-3. The first indication of insufficient range between the target and radar (near field effects) is that the nulls in the

---

\* After working with post-calibrated data on this contract, we are convinced of the convenience of this format and have changed our own calibration technique at the Radiation Laboratory, University of Michigan accordingly.

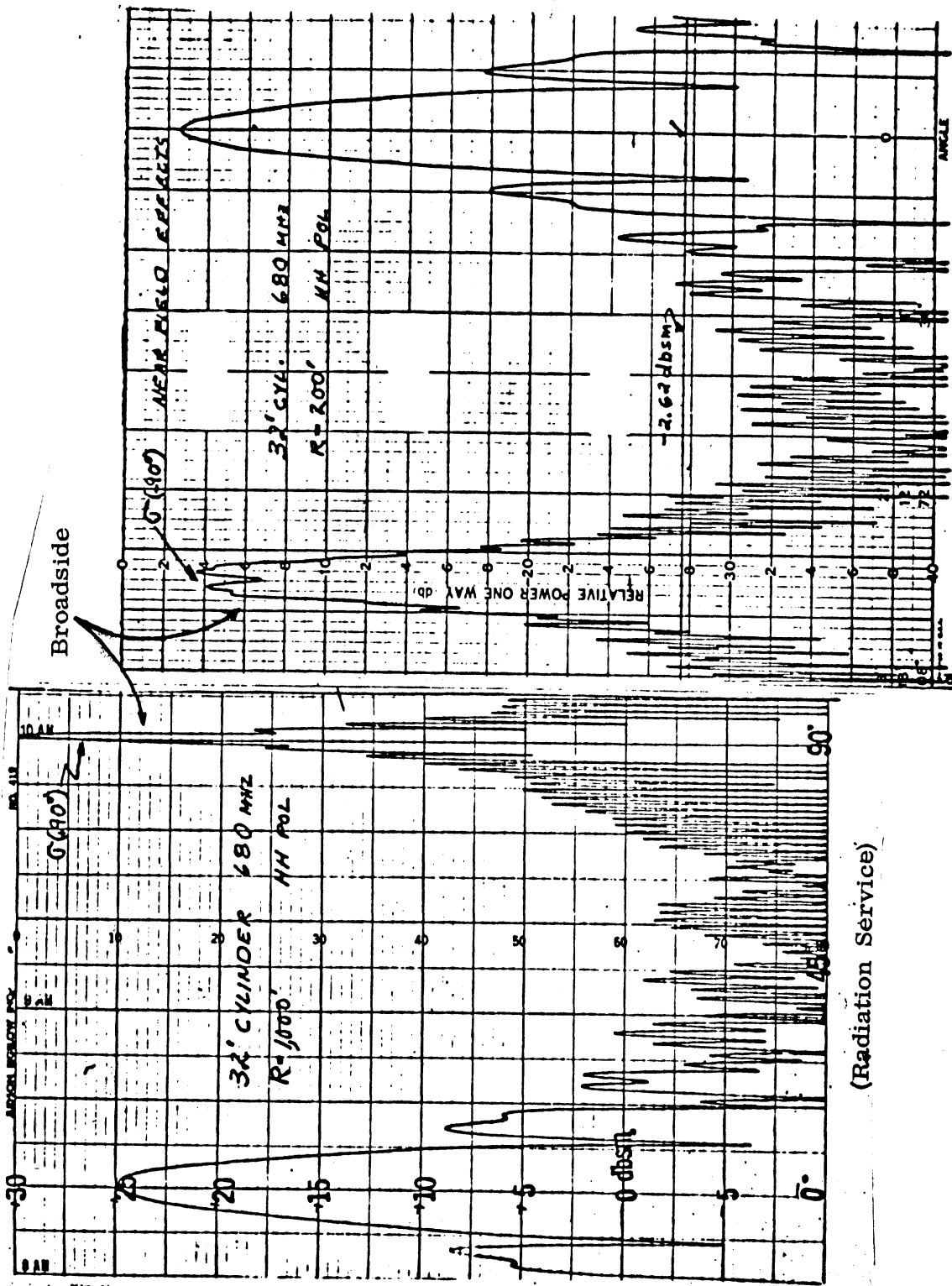


lobes just off broadside ( $\theta = 90^\circ$ ) become shallow. Compare Fig. 4-3 with any of the full scale data to see this behavior. As the range is further reduced, the target passes from the Fraunhofer (far) zone to the Fresnel (near) zone. This progressive degeneration in range requirements is exemplified by passing from Fig. 4-3 (Fraunhofer pattern) to Figs. 4-7 or 4-2 and 4-6 or 4-11 (transition region) and then to Fig. 4-16 (Fresnel pattern). The second effect which becomes noticeable in the near field is the amplitude reduction in the broadside peak. This was mentioned indirectly at the close of the last section where it was noticed that there was closer to a 5 dB rather than 6 dB difference in the full and 1/2 scale data for  $ka = 5.44$ .

Ideally, it is desirable to have the target illuminated by a plane wave when its cross section is being measured because then the shape and form of the scattering pattern are constant and only the power level varies as  $1/R^4$ . The illumination is considered to be sufficiently plane when there is less than  $\lambda/16$  phase variation over the target at the time its maximum dimension  $L$  is exposed to the radar. To satisfy this phase requirement the range  $R$  must be (Kouyoumjian and Peters, 1965)

$$R \geq \frac{2(D + L)^2}{\lambda}$$

where  $D$  is the maximum dimension of the radar antenna. If  $D$  is small compared to  $L$ , it may be ignored and the above expression reduces to the  $2L^2/\lambda$  criteria introduced in Chapter II. Disregarding  $D$  which varies from one facility to another the necessary ranges  $R$  for the various cylinder models are listed in Table IV-1.



(Conductron)

(Radiation Service)

FIG. 4-16: NEAR FIELD DISTORTIONS FOR HH POLARIZATION AT  $ka = 10.9$ . THE PATTERN ON THE RIGHT SHOW THE EFFECT OF BEING IN THE FRESNEL ZONE NEAR  $\theta = 90^\circ$ .

TABLE IV-1  
 REQUIRED RANGE DISTANCE (FEET) AS  
 DETERMINED BY  $2L^2/\lambda$

Frequency MHz	Model Length (feet)				
	32	16	8	4	2
170	354	88	-	-	-
340	708	177	44	-	-
680	1416	354	88	22	-
1360	2832	708	177	44	11
2720	-	1416	354	88	22

Further explanation is needed for Fig. 4-16 which is an example of severe near field distortion. These are experimental patterns for the full scale cylinder measured at 680 MHz ( $ka = 10.9$ ) and HH polarization. The pattern on the left was measured at a range of 1000 feet ( $1.4 L^2/\lambda$ ) while the one on the right was measured at 200 feet ( $0.3 L^2/\lambda$ ). According to Table IV-1 the minimum range should have been 1,416 feet. Note that these two patterns are arranged with their broadside returns in the center of the figure; the left pattern covers the aspect range between  $0$  and  $+90^\circ$  while the right one covers between  $-90^\circ$  and  $0^\circ$ . The vertical placement of the two patterns in Fig. 4-16 is such that equal dBsm levels are aligned. In this example near field distortion caused about a 12 dB difference in the broadside return. There is a 2.5 dB difference in the end-on region ( $\theta = 0^\circ$ ). As it turns out the Radiation Service pattern (left) is about 1.5 dB high and Conductron (right) pattern 1.0 dB low compared to theory at  $\theta = 0^\circ$ , so discrepancies in this region are not near field errors.

Near field errors as serious as those shown in the right hand portion of Fig. 4-16 occurred in eight patterns ( six from Conductron and two from Micro-netics). Errors due to this cause are the largest and occur most frequently in this test program. Their occurrence is, however, predictable in that an examination of the maximum target dimension, the incident wavelength and the antenna-to-target separation distance indicates whether or not this problem will exist. More suggestions and discussion concerning the near field effects are found in Volume I.

#### 4.4 Comparison Between Theory and Experiment

In this section we make some selected comparisons between theory and experiment, and although we use four distinct theories, the comparisons are summarized in three figures. Table IV-2 lists the figures and  $ka$  values for which the various theories apply.

TABLE IV-2: LIST OF CONDITIONS IN WHICH THEORY IS COMPARED WITH EXPERIMENT.

Fig. No.	Theory Used	Aspect Angle at Which Comparison is Made .	$ka$ Values for Which Comparison is Made.
4-17, 4-18	Norair SDT	End-on, broadside, and at peaks of five other lobes.	1.36
4-19	Schmitt-Andrejewski	End-on.	1.36, 2.72, 5.43
4-19	Infinite Cylinder (exact)	Broadside.	1.36, 2.72, 5.43
4-19	Physical Optics	End-on, broadside.	10.86, 21.72

Although there were 18 cylinder-frequency combinations measured by each range, these data can all be collected into five groups according to  $ka$ . In order to make the best use of all the data, we reduced the radar cross sections from dBsm to  $dB\lambda^2$  by simply adding or subtracting a correction factor (in dB). This resulted in a large number of samples, producing, for example, as many as 52

values for analysis of the end-on return for  $ka = 2.72$ . For each comparison we draw in Figs. 4-17 through 4-19 we show the mean value of the data and the standard deviation. If the individual deviations are assumed to be entirely random, the standard deviation represents a confidence level of 68.3 percent; that is to say, if ten more measurements are made, and if the errors are truly random, seven of them will fall within the range bracketed by the mean value plus or minus the standard deviation.

Norair's SDT prediction is shown in Fig. 4-17 for HH polarization and  $ka = 1.36$ , the smallest electrical size involved in the measurements program. Note that the worst disagreement is about 1.1 dB and it occurs at end-on and  $63^\circ$  aspect. The broadside return is predicted within 0.3 dB and the standard deviations are usually less than 1 dB. The Norair theory for VV polarization is shown in Fig. 4-18. Note that the standard deviations are much greater for this than HH polarization, reaching a value of nearly 2.5 dB at the  $66.5^\circ$  aspect angle. The experimental end-on return is precisely the same as for HH polarization, and again the broadside return is within 0.3 dB of the theoretical prediction. The point of poorest agreement lies at  $54.5^\circ$  and the difference between theory and experiment is 1.6 dB. For both polarizations the experimental data lie consistently below the theory (except for VV polarization at broadside). At best we can say the Norair SDT theory does well or it does poorly, depending what aspect angle is of interest.

We have not made any comparisons of null depth or null locations, and there is no reason to believe the theory will predict these returns any better than it does the lobe amplitudes in Figs. 4-17 and 4-18. (Inspection of Figs. 6-5 through 6-6 show that range performance becomes progressively worse away from the peaks of the lobes, especially for this low  $ka$ .) It is apparently more difficult to produce accurate VV patterns than HH patterns, presumably because the ground reflects this polarization more readily into the target area

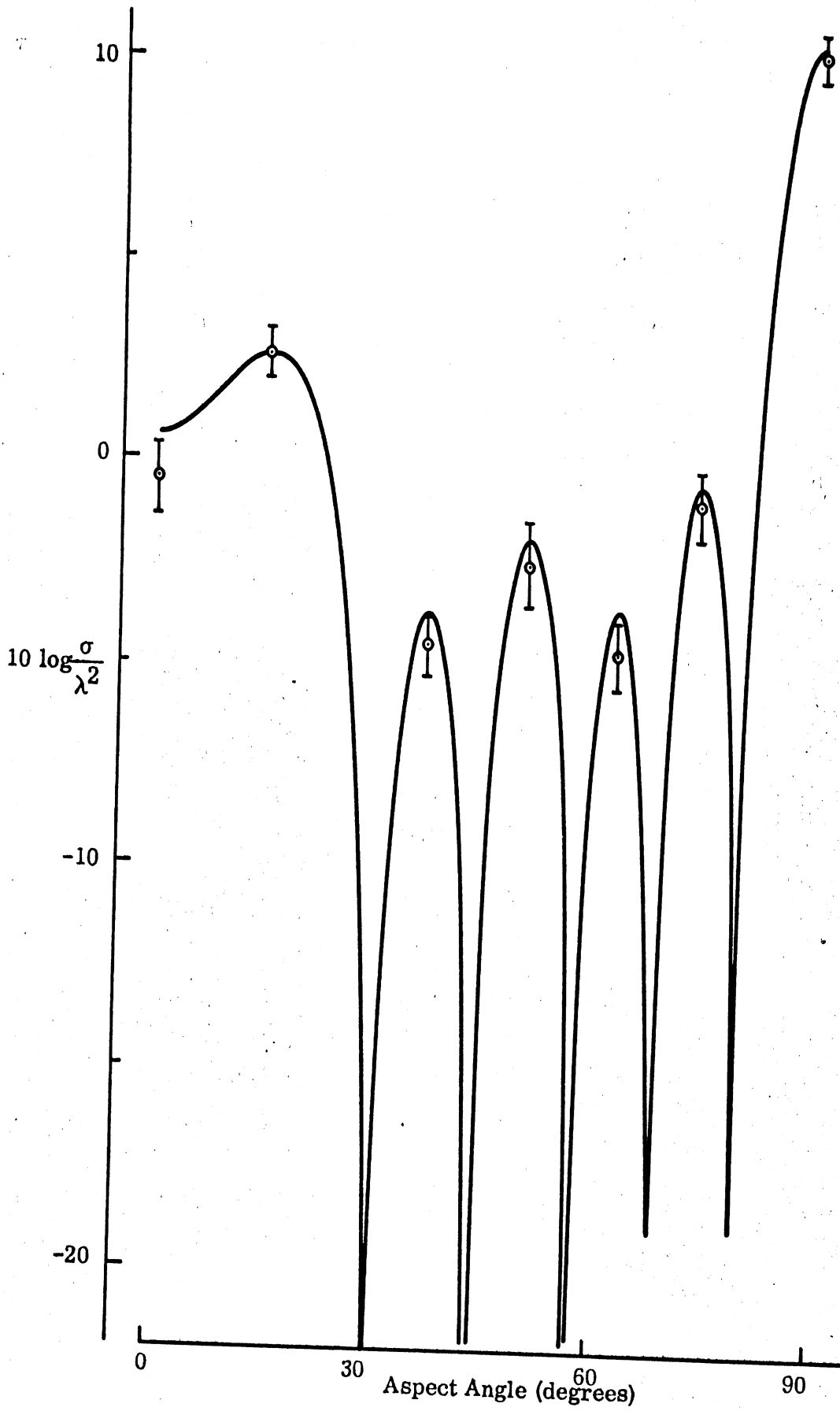


FIG. 4-17: COMPARISON OF NORAIR SDT THEORY WITH RANGE DATA FOR HH POLARIZATION ( $ka=1.36$ ). Each mean value and standard deviation is based on 21 data samples.

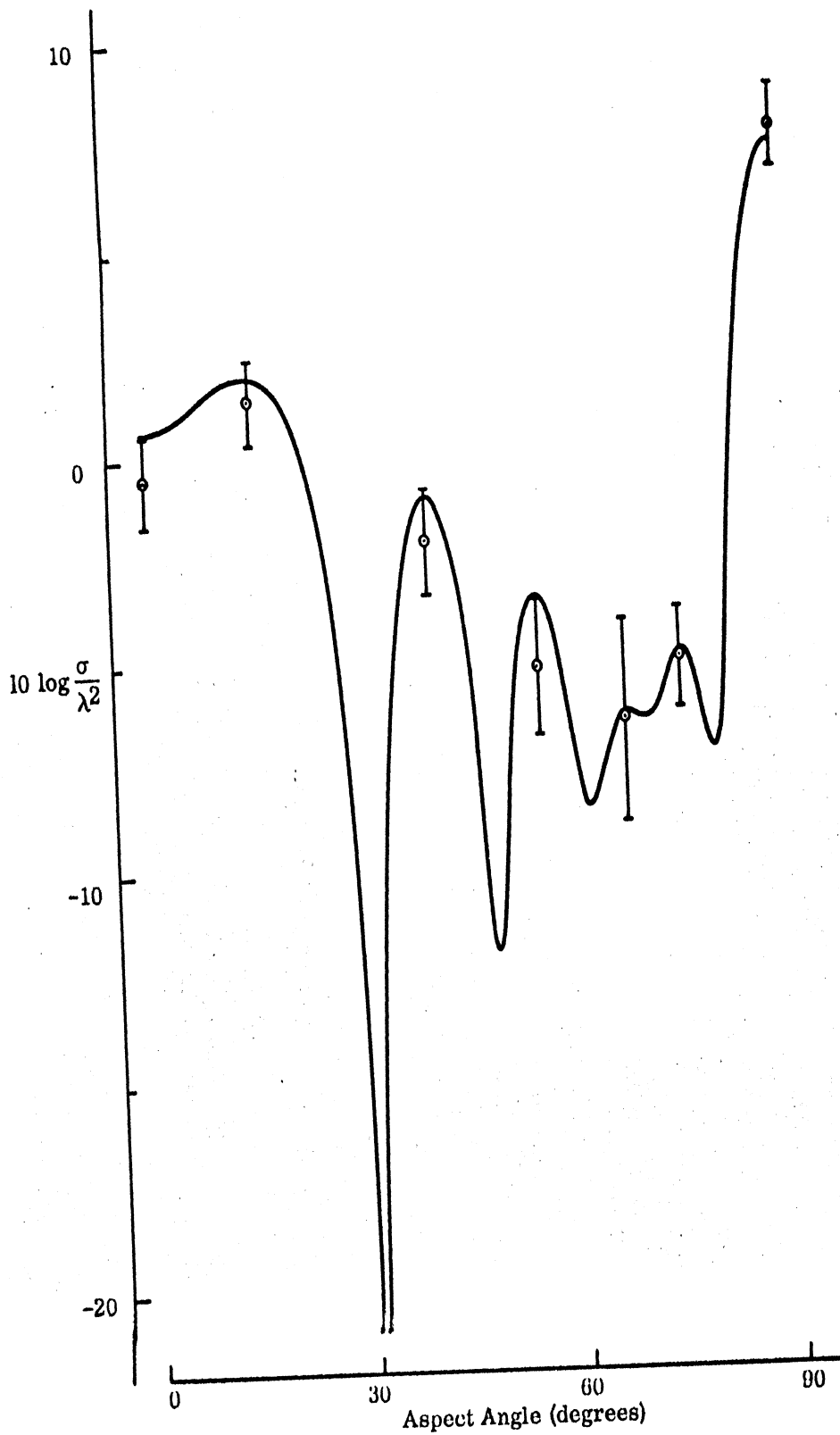


FIG. 4-18: COMPARISON OF NORAIR SDT THEORY WITH RANGE DATA FOR VV POLARIZATION ( $ka=1.36$ ). Each mean value and standard deviation is based on 21 data samples.

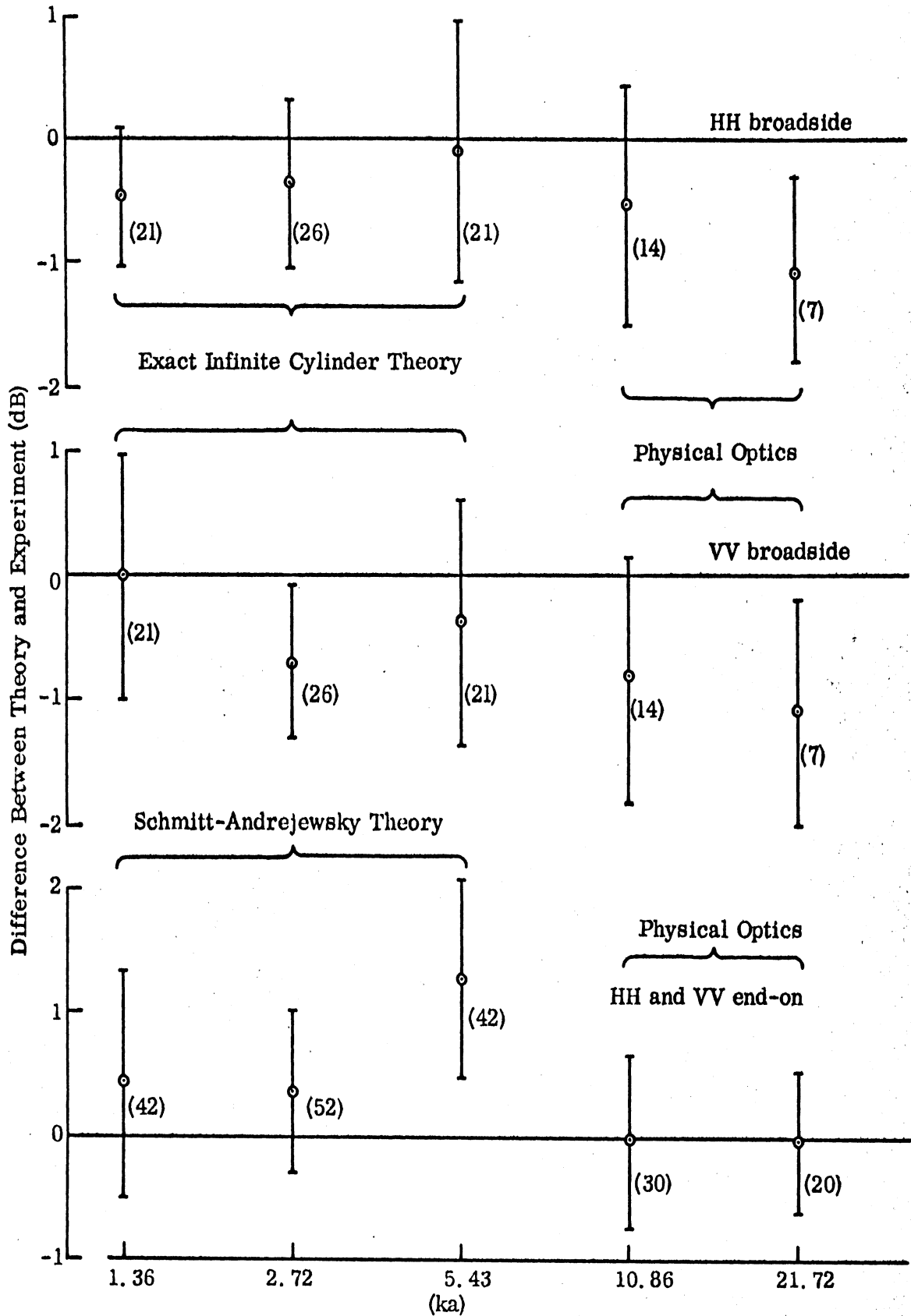


FIG. 4-19: DIFFERENCES BETWEEN THEORY AND EXPERIMENT ARE SUMMARIZED FOR END-ON AND BROADSIDE ASPECT ANGLES. The quantities in parentheses show the number of data samples used to obtain the means and standard deviations.



as an interference signal. As we will point out later, the ranges turned in poorer performances on the larger cylinders than the smaller ones for  $ka = 1.36$ .

Turning now to Fig. 4-19, we present a comparison of three theoretical methods with experiment, this time for all five values of  $ka$ , but only for end-on and broadside viewing angles. The exact infinite cylinder solution was used to predict the theoretical broadside returns for both polarizations for the first three  $ka$  values. For end-on incidence, the Schmitt-Andrejewski theory was used, again for the first three  $ka$  values. Beyond  $ka = 10$ , both theories become indistinguishable from physical optics theory and the latter was used for both broadside and end-on incidence for the two highest  $ka$  values. Note that the differences between theory and experiment are plotted in Fig. 4-19.

For broadside incidence, the theory seems to be no better than 1 dB for either polarization, and this occurs, moreover, for the highest  $ka$ . Since physical optics becomes progressively more successful as  $ka$  increases, and since the frequency was high, we believe it is the experiment that should be doubted. Near field effects were particularly severe for this high  $ka$  and the theory should be accurate within 0.5 dB here. By discounting the high  $ka$  experimental data, we venture to state that the exact infinite cylinder theory predicts the broadside return within  $\pm 1.4$  dB with a confidence level of about 70 percent.

For end-on incidence, physical optics does very well for higher  $ka$  (10.86 and 21.72). There was no near field problem in this case and the mean values lie less than 0.05 dB from the physical optics prediction. For  $ka = 1.36$  and 2.72, the Schmitt-Andrejewski theory lies less than 0.5 dB below the experimental mean, but at  $ka = 5.43$ , it fails by 1.3 dB. Based on Fig. 4-19, we contend that the theory will be no more than 2 dB greater, nor 0.8 dB less, than experiment with a confidence of 68 percent.

None of the mean experimental values presented in Figs. 4-17 through 4-19 lie more than 1.6 dB from the various theories used for comparison and we would like to attribute the theory with more accuracy than we have stated. Indeed, we will take the liberty of endowing the theory with absolute truth in Chapter VI, but Figs. 4-17 through 4-19 do not tell us if theory or experiment is in error; they merely say there is a difference.

## INTRA-RANGE EVALUATION TESTS

Having considered the background material in the first four chapters, we now turn our attention to the reduction and evaluation of the VV and HH measured data. In this chapter we examine the measurements by the intra-range technique which is independent of theory, and is a comparison of separate data (from the same range) that have some relationship to one another through scaling or symmetry. In the following chapter (Chapter VI) data from all the ranges are compared directly with theory.

Earlier in Chapters I and IV we noted how the test data would be reduced and evaluated. Reduction of the data has consisted of recording the amplitude of lobe peaks and the angular location of nulls from each scattering pattern in tables like that shown in Table V-1. The locations of the numbered peaks and the lettered nulls in Table V-1 are indicated on the sample pattern in Fig. 5-1. This pattern is for the lowest  $ka$ , 1.36. As  $ka$  grows, evaluation points 8, 9 and 10 and letters E and F migrate closer to  $\theta = 90^\circ$  and numbers 4, 5 and 6 and letters A, B, C and D move closer to  $\theta = 0^\circ$ , but lobe peak 7 remains in the aspect region near  $45^\circ$ . In the reduction method data recorded for smaller  $ka$  values are equally distributed throughout the region for  $\theta$  between  $0^\circ$  and  $90^\circ$ . As  $ka$  increases the recorded points begin to cluster about the  $0^\circ$  and  $90^\circ$  regions and only one point is recorded in the mid region near  $45^\circ$ . This is an acceptable approach since, as  $ka$  increases, the lobe peaks in the mid region become small in amplitude compared to those at  $0^\circ$  and  $90^\circ$ .

Because our method of reducing and recording the measurements tends to accent the end-on and broadside regions, it follows that our evaluation and grading of the data is based primarily on the performance in these same regions. After recording and examining 60 percent of all the data and knowing that the remaining 40 percent would not be available until the last few days before the final reports would be due, we were forced to further limit the number of points that we could formally evaluate and grade. We concluded that the most efficient

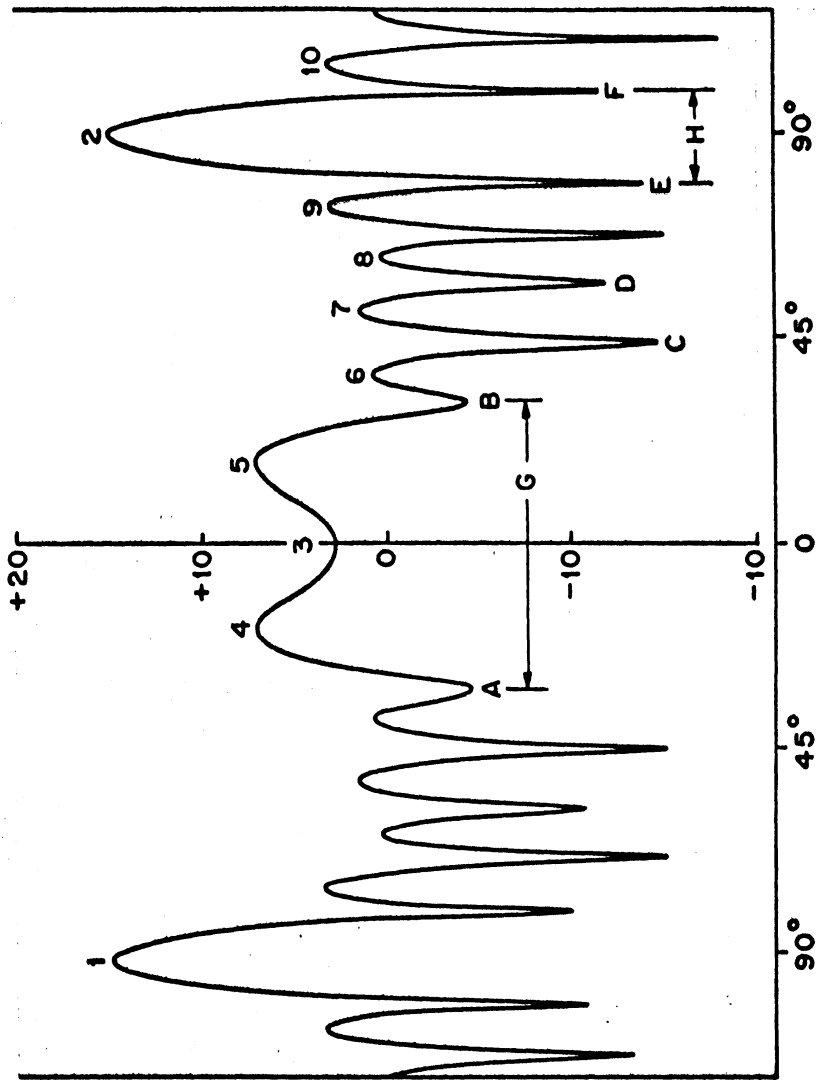


FIG. 5-1: SCATTERING PATTERN SHOWING THE POINTS RECORDED IN TABLE V-1.

TABLE V-1: EXAMPLE OF HOW DATA WAS REDUCED FOR EACH PATTERN FROM EACH RANGE.

Scale: 1/2, Frequency 170 MHz, Polarization, HH, ka = 1.36. See Fig. 5-1 for the location of the points given here.

(dBsm)	1	2	3	4	5	6	7	8	9	10
CC	+15.5	+15.5	+3.0	+6.75	+6.75	0.0	+4.25	+1.0	+2.75	+3.0
RSC	+15.0	+15.0	+2.75	+7.25	+7.25	+0.75	+1.5	+0.5	+4.0	+3.25
/GD/FW	+15.5	+15.5	+3.5	+6.0	+6.0	+0.5	0.0	+1.0	+4.0	+3.75
RSS	+15.0	+15.0	+4.2	+7.2	+7.2	+0.1	+2.5	-0.7	+3.5	+3.5
MC	16.75	17.0	5.0	8.7	8.8	1.3	4.3	1.0	6.0	6.0
THEO	15.6	15.6	5.6	8.1	8.1	1.6	3.1	1.6	4.6	4.6

Lobe Amplitude

(Degrees)	A	B	C	D	E	F	G	H
CC	-33.5	+29.5	+41	+57	+77.5	+99	63	21.5
RSC	-34	+31	+44	+57	+79	+100	65	21
GD/FW	-30	+30.5	+44.5	+56.5	+79.5	+102	60.5	24.5
RSS	-31.0	+31.7	+44.5	+68.4	+80.0	+101	62.7	21
MC	-31	+32	45	+68.2	80.0	100.5	63	20.5
THEO	-30	+30	44	57	79	101	60	22

Null Positions - A through F

Angular Widths - G and H

approach would be to limit our attention to points 2 and 3 in Fig. 5-1. Preliminary examination of these two points indicated that a meaningful insight into the performances of the ranges can be obtained from these samples. At the same time this limitation in our analysis would prevent us from being overwhelmed with too many details. After analyzing the ranges based on the data at end-on and broadside, we believe that we have displayed the weak and strong attributes of the ranges.

The intra-range evaluations consist of constant  $ka$  tests and end-on polarization comparisons. In the constant  $ka$  tests the VV and HH experimental cross sections at end-on and broadside are tabulated in a frequency-model scale display similar to that in Table III-1. The data from each range are presented in a separate table. Comparisons are made within each table along diagonal (constant  $ka$ ) lines; thus the name "constant  $ka$  test" has been assigned to this form of evaluation.

In the end-on polarization comparison the cross section values at  $\theta=0$  are displayed on a graph like that in Fig. 3-8. Measurements from all the ranges are presented in the same graph. In this test, differences are noted between the VV and HH returns at end-on incidence. Theoretically these two values should be equal.

All the measurements involved in the evaluation were read directly from the test patterns submitted by the ranges. No corrections, additions or deletions have been introduced. The estimated accuracy for reading the patterns is  $\pm 0.25$  dB or better, depending on the recording paper submitted to us. The raw data listed in Tables V-2 through V-7 contain the entire family of sample points that will be used in all subsequent evaluations.

## 5.1 Constant ka Tests

Constant ka displays are shown in Tables V-2 through V-6 for the outdoor ranges and a small display for the indoor range in Table V-7. Four cross section values in dBsm are given in each box, these are VV and HH cross sections for end-on and broadside as indicated in the example below.

$\sigma_{VV}(\theta=0^\circ)$	End-on
$\sigma_{HH}(\theta=0^\circ)$	End-on
$\sigma_{VV}(\theta=90^\circ)$	Broadside
$\sigma_{HH}(\theta=90^\circ)$	Broadside

In these tables the frequency is constant across each row and is given along the left margin. Model size is constant in each column and is indicated at the top of the columns.

The diagonal lines connect boxes with the same ka. Cross sections in the same position in adjacent boxes along the same diagonal should differ by 6 dB while those separated by one or two boxes should differ by 12 and 18 dB respectively.

As an example, consider Table V-2 (Conductron data) for the 1/8 and 1/16 scale models when  $ka=1.36$ . Here  $\sigma_{VV}(\theta=0^\circ)$  and  $\sigma_{HH}(\theta=0^\circ)$  both differ by 7 dB,  $\sigma_{VV}(\theta=90^\circ)$  by 6.5 dB, and  $\sigma_{HH}(\theta=90^\circ)$  by 6.0 dB. For the same case in Table V-3 (Radiation Service data) the corresponding differences are 6.5, 6.25, 5.5 and 5.25 dB. Similar comparisons may be made between the 1/8 and the 1/4; then 1/4 and the 1/2 scale measurements, and so on for each line of equal ka. Deviations from the expected 6 dB difference are noted as errors.

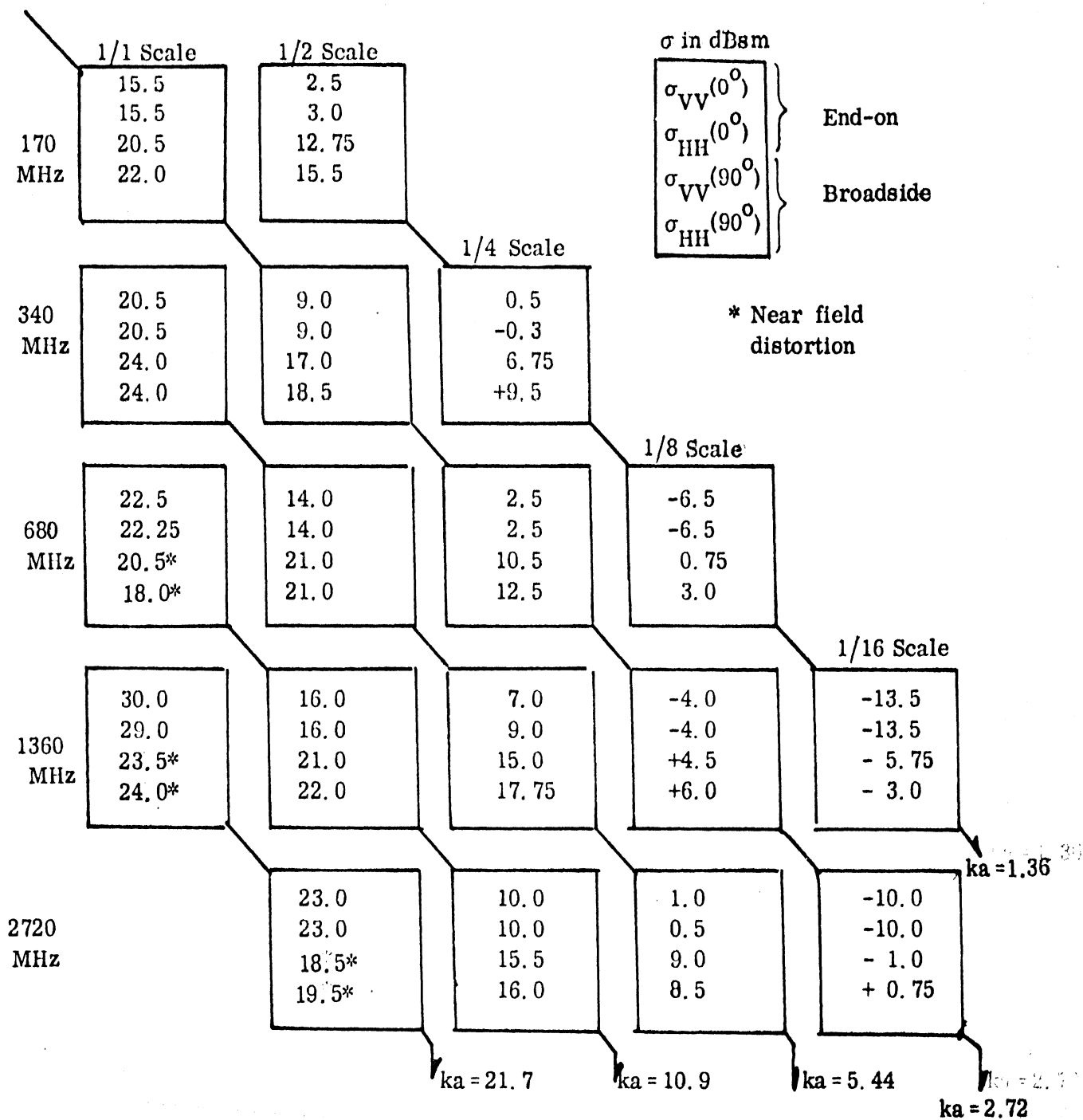


TABLE V-2: CONDUCTRON CONSTANT  $k_a$  TEST.

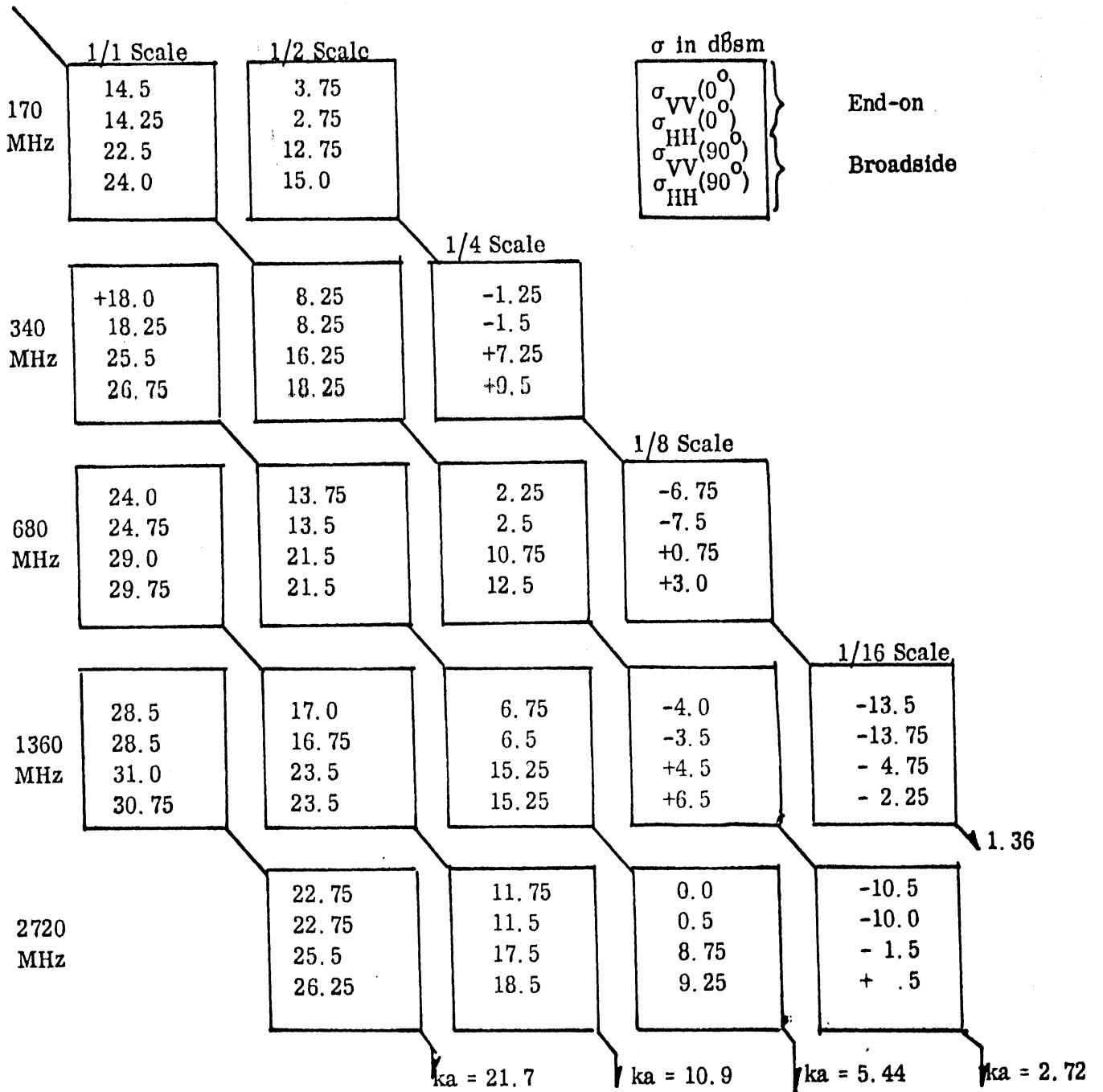


TABLE V-3: RADIATION SERVICE CONSTANT  $ka$  TEST.



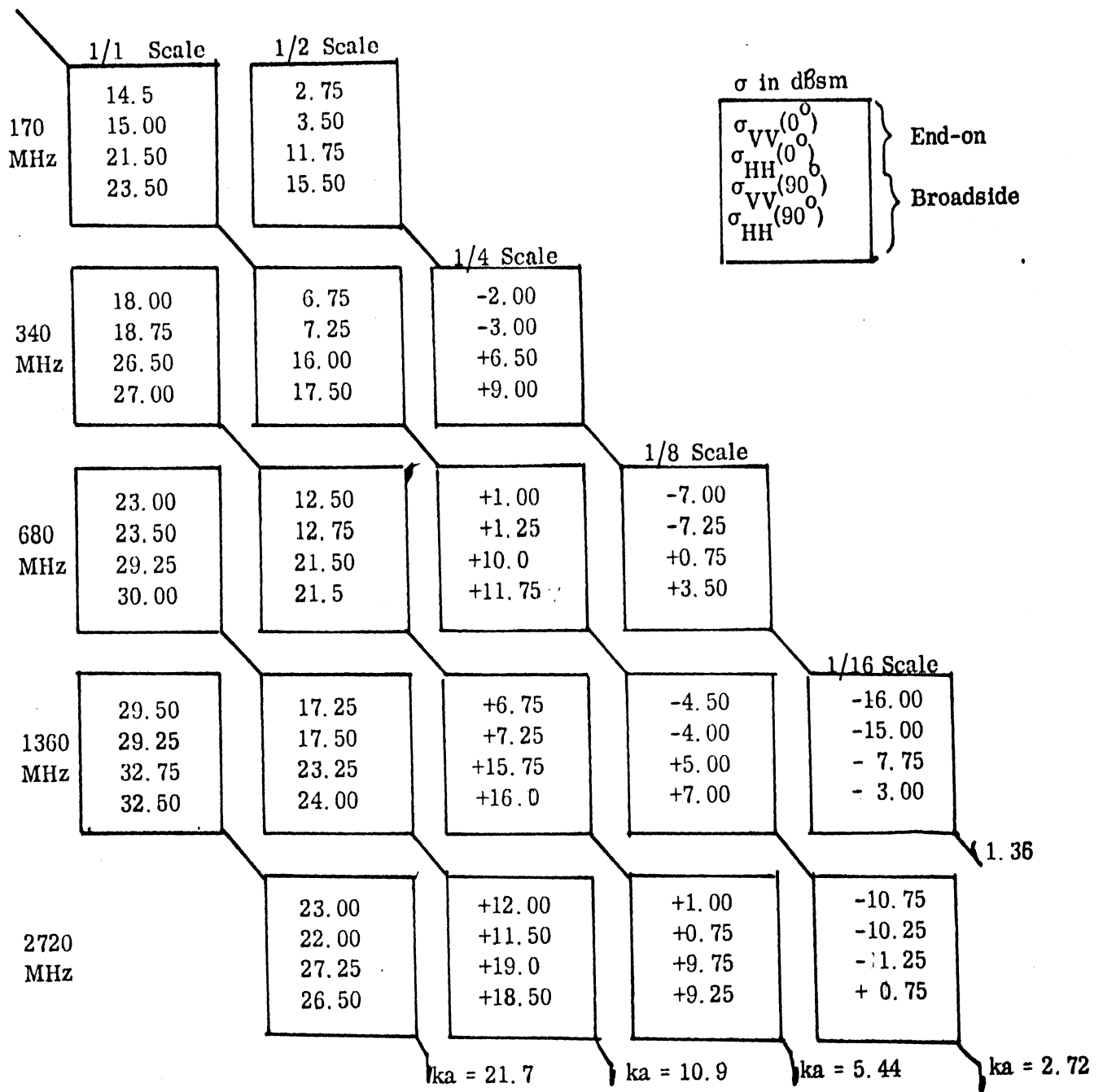


TABLE V-4: GD/FW CONSTANT  $k_a$  TEST.

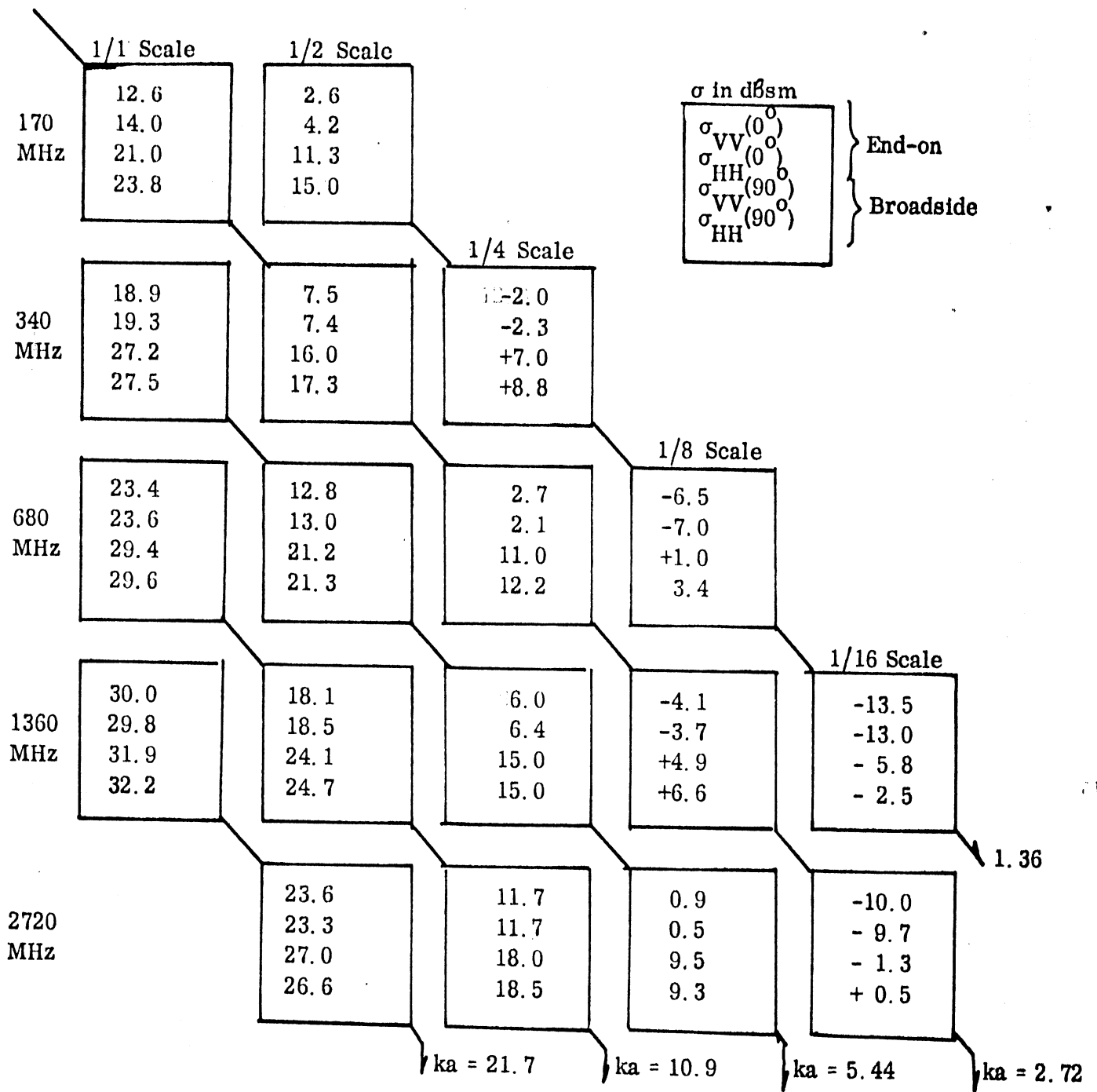


TABLE V-5: RAT SCAT CONSTANT  $ka$  TEST.

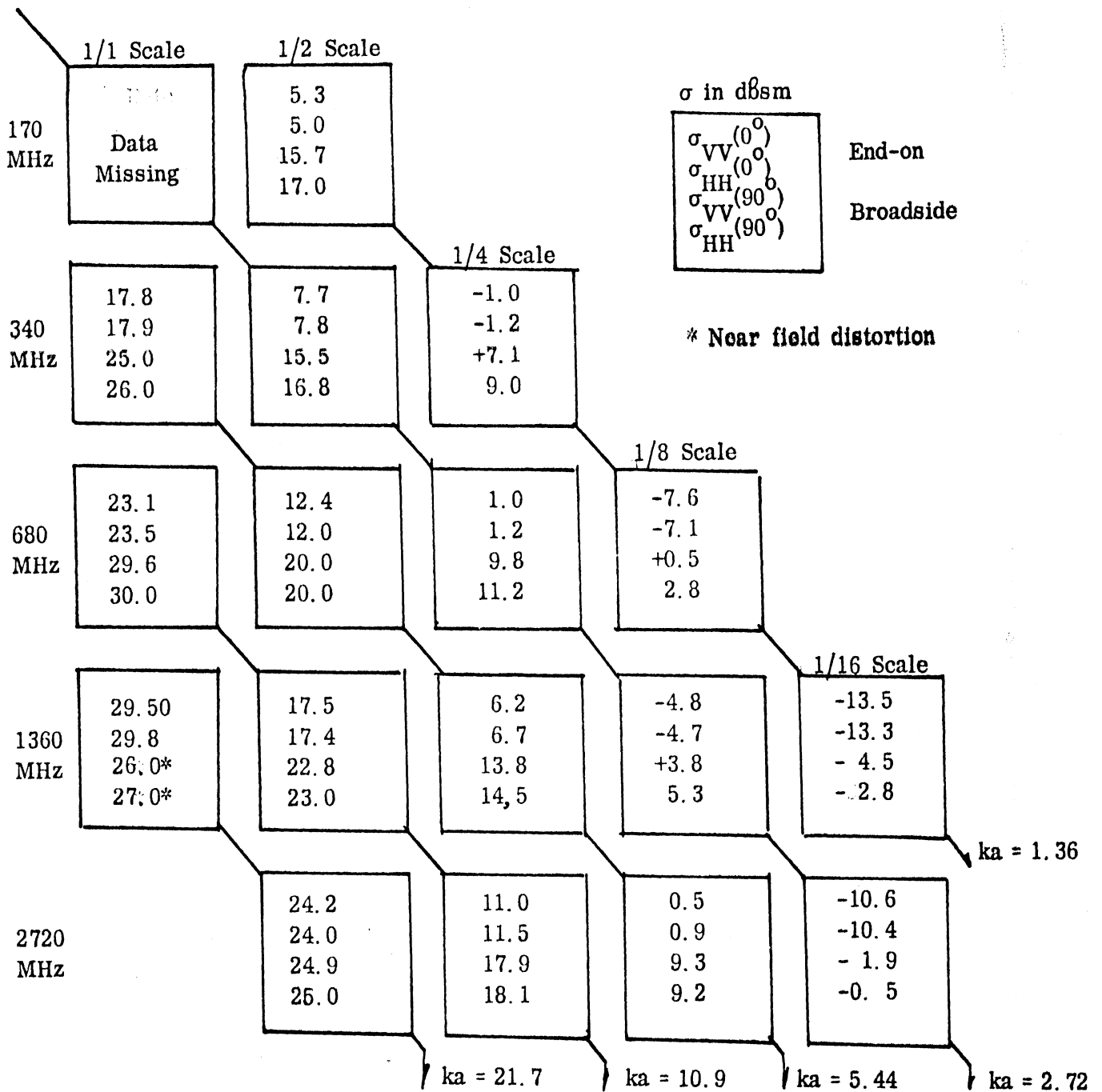


TABLE V-6: MICRONETICS CONSTANT ka TEST.

	1/8 Scale	1/16 Scale	
1360 MHz	- 2.8 - 3.1 + 4.0 5.7	-12.7 -13.1 - 5.3 - 4.2	ka=1.36
2720 MHz	+2.9 + 1.9 +10.0 10.0	- 9.4 -9.6 - 1.7 0.0	
			ka=5.44
			ka=2.72

TABLE V-7: AVIONICS LABORATORY CONSTANT  
ka TEST.

Figure 5-2 shows the distribution of errors for the constant ka tests. In this figure the number of errors is given as a function of error size. For the upper three cases the errors are more discrete in their spread than in the lower two cases. This represents a difference in reading accuracy. Early in the program we read data to the nearest  $\pm 1/4$  dB while later on we attempted to read it to the nearest  $\pm 1/10$  dB. This change is due in part to the finer graduation on the recording paper used by some of the ranges.

The final tally for the errors found in the constant ka tests for Tables V-2 through V-7 are given in Table V-8. A total of 52 comparisons were made for each table except Table V-7. Extreme near field errors in the Conductron and Micronetics data are indicated by an asterisk (\*). Although these errors may be between 6 and 12 dB in size, we treat them as any other error which exceeds 1 dB. Micronetics is missing data for the full scale model at 170 MHz because this target was dropped from the pedestal during its last test at this range. This missing data is also treated as an error of greater than 1 dB and therefore reduces this range's performance.

TABLE V-8: CONSTANT ka TEST RESULTS

Range	Errors 1dB and Less		Grade
	Total No. 52	Percent	
CC	39	75	C
RSC	46	88	B
GD/FW	43	84	B
RSS	45	87	B
MC	41	79	C
AL	4	100	A

Displays like Table V-8 above are used to summarize the evaluation results for other tests also. In these tables and some of the graphs the range names are abbreviated; CC (Conductron), RSC (Radiation Service) GD/FW (General Dynamics, Fort Worth), RSS (RAT SCAT Site), MC (Micronetics)



and AL for Avionics Laboratory. The number of errors and the corresponding percentage of the total number of cases are listed according to range. A letter grade is found on the far right and is based on the percentage of errors 1 dB or less. As in Volume I the letter grades are defined as:

	A	Very Good	(90 to 100 percent)
	B	Good	(80 to 89 percent)
	C	Acceptable	(70 to 79 percent)
	D	Barely Acceptable	(60 to 69 percent)
	E	Intolerable	( 0 to 59 percent)

The constant ka test is independent of theoretical calculations and it seems reasonable to expect that no errors in scaled measurements should exceed 1 dB. Generally speaking, we found that most of the errors greater than 1 dB were due to near field distortion. In these cases the errors would be located in the lower left portion of the constant ka test tables where the measurements for the larger models at higher frequencies are found.

There are other errors which are not due to near field effects; most noticeable in this regard is the difference between the 1/2 and 1/4 models for  $ka=1.36$  for all the ranges but particularly for GD/FW and RAT SCAT. GD/FW had one 3 dB error between the 1/8 and 1/16 scale data for  $\sigma_{VV}(0^\circ)$ . This was the largest error in this test not due to near field effects. It is hard to find a reason for such a large error other than carelessness. With the exception of the cases just mentioned, the performances of the ranges in this test are satisfactory, but are far from outstanding as reflected in the grades of Table V-8 .

## 5.2 End-on Polarization Comparison

The end-on cross sections for VV and HH polarization given in the tables of the last section are now arranged in another form in Fig. 5-3. At first glance this dense collection of data may be hard to digest, but after referring back to Fig. 3-8, this display hopefully will become more meaningful. Constant ka lines are labelled in Fig. 3-8 but have been omitted from Fig. 5-3 to reduce conjection. The one inch long horizontal lines in Fig. 5-3 are the same

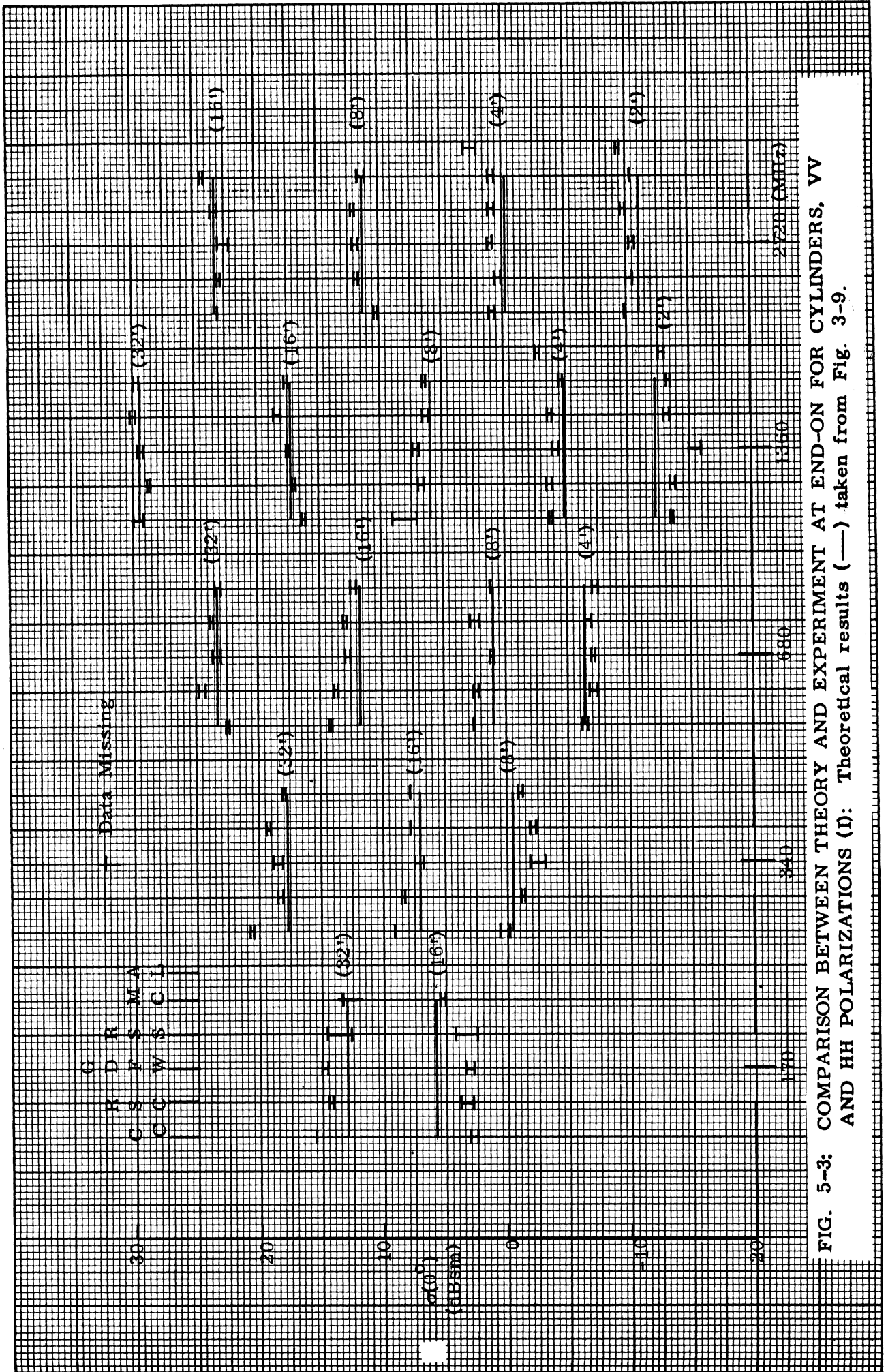


FIG. 5-3: COMPARISON BETWEEN THEORY AND EXPERIMENT AT END-ON FOR CYLINDERS, VV AND HH POLARIZATIONS (I): Theoretical results (—) taken from Fig. 3-9.



theoretical values denoted by points in Fig. 3-8. The short pairs of horizontal lines connected by a vertical line (generally there are five pairs per theoretical line) show the level of the experimental data from the ranges. In each case they are listed from left to right as Conductron, Radiation Service, General Dynamics, RAT SCAT, Micronetics, and in four instances, Avionics Laboratory.

The lengths of the vertical lines in this display are equal to the error between the VV and HH end-on returns but no attempt is made to show which of the short horizontal lines is VV and which is HH. Although the theoretical, as well as experimental, results are shown in Fig. 5-3, the evaluation test is like the constant  $k_a$  test in that it is essentially independent of theory. For the present case we depend upon theory only for the proof that for end-on incidence the VV and HH polarized returns are equal. If one accepts this statement there is no further need for any theoretical arguments for the polarization comparison tests.

Therefore, for the present test we should concern ourselves only with the length of the vertical line connecting the VV and HH cross sections in Fig. 5-3. The distribution for the polarization errors shown in Fig. 5-3 are displayed in bar graph form in Fig. 5-4. This display has the same format as Fig. 5-2. Note that Micronetics has a very good cluster of errors less than 1 dB but failed to score perfectly because of missing data. Errors 1 dB and less are tabulated in Table V-9 along with the percentages and grades.

TABLE V-9: END-ON POLARIZATION TEST RESULTS

<u>Range</u>	<u>Errors 1 dB and Less</u>		<u>Grade</u>
	<u>Total No. 18</u>	<u>Percentage</u>	
CC	17	95	A
RSC	18	100	A
GD/FW	18	100	A
RSS	16	89	B
MC	17	95	A
AL	4	100	A

So far as grades are concerned this test produced the highest marks of all the evaluation tests, with three ranges registering errors of 1 dB or less

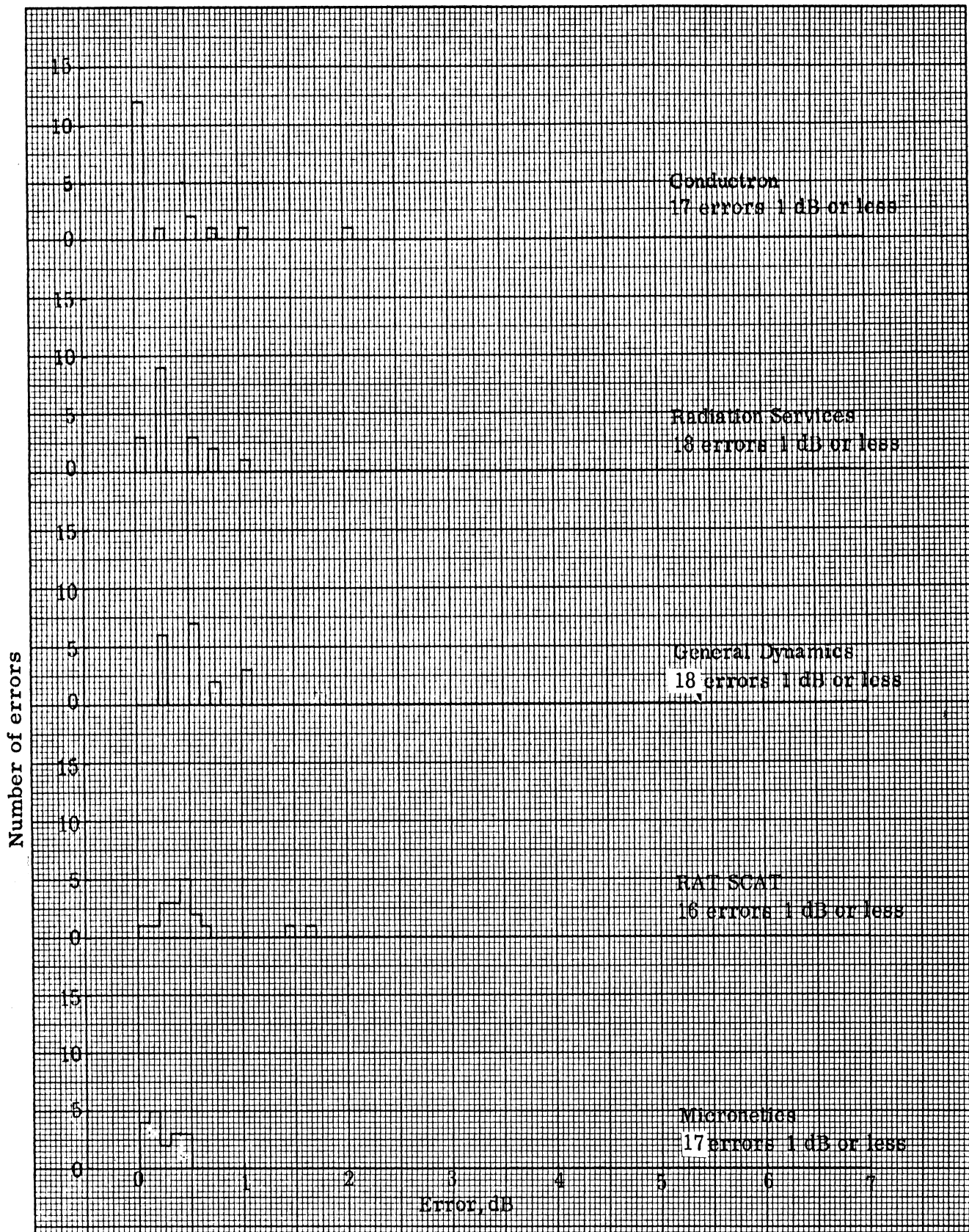


FIG. 5-4. DISTRIBUTION OF ERRORS BETWEEN HH AND VV MEASUREMENTS OF END-ON RETURNS. BEST POSSIBLE SCORE IS 18.

for all the comparisons. The four cases in which errors exceeded 1 dB stand out in Figs. 5-3 and 5-4. At 170 MHz RAT SCAT had two errors of 1.75 dB and Micronetics was missing the full scale measurements. At 1360 MHz for the 1/4 scale model Conductron achieved the low point with a 2 dB error.

It is to be expected that for this type of evaluation all the ranges should do well. The agreement between VV and HH polarization for an aspect view with total roll symmetry should be one of the first things checked by the range operator when he is analyzing cross section data. Another reason for the good performance in this test is that near field effects are not present at end-on incidence because at this aspect angle the target always exposes a sufficiently small view of itself to the radar so that it is in the far field. We should emphasize, perhaps, that this has been a test for consistency by making use of a well known theoretical fact. Results which rate high in this test may have an inferior rating when we examine the absolute level of the end-on cross section in the next chapter.

This concludes the intra-range tests where data from each range were compared and judged by themselves, independently of theory and the other ranges. The separate results for each range were then compared with one another in Tables V-8 and V-9. For the inter-range tests in the next chapter, bar graphs like that in Fig. 5-3 are used to compare measurements with theory.

## VI

### INTER-RANGE EVALUATION TESTS

In the inter-range evaluation tests, cross section measurements for end-on and broadside aspect angles are compared with one another and with theory. These comparisons are presented in the same form as in Fig. 5-2, in fact the data in this figure is one of the cases analyzed in these tests. Data for broadside (VV and HH) are grouped in the form shown in Figs. 3-10 and 3-11. Also included here are VV and HH measurements for the sidelobe peaks next to broadside.

If near field distortions are excluded, we find that broadside measurements agree better with theory than do the end-on measurements. For a fixed frequency-model size situation there is also better agreement for broadside than end-on measurements when related experimental data are compared. As should be expected, near field distortions become even more pronounced in the data for the first sidelobe away from broadside than for the specular flash.

#### 6.1 End-on Data

To rate the ranges on the basis of the measured end-on returns, we computed the differences between the theory and the experiment for both polarizations. These differences can be inspected in the graphical presentation of Fig. 5-2 or they can be calculated from the raw and theoretical data presented in Tables III-1 and V-2 through V-7. The distribution of the errors is displayed in Fig. 6-1 and, as in the error distributions shown in Chapter V, we make no distinction between positive or negative errors. Notice that Micronetics' errors were all clustered below 1.3 dB and that this range did better than all the other ranges in spite of its failure to measure the full scale cylinder at 170 MHz. Conductron shows the largest spread in errors and turned in the poorest performance, while the remaining three lie between these extremes.

The Avionics Laboratory error distribution is not included in Fig. 6-1 because it performed far fewer tests. Its performance is tabulated, however, along with those of the other ranges, in Table VI-1. Because AL turned in only

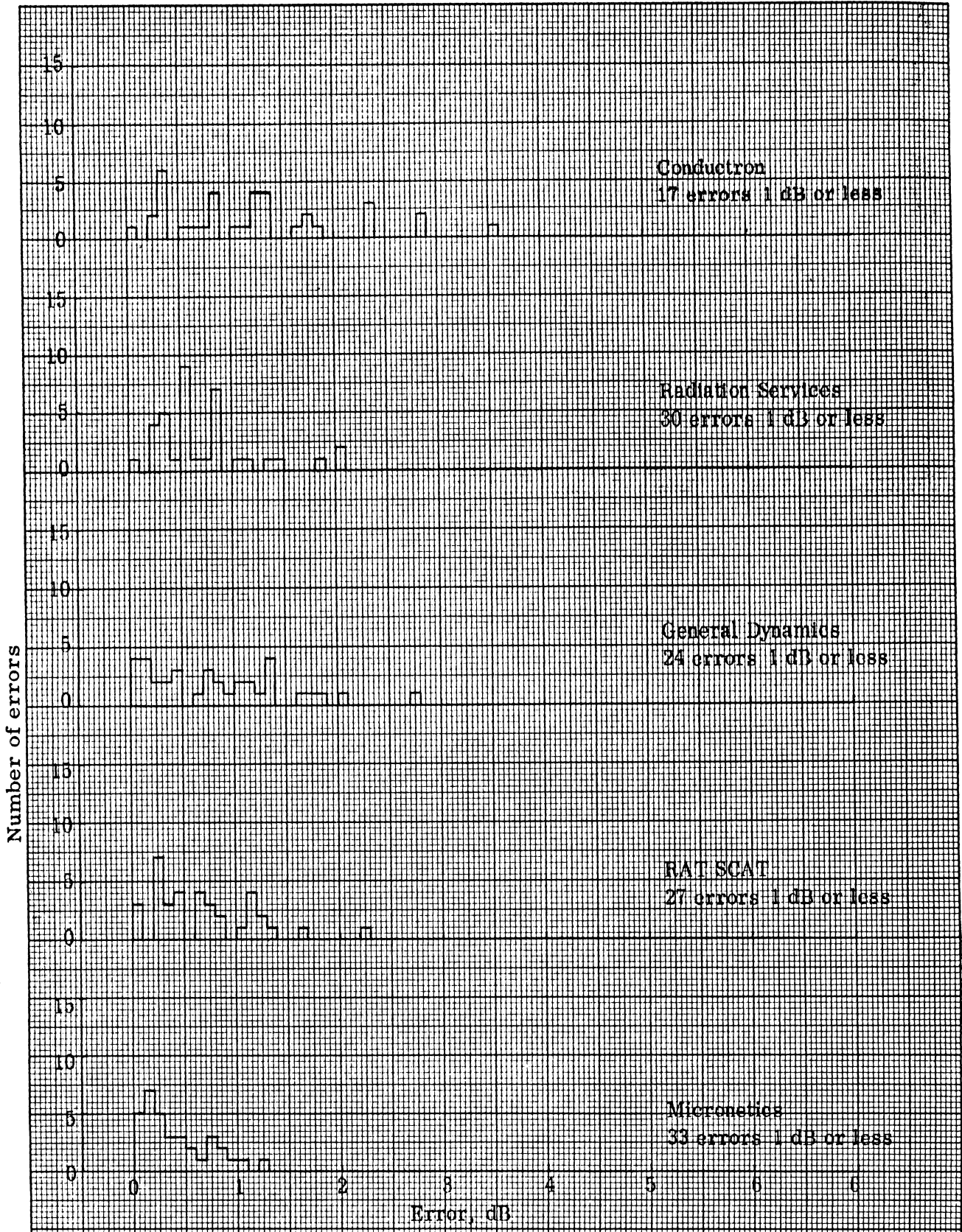


FIG. 6-1: DISTRIBUTION OF ERRORS BETWEEN THEORY AND EXPERIMENT FOR END-ON INCIDENCE, BOTH POLARIZATIONS. BEST POSSIBLE SCORE IS 36.

four errors less than 1 dB of a total of 8 measurements, it receives an E.

**TABLE VI-1: ERRORS BETWEEN THEORY AND EXPERIMENT FOR END-ON INCIDENCE (see Fig. 6-1).**

Range	Errors 1 dB and Less		Grade
	No.	Percent	
CC	17	47	E
RSC	30	83	B
GD/FW	24	67	D
RSS	27	75	C
MC	33	92	A
AL	4*	50	E

\* of a possible 8 .

The poor results in Table VI-1 cases some suspicion on the reliability of the theory, but we pointed out in Chapter III that the end-on theoretical model was not expected to be as accurate as the broadside model. In the mathematical formulation for end-on incidence, we assumed the cylinder to be an isolated disc rather than one attached to a cylinder of finite length with another disc at the opposite end. For smaller  $ka$ , effects from the far end of the cylinder occur in the form of reflected traveling waves that weaken the end-on theory. This is, in fact, seen in the measurements of Fig. 5-2 in which the theory and experiment match better for increasing  $ka$ . In most instances of disagreement between theory and experiment in Fig. 5-2 a shift of one dB or less in the theory would align it with the average of the experimental data.

More disturbing than the lack of agreement between theory and measurement are the variations between the measurements themselves. If the measurements were more consistent among themselves it would be easy to conclude that the theory was in error by a given amount, but in many cases in Fig. 5-2 it is difficult to assign a "correct" radar cross section value.

In summary, for the end-on comparison with theory, Micronetics did very well, perhaps because its crew used an auxiliary flat plate calibration in addition to a sphere. Both Conductron and the Avionics Laboratory did poorly; General Dynamics performed only somewhat better. Radiation Service and RAT SCAT take second and third place honors, respectively, behind Micronetics.



## 6.2 Broadside Data

As in the end-on tests, we computed the differences between theory and experiment for broadside incidence. Since the broadside return depends upon polarization, the computations were performed for the VV and HH polarizations separately, but the errors are presented as a single group. The errors can be ascertained from the graphical displays of Figs. 6-2 and 6-3 or they can be computed by taking differences between the theoretical values of Table III-1 and the experimental values reported in Tables V-2 through V-7.

The asterisks in Figures 6-2 and 6-3 indicate that severe near field pattern distortions were observed in the experimental results. These distortions were so great that the data belonging with a particular theoretical value in some cases fell on that associated with an entirely different target. The inclusion of the distorted values in Figs. 6-2 and 6-3 would have caused much confusion, hence we omitted plotting them and merely indicated the presence of these large errors by the asterisks. The missing values are available, of course, in the tables of Chapter V.

We find better overall agreement between theory and experiment in Figs. 6-2 and 6-3 than we did in Fig. 5-2 (the end-on results). Most of the discrepancies in the broadside data are due to near field distortions which we know exist. One noticeable exception is the General Dynamics measurements of the 2-foot (1/16 scale) cylinder at 1360 MHz in Fig. 6-2. This result is almost 3 dB below the theory and measurements of the other ranges. Equally poor measurements for this case were found in Fig. 5-2, but in Fig. 6-3 (HH polarization, broadside) good agreement is found for this case both with theory and the other measurements. The errors in the GD/FW data and the other errors not attributable to near field effects, are thought to be due to one or more effects, e. g. lack of field uniformity, secondary reflections or lack of sufficient care in normal calibration procedures.

The distributions of the errors in the broadside measurements are shown

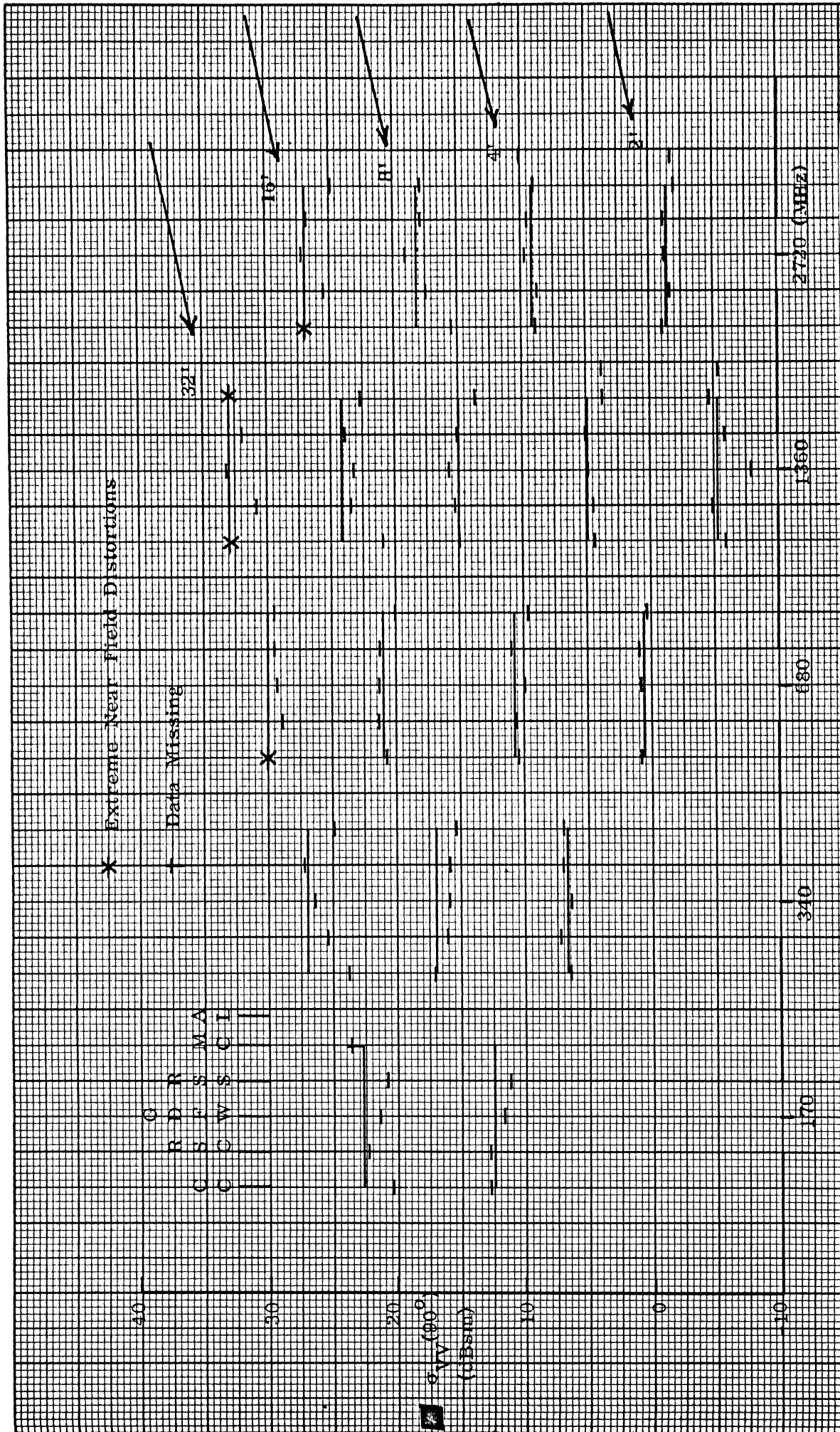


FIG. 6-2: COMPARISON BETWEEN THEORY AND EXPERIMENT AT BROADSIDE FOR CYLINDERS, VV POLARIZATION. Theoretical results (—) taken from Fig. 3-10.



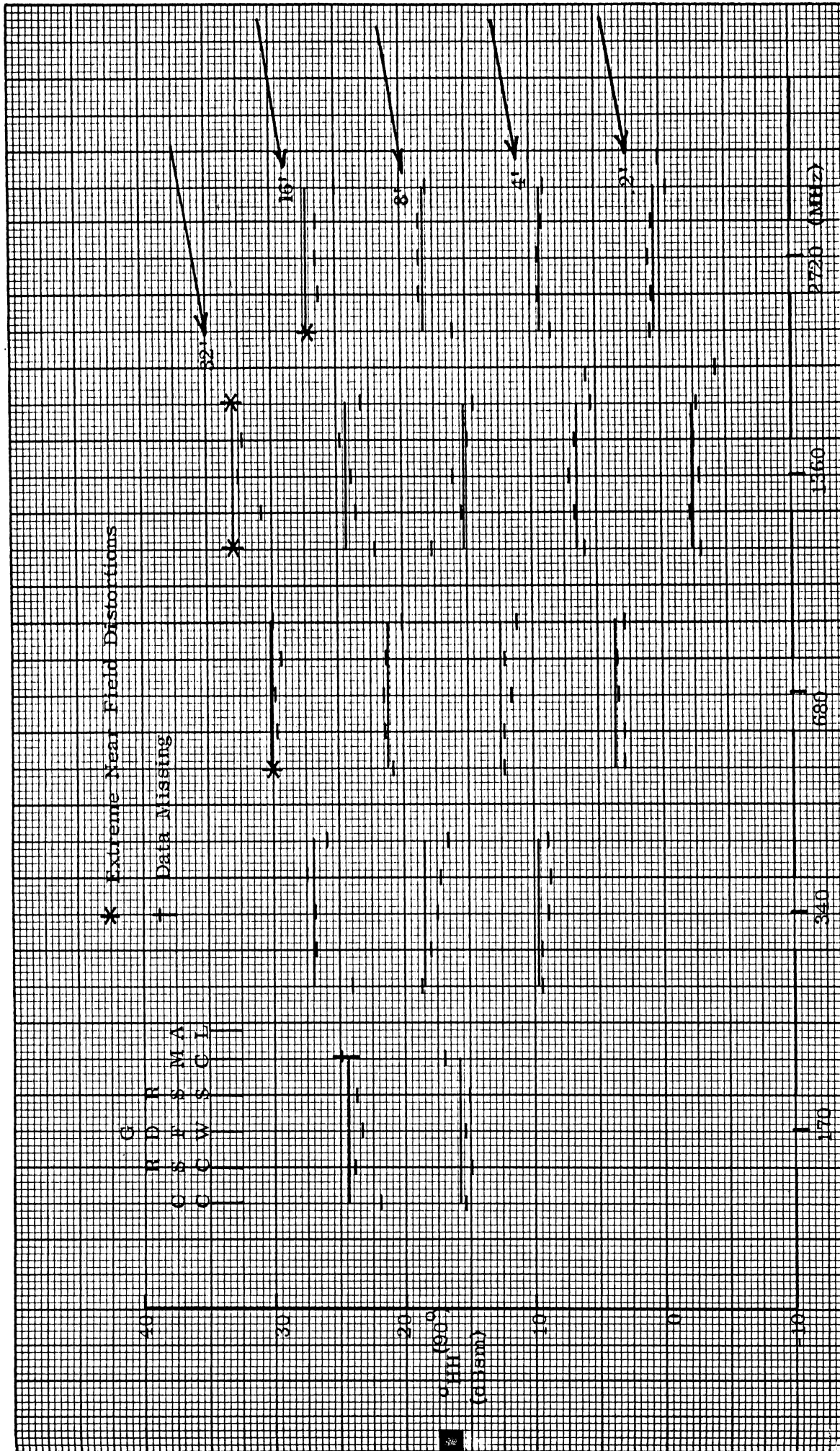


FIG. 6-3: COMPARISON BETWEEN THEORY AND EXPERIMENT AT BROADSIDE FOR CYLINDERS, HH POLARIZATION. Theoretical results (—) taken from Fig. 3-11.

in Fig. 6-4 and are summarized in Table VI-2. Note that because many of Micronetics' errors are greater than 1 dB, this range turned in the worst performance. General Dynamics shows the best performance of the outdoor ranges, but as indicated in the summary of Table VI-2, Avionics Laboratory outperformed them all.

TABLE VI-2: ERRORS BETWEEN THEORY AND EXPERIMENT AT BROADSIDE FOR BOTH POLARIZATIONS

Range	Errors 1 dB and Less		Grade
	No.	Percent	
CC	21	58	E
RSC	30	83	B
GD/FW	34	94	A
RSS	33	92	A
MC	15	42	E
AL	8*	100	A

\* of a possible 8.

### 6.3 Sidelobe Symmetry

Measurements and theory for the sidelobes immediately to the left and right of the broadside specular return are shown in Fig. 6-5 for VV and Fig. 6-6 for HH polarization. These displays should not be confused with those in Fig. 5-2, in which differences in polarization are given. In this case the two short lines are the measured levels of the right and left sidelobes. The sidelobe data are being examined in ascertain the degree of pattern symmetry. Ideally the two short horizontal lines connected by the vertical line should be equal. Any differences, and these are indicated by the length of the vertical line, are indicative of pattern "sloppiness" or near field problems. One of the first signs of near field distortion is the disappearance of the first sidelobes, indicated by the asterisks, thus more field field problems are seen in these figures than in the broadside data.

For  $ka \geq 2.72$  the theoretical sidelobe level is found by subtracting 13 dB from the broadside return since the pattern response for this aspect region is

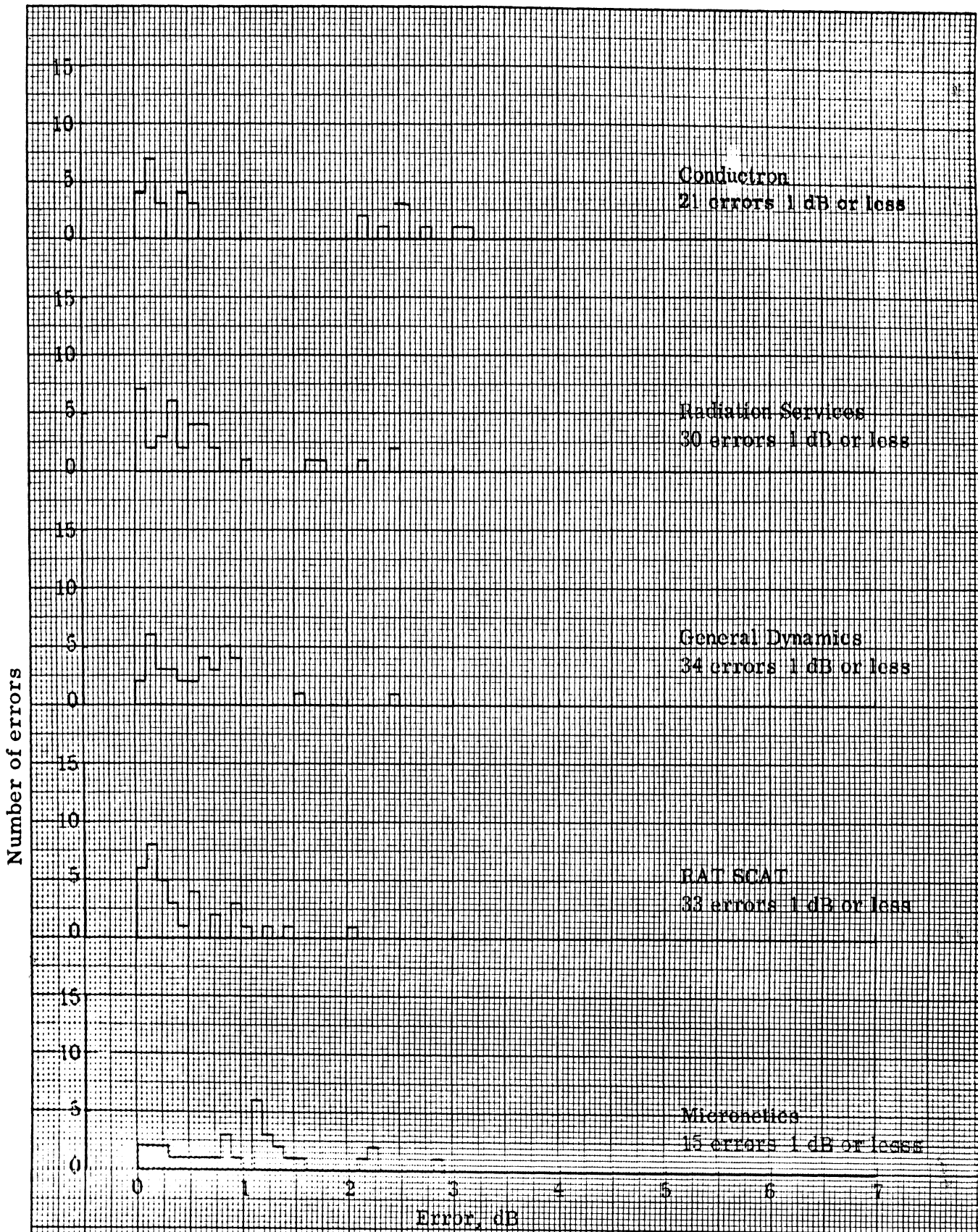


FIG. 6-4: DISTRIBUTION OF ERRORS BETWEEN THEORY AND EXPERIMENT FOR BROADSIDE INCIDENCE, BOTH POLARIZATIONS. BEST POSSIBLE SCORE IS 36.

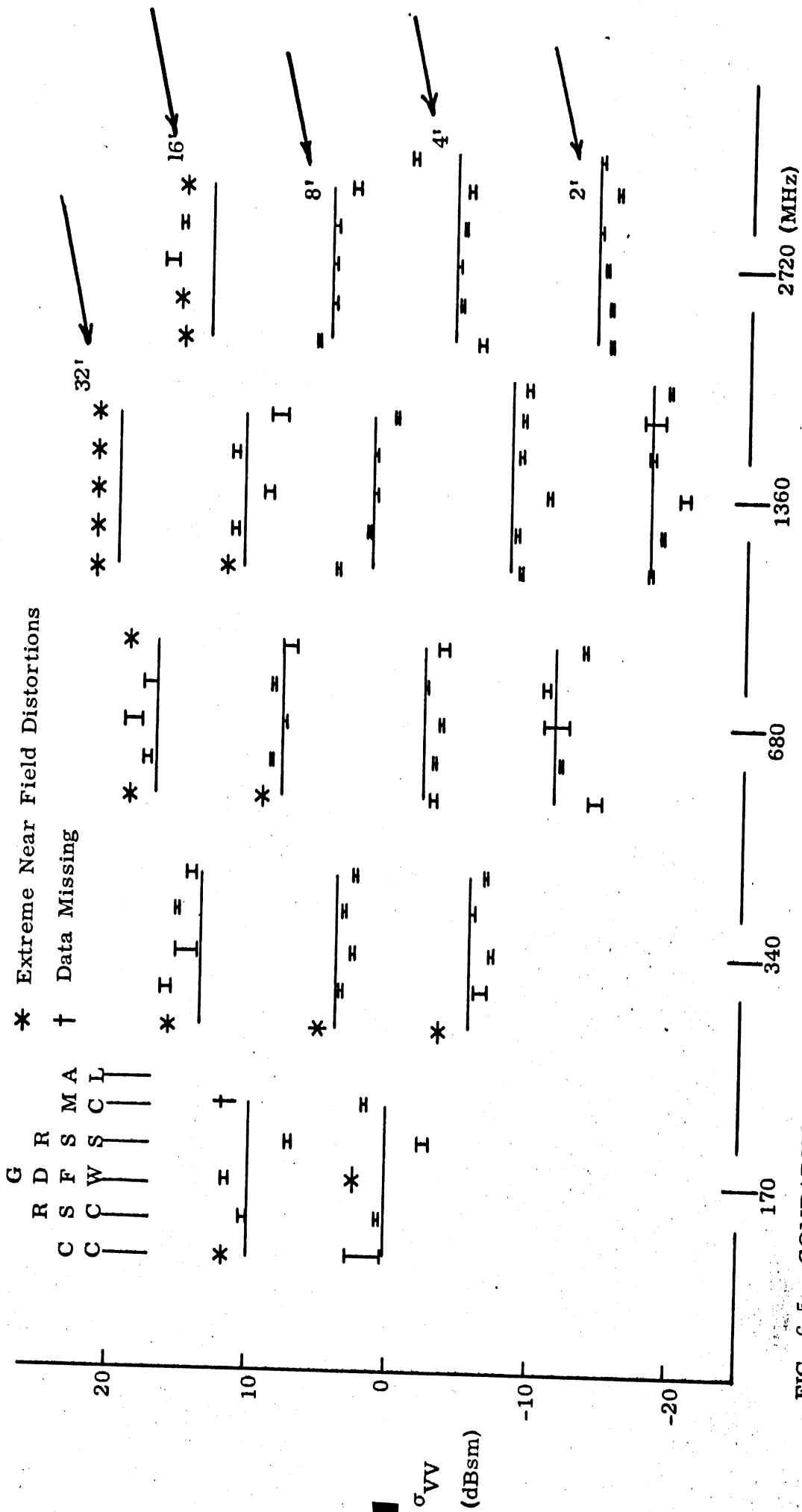


FIG. 6-5: COMPARISON BETWEEN THEORY AND EXPERIMENT AT FIRST SIDELOBES NEXT TO BROADSIDE (1) FOR CYLINDER, VV POLARIZATION.

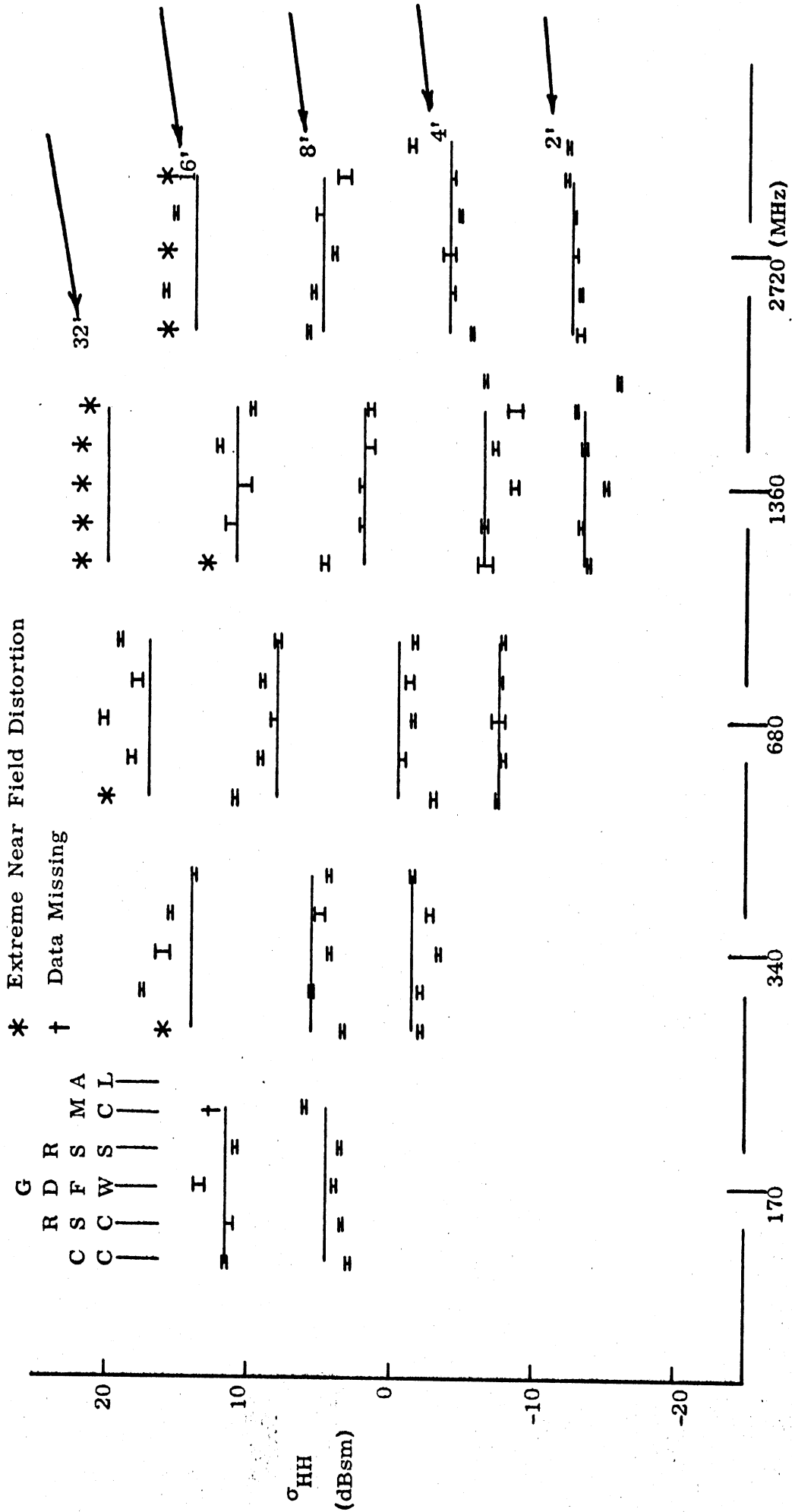


FIG. 16-6: COMPARISON BETWEEN THEORY AND EXPERIMENT AT FIRST SIDELOBES NEXT TO BROADSIDE (I) FOR CYLINDER, HH POLARIZATION.

governed by a  $\sin x/x$  behavior (see Eq. 3.13),. For the case of  $ka=1.36$  the sidelobe level is read directly from Fig. 3-2 in  $\text{dB}\lambda^2$  and converged to  $\text{dBm}^2$  for each model size.

No grades have been assigned to these measurements because they do not reveal any new sources of errors. Most of the troubles shown in Figs. 6-5 and 6-6 can be seen in the broadside and end-on comparisons. These results have been included to give additional examples showing how the data can be reduced as well as to emphasize that a primary cause of error in the test program is due to near field distortions. Another area where errors were noticeable is the  $ka=1.36$  region and some of the evaluation tests suggest this target size is a troublesome one independently of near field effects. See the discussion on secondary reflections in Section 4.1.2.5 of Volume I.

#### 6.4 Special Evaluation for $ka=1.36$

Of all the measurements submitted to us by the ranges, the  $ka=1.36$  patterns showed the widest unexplained spread in values. To demonstrate the divergence of the data, we present the four patterns in Figs. 6-7 through 6-10, all for  $ka=1.36$ . The first two (6-7 and 6-8) summarize the measurements of the  $1/2$  scale cylinder at 170 MHz and the last two (6-9 and 6-10) summarize the measurements of the  $1/8$  scale cylinder at 680 MHz. The ranges performed somewhat better at the higher frequency than the lower.

To arrive at an evaluation of this special case, we sampled the individual range patterns at all integral values of  $5^\circ$  of aspect lying between (and including) end-on and broadside. This produced 19 radar cross section values for each range and polarization for 170 and 680 MHz. In addition, we treated the theory as given by the Norair SDT (Figs. 4-17 and 4-18) as though it represented data from a sixth range. Having effectively six sets of range data (five actually from the ranges and one from the theory) we computed the mean radar cross section at each of the aspect angles shown in the figures and used these values as "standards". The departure of individual range returns from these mean values constituted "errors", which we listed and tabulated. Each range (including the theory) pattern thus bears 19 values of error for each of the four patterns, leaving us with 76 numbers to evaluate per range.

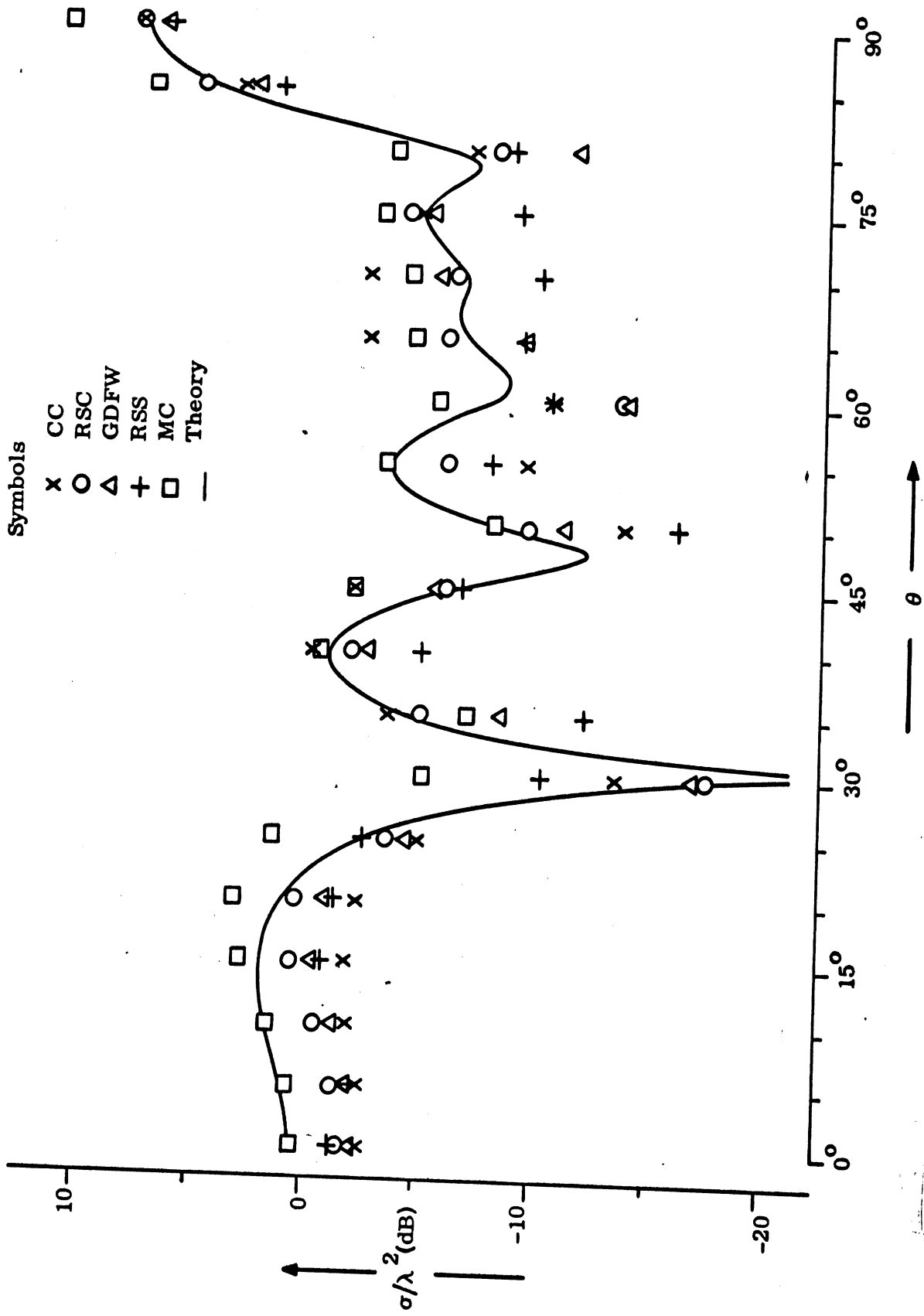


FIG. 6-7: COMPARISON BETWEEN THEORY AND EXPERIMENT FOR THE 16 FOOT CYLINDER FOR VV POLARIZATION AT 170 MHZ.

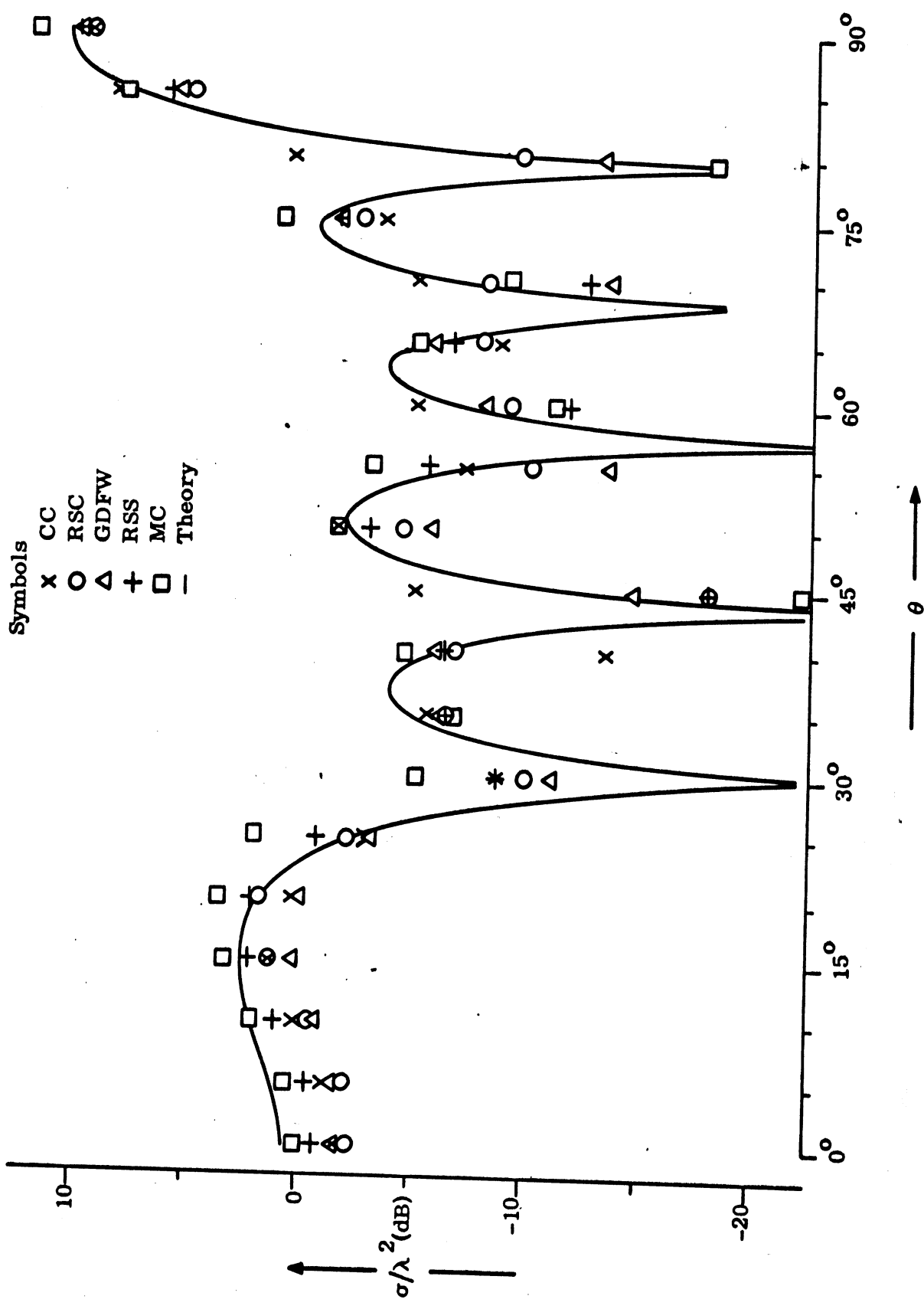


FIG. 6-8: COMPARISON BETWEEN THEORY AND EXPERIMENT FOR THE 16 FOOT CYLINDER FOR HH POLARIZATION AT 170 MHZ.



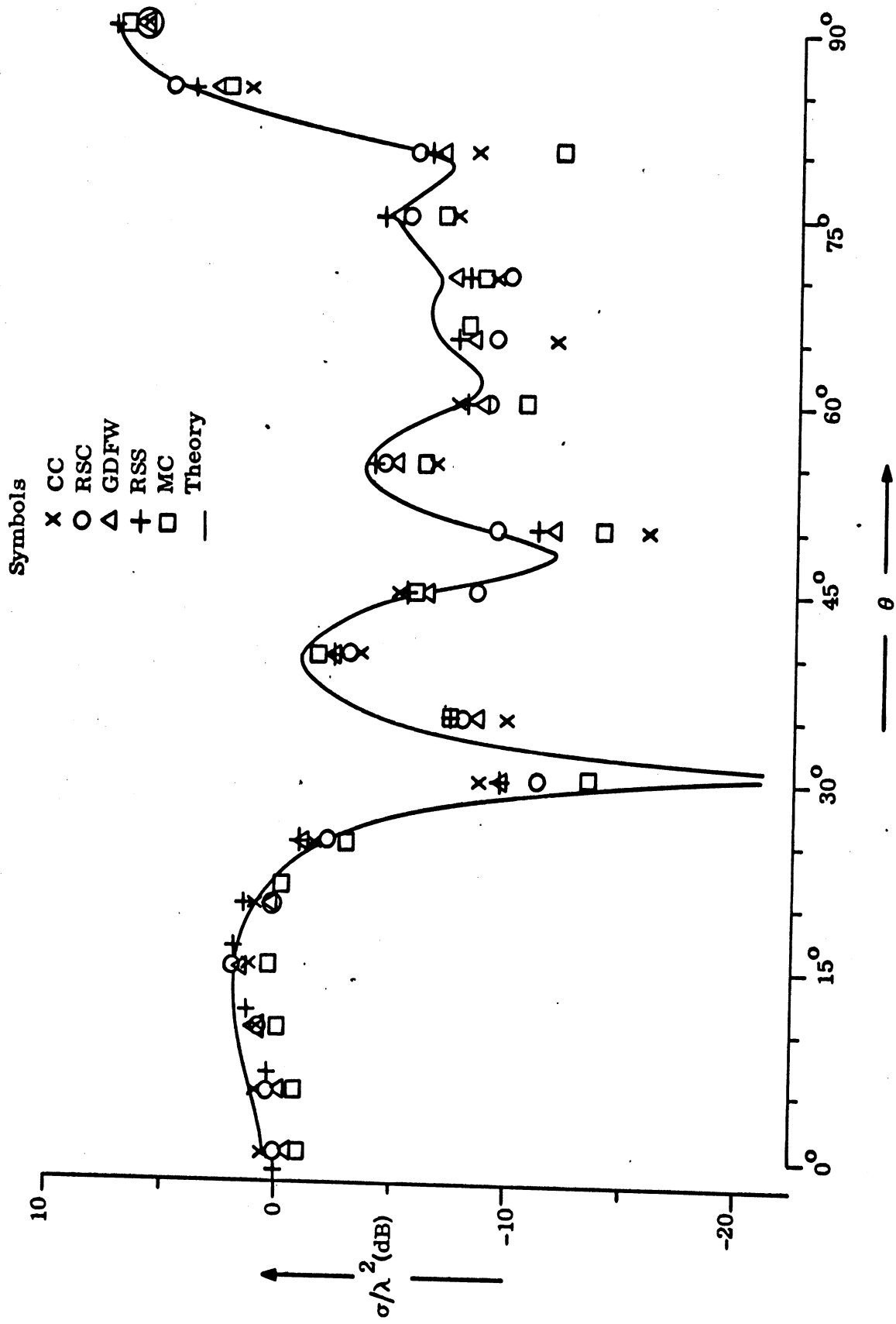


FIG. 6-9: COMPARISON BETWEEN THEORY AND EXPERIMENT FOR THE 4 FOOT CYLINDER FOR VV POLARIZATION AT 680 MHZ.

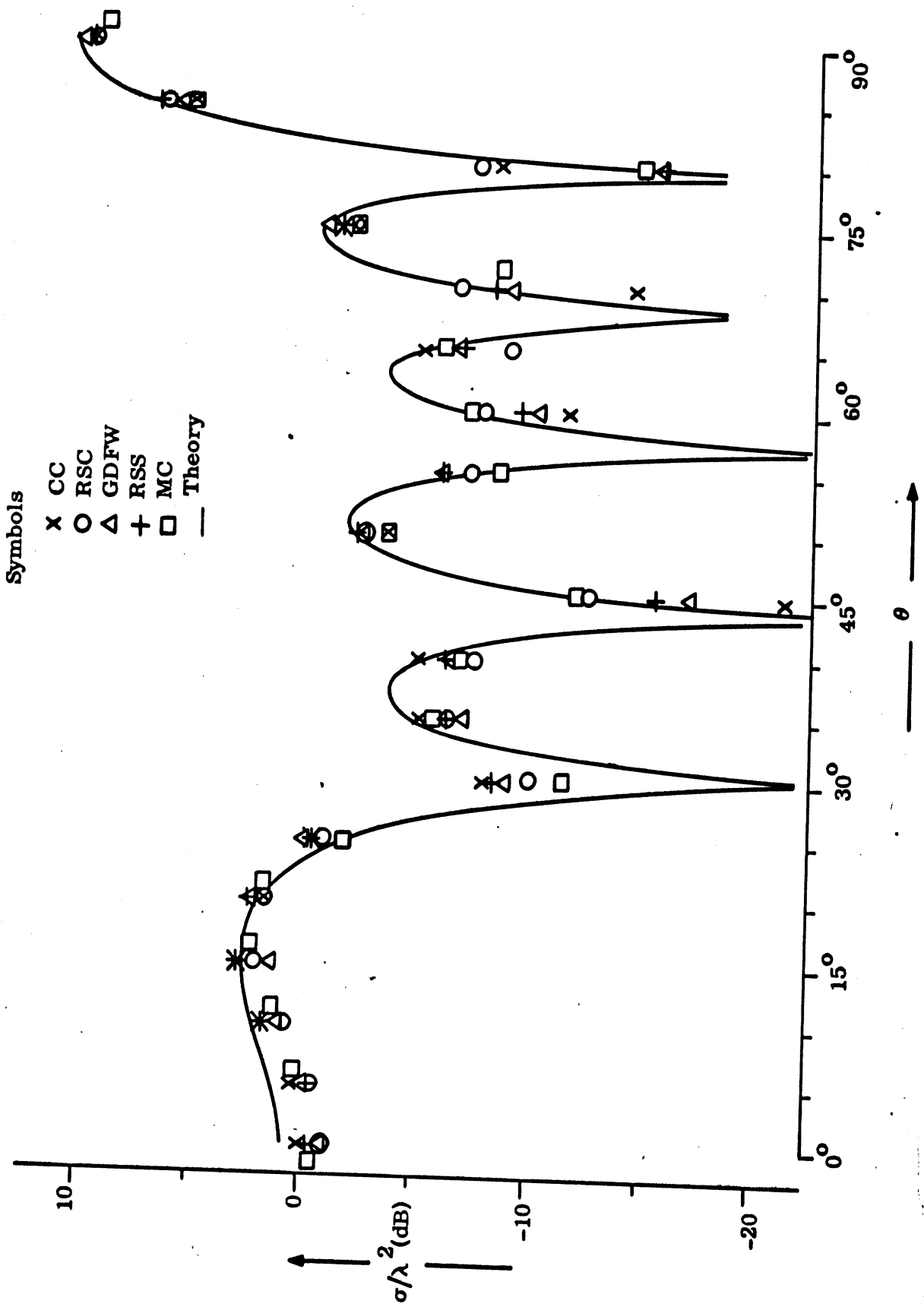


FIG. 6-10: COMPARISON BETWEEN THEORY AND EXPERIMENT FOR THE 4 FOOT CYLINDER FOR HH POLARIZATION AT 680 MHZ.

The theoretical cross sections were not considered in two instances because of the deep nulls it predicts at the 30° aspect angle. We therefore excluded the two largest errors of each range from the analysis, leaving each of the six (five ranges and the theory) with 74 error values. The error distribution generated by the above analysis is shown in Fig. 6-11 and the reader will surmise from the plots that this was a severe test for all the ranges because there are substantial numbers of large errors.

The range performance for this special low ka test are summarized in Table VI-3. Note that, although we did not present the error distribution for the theory, its performance is carried in Table VI-3 like those of the five ranges. Observe that the theory "flunked" along with two other ranges, but remember that the errors summarized in Table VI-3 were generated by a comparison against mean performances, and not against theory. No range did better than "C" for this test and Micronetics, Conductron, and the theory all received an "E" grade. We want to emphasize that the poor performance of the theory in this test should not reflect on the theory used in comparisons at end-on and broadside, which is more dependable than that over the entire aspect range.

TABLE VI-3: RANGE RATINGS FOR SPECIAL PATTERN TEST ( $ka=1.36$ ).

Range	Number of Errors	Percentage of Errors	Grade
	<u>1 dB or less</u>	<u>1 dB or less</u>	
Theory	40	54	E
CC	36	49	E
RSC	53	72	C
GD/FW	52	70	C
RSS	46	62	D
MC	30	41	E

Number of errors

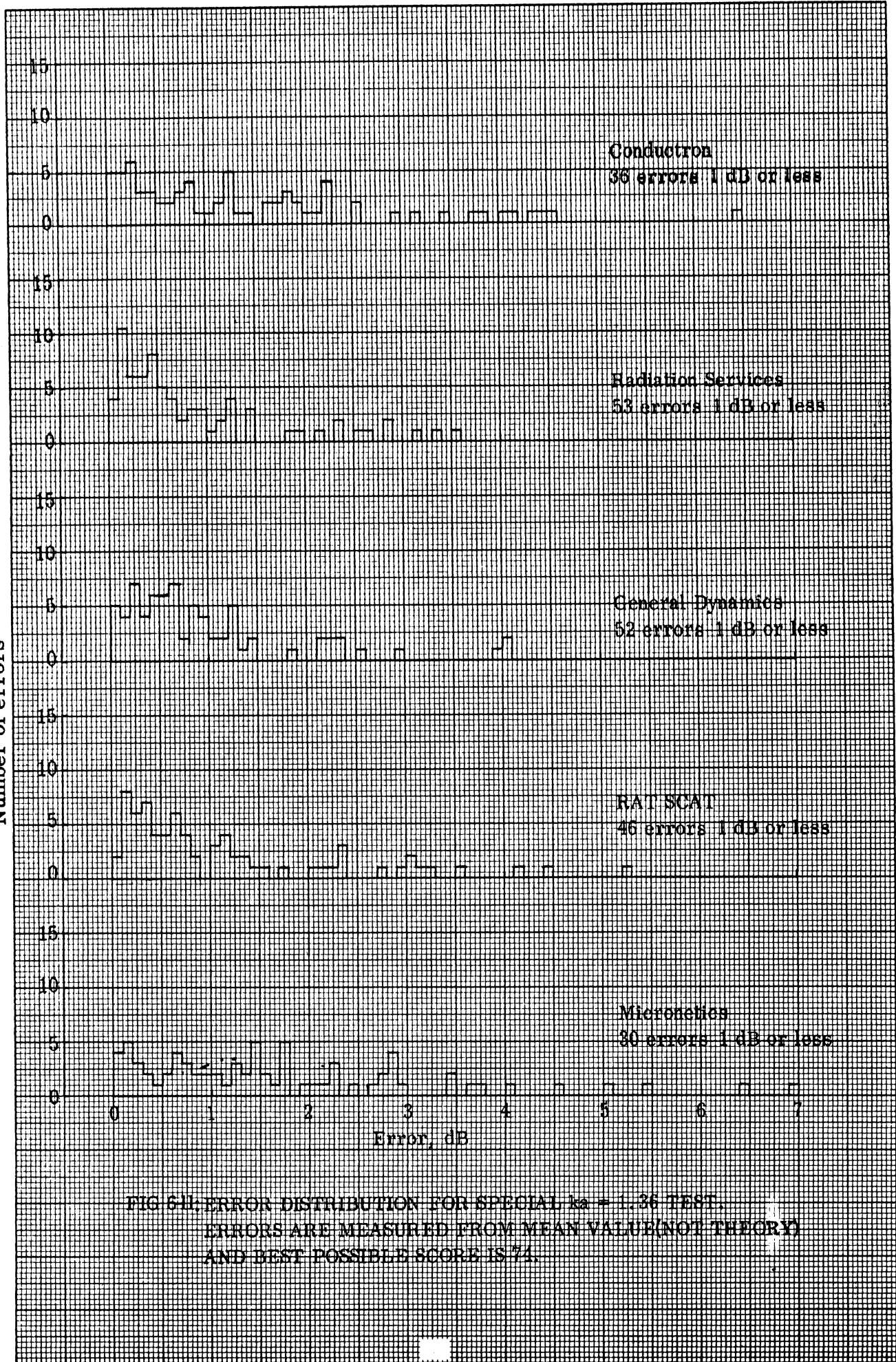


FIG 6-11: ERROR DISTRIBUTION FOR SPECIAL  $k_a = 1.36$  TEST.  
ERRORS ARE MEASURED FROM MEAN VALUE (NOT THEORY)  
AND BEST POSSIBLE SCORE IS 74.

concord

## 6.5 Summary of Co-Polarized Measurements

In Chapters V and VI we presented an error distribution plot and a table summarizing range performance for each of five evaluation tests. The distribution of all the errors of these tests is collected and shown in Fig. 6-12, and Table VI-4 summarizes the overall range performances. Note that Avionics Laboratory was not evaluated in the special low ka test. Figure 6-12 shows that each range had a few large errors, some as large as 7 dB, but that Radiation Service is the best overall performer. Had we decided to rate the ranges on errors 0.1 dB or less, Conductron would have been the best performer.

Table VI-4 clearly shows that the poor performance with which we credit Conductron and Micronetics has been built up from a cumulation of relatively poor performances throughout the five tests. Radiation Service comes out number 1 in three tests and number 2 in two tests and number 3 in one test. The result is that this range is at the head of the list in the total accuracy evaluation of the co-polarized tests. Note that only five percentage points separate the top three positions in the outdoor ranges; it was a close race.

Two problem areas were found in the evaluation of the co-polarized data; a) in the measurement of the larger models at the higher frequencies, and b) for model-frequency combinations when  $ka=1.36$ . The cause of problem (a) was insufficient distance between target and the radar or near field distortion. Conductron had the most difficulty with this problem because their maximum range was limited to 200 feet. Micronetics also had near field distortion. For the other three ranges, these effects were just becoming visible, particularly in the sidelobe data in the last section.

The second problem (b) with the  $ka=1.36$  data seemed to bother all the ranges especially for the 16-foot (1/2 scale) model at 170 MHz. Lack of agreement

Number of errors

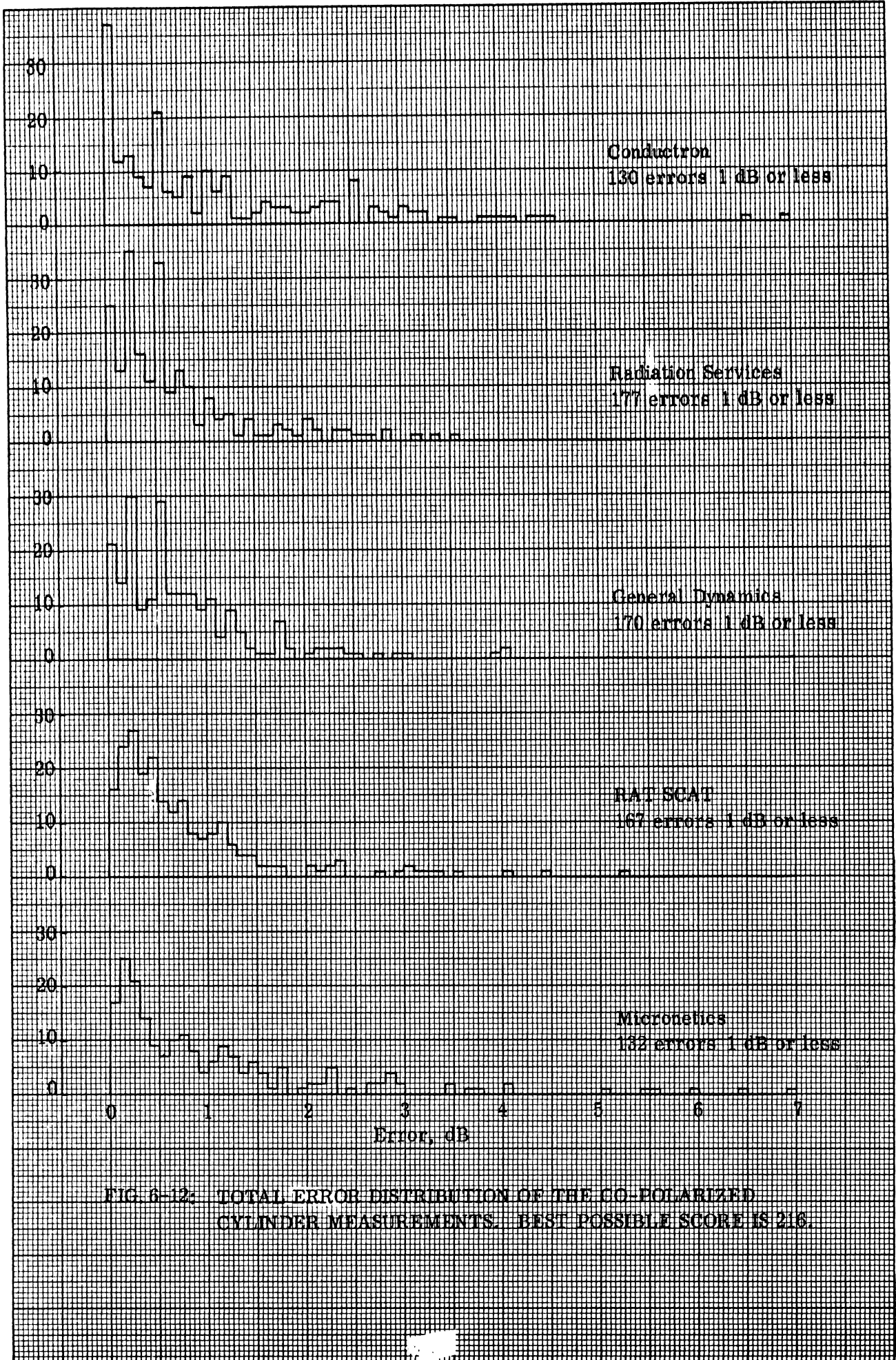


FIG. 6-12: TOTAL ERROR DISTRIBUTION OF THE CO-POLARIZED CYLINDER MEASUREMENTS. BEST POSSIBLE SCORE IS 216.

**TABLE VI-4: SUMMARY OF RANGE TESTS FOR FIVE POINTS OF EVALUATION. Numbers indicate errors 1 dB or less for the range listed.**

<b>Range Test</b>	<b>CC</b>	<b>RSC</b>	<b>GD</b>	<b>RSS</b>	<b>MC</b>	<b>AL</b>
<b>Constant ka (52 possible)</b>	40	46	43	45	41	4 (of possible 4)
<b>End-on Polarization (18 possible)</b>	17	18	18	16	17	4 (of possible 4)
<b>End-on Theory (36 possible)</b>	17	30	24	27	33	4 (of possible 8)
<b>Broadside Theory (36 possible)</b>	21	30	34	33	15	8 (of possible 8)
<b>Special Low ka Test (74 possible)</b>	36	53	52	46	30	not evaluated
<b>Total Number of Errors (216 possible)</b>	131	177	171	167	136	20 (of possible 24)
<b>Percent</b>	60	82	79	77	63	83
<b>Grade</b>	D	B	C	C	D	B



of the measurements with themselves and with theory was more noticeable in the end-on and sidelobe data than in the broadside data. The errors with the  $ka=1.36$  data were not nearly as large in amplitude as the near field errors.

It is not obvious what the cause or causes for the difficulties with the measurements are when  $ka=1.36$ , particularly since there is a randomness about the types of troubles encountered. One explanation which could account for the randomness of the errors is the following. For  $ka=1.36$ , the lobe structure of the backscatter patterns is the broadest, therefore, more energy is scattered in all directions than for the larger  $ka$  cases. This is shown in the theoretical and experimental patterns in Chapters III and IV where, as  $ka$  decreases, it is seen that the backscattered power becomes more evenly distributed over this entire aspect region. Similar behavior will also occur in bistatic directions so that the power directed towards the ground and to the sides of the target increases with smaller values of  $ka$ . In other words, for smaller  $ka$  values the scattering tends to be more omnidirectional. The broader beam structure would enhance the scattering from spurious objects such as the pit, the supporting columns and other objects in the vicinity of the target, thus tending to introduce random type errors. This is a problem which all range operators are aware of and it is discussed under the heading of Secondary Reflections in Volume I. In some cases such as the General Dynamics measurements on the 2' (1/16-scale) model at 1360 MHz, it appears as though carelessness in this regard might have caused these errors.

In Volume I additional possible causes for the random errors in the  $ka=1.36$  data are mentioned. A possible serious problem discussed there is the lack of uniformity of the incident field in the target area, particularly the fields along the radial direction between the target and radar. This is a direction which is usually not checked as carefully as that normal to this line at the pit. Since at end-on incidence the target extends the furthest into this region, it may well be causing problems in the  $ka=1.36$  tests. Most likely there is more than a single cause for these random errors and different combinations of them exist



at each range.

In the interest of making this report as readable as possible, all the test patterns are not shown. It should be noted that measurements for the same model-frequency tests from the different ranges did agree well insofar as pattern shape is concerned. The evaluation procedures in this chapter and in Chapter V concentrated on pattern amplitudes relative to one another, and to theory, which is a more sensitive test than analyzing pattern shapes.



## VII

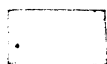
### CROSS POLARIZATION THEORY AND EXPERIMENT

Theoretical, experimental and evaluation aspects of the VH and HV cross polarization tests are discussed in this chapter. Simple theoretical arguments based on image theory are used to show why the cross polarized returns, VH and HV, should be zero when a perfectly conducting target is measured in a plane of symmetry. When experimental patterns are examined it is found that measured VH and HV returns in many cases resemble the co-polarized cross section patterns with the power level reduced by 20 to 30 dB. The level of the measured cross polarized return is too high and is generally due to coupling between the transmitting and receiving antennas; this is obvious if the cross polarized pattern is similar to the co-polarized pattern.

Our evaluation tests consists of comparing isolation levels between the cross polarized and co-polarized returns. Comparisons are made in the broad-side aspect region where the largest returns are usually found for both the direct and orthogonal patterns.

#### 7.1 Cross Polarized Theory

Combinations of image theory, the equivalence principle, and the reciprocity theorem can be invoked to prove that there is no cross polarized return from the cylinder models when measured as in this program. All of these concepts are adequately introduced and explained by Harrington (1961). When the plane in which the target is rotated is also a plane of symmetry of the target, the plane of symmetry can be replaced with a perfect conductor, S, and the lower portion of the model can be removed as in Fig. 7-1. If the conducting plane is sufficiently polished we observe the optical image of the upper portion of the model reflected from the surface as though it were the lower portion, thus making it appear as if the complete cylinder were still present. An additional condition which the target model satisfies is that it must be a good conductor like the image



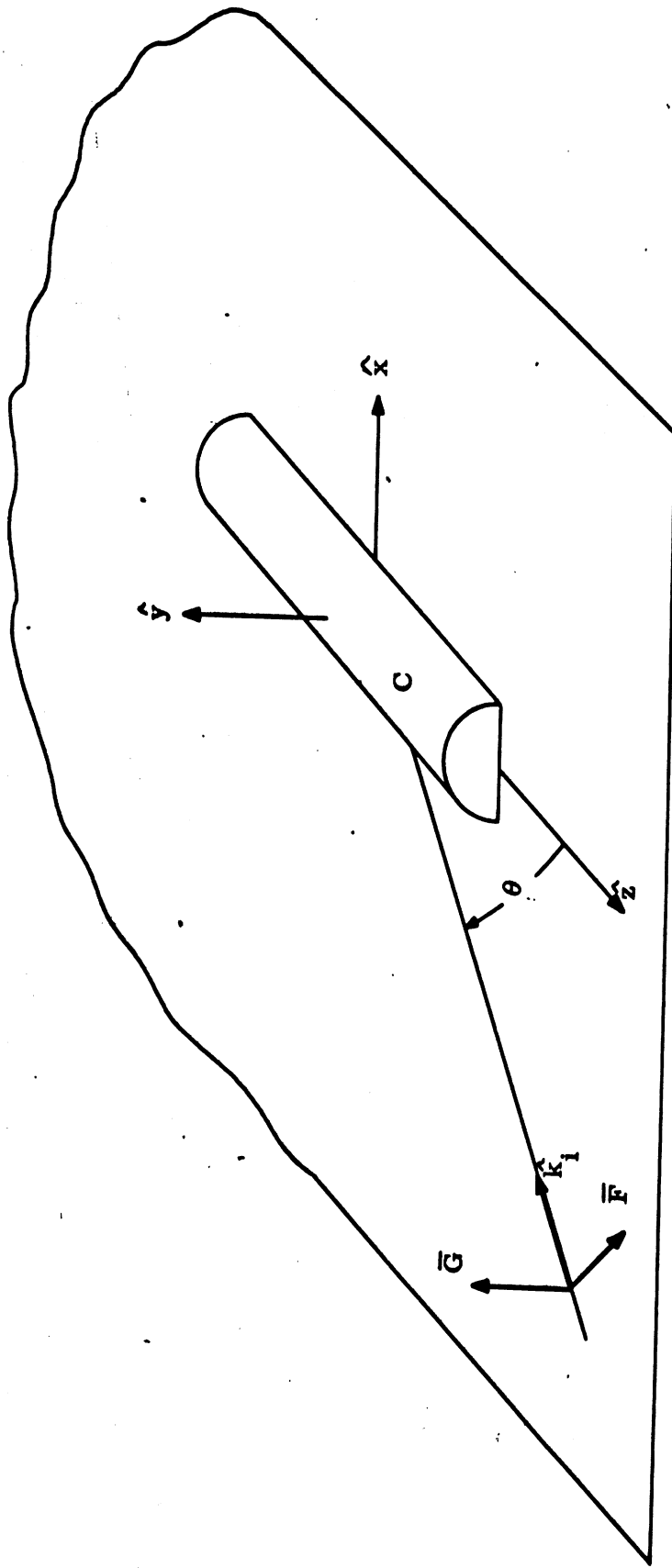


FIG. 7-1: IMAGE PLANE GEOMETRY FOR THE CYLINDER MODEL.

plane S. If the model retained all the necessary symmetry but was coated with a dielectric or plasma layer, image theory would no longer hold and, in general, cross polarized returns would be present for aspect angles different from  $0^\circ$  and  $90^\circ$ .

The polarization of the incident electric field  $\bar{E}$  is divided into the usual vertical (V) and horizontal (H) components and analyzed separately. Assume the incident field is directed along the  $\hat{k}_i$  vector at an aspect angle  $\theta$  as shown in Fig. 7-1. For the first case allow the vector  $\bar{G}$  which is normal to S to be the  $\bar{E}$  field and the vector  $\bar{F}$ , which is tangent to S, to be the magnetic field  $\bar{H}$ ; this then is the V polarization. If it is further stipulated that S is a perfect electric conductor then  $\hat{y} \times \bar{E} = 0$  which means that all electric fields in the plane S are zero by definition. Thus no component of the backscattered  $\bar{E}$  field can exist in the x-y plane, indicating that the VH return must be zero. This conclusion is valid so long as the radar lies in a plane of incidence which is also a plane of symmetry for a conducting target.

The line of reasoning for the cross polarized arguments may take at least two paths. One argument calls upon the reciprocity theorem, stating that the response of a system is unchanged if the transmitter and receiver are interchanged. All the fields and target satisfy the usual linear, bilateral conditions necessary for reciprocity. From this theory it follows that the HV return is zero if the VH return is zero.

A somewhat more physical, but less familiar, argument for the HV case is found in the equivalence principle stating that one need not know the actual sources to determine the fields in a given region; any accurate equivalent source or group of sources will suffice. This principle permits us to allow S to be a perfect magnetic conductor which in turn implies that  $\hat{y} \times \bar{H} = 0$  or  $\bar{H}$  is zero on the surface S. We now return to Fig. 7-1 and interchange  $\bar{G}$  and  $\bar{F}$  so that  $\bar{G} = \bar{H}$  and  $\bar{F} = -\bar{E}$  in order to have the appropriate propagation in the  $\hat{k}_i$  direction. The target may be represented by a perfect magnetic conductor even though it is physically an electric conductor. The boundary conditions on C are such that

the incident field will be scattered back to the receiver in the correct manner. Because  $\hat{y} \times \bar{H} = 0$  there can be no HV return for the horizontally polarized case either.

## 7.2 Cross Polarized Measurements

Unfortunately in the real world accurate cross polarized measurements are difficult to make, particularly when the VH and HV returns should be zero. In performing these measurements one invariably discovers a small but finite return when there should be none at all. Some of the causes for the erroneous returns are

- a) antenna alignment and isolation
- b) target alignment,
- c) depolarized returns from alien scatterers.

For the test made during this program, it appears that antenna isolation problems were the main cause of spurious (finite) VH and HV returns. This conclusion follows from the fact that most of cross polarized patterns definitely resembled the VV and HH patterns as shown in Fig. 7-2. The pattern on the left in this figure is a portion of the HH pattern in Fig. 4-12 for the 32-foot cylinder at 340 MHz. On the right in Fig. 7-2 is the VH return for the same target which appears similar to the co-polarized return, but is 20 dB lower in power level.

For the VH pattern in Fig. 7-2 the peak return is located at  $90^\circ$ . As a rule the peak return for all the VH and HV patterns are located near, but not always exactly on, broadside. Cross polarized (VH and HV) data for peak returns near broadside in dBsm are summarized in Tables VII-1 and VII-2 for all the ranges. In these displays the values in each box are arranged according to the measuring facility as indicated in the sample box in the upper right part of the table. The frequency axis and the model size axis are the same as those used in other displays.

There are many measurements missing in these tables. The symbol (\*) indicates near field distortions and (-) indicates that no data were submitted for these cases. It is not meaningful to compare cases having near field errors,

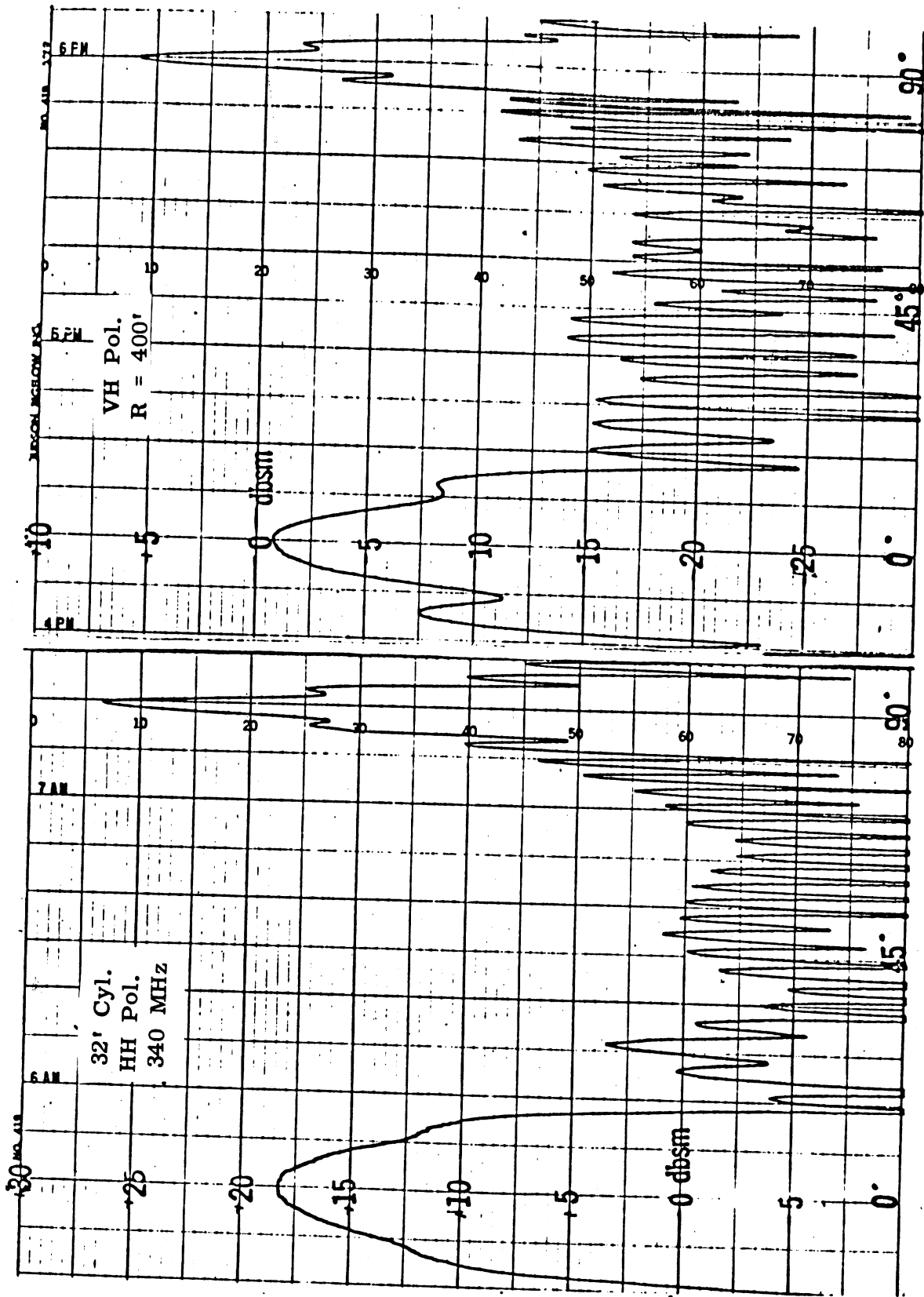


FIG. 7-2: COMPARISON BETWEEN HH AND VH POLARIZATIONS,  
 $ka = 5.44$ , 32 FOOT CYLINDER, 340 MHz.

	1/1 Scale	1/2 Scale
170 MHz	-	-
	-3.8	-11.5
	-	-
	+4.0	-5.0
	-	+1.0

\* Near Field Distortion  
 - No Test Data Submitted

		1/4 Scale	
340 MHz	-	-	-
	+5.6	-6.75	-14.25
	+6.6	-2.6	-4.25
	+4.5	-4.5	-18.9
	+7.0	-8.0	-19.3

- |   |      |
|---|------|
| 1 | CC   |
| 2 | RSC  |
| 3 | GDFW |
| 4 | RSS  |
| 5 | MC   |

			1/8 Scale
680 MHz	-	-	-
	+1.0	-13.5	-24.8
	-0.4	-9.25	-15.25
	-10.4	-20.1	-26.5
	+7.7	-5.1	-14.8
			-33.0
			-25.0
			-36.5
			-23.3

				1/16 Scale
1360 MHz	*	-10.6	-18.0	-24.0
	+3.4	-13.0	-22.0	-26.25
	+2.0	-6.5	-9.5	-19.75
	-2.3	-16.1	-16.1	-25.0
	*	-1.2	-14.9	-26.6
				-30.5
				-31.5
				-29.75
				-34.5
				-37.0

2720 MHz	*	-25.0	-22.0	-29.0
	-5.5	-20.4	-34.5	-35.5
	-13.0	-29.75	-36.0	-33.0
	-0.5	-18.5	-27.2	-27.2
	*	-10.0	-24.3	-34.5

TABLE VII-1: SUMMARY OF VH CROSS POLARIZED DATA (in dBsm) FOR PEAK RETURNS NEAR BROADSIDE.





since we know they are distorted. General Dynamics made no cross polarized tests at 170 MHz and Conductron made cross polarized tests only at 1360 and 2720 MHz. Below these frequencies Conductron used the same antenna for transmitting and receiving and felt that its isolation was insufficient to record accurate data.

### 7.3 Evaluation of Cross Polarized Data

Many times throughout this report it has been mentioned that there are numerous ways to evaluate the results for the different tests. For the cross polarized measurements we decided to compare isolation levels between the direct and cross polarized returns. The isolation comparisons were further limited to the broadside aspect region, because these returns are the largest and easiest to recognize.

The VH and HV values in Tables VII-1 and VII-2 were subtracted from the corresponding HH and VV broadside values in Tables V-2 through V-6 according to the expressions

$$\sigma_{HH}(90^\circ) - \sigma_{VH}(\approx 90^\circ)$$

and

$$\sigma_{VV}(90^\circ) - \sigma_{HV}(\approx 90^\circ) .$$

The isolation differences for these comparisons are given in Tables VII-3 and VII-4.

A comparison of the numbers in any of the four tables in this chapter within a range or between the ranges shows only random behavior. This is to be expected since all the VH and HV returns are a form of noise in that the returns should be zero. For the same reason the VH and HV returns for the same frequency-model tests should not look alike. Generally one would expect the VH and HV cross sections to be equal from reciprocity considerations, but when the return looks like random noise this is not the case.

The average isolation levels for the cross polarization comparisons for each of the ranges are listed in Table VII-5 with the number of tests which the

	1/1 Scale	1/2 Scale				
170 MHz	-	-	* Near Field Distortion - No Test Data Submitted			
	27.9	26.5				
	-	-				
	19.8	20.1				
	-	16.0				
			1/4 Scale			
340 MHz	-	-	-	1 CC 2 RSC 3 GDFW 4 RSS 5 MC		
	21.15	25.0	23.75			
	20.4	20.1	13.25			
	23.5	21.8	27.7			
	19.0	24.8	28.3			
			1/8 Scale			
680 MHz	-	-	-			
	29.0	35.0	37.05			36.0
	31.0	30.75	27.45			28.9
	40.0	41.3	38.7			40.0
	22.3	25.9	26.0			26.0
			1/16 Scale			
1360 MHz	*	32.1	35.8	30.0	27.5	
	27.35	36.0	37.25	32.75	29.3	
	30.5	30.7	25.5	26.75	26.25	
	34.4	41.7	31.0	31.5	32.0	
	*	24.2	29.4	31.9	34.2	
2720 MHz		*	41.0	30.5	28.0	
		31.8	38.9	43.75	36.0	
		39.5	48.25	45.25	33.6	
		27.1	37.2	36.5	27.7	
		*	33.3	33.6	34.0	

TABLE VII-3: ISOLATION COMPARISONS FOR  $\sigma_{HH}(90^\circ) - \sigma_{VH}(\approx 90^\circ)$ .

	1/1 Scale	1/2 Scale
170 MHz	-	-
	31.0	26.0
	-	-
	18.8	17.1
	-	15.1

\* Near Field Distortion  
 - No Test Data Submitted

		1/4 Scale	
340 MHz	-	-	1 CC
	20.25	23.25	2 RSC
	27.75	24.6	3 GDFW
	36.5	33.0	4 RSS
	18.0	23.3	5 MC
		22.0	
		12.0	
		31.6	
		26.0	

			1/8 Scale
680 MHz	-	-	-
	28.0	34.5	33.75
	24.25	24.5	25.1
	44.2	42.0	37.8
	21.9	25.3	23.3
		35.0	
		30.25	
		37.5	
		24.4	

				1/16 Scale	
1360 MHz	*	31.2	32.0	27.50	25.2
	27.25	27.4	38.25	30.85	27.3
	25.05	28.25	27.55	26.75	26.9
	32.4	37.3	28.0	27.0	26.4
	*	24.1	31.1	30.2	33.2

2720 MHz	*	41.0	30.25	30.5
	29.5	37.3	40.25	41.0
	32.5	33.1	33.25	28.8
	27.0	31.5	31.9	26.9
	*	27.9	32.3	30.5

TABLE VII-4: ISOLATION COMPARISONS FOR  $\sigma_{VV}(90^\circ) - \sigma_{HV}(\approx 90^\circ)$ .

ranges successfully complete. A maximum of 36 VH and HV tests were considered in the isolation evaluations. RAT SCAT and Radiation Service completed all the tests and had the best overall performance with 31.5 and 30.7 dB isolation levels. Conductron had the highest level but successfully completed less than half the tests. Micronetics has a slightly lower average for this comparison because it uses the same antenna for transmitting and receiving for most of its tests, creating isolation difficulties.

TABLE VII-5: ISOLATION AVERAGES

Range	No. Tests Completed	Grade	Average Isolation for These Tests	Grade
CC	14	E	32.2 dB	C
RSC	36	A	30.7 dB	C
GD/FW	32	B	27.2 dB	D
RSS	36	A	31.5 dB	C
MC	30	B	27.5 dB	D

The required isolation needed to perform satisfactory cross polarized measurements is subject to question. Based on target identification studies we are conducting at The University of Michigan, we feel that a 30 dB isolation level is the minimum acceptable value and for some applications this may be insufficient. Additional comparisons of the cross polarized data are possible and if this is an area of interest to the reader he might wish, for example, to make evaluation tests similar to those in Chapters V and VI. Recommendations for improving cross polarized measurements are given in Volume I. Improvements in antenna design alone would produce better isolation levels.

As we demonstrated earlier in this chapter, the cross polarized echo from any conducting body of roll symmetry is theoretically zero along the principal planes. Measurement of the cross polarized return of such a target, then, represents an extremely difficult task whose only utility is to assess the isolation of the two channels and to perhaps judge the general condition of the range. A much more meaningful cross polarized measurement would have been along the

planes of maximum return. These planes lie  $45^\circ$  from the principal planes, as shown in Fig. 7-3, and theoretically the cross polarized echoes can be computed from the phase and amplitude of the VV and HH returns. Depending on the complexity of the antenna feeds, this technique can range from extremely simple to unduly complex, and some radar cross section ranges may be quite incapable of performing such a measurement.

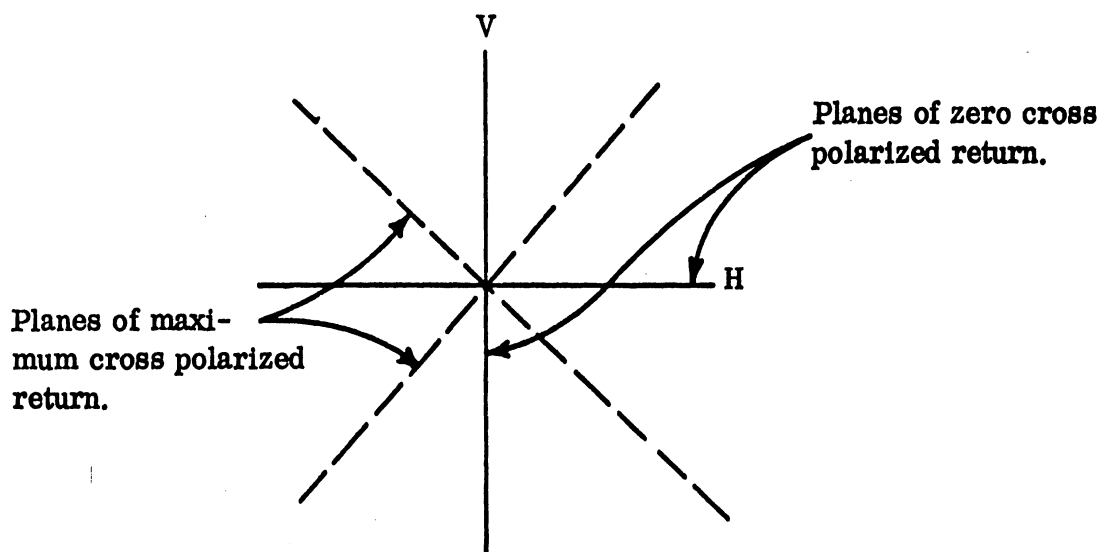


**FIG. 7-3: CROSS POLARIZED MEASUREMENTS ARE BEST PERFORMED IN CUTS ANGLED  $45^{\circ}$  TO THE PRINCIPAL PLANES. The boresight axis is normal to the plane of the diagram.**

## VIII

### CONCLUSION

Much of Volume I could be considered as a conclusion to Volume IIa, but for the sake of completeness some topics are discussed here which also are found in the first volume. Topics such as recommendations for the improvement of deficiencies and guides to optimum utilization of facilities are not restated here. We limit our concluding remarks in this chapter to the material specifically covered in Volume IIa.

Two topics mentioned at the beginning of this report are phase measurements and digital data. Only two of the ranges had the capability to measure phase. General Dynamics is equipped to measure phase over all the frequency bands in this test program (170 to 2720 MHz) but RAT SCAT can measure phase only at L band (1000 MHz to 2000 MHz). Unfortunately there were not enough accurate phase data to make meaningful comparisons. General Dynamics submitted phase patterns for all frequency-model combinations but from what we have learned, these patterns would be difficult to use because of the way they were calibrated. In order to speed up our seriously lagging time schedule at RAT SCAT, we waived the need for phase measurements there, except for the 32' and 16' cylinders at 1360 MHz. A theoretical phase pattern is presented in Fig. 3-7 to show typical phase behavior. The importance of improving phase measuring capabilities for all the ranges is discussed in Volume I.

All the ranges recorded digital data as well as the analog patterns and the various forms of digital equipment used at the ranges are shown in Table II-2. Of all the digital recording equipment, the magnetic tape system at Micronetics seemed to be the most desirable. At the beginning of the contract Rome Air Development Center was processing all digital data to verify their correspon-

dence with the analog recordings. Rome discovered several problems in converting the various formats of the individual ranges to its computer program for analysis. Digital data from RAT SCAT and Micronetics were not available until the end of the program and because of these difficulties, no overall evaluation was made of the digital data. In Volume I we discuss the need for equipment that would permit the range operators to make an immediate check of the correctness of the digital data.

The remainder of our remarks below are directed towards the theoretical models in Chapter III, the co-polarized tests in Chapters V and VI, and the cross polarized tests in Chapter VII. Finally, we offer some subjective views about the outcome of these tests.

#### 8.1 Remarks on the Theoretical Models

One of the objectives of this program was to compute expected radar cross sections for each of the cylinders under the experimental frequency and polarization conditions specified. This was done in Chapter III for the co-polarized (HH and VV) tests and in Section 7.1 for the cross polarized (VH and HV) tests. The spirit of this task was to determine the cross section with existing methods rather than to develop new theoretical approaches for calculating cross sections of finite cylinders. We believe that this portion of the contract was amply discharged and that a sound theoretical base was established for making comparisons with experimental measurements.

Theoretical calculations were made for two reasons: first, continuous patterns as a function of aspect angle can be obtained and second, accurate cross sections at end-on and broadside aspect positions are available. The continuous theoretical patterns were used to check the gross pattern structure shown by the experimental data. Accurate cross section calculations at end-on and broadside aspect angles were compared directly with measured data in the main evaluation program. Theoretical arguments based on image theory were developed to show



that no cross polarized return should be expected for the tests made on the cylinders.

A weak point in our theoretical models for the co-polarizations at end-on incidence for the smaller  $ka$  values may be noted. We expected this to be troublesome because the mathematical formulation was based on the assumption that the cylinder at end-on would behave like a disc alone, but nevertheless, this model still appeared to be accurate to within  $\pm 1$  dB. The disagreement in the measurements from the separate ranges for this aspect region emphasized this weak spot in theory.

Considering that there is no exact solution for the fields scattered by a finite cylinder, the mathematical models employed here yielded good results. In the near future there will be improved numerical computer techniques for obtaining even more accurate cross section calculation over larger values of  $ka$ . During the course of this contract (1965-1968) developments in computer techniques have come a long way (see the references mentioned in the beginning of Chapter III) and it is reasonable to expect they will continue.

## 8.2 Remarks on the Co-Polarized Data

The intra-range and inter-range tests required data reduction and evaluation procedures for the co-polarized data and grades reflecting relative performance were assigned to these tests for each of the ranges. Other display and reduction techniques were included, such as the comparison of experimental data with continuous theoretical patterns over five-degree intervals and the examination of the amplitudes of the sidelobes adjacent to broadside. We felt the sidelobe tests added no significant information above that obtained in the intra-range and inter-range tests and we therefore assigned no grades to them.

A summary of the intra- and inter-range evaluations and grades has been presented at the end of Chapter VI. The grades for each test and the overall average grade for each range, assuming the five tests are of equal weight,

are shown in Table VIII-1 which is a condensed form of Tables V-8 and V-9 of Chapter V and VI-1, VI-2 and VI-4 of Chapter VI. General Dynamics and RAT SCAT both achieved overall grades of C while Radiation Services did slightly better with a grade of B. For all practical purposes these three ranges performed their tests well and had no consistent sources of error. Yet we must stress that on occasions these ranges did have noticeable errors, particularly for the lower ka cases.

TABLE VIII-1: SUMMARY OF GRADES FOR ALL EVALUATION TESTS AND AVERAGE GRADES

Range	Constant ka	End-on Polarization Comparison	End-on Theory Comparison	Broadside Theory Comparison	Special Low ka Test	Overall Performance
CC	C	A	E	E	E	D
RSC	B	A	B	B	C	B
GDFW	B	A	D	A	C	C
RSS	B	B	C	A	D	C
MC	C	A	A	E	E	D
AL	A	A	E	A	--	B

Our grading criterion was such that errors 1 dB or smaller were considered acceptable. Micronetics had many errors between 1 and 1.5 dB and this accounts for its lower grade. Micronetics also had near field distortions in a few of its patterns, but this was a minor problem compared to Conductron's difficulties in this area. Due to an accident in which the 32 foot cylinder was dropped, Micronetics was unable to make any tests on this target at 170 MHz. In our

evaluation the missing data were treated as if they had an error greater than 1 dB. Only two models were measured at two frequencies on the Avionics Laboratory range. Grades were assigned to most of its results, but since there were so few tests, one cannot attach high significance to these grades.

Near field distortions in the broadside aspect region were the reasons for errors in several of Conductron's patterns. The maximum antenna-to-target distance used at this facility was 200 feet, and this fell far short of the commonly accepted  $2L^2/\lambda$  range criterion for many of the tests (see Table IV-1). Conductron mathematically transformed near field data to far field predictions to correct the distorted broadside pattern structure, but when the distortion is severe it extends to other lobes in the broadside region. Because of this the "corrected" values were not included in our evaluation; instead, the raw data from the patterns was used for the evaluation tests.

Secondary causes of errors in the co-polarized data are less easy to identify. We refer to the errors in the low ka value tests which were mostly random yet present in all the range data. These errors may have been due to lack of a uniform incident field, secondary reflections, or insufficient observance of other proven measurement procedures. These and other problem areas are discussed in detail in Chapter IV of Volume I.

### 8.3 Remarks on the Cross Polarized Data

The ranges were graded both on their capabilities to perform cross polarized measurements and on their results. It turns out that, since there is theoretically no cross polarized return from the cylinder targets, this represented a rather difficult and relatively uninformative test. The grades we assign should not be as heavily weighted as those given in the co-polarized evaluation.

There were 36 VH and HV tests to be made at each range but only Radiation Services and RAT SCAT were able to do them all. Both of these

ranges had better than 30 dB average isolation between the cross and co-polarized measurements. General Dynamics was unable to measure cross-polarization at 170 MHz; for other tests, they had a 27.2 dB isolation level.

Conductron made cross polarized measurements only at S and L bands (1000 MHz - 3000 MHz) because at lower frequencies it uses the same antenna for transmitting and receiving and in this mode of operation it felt there was insufficient isolation to obtain accurate measurements. It is interesting to note that Micronetics used one antenna for transmitting and receiving for most of its tests, yet it chose to make cross polarized measurements at all frequencies. Micronetics' average isolation was 25.7 dB, just a little poorer than General Dynamics' isolation level.

From our own experiences at the Radiation Laboratory, we feel that a minimum average isolation of 30 dB should exist between the cross and co-polarized levels when no cross polarization should be present. It would be desirable to strive for a 40 dB isolation level for these cases. By improving antenna design for better isolation, much of the additional 10 dB should be attainable. A more significant test of cross polarized measurements for a cylinder is one in which a  $45^{\circ}$  polarization is transmitted and a  $135^{\circ}$  polarization received.

#### 8.4 Final Remarks

We found that accurately scaled cylindrical targets represent good targets with which to evaluate radar cross section ranges. The cylinder is a simple enough shape for which the end-on and broadside returns can be predicted with an accuracy of one dB or better, yet its scattering behavior is sufficiently complex to test range performance. The cylinder is also a practical shape because it is often a component of many aerospace vehicles and boosters.

Our analysis of the range data acquired for the cylindrical targets shows that some ranges have difficulty in measuring large objects at some of the higher frequencies and that all ranges have difficulty if the accuracy requirements are unduly stringent. In this program we arbitrarily refer to errors less than or equal to one dB, and this error level is reflected in the results of Table VIII-1. If we had set our sights a little higher, say at 0.5 dB, no range would have been acceptable; had we specified 2 dB, on the other hand, all would have turned in very good performances. Thus we emphasize that, depending on the rating system adopted, range performances can run the gamut of totally unacceptable to totally acceptable.

The evaluations presented in this Volume IIa of the Final Report are summarized in less detail in Volume I, but form a part of a more general comparison of range capabilities. The reader will find in Volume I a critique of the shortcomings of radar cross section ranges and a list of possible improvements that can be made. Among these improvements is the recommendation that the range customer establish a close liaison with range personnel, who, in turn, must be unusually diligent in performing their tasks. The acquisition of highly accurate and reliable data is accomplished only through the expenditure of hard work and honest endeavor.

## REFERENCES

- Air Force Missile Development Center (1965), "RAT SCAT Radar Target Scatter Site Brochure."
- Bachman, C. G., H. E. King and R. C. Hansen (1963), "Techniques for Measurement of Reduced Radar Cross Sections," Microwave J., 6, Pt. 1, pp. 61-67 (February), Pt. 2, pp. 95-101 (March), Pt. 3, pp. 80-86 (April).
- Bahret, W. F. (1964), "Avionics Laboratory Radar Cross Section Measurements Facility," Radar Reflectivity Measurements Symposium, II, AD 601365, pp. 201-202.
- Blacksmith, P., R. E. Hiatt and R. B. Mack (1965), "Introduction to Radar Cross Section Measurements," Proc. IEEE, 53, pp. 901-920.
- DiFrancia, G. T. (1953), Electromagnetic Waves, Interscience Publishers, New York, p. 37.
- General Dynamics (1964), "Radar Cross Section Measurement Capabilities," General Dynamics/Fort Worth Brochure FZE-366.
- Fisher, F. E. (1967), "Theoretical Approximation to Resonant Cylinder Scattering," Company Publication, Radiation Service Co., Radiation Inc., Melbourne, Florida, August 1967.
- Harrington, R. F. (1961), Time-Harmonic Electromagnetic Fields, Chapter 3, McGraw-Hill, New York, New York.
- Honer, R. E. and W. D. Fortner (1964), "Outdoor Pulsed Radar Reflectivity Range," Radar Reflectivity Measurements Symposium, II, AD 601365, pp. 274-285.
- Kouyoumjian, R. G. and L. Peters (1965), "Range Requirements in Radar Cross Section Measurements," Proc. IEEE, 35, No. 8, pp. 920-929.
- Landfried, J. E. and W. L. Williamson (1964), "Static Radar Reflectivity Measurement Facilities at Radiation Incorporated," Radar Reflectivity Measurements Symposium, II, AD 601365, pp. 299-302.
- Marlow, H. C., D. C. Watson, C. H. VanHoover and C. C. Freeny (1965), "The RAT SCAT Cross Section Facility," Proc. IEEE, 53, pp. 946-953.
- Mentzer, J. R. (1955), Scattering and Diffraction of Radio Waves, Pergamon Press, p. 34 and p. 64.

Oshiro, F.K. and C.W. Su (1965), "A Source Distribution Technique for the Solution of General Electromagnetic Scattering Problems," Northrop-Norair Report No. NOR-65-271.

Oshiro, F.K. et al (1967), "Calculation of Radar Cross Sections," Northrop-Norair Second Quarterly Report No. NOR-67-31 (January).

Schmitt, H. J. (1959), "Back Scattering Measurements with a Space-Separation Method," IRE Trans. Ant. and Prop., AP-7, No. 1, January, pp. 15-22.

Also, see King, R.W.P. and T.T. Wu (1959), Scattering and Diffraction of Waves, Harvard University Press, p. 129.

Wren, A.W. (1964), "Conductron Corporation's Cross Section Range," Radar Reflectivity Measurements Symposium, II, AD 601365, pp. 359-362.

## APPENDIX A

### PHYSICAL OPTICS MODEL FOR SCATTERING BY A FINITE CYLINDER

In this appendix expressions are derived for the amplitude and phase of the scattered fields from a finite cylinder. Knowing the scattered fields, one can estimate the radar cross section of the cylinder. The physical optics procedure, which is used to evaluate the fields, is an approximate technique whose accuracy increases for growing values of  $ka$ .

The monostatic (or back) scattering cross section of an object is defined as (Blacksmith, 1965)

$$\sigma = 4\pi R^2 \left| \frac{\bar{H}^s}{\bar{H}^i} \right|^2 \quad (\text{A. 1})$$

where  $\bar{H}^i$  and  $\bar{H}^s$  are the magnetic field intensities of the incident and back-scattered fields respectively and  $R$  is the distance from the scattering target to the transmitter-receiver location in the far field. For the monostatic case the transmitter and receiver are located at the same position  $P(R)$ . When the transmitter is placed in the far field, the incident field  $\bar{H}^i$  may be treated as a plane wave.

In this analysis the scattering object is a finite cylinder of length  $l$  and radius  $a$  as shown in Fig. A-1. Since there is no exact solution for the scattered fields from a finite cylinder, an approximate model is introduced to obtain an expression for the fields. In the approximate model the fields scattering from a cylinder  $\bar{H}_c^s$  and a circular flat plate  $\bar{H}_p^s$  are summed as phasors to obtain an expression for the total backscattered field  $\bar{H}^s$ .

$$\begin{aligned} \bar{H}^s &= \bar{H}_c^s + \bar{H}_p^s \\ \bar{H}^s &= \bar{H}_c e^{j\psi_c} + \bar{H}_p e^{j\psi_p} \end{aligned} \quad (\text{A. 2})$$



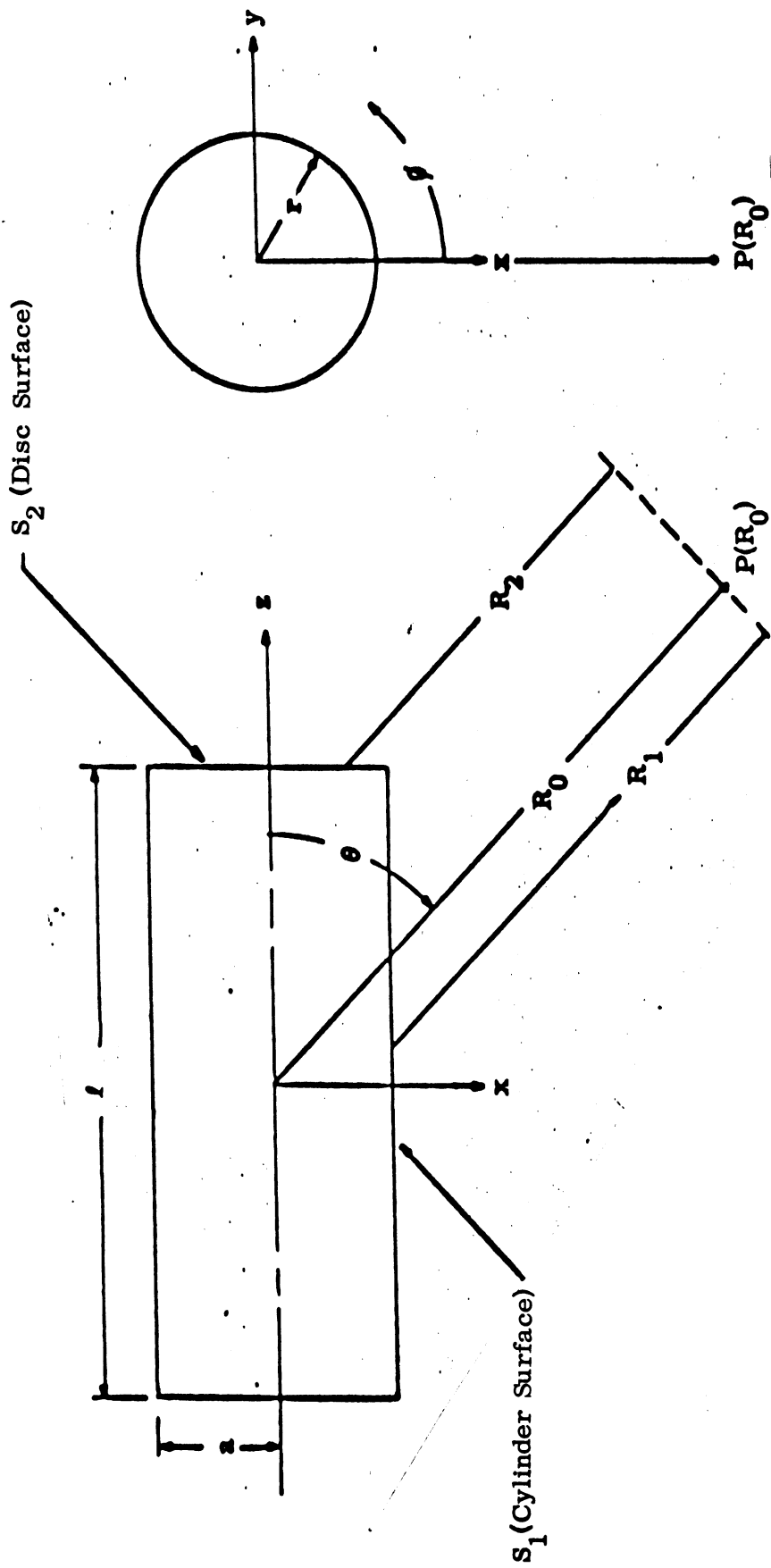


FIG. A-1: FINITE CYLINDER GEOMETRY.

where  $\bar{H}_c$  and  $\bar{H}_p$  are the amplitude and  $\psi_c$  and  $\psi_p$  are the phase components of the scattered field from the cylinder and the plate. No attempt is made to consider the scattering contribution from the edge where the cylinder and plate are joined. This omission of the edge effect produces noticeable but small errors in the aspect region near and about  $45^\circ$ . If more accurate behavior of the edge effects are desired, the reader is referred to method (b).

If the backscattered fields of (A.2) are substituted into (A.1), then

$$\sigma = 4\pi R_o^2 \left[ \frac{|\bar{H}_c|^2 + |\bar{H}_p|^2 + 2|\bar{H}_c| |\bar{H}_p| \cos(\psi_c - \psi_p)}{|\bar{H}^i|^2} \right] \quad (\text{A. 3})$$

The amplitudes  $\bar{H}_c$  and  $\bar{H}_p$  are well known and are found in cross section tables (e.g. Oshiro and Su, 1965), but the phase components  $\psi_c$  and  $\psi_p$  are not easily found. In order to determine the precise value of  $\psi_c$  and  $\psi_p$ ,  $\bar{H}_c^s$  and  $\bar{H}_p^s$  are evaluated by the physical optics procedure. Even though the physical optics model becomes effective only when  $ka$  is greater than 5.44, this procedure does offer a physical insight into the scattering behavior irrespective of the  $ka$  value.

Assume a plane parallel-polarized field is obliquely incident upon a perfectly conducting cylinder of finite length at an aspect angle  $\theta$  as shown in Fig. A-1. The field  $\bar{H}^i$  originates at  $P(R_o)$  in the far field and in the vicinity of the cylinder is represented as

$$\bar{H}^i = \hat{y} H_o e^{jk(z \cos \theta + x \sin \theta)} \quad (\text{A. 4})$$

where  $k$  is the wave number,  $H_o$  the harmonic amplitude of the magnetic field intensity, and  $\hat{y}$  is a unit vector. Harmonic time dependence has been assumed to be  $e^{j\omega t}$ . A formulation of this problem in terms of the incident electric field

will lead to the same expressions as the magnetic field formulation which demonstrates that the physical optics approximation is polarization independent (i. e. VV and HH patterns are the same).

The surface current density  $\bar{J}_s$  generated on the scattering surface by the incident field is  $\bar{J}_s = 2(\hat{n} \times \bar{H}^i)$  for the physical optics model, where  $\hat{n}$  is the outward normal to the scattering surface. This representation of the current is valid for surfaces which are large and flat compared to a wavelength. As curvature is introduced in the scattering surface, the model becomes less valid. When the radius of the cylinder is on the order of or smaller than a wavelength ( $ka \leq 6$ ) the model no longer applies and the polarization effects are noticeable.

Following the procedures outlined by Mentzer (1955), the physical optics expression for the scattered field  $\bar{H}^s(R_o)$  is

$$\bar{H}^s(R_o) = \frac{-1}{4\pi} \iint_S 2(\hat{n} \times \bar{H}^i) \times \nabla \psi dS \quad (A.5)$$

where  $S$  is the portion of the scattering surface illuminated by  $\bar{H}^i$  and  $\psi$  is the spherical Green's function. Equation (A.5) has been derived from Maxwell's equations. When  $kR$  is large,  $\nabla \psi$  is approximately

$$\nabla \psi \cong -j \frac{\hat{R} k e^{-jkR}}{R} \quad (A.6)$$

where  $\hat{R} = \hat{x} \sin \theta + \hat{z} \cos \theta$  is the unit vector which is always in the plane of incidence ( $x - z$  plane).

For the finite cylinder the illuminated surface is broken into two parts, the cylinder  $S_1$  and the flat circular plate  $S_2$ . All fields in the shadow region are assumed to be zero. Due to the symmetry of the cylinder,  $\bar{H}^s$  has to be determined only for  $\theta$  between  $0^\circ$  and  $90^\circ$ . When  $\theta = 0^\circ$ ,  $P(R_o)$  is located at the end-on

position and when  $\theta = 90^\circ$ , at the broadside position. If  $S_1$  is divided into  $S_1$  and  $S_2$ , Eqs. (A.5) and (A.6) lead to

$$\bar{H}^s(R_0) = \frac{jk}{2\pi R_0} \left[ \iint_{S_1} (\hat{n}_1 \times \bar{H}^i) \times \hat{R} e^{-jkR_1} dS_1 + \iint_{S_2} (\hat{n}_2 \times \bar{H}^i) \times \hat{R} e^{-jkR_2} dS_2 \right]. \quad (A.7)$$

In the denominator of (A.7) the far field approximation allows  $R_1 = R_2 = R_0$ . With the aid of Fig. A-1, the parameters related to  $S_1$  are

$$\hat{n}_1 = \hat{x} \cos \phi + \hat{y} \sin \phi$$

$$dS_1 = a d\phi dz, \quad -\pi/2 \leq \phi \leq \pi/2 \quad \text{and} \quad -l/2 \leq z \leq l/2$$

$$R_1 = R_0 - a \cos \phi \sin \theta - z \cos \theta$$

and those related to  $S_2$  are

$$\hat{n}_2 = \hat{z}$$

$$dS_2 = r dr d\phi, \quad 0 \leq r \leq a \quad \text{and} \quad 0 \leq \phi \leq 2\pi$$

$$R_2 = R_0 - r \cos \phi \sin \theta - l/2 \cos \theta$$

The above parameters are substituted into (A.7) and four integrations are performed. Only one of the integrations is difficult and it is accomplished by taking

advantage of the physical optics approximation that  $2ka \sin \theta$  is large in the integral over  $S_1$ . The troublesome integral has the form

$$\int_{-\pi/2}^{\pi/2} e^{j\beta \cos \phi} \cos \phi \, d\phi \quad (\text{A.8})$$

where  $\beta = 2ka \sin \theta$ . When  $\beta$  is large, (A.8) yields to the method of stationary phase (De Francia, 1953) and

$$\int_{-\pi/2}^{\pi/2} e^{j\beta \cos \phi} \cos \phi \, d\phi \longrightarrow \left(\frac{2\pi}{j\beta}\right)^{1/2} e^{j\beta} \quad (\text{A.9})$$

The solutions for the two double integrals in (A.7) are

$$\bar{H}_c^s = \hat{y} \frac{H_o \sqrt{ka l^2 \sin \theta}}{2R_o \sqrt{\pi}} \left[ \frac{\sin(kl \cos \theta)}{kl \cos \theta} \right] e^{-jkR_o} e^{j\left[\frac{\pi}{4} + 2ka \sin \theta\right]} \quad (\text{A.10})$$

and

$$\bar{H}_p^s = \hat{y} \frac{H_o ka^2}{2R_o} \left[ \frac{J_1(2ka \sin \theta)}{ka \tan \theta} \right] e^{-jkR_o} e^{j\left[\frac{\pi}{2} + kl \cos \theta\right]} \quad (\text{A.11})$$

where  $J_1(2ka \sin \theta)$  is the Bessel function of order unity. The phase difference  $\psi_c - \psi_p$ , which is being sought for (A.3), can be determined from the exponential terms in (A.10) and (A.11) and is

$$\psi_c - \psi_p = 2ka \sin \theta - kl \cos \theta - \frac{\pi}{4} \quad (\text{A.12})$$

With the proper substitution of (A.10), (A.11) and (A.12) into (A.9) the total backscattering cross section is

$$\sigma = \sigma_c + \sigma_p + 2\sqrt{\sigma_c \sigma_p} \cos \left[ 2ka \sin \theta - kl \cos \theta - \frac{\pi}{4} \right] \quad (\text{A.13})$$

where

$$\sigma_c = ka l^2 \sin \theta \left[ \frac{\sin(kl \cos \theta)}{kl \cos \theta} \right]^2$$

and

$$\sigma_p = \pi(ka^2)^2 \left[ \frac{J_1(2ka \sin \theta)}{ka \tan \theta} \right]^2$$

The expressions in (A.13) can be normalized relative to a square wavelength ( $\lambda^2$ ) in which case they become

$$\frac{\sigma}{\lambda^2} = \frac{\sigma_c}{\lambda^2} + \frac{\sigma_p}{\lambda^2} + \frac{2}{\lambda^2} \sqrt{\sigma_c \sigma_p} \cos \left[ 2ka \sin \theta - kl \cos \theta - \frac{\pi}{4} \right] \quad (\text{A.14})$$

and

$$\frac{\sigma_c}{\lambda^2} = ka \left( \frac{kl}{2\pi} \right)^2 \sin \theta \left[ \frac{\sin(kl \cos \theta)}{kl \cos \theta} \right]^2$$

$$\frac{\sigma_p}{\lambda^2} = \frac{(ka)^4}{\pi} \left[ \frac{J_1(2ka \sin \theta)}{2ka \tan \theta} \right]^2$$

As  $ka$  and  $kl$  increase in value beyond six, (A.13) and (A.14) become better representations for the backscattering cross section of finite circular cylinders and VV and HH patterns tend to become indistinguishable.

It is possible to derive theoretical expressions from the physical optics model which indicate roughly how the measured phase data should appear. By substituting the scattering expressions of (A. 10) and (A. 11) into (A. 2), the total scattered field  $\bar{H}^s$  may be factored into the form

$$\bar{H}^s = \hat{y} \left[ H_c \cos \psi_c + H_p \cos \psi_p \right] \left[ 1 + j \tan \delta \right] \quad (\text{A. 15})$$

where  $\delta$  is the phase angle for the scattered field measured relative to the center of the cylinder ( $R_o = 0$  in Fig. A-1). The other parameters in (A.15) are

$$H_c = \frac{H_o}{2R_o} \sqrt{\frac{ka l \sin \theta}{\pi}} \left[ \frac{\sin(kl \cos \theta)}{kl \cos \theta} \right]$$

$$H_p = \frac{H_o ka^2}{2R_o} \left[ \frac{J_1(2ka \sin \theta)}{ka \sin \theta} \right]$$

$$\psi_c = \frac{\pi}{4} + 2ka \sin \theta \quad \psi_p = \frac{\pi}{2} + kl \cos \theta$$

The phase angle  $\delta$  is defined as

$$\delta = \tan^{-1} \left[ \frac{H_c \sin \psi_c + H_p \sin \psi_p}{H_c \cos \psi_c + H_p \cos \psi_p} \right] \quad (\text{A. 16})$$

Like the cross section expressions in (A.13) and (A.14), the physical optics approximation for phase becomes meaningful only for larger values of  $ka$ .

**DOCUMENT CONTROL DATA - R & D**

*(Security classification of title, body of abstract and indexing annotation must be entered when the overall report is classified)*

1. ORIGINATING ACTIVITY (Corporate author) The University of Michigan Radiation Laboratory, Dept. of Electrical Engineering, 201 Catherine Street, Ann Arbor, Michigan 48108		2a. REPORT SECURITY CLASSIFICATION Unclassified	
		2b. GROUP	
3. REPORT TITLE Evaluation of Selected Radar Cross Section Measurement Ranges - Volume IIa: Cylinder Tests and Range Evaluation Procedures			
4. DESCRIPTIVE NOTES (Type of report and inclusive dates) Final Report (July 1965 - April 1968).			
5. AUTHOR(S) (First name, middle initial, last name) Thomas M. Smith, Eugene F. Knott and Ralph E. Hiatt			
6. REPORT DATE December 1968	7a. TOTAL NO. OF PAGES 135 /	7b. NO. OF REFS 17	
8a. CONTRACT OR GRANT NO. AF 30(602)-3872	9a. ORIGINATOR'S REPORT NUMBER(S) 7462-1-F		
b. PROJECT NO. 6512	9b. OTHER REPORT NO(S) (Any other numbers that may be assigned this report)		
c. Task 651207			
d.			
10. DISTRIBUTION STATEMENT			
11. SUPPLEMENTARY NOTES		12. SPONSORING MILITARY ACTIVITY Rome Air Development Center Griffiss Air Force Base, New York	
13. ABSTRACT  This is the second part of a three part final report on the evaluation of radar cross section measuring facilities. In Volume IIa, the results from measurements on five right circular cylinders, which are scale models of one another, are discussed in detail. Evaluation procedures are set forth in order to determine how well each of the ranges performed their tasks. These procedures involve the comparison of measurements on cylinders which should give the same results, or results which should differ by known scale factors, and secondly the comparison of theoretical and experimental results for end-on and broadside aspect angles. Five outdoor radar ranges took part in this evaluation program. Limited tests were made on two of the smaller cylinder models at a sixth facility, an indoor range.			



14. KEY WORDS	LINK A		LINK B		LINK C	
	ROLE	WT	ROLE	WT	ROLE	WT
Cylinder Models Ground Plane Range Large Radar Targets Outdoor Range Radar Range Evaluation Theoretical Cross Sections						